

**The early evolution of jawed vertebrates
(gnathostomes), with a special focus on
sensory systems and the application of
Bayesian phylogenetic methods**

by

Benedict King

*Thesis
Submitted to Flinders University
for the degree of*

Doctor of Philosophy
College of Science and Engineering
9th November 2018

Dedicated to Dr. Bernward Neelsen

(1930-2015)

Contents

Declaration.....	vii
Abstract.....	viii
Acknowledgements.....	x
List of published papers.....	xii
Chapter 1 – General introduction.....	1
Aims.....	1
Living and fossil jawed vertebrates.....	2
Ordovician and Silurian gnathostomes.....	3
The Devonian fossil record of gnathostomes.....	5
The use of fossils and stratigraphy in phylogenetic inference.....	8
Recent advances in early gnathostome phylogenetics.....	11
Character polarity and outgroups for early gnathostomes.....	15
Bayesian tip-dated phylogenetics.....	17
Vertebrate lateral line and electroreceptor sensory systems.....	19
References.....	22
Chapter 2 – Electoreception in early vertebrates: survey, evidence and new information	39
Context.....	39
Statement of authorship.....	39
Abstract.....	40
Introduction.....	41
Materials and methods.....	44
Survey of electroreceptors in living vertebrates.....	47

Jawless stem gnathostomes.....	54
Placoderms.....	59
Osteichthyans (bony fish).....	77
Discussion.....	95
Conclusions.....	98
Acknowledgements.....	99
References.....	99
Chapter 3 – Bayesian morphological clock methods resurrect placoderm monophyly and reveal rapid early evolution in jawed vertebrates.....	125
Context.....	125
Statement of authorship.....	126
Abstract.....	126
Introduction.....	127
Materials and methods.....	129
Revisions to characters supporting placoderm paraphyly.....	134
Results.....	140
Discussion.....	154
Acknowledgements.....	159
References.....	159
Chapter 4 – New information on <i>Brindabellaspis stensioi</i> Young, 1980, highlights morphological disparity in Early Devonian placoderms.....	168
Context.....	168
Statement of authorship.....	168

Abstract.....	169
Introduction.....	169
Systematic Palaeontology.....	171
Materials and methods.....	174
Results.....	175
Discussion.....	187
Acknowledgements.....	191
References.....	191
Chapter 5 – New information on the enigmatic early osteichthyan ‘<i>Ligulalepis</i>’.....	198
Context.....	198
Statement of authorship.....	199
Abstract.....	199
Introduction.....	200
Materials and methods.....	202
Skull roof and braincase.....	205
Cranial endocast.....	217
Sensory canals.....	225
Phylogenetic analysis.....	226
Discussion.....	230
Acknowledgements.....	234
References.....	234
Chapter 6 – Bayesian tip-dating methodology: topological effects, stratigraphic fit and the relationships of early osteichthyans.....	241
Context.....	241

Abstract.....	242
Introduction.....	242
Materials and methods.....	244
Results.....	249
Discussion.....	256
References.....	259
Chapter 7 – General discussion.....	265
Are placoderms monophyletic or paraphyletic?.....	265
Untangling early osteichthyan phylogeny.....	269
Tip-dating methods: assumptions and problems.....	271
Comparisons of different phylogenetic methods applied to morphology.....	274
Vertebrate laterosensory systems, an underutilized source of information.....	275
Future research.....	277
References.....	278
Bibliography.....	285

Declaration

I certify that this thesis does not incorporate without acknowledgment any material previously submitted for a degree or diploma in any university; and that to the best of my knowledge and belief it does not contain any material previously published or written by another person except where due reference is made in the text.

Signed 

Date: 01/12/2017

Abstract

The jawed vertebrates, or gnathostomes, are a highly diverse group that have conquered almost every habitat on earth. Indisputable articulated gnathostome fossils first appear in the Silurian Period, following which the group underwent a major radiation. Modern gnathostomes include osteichthyans (bony fishes, including tetrapods) and chondrichthyans (cartilaginous fishes i.e. sharks, rays and ratfishes). Extinct gnathostome groups include placoderms (“armoured fish”) and acanthodians (“spiny sharks”). In this thesis, three main approaches are taken to study the early evolution of gnathostomes. First, studies of sensory systems, particularly electroreception, provide insights into ecological function. Second, phylogenetic studies aim to reveal sequences of character change and rates of morphological evolution. Third, descriptions of new fossils of key taxa provide new character information and ecological interpretations.

Electroreception, the ability to detect electric fields, is phylogenetically widespread in vertebrates, suggesting it may be an ancestral feature. However, the deep evolutionary history of electrosensory systems is largely unknown. In this thesis, I utilise computed tomography (CT) scans and digital segmentation to study putative electroreceptors in early vertebrate fossils. I conclude that there is currently no evidence for electroreception in placoderms. However, the “pore-group” pits on the snouts of some early osteichthyans (which are particularly developed in early lungfishes) are shown to have several features consistent with identification as electroreceptors.

The phylogenetic relationships of early gnathostomes are a major source of debate. Current hypotheses favour a scenario in which the placoderms are paraphyletic with respect to other gnathostomes. In this thesis, tip-dated (or morphological clock) Bayesian methods, which model morphological evolution, speciation, extinction and fossil sampling, are for the first time applied to the problem of early vertebrate phylogeny. These methods strongly support placoderm monophyly, despite morphological evidence being essentially equal for paraphyly and monophyly.

Fossils of the placoderm *Brindabellaspis* have been central to discussions of early gnathostome phylogeny. New material of *Brindabellaspis* reveals a bizarre elongate rostrum supported by a thin anterior expansion of the braincase. The dorsal surface has a midline sensory canal, which CT scans reveal to be equivalent to a transverse canal in other placoderms that has doubled back and fused on itself. The new specimens highlight morphological disparity in early gnathostomes.

The skull of the osteichthyan "*Ligulalepis*" revealed an unexpected combination of features when first described. I describe a second specimen, together with substantial new information from CT scans. "*Ligulalepis*" has an unusual combination of morphological features, including a placoderm-like pituitary vein, a chondrichthyan-like labyrinth. Presence of a lateral cranial canal is variable between specimens.

The effect of Tip-dated Bayesian methods on the recovery of evolutionary relationships is relatively unexplored. Here I show that these methods favour trees with better stratigraphic fit, which have a higher prior probability. These prior probabilities are particularly influential in parts of phylogenetic trees with weak character evidence. As applied to early osteichthyan phylogeny, tip-dated methods favour an actinopterygian position for "*Ligulalepis*" over a stem osteichthyan position.

Acknowledgements

Thanks first and foremost thanks to my supervisors John and Mike. Thanks to John for the opportunity to do this PhD, his infectious enthusiasm for fossil fishes, and the freedom to push projects in my own directions. Of course I am also grateful for the opportunities I have had to go on awesome field trips! Many thanks also to Mike, for taking me on when I first arrived in Australia, and basically setting up this PhD. Mike's open-minded approach and deep thinking are a great inspiration.

Thanks also to Trev and Gav for general advice and guidance. Thanks in particular to Trev for stepping in when I needed references. The most important acknowledgement of all goes to Gav for the many free tickets to see Port Adelaide in action. Attempting to understand the complexities of the holding the ball and deliberate out of bounds rules set my struggles with Bayesian phylogenetic analysis in perspective.

Brian and Alice, our ichthyology postdocs, provided helpful guidance in all things fossil fish, and general moral support.

Thanks to Carey for helping with preparation of fossils, particularly the delicate gluing of *Ligulalepis*.

Many thanks to all my co-authors, who are listed in each chapter. I have also had the pleasure of discussing early vertebrate anatomy and phylogenetic methods with many experts. Special mention goes to Gavin Young and Marco Castiello.

Doing a PhD is not possible without the support of a fantastic lab group, who are usually around for a beer and a chat after work (or sometimes during). Thanks to Aidan, Jake, Lisa, Diana, Gully, Warren, Kailah, Amy, Matt, Carmel, Rach, Elen, Ellen, Aaron etc. If I forgot anyone, it's because the lab is too successful. Special thanks to Sam Arman because I was in his acknowledgements as a joke and now I'm returning the favour.

Last but not least I would like to thank my parents and brother for listening to me complain about my PhD and tolerating me living on the other side of the planet. Special thanks to my wife Po-Yuan for being my rock throughout the past three and a half years.

List of published papers

Chapter 2. King, B., Hu, Y. and Long, J.A. (2018). Electroreception in early vertebrates: survey, evidence and new information. *Palaeontology* **61**:325-358.

Chapter 3. King, B., Qiao, T., Lee, M.S.Y., Zhu, M. and Long J.A. (2017). Bayesian morphological clock methods resurrect placoderm monophyly and reveal rapid early evolution in jawed vertebrates. *Systematic Biology* **66**:599-516.

Chapter 4. King, B.*, Young, G.C.*, and Long, J.A. (2018). New information on *Brindabellaspis stensioi* Young, 1980, highlights morphological disparity in Early Devonian placoderms. *Royal Society Open Science* **5**: 180094.

Chapter 5. Clement, A.M.*, King, B.*, Giles, S.*, Choo, B., Ahlberg, P.E., Young, G.C., Long, J.A. (2018). Neurocranial anatomy of an enigmatic Early Devonian fish sheds light on early osteichthyan evolution. *eLife* **7**: 34349.

* denotes equal contribution

Chapter 1

General introduction

Aims

The aim of this thesis is to study the early radiation of jawed vertebrates (gnathostomes). Two major research questions are addressed. The first is the phylogenetic tree of early gnathostomes, which is vital for reconstructing the evolution of key traits and for inferring macroevolutionary patterns. The second concerns the sensory systems of early gnathostomes, in particular this thesis aims to understand whether or not electroreception was present in early gnathostomes and in what form.

Two techniques are applied in these investigations: computed tomography (CT) scanning and Bayesian tip-dated phylogenetics. In Chapter 2 CT scanning is used across a broad range of vertebrates to study a neglected sensory modality: electroreception. CT scanning is used to elucidate the neurocranial anatomy of key early gnathostome fossils in chapters 4 and 5, providing new character information for studying early vertebrate phylogeny.

Bayesian tip-dating is a recently developed method of phylogenetic analysis (Ronquist et al. 2012), combining the ages of fossils with morphological data and models of evolution. Here it is applied with two key aims. Firstly, this method may produce improved estimates of early vertebrate relationships, and the effect of tip-dating on tree topology is investigated in chapters 3 and 6. Secondly, tip-dating is a tool to understand macroevolution, and chapter 3 examines rates of evolution in early vertebrates.

Living and fossil jawed vertebrates

The vertebrates comprise approximately 68,000 living species (IUCN 2017) and can be divided into jawless forms (the hagfishes and lampreys, collectively known as Cyclostomata) and the jawed forms (Gnathostomata). Traditionally, vertebrates have been considered distinct from craniates: vertebrates comprised the gnathostomes and lampreys but excluded the hagfishes, whereas craniates also included the hagfishes (Janvier 1996). The hypothesis that lampreys were closer to gnathostomes than hagfishes is supported by many morphological characteristics (Løvtrup 1976), including presence of vertebrae, at least two semicircular canals, osmoregulation, mechanosensory neuromasts and electroreception. However, molecular data now places the hagfish together with lampreys in a monophyletic Cyclostomata (Heimberg et al. 2010). This meant that vertebrates as traditionally defined (and comprising lampreys and gnathostomes) no longer form a natural (monophyletic) group, although this conundrum is somewhat alleviated by the discovery of vestigial vertebrae in some hagfishes (Ota et al. 2011; Ota et al. 2013). Today, vertebrates and craniates are typically considered synonymous, with the term craniate falling out of use (Janvier 2015).

The gnathostomes comprise the vast majority of vertebrate species. Besides jaws, defining features of the gnathostomes include three semicircular canals in the inner ear, a branchial skeleton internal to the gills, myelinated nerves, paired fins and the trabeculae cranii of the braincase (Maisey 1986). Modern gnathostomes are further divided into the chondrichthyans and the osteichthyans. The chondrichthyans are the cartilaginous fishes, which includes sharks, rays and chimaeras. Their diagnostic feature is the presence of tessellate prismatic calcified cartilage. The osteichthyans are the bony fishes (which includes the tetrapods), defined by the presence of endochondral bone replacing endoskeletal cartilage.

There are two completely extinct groups of gnathostomes that need to be introduced. The first is the acanthodians. They are characterised by the presence of spines on their paired fins as well as their dorsal and anal fins (Janvier 1996). Like the chondrichthyans, they lack endochondral bone, and do

not have large dermal bone plates covering their skulls (with a few exceptions). The lack of preservation of endocranial details in most taxa, and the lack of skull roof bones, means that relatively few characters are available to determine their phylogenetic relationships. The second extinct group is the placoderms. Placoderms, like osteichthyans, have skulls made of large dermal bone plates (the macromeric condition). Placoderms also have trunk armour that forms a complete ring around the body, and this often has a movable articulation with the skull.

Ordovician and Silurian gnathostomes

Well preserved macrofossils of gnathostomes from before the Devonian period (c. 419-358 million years ago) are rare, although microfossils are well-represented. There are a handful of putative gnathostomes from the Ordovician (Sansom et al. 2001). The Harding sandstone (Middle Ordovician) has a number of taxa known only from scales including *Skiichthys*, a possible placoderm or acanthodian (Smith and Sansom 1997), as well as a number of chondrichthyan-like scales (Sansom et al. 2001). From the Ordovician of Central Australia, *Tantalepis* (Sansom et al. 2012) and *Areyongalepis* (Young 1997) are possible chondrichthyan scales.

Silurian gnathostomes have been reviewed by Qu et al. (2010). Previously, the oldest record of placoderms was thought to be two antiarchs (including one named taxon *Shimenolepis*) from Hunan province, China, initially dated as Wenlock. This occurrence has now been revised to Upper Ludlow (Zhao et al. 2016). The placoderm '*Wangolepis*', which remains a *nomen nudum*, is from the Wenlock of Hunan (Pan 1986; Qu et al. 2010). In addition, Tông-Dzuy et al. (1997) report *Myducosteus*, a placoderm of unknown affinity from the Ludlow and Pridoli of Vietnam. *Silurolepis* from the Ludlow Kuantu Formation was initially described as a partially articulated antiarch trunk armour (Zhang et al. 2010), but ongoing investigations suggest that its identification as an antiarch is probably erroneous (pers. comm. Brian Choo).

Silurian acanthodians are mainly known from scales, isolated spines and dentigerous jaws (Hanke et al. 2001). A partially articulated specimen of the putative acanthodian *Yealepis* is known from the Silurian of Australia (Burrow and Young 1999), but this taxon lacks fin spines, the traditional characteristic feature of acanthodians. *Nerepisacanthus denisoni*, a partially articulated acanthodian from New Brunswick, Canada, has been assigned to a family of ischnacanthiform acanthodians (Burrow 2011; Burrow and Rudkin 2014). *Yealepis* does not preserve a head, making more detailed studies impossible.

Putative Silurian chondrichthyans are known only from scales. Mongolepids were first described from the Llandovery of Mongolia (Karatujute-Talimaa et al. 1990), but are also known from Siberia and China (Qu et al. 2010). Recently the mongolepid *Solinalepis* has been described from the Ordovician of North America (Andreev et al. 2016). If mongolepids are indeed chondrichthyans (as supported by Andreev et al. 2016), they occur in the fossil record 50 million years before the first chondrichthyan teeth in the Early Devonian. Other putative chondrichthyan scales from the Silurian are the elegestolepids (Karatujute-Talimaa and Predtechenskyj 1995) and *Pilolepis* from arctic Canada (Thorsteinsson 1973).

Silurian osteichthyans were until relatively recently only known from fragmentary material for example the osteichthyans *Andreolepis* and *Lophosteus* from the Baltic region (Gross 1968; Gross 1969). Jaw specimens of *Lophosteus* and *Andreolepis* show features that indicate a probable stem osteichthyan position (Botella et al. 2007). Material from the late Silurian of Qujing, China, was suggested to belong to a sarcopterygian (Zhu and Schultze 1997). This material, consisting of two isolated jaws, a skull roof bone and a fin spine was informally assigned to *Psarolepis*, an early Devonian taxon also from Qujing (Yu 1998). There are also osteichthyan scale taxa *Naxilepis gracilis* and *Ligulalepis yunnanensis* from the Silurian of China (Zhao et al. 2016).

Recently, articulated gnathostome remains have been discovered in the Kuantu Formation (Ludlow of Yunnan). The key taxa are *Entelognathus* (Zhu et al. 2013) and *Qilinyu* (Zhu et al. 2016), placoderms

with osteichthyan-like jawbones, and *Guiyu* (Zhu et al. 2009), the oldest articulated osteichthyan. These discoveries have revolutionised our understanding of early vertebrate evolution, and are introduced in more depth in the section on recent advances in early vertebrate phylogenetics (below). The new taxa have blurred the boundaries between the major gnathostome groups, and call into question the identity of Silurian and Ordovician vertebrates known from isolated material, particularly ‘acanthodian’ fin spines.

The Devonian fossil record of gnathostomes

The study of Devonian gnathostomes relies heavily on a relatively small number of fossil sites (Brazeau and Friedman 2015), which will be briefly reviewed here. These sites have produced the majority of taxa used in phylogenetic discussion of early vertebrates, including chapter 3 of this thesis. Each site has particular taphonomic features that make its specimens particularly useful for study. The sites can be approximately divided into those that preserve complete articulated fishes, and those that preserve delicate braincase material in exceptional three-dimensional detail.

The Lochkovian MOTH (Man On The Hill) site in Canada, and the Turin Hill site in Scotland are unusual in being completely (Turin Hill) or almost completely (MOTH) dominated by acanthodians (Brazeau and Friedman 2015). These sites preserve complete articulated acanthodians (Watson 1937; Gagnier et al. 1999; Hanke and Wilson 2006; Hanke 2008) and provide the majority of acanthodians in phylogenetic analyses of early gnathostomes (Brazeau 2009). The acid-prepared fossils of the MOTH locality in particular allow the comparison of scale and body form characters in the same specimens (Hanke and Wilson 2010), which will be discussed in more detail below. Increasingly, acid preparation is now being applied to fossils from Turin Hill, revealing new information (Burrow et al. 2013).

The Xishancun and Xitun formations are from the Lochkovian of South China, the Xitun Formation overlying the Xishancun. Osteichthyan taxa from these formations dominate discussions of early

sarcopterygian evolution (Chang 1982; Yu 1998; Zhu et al. 1999; Zhu and Yu 2002), and include early branches of the coelacanth and lungfish groups (Chang 1995; Friedman 2007). There are also abundant antiarchs, which have been central to discussions of this group of placoderms (Zhang 1980; Zhu 1996; Zhu et al. 2012b).

The Late Lochkovian Wood Bay Formation of Spitzbergen has abundant arthrodire specimens (Goujet 1984a) as well as the sarcopterygians *Porolepis* (Jarvik 1972) and *Powichthys* (Clément and Janvier 2004). It is also an extremely important formation for fossils of the jawless osteostracans, which have been the subject of detailed studies of neurocranial anatomy (Janvier 1985). These specimens are the source of many of the outgroup comparisons used to reconstruct gnathostome phylogeny (Brazeau 2009).

The late Pragian or early Emsian Hunsrück Slate preserves articulated specimens, and is a rare source of information for two of the less common groups of placoderms: the rhenanids and the petalichthyids (Gross 1961; Gross 1963). Recently it has also produced information on one of the only known placoderm pharyngeal skeletons (Brazeau et al. 2017).

The Emsian Taemas-Wee Jasper Formation is the oldest known fish fauna from a tropical reef (Young 2011). Although specimens are mostly disarticulated (but see Young et al. (2001)), exceptional detail of the neurocranium is visible in the acid-prepared specimens. Studies on the arthrodire placoderm *Parabuchanosteus* and the 'acanthothoracid' placoderm *Brindabellaspis* are the source of classic studies on placoderm neurocranial characters (Young 1979; Young 1980). New information on *Brindabellaspis* and the osteichthyan '*Ligulalepis*' (Basden et al. 2000; Basden and Young 2001) from Taemas-Wee Jasper are the subjects of chapters 4 and 5 and material from Taemas-Wee Jasper is central to the studies of sensory systems in chapter 2.

The Orcadian Basin of Northern Scotland and Orkney contains a series of Middle Devonian ephemeral lake deposits (Hamilton and Trewin 1988). The fossil fishes are thought to be preserved

in mass mortality events following the deoxygenation of lake waters (Trewin 1985). There are several localities, of which three deserve a special mention: Achanarras quarry in Caithness and its equivalent in Orkney (the Sandwich fish bed) preserve a high diversity of complete articulated specimens (Trewin 1985), and Tynet burn in Moray is a good source of 3-dimensional neurocranial detail (Thomson 1965; Giles et al. 2015a). The Orcadian basin has produced many placoderms, sarcopterygians, an actinopterygian and acanthodians.

Mount Howitt, from the Givetian of Victoria of Australia, preserves many complete specimens. These are preserved as impressions, and studied from latex peels, so little neurocranial detail is available. Important specimens of placoderms, acanthodians, sarcopterygians and actinopterygians are known from Mt Howitt, which is especially important in preserving the tail fin of these fishes (e.g. Long 1984; Long 1988; Long 1999).

The early Frasnian Gogo Formation from the Kimberley region of Western Australia is a reef formation, where the fossil fish are preserved in nodule fields between the reef outcrops (Long and Trinajstić 2010). The specimens are preserved as complete fish and are undistorted: following acid preparation the individual bones can be reassembled into complete skeletons. About 50 species of fishes are known from Gogo; lungfish and arthrodiras are particularly diverse (Long and Trinajstić 2010). Early actinopterygians are typically more delicate than sarcopterygians and are poorly known from other sites, so the fine preservation of the actinopt *Mimipiscis* and *Moythomasia* at Gogo has led to these taxa being central to discussions of early actinopt evolution (Gardiner 1984). The undistorted nature of the Gogo fossils allows unambiguous reconstruction of anatomy, such as showing definitively the presence of a choana (internal nostril) in 'osteolepiform' fishes (Long et al. 1997). Gogo is a bona fide *Lagerstätten*", preserving embryos, stomach contents and soft tissue (Nicoll 1977; Trinajstić et al. 2007; Long et al. 2008; Trinajstić et al. 2013). Unfortunately, placoderms from this fauna almost completely lack braincase ossification. Specimens from the Gogo Formation are used extensively in the investigations of early vertebrate sensory systems in chapter 2.

The Frasnian Escuminac Formation of Miguasha, Canada, is thought to be an estuarine deposit, although a number of possible environmental interpretations have been considered (Prichonnet et al. 1996). The quality of preservation is perhaps second only to Gogo among Devonian fish fossil sites, and there is a diverse fauna of placoderms, acanthodians, sarcopterygians and actinopterygians (Schultze 1996). The tetrapodomorph sarcopterygian *Eusthenopteron* was the subject of detailed serial grinding studies (Jarvik 1980), and as such forms something of a “standard model” with which other Devonian vertebrates are compared. The Escuminac Formation also preserves the last known representative of the jawless osteostracans, and the only one to preserve the internal structure of the pectoral fins (Janvier et al. 2004). The late Frasnian Kellwasserkalk has produced abundant placoderm fossils (Stensiö 1963a; Maisch 1998), notable for the excellent preservation of 3-dimensional braincase details (Stensiö 1963b). The particular importance of this site is the preservation of braincase material of otherwise rare groups: *Cladodoides* for chondrichthyans (Maisey 2005), *Jagorina* for rhenanid placoderms (Stensiö 1969) and *Diplocercides* for coelacanth (Stensiö 1937).

The Famennian Cleveland shale from Ohio, USA, is a deep marine deposit preserving fossil fishes, often in concretions (Carr and Jackson 2010). It contains many placoderms, but is particularly important for the early chondrichthyans *Cladoselache* and *Tamiobatis* (Harris 1938; Williams 1998; Maisey 2007), and the actinopterygian *Tegeolepis* (Dunkle and Schaeffer 1973) which may be the sister group to most other actinopterygians (Giles et al. 2015b).

The use of fossils and stratigraphy in phylogenetic inference

Phylogenetic systematics, or cladistics (Hennig 1966), introduced the possibility of reconstructing phylogeny and historical processes without reference to the fossil record. The key advance of cladistics is the use of only derived characters to specify evolutionary relationships; plesiomorphic characters (inherited from a common ancestor of all taxa under consideration) are not taken as

evidence of phylogenetic relationship. As such, the process of evolution, with historical sequences of character change, is implicit in cladistic studies, and Hennig (1966) went to great lengths to justify the assumption of evolution. An early and influential example of cladistics in practice was the a phylogeny of chironomid midges, which showed concordance between phylogenetic relationships and plate tectonic movements (Brundin 1966).

The use of fossils in inferring the relationships of modern taxa has subsequently been downplayed (Nelson 1969; Patterson 1981). Palaeoichthyologists were particularly active in this debate. Rosen et al. (1981) criticised the “search for ancestors” typical of palaeontological studies. Many examples of this occur in the literature for early vertebrates, including hypotheses regarding the evolution of hagfishes from heterostracans and lampreys from osteostracans (Stensiö 1927), salamanders from porolepiformes and other tetrapods from osteolepiformes (Jarvik 1942), and various groups of sharks independently from within placoderms or acanthodians (Ørvig 1962; Stensiö 1963a; Stensiö 1969; Jarvik 1977). Patterson (1981) instead relegated the use of fossils to being placed within the framework provided by living species: they could inform divergence dates and sequences of character evolution, but not change the inferred relationships of living taxa. Although examples were put forward where fossils do make a difference (Gauthier et al. 1988; Kemp 1988), the advent of large-scale molecular data means that this is increasingly unlikely to happen. Indeed, Patterson’s ideas largely resemble the current approach to studying fossils, fossils are assigned to the stem and crown groups of living clades. Crown groups include all descendants (living and fossil) of the common ancestor of a set of living species, whereas stem groups are the paraphyletic assemblage of extinct forms that are more closely related to a particular crown group than to anything else.

The use of stratigraphic or age data in the reconstruction of phylogeny has been controversial and is not general accepted. Schaeffer et al. (1972) rebutted the idea of inferring character polarity from temporal data, but this is by no means the only way of using stratigraphic data. Stratophenetics (Gingerich 1979) involves linking taxa within and between horizons to trace phylogeny, and requires

a fossil record so dense and continuous that phylogeny can be essentially observed directly. It is not therefore useful outside relatively localised parts of the fossil record (Patterson 1981).

Stratocladistics (Fisher 2008), in contrast to stratophenetics, builds upon the foundations of cladistics. Under this methodology, morphological debt (the number of steps as in a typical parsimony analysis) is supplemented with 'stratigraphic parsimony debt'. If a lineage in a tree crosses a time interval without preserving a fossil, but other coeval lineages are preserved, this stratigraphic debt confers an additional parsimony step. Morphological and stratigraphic debt is then summed. Similar to the way convergent evolution in morphological characters are considered *ad hoc* hypotheses in a parsimony analysis (Farris 1983), unpreserved lineages (when other lineages are preserved) are considered *ad hoc* hypotheses in stratocladistics, requiring assumptions of heterogeneous preservation rates (Fisher 2008). Fossils can be placed in ancestral positions during the tree search. Trees obtained from a stratocladistic analysis might not be the same as the most parsimonious trees obtained from a purely morphological analysis, if the most parsimonious purely morphological trees are inconsistent with the stratigraphic record.

A criticism of the use of stratigraphic data in phylogenetic analysis comes from 'transformed cladistics' (Platnick 1979). In transformed cladistics, trees are considered distinct from cladograms. Cladograms are nested hierarchies or schemes of synapomorphies where all taxa are in terminal positions. Trees on the other hand have an explicitly temporal component and taxa can be placed in ancestral positions; several trees are compatible with a single cladogram. According to transformed cladistics, cladograms must be reconstructed before the consideration of trees. Although transformed cladistics was not widely adopted (in particular the idea that plesiomorphic and derived states of a character can be identified without the assumption of an underlying process of evolution has not been popular) the distinction of cladograms and trees has been influential. In stratocladistics however, analyses are performed directly at the tree level: cladograms are optional simplifications (Fisher 2008).

A number of arguments against stratocladistics have been raised (Heyning and Thacker 1999; Geiger et al. 2001), but have been met with counterarguments (Alroy 2002; Fisher 2008). The most cogent criticisms concern not the philosophy but the practice: attempts to use stratocladistic methodology failed to find the shortest trees (Fox et al. 1999; Heyning and Thacker 1999). Indeed, only relatively recently has a computer program been written to perform stratocladistic analyses (Marcot and Fox 2008), and this has not been updated from its initial experimental form. This, and the guilt-by-association with stratophenetics, may explain why stratocladistics has not been widely adopted.

Recently, tip-dated Bayesian methods (Ronquist et al. 2012; Gavryushkina et al. 2014; Lee et al. 2014b; Gavryushkina et al. 2017) have provided a new and more sophisticated way of integrating stratigraphic and morphological data. As with stratocladistics, tip dating methods do not distinguish between cladograms and trees, and the probability of each taxon falling into an ancestral position can now be estimated during the analysis (Gavryushkina et al. 2014). In Chapter 6 I show that the use of tip-dated methods can influence the inferred evolutionary relationships as a result of the incorporation of stratigraphic data, as in stratocladistics.

Recent advances in early gnathostome phylogenetics

Discoveries in the last 20 years have led to advances in our knowledge of early vertebrates and their characters, and have increasingly blurred the boundaries between placoderms, acanthodians, chondrichthyans and osteichthyans. These advances are reviewed in Brazeau and Friedman (2015).

Pucapampella, from the Middle Devonian of Bolivia is the earliest chondrichthyan braincase known in detail (Maisey 2001). A key finding was that it possessed a ventral cranial fissure, a feature previously known from osteichthyans and the acanthodian *Acanthodes*. This suggests that a ventral cranial fissure is a crown gnathostome synapomorphy (lost in other chondrichthyans), and weakens support for an acanthodian-osteichthyan relationship, which was suggested partly on the basis of this feature (Miles 1973b). *Doliodus*, an even earlier articulated shark from the Early Devonian of

Canada, was found to have paired pectoral fin spines, a feature previously unknown in chondrichthyans (Miller et al. 2003). However, the braincase of *Doliodus*, which is not as well preserved as *Pucapampella*, lacks a cranial fissure (Maisey et al. 2009).

Acanthodians from the MOTH locality also weaken support for acanthodian monophyly. Scale taxa that were originally attributed to chondrichthyans (due to the presence of marginal accretion of odontodes) were found in articulated acanthodian-like body fossils with a full complement of fin spines (Hanke and Wilson 2010).

Neurocranial anatomy of acanthodians is only known in detail from *Acanthodes bronni*, which is preserved in nodules in the Lebach ironstone (Early Permian, Germany). It is among the latest occurring acanthodians, and has anatomical specialisations suggesting a suspension-feeding lifestyle (Watson 1937). Because of this, it is often suspected not to be representative of the earlier acanthodians, but still serves as the main focus for discussions of acanthodian phylogeny due to the lack of alternatives. The study of Miles (1973b) made the argument of an acanthodian-osteichthyan relationship based on *Acanthodes* and this was generally accepted for several decades. More recent description of the braincase of *Acanthodes* have shown more similarities with chondrichthyans (Davis et al. 2012), including the position of the hyoid arch attachment (Brazeau and de Winter 2015).

Partial neurocranial remains were known from the Early Devonian acanthodian *Ptomacanthus* (Miles 1973a), but were initially undescribed. The *Ptomacanthus* neurocranium was finally described in detail by Brazeau (2009), revealing an anatomy quite different from *Acanthodes*, with a short wide basisphenoid more similar to placoderms than osteichthyans or chondrichthyans. This study also included the first cladistic test of acanthodian monophyly, and the results instead suggested that acanthodians were a paraphyletic assemblage of stem osteichthyans, stem chondrichthyans and stem gnathostomes.

Placoderms have been regarded as a monophyletic group since the work of Goujet and others (Goujet 1982; Goujet 1984b; Goujet 2001). This hypothesis was challenged by Johanson (2002), who argued that the fin vasculature penetrated the postbranchial lamina in osteostracans and antiarch placoderms, suggesting placoderms are paraphyletic with the antiarchs occupying a basal position. However, this interpretation of the fin vasculature of antiarchs was later rejected (Young 2008). The cladistic analysis of Friedman (2007), although focussing on osteichthyans, hinted at the possibility of placoderm paraphyly. Brazeau (2009) tested the relationships of placoderms more thoroughly, and the results once again indicated that placoderms were paraphyletic, with antiarchs basal. Both these analyses included Johanson's (2002) character concerning the pectoral fin vasculature, but deletion of this character in an updated matrix (Davis et al. 2012) resulted in a largely similar view of placoderm relationships (i.e. paraphyly with a basal position for antiarchs). Other characters introduced by Brazeau (2009) produced placoderm paraphyly, and were retained in subsequent analyses (Davis et al. 2012; Zhu et al. 2013; Dupret et al. 2014; Giles et al. 2015c; Long et al. 2015). These characters are discussed in detail in chapter 3.

The debate regarding placoderms as a monophyletic or paraphyletic group has continued. Young (2010) provided a list of characters shared by placoderms. However these characters are almost all disputed, lacking polarity from outgroup comparisons, amongst other problems (Brazeau and Friedman 2014). New discoveries of claspers (reproductive organs for internal fertilisation) in placoderms have particular significance to the debate about placoderm relationships. Claspers were well-known from ptyctodontids (Miles and Young 1977), and have subsequently been discovered in arthrodires (Ahlberg et al. 2009) and antiarchs (Long et al. 2015). Embryos in ptyctodontids and arthrodires (Long et al. 2008; Long et al. 2009) show that at least some placoderms were viviparous in addition to having internal fertilisation. The claspers of placoderms appear to be homologous (Long et al. 2015), and as such present a challenge to placoderm paraphyly as it necessitates reversal from internal fertilisation to external fertilisation at the gnathostome crown node (Brazeau and

Friedman 2015; Long et al. 2015). There is little or no evidence for such reversal occurring amongst living taxa, despite multiple origins of internal fertilisation (Blackburn 2015).

Discoveries of early osteichthyans in the last 20 years have shown a number of features previously only known from other groups of gnathostomes. *Psarolepis*, from the Silurian and Early Devonian of China (Zhu and Schultze 1997; Yu 1998; Zhu et al. 1999), displays a mix of sarcopterygian characters (e.g. jointed braincase, cosmine covered dermal bones), actinopterygian characters (e.g. shape of the maxilla) and characters previously known only from acanthodians and placoderms, most notably fin spines. Although *Psarolepis* was initially tentatively reconstructed from disarticulated remains, a similar mix of characters was later confirmed in the Silurian osteichthyan *Guiyu* (Zhu et al. 2009), which possessed a placoderm-like median dorsal plate and dermal pelvic girdle in addition to dorsal and pectoral fin spines (Zhu et al. 2009; Zhu et al. 2012a).

An isolated skull and braincase of '*Ligulalepis*' from the Taemas-Wee Jasper limestones of Australia showed the first evidence for an eyestalk (a cartilaginous attachment for the eyeball) in an osteichthyan (Basden et al. 2000; Basden and Young 2001), a feature better known from placoderms and chondrichthyans. It is recognised in placoderms (and subsequently '*Ligulalepis*') as a large irregular foramen with an outwardly turned lip of perichondral bone. '*Ligulalepis*' has been considered either as a stem osteichthyan or stem actinopterygian (and once as a stem sarcopterygian) in various analyses, and solving this debate will be vital for reconstructing the ancestral character complement of osteichthyans. A thorough redescription of the anatomy of '*Ligulalepis*', including a new specimen, is the subject of chapter 5.

The discovery of *Entelognathus* from the Silurian Kuantu Formation of China led to a major reassessment of character evolution in gnathostomes (Zhu et al. 2013). Much of the morphology of *Entelognathus* is typical for placoderms, particularly arthrodires, but its jawbones are far more similar to osteichthyans. *Entelognathus* has usually been resolved as a stem gnathostome (Zhu et al. 2013; Dupret et al. 2014), although once has been placed on the osteichthyan stem (Long et al.

2015). The inclusion of *Entelognathus* in phylogenetic analyses of early gnathostomes invariably shifts the acanthodians entirely onto the chondrichthyan stem (Zhu et al. 2013; Long et al. 2015). This has the implication that the macromeric dermal bones of osteichthyans and placoderms are homologous and the macromeric condition is ancestral for crown gnathostomes.

The idea that the ancestral crown gnathostome had a macromeric dermal skeleton was further corroborated by the study of the *Janusiscus* from the Early Devonian of Siberia (Giles et al. 2015c). Previously assigned to the putative actinopt genus *Dialipina* (Schultze 1992), *Janusiscus* showed features of the braincase that suggested it was in fact a stem gnathostome, notably absence of a ventral cranial fissure. The discovery of *Janusiscus* also led to attempts to homologise the various neurocranial processes of gnathostome groups (Giles et al. 2015c).

Character polarity and outgroups for early gnathostomes

Phylogenetics typically requires the use of an outgroup, a taxon or taxa “known” to lie outside the clade of interest, the ingroup. The outgroup provides polarity to the characters, distinguishing plesiomorphic from derived character states. Selection of a suitable outgroup is something of a balance: the outgroup must be sufficiently different from the ingroup that it can be confidently assumed to lie outside the ingroup clade. However, if the outgroup is too different morphologically, it may be misleading, or there may be difficulties in finding homologous characters shared by both the ingroup and the outgroup. One common approach is to base the ingroup on a particularly important character, for example jaws. The acquisition of jaws is thought to have led to such a great rearrangement of the morphology of the head that it is assumed to be irreversible. Thus any jawless vertebrate can (theoretically) be used as an outgroup, but this does not necessarily mean that it will be useful for polarising characters.

Character polarity and outgroups are a significant problem in studies of early gnathostomes due to the difficulty in finding homologous characters across both jawless and jawed vertebrates. The living

jawless vertebrates, the hagfishes and lampreys, are too highly specialised to be useful as outgroups. From the groups of fossil jawless fishes, only the galeaspids and osteostracans preserve details of the neurocranium. Osteostracans are considered to be the closest sister group to gnathostomes and share a number of derived characteristics with them, including an epicercal tail, ossified sclerotic rings, perichondral and cellular bone (Janvier 1981). Galeaspids are also thought to possess perichondral bone (Zhu and Janvier 1998), and are usually regarded as the next outgroup to gnathostomes after osteostracans (Sansom et al. 2010). A third group, the pituriaspids (Young 1991), are thought to have a calcified endoskeleton (possibly of perichondral bone), and are usually thought to lie close to galeaspids and osteostracans in vertebrate phylogeny. Pituriaspids are known only from a handful of specimens from a single site, preserved as natural moulds, and are not known in enough detail to factor in discussions of gnathostome character polarity. As a result galeaspids and osteostracans are used as the only outgroups in cladistic analyses of early gnathostomes (Brazeau 2009).

Although detailed braincase anatomy for both galeaspids and osteostracans is known (Janvier 1985; Gai et al. 2011), these taxa are still of limited use for polarising gnathostome characters. The dermal exoskeleton of galeaspids and osteostracans consist of an interlocking network of tesserae, so the dermal plate characters of placoderms and osteichthyans cannot be polarised. Characters concerning the nature of the jaws and their attachments are a rich source of gnathostome characters, but by definition cannot be polarised by jawless outgroups. There are also puzzling character incongruences between galeaspids and osteostracans, most notably in the layout of the nasal sacs and hypophyseal duct (Gai et al. 2011). Galeaspids have paired nasal sacs and a separate hypophyseal duct, resembling the gnathostome condition, whereas osteostracans have a single median nasohypophyseal duct, resembling the condition in cyclostomes. The cyclostome-like condition of osteostracans is now thought to have evolved in parallel (Janvier 1981; Gai et al. 2011).

Partly in an attempt to gain traction on the polarity issue in early vertebrate phylogeny, chapter 3 applies tip-dated Bayesian methods of phylogenetic analysis, which will be outlined in the following section.

Bayesian tip-dated phylogenetics

Model-based methods of phylogenetic analysis for morphology originate from Lewis (2001), who described a simple model of discrete character change that remains the only model of morphological character change widely used. Although models for continuous traits were available since the infancy of statistical phylogenetics (Felsenstein 1973), morphological datasets typically consist of discrete characters. Availability of a model for morphological evolution allows phylogenetic analysis to be performed in a maximum likelihood or Bayesian inference framework. Bayesian inference has a number of advantages over maximum likelihood methods including the ability to isolate parameters of interest whilst accounting for uncertainty in other model parameters (for example tree topology), estimation of meaningful support values during the initial estimation of phylogeny, and the estimation of divergence times using fossil calibrations (Huelsenbeck et al. 2001). Bayesian inference is also intuitive in the sense of combining prior knowledge (for example the age of fossils) and information from new data to provide a posterior distribution of trees.

The use of tip-dating in palaeontology grew out of the so-called total-evidence approach (Pyron 2011; Ronquist et al. 2012). The name tip-dating refers to the direct inclusion of fossils and their ages as “tips” in a phylogenetic analysis, rather than applying temporal information from fossils to calibrate the ages of internal nodes (node-dating). In the total-evidence tip-dating approach molecular and morphological data for living taxa are combined with morphological data for fossils. This has the significant advantage of allowing direct estimation of the phylogenetic position of the fossils from the data, and it does not require the fossils to have an assumed fixed position. Use of total evidence dating relies on the assumption of a morphological clock in addition to a molecular

clock (Ronquist et al. 2012). Tip-dating approaches were subsequently applied to purely palaeontological datasets (Lee et al. 2014a; Lee et al. 2014b): effectively total evidence dating without the molecular data.

Since these early studies, improvements to tip dating methods have accumulated rapidly. Most notably, serial sampled tree priors model the speciation, extinction and sampling process through time (Stadler 2010; Heath et al. 2014). These tree priors are more appropriate and give more sensible results than the uniform tree priors used in previous studies, which produced unrealistically ancient divergence dates (Matzke and Wright 2016). There are also new models that estimate the probability of fossils being sampled ancestors (Gavryushkina et al. 2014).

Tip-dating methods are often used for inferring macroevolutionary patterns of evolutionary rates (Lee et al. 2014a; Close et al. 2015) or for inferring divergence times (Beck and Lee 2014; Gavryushkina et al. 2017). Topological differences between tip-dating and other methods have received some attention (Bapst et al. 2016), but have not been explored in detail. Chapters 3 and 6 explore the effect of tip-dating on tree topology, showing that it can be significant.

Tip-dating also has the potential to contribute to the outgroup problem in early gnathostome phylogeny. The root position of a phylogenetic tree can be estimated using the molecular clock instead of an outgroup (Huelsenbeck et al. 2002). It is now common practice not to use an outgroup in molecular clock Bayesian analyses. The morphological clock could potentially be used in a similar way, and this forms a major component of Chapter 3. It is not necessary to remove the outgroup entirely, and Chapter 3 still employs outgroups. The morphological clock is used in conjunction with the outgroup in the hope that the two imperfect forms of evidence can together find the root position of the gnathostome phylogenetic tree.

Vertebrate lateral line and electroreceptor sensory systems

The lateral line system (for detecting mechanical stimuli) and electrosensory system (for detecting electric fields) are thought to be ancestral vertebrate features (Bullock et al. 1983; Northcutt 1989; Baker et al. 2013). These systems are potentially a rich source of character data for early gnathostome phylogeny, but have received less attention than other parts of anatomy. The presence of electroreception in early gnathostomes is generally unknown: chapter 2 is the first broad-scale study of electroreception across early vertebrates. For lateral line systems, chapter 4 describes a novel adaptation of the ethmoid commissure line of the placoderm *Brindabellaspis*, unknown in any other vertebrate, chapter 5 includes a description of sensory line structure in '*Ligulalepis*' and chapter 3 includes a reassessment and expansion of the lateral line system characters used in early vertebrate phylogenetics.

The lateral line and electroreception sensory systems form, together with the inner ear, the octavolateralis system, united by development from cranial placodes and similar sensory cell morphology (Jørgensen 1989). Further similarities were found recently when it was shown that membrane voltage oscillations mediated by calcium and potassium ion channels form the molecular basis of electroreception in skates (Bellono et al. 2017). A similar mechanism is found in mechanosensory hair cells, and is responsible for frequency-tuning in the inner ear (Fettiplace and Fuchs 1999).

The octavolateralis system is innervated by a series of placode-derived nerves (the lateral line and auditory nerves), which are considered a distinct series of cranial nerves due to their different developmental origins from other cranial nerves (Northcutt 1989). Traditionally, the lateral line nerves have been considered a specialised component of the dorsal cranial nerves (trigeminal, facial, glossopharyngeal, vagal), and the lateral line nerves are indeed closely associated with the dorsal cranial nerves peripherally. The consideration of lateral line nerves as part of the dorsal cranial nerves is closely associated with old ideas about segmentation of the vertebrate head (Northcutt

1989), which are no longer widely accepted (Northcutt 2008). The idea that lateral line nerves form a separate series of cranial nerves is more compatible with their development from cranial placodes (rather than neural crest as for the dorsal cranial nerves) and does not require an unparsimonious series of losses of cranial nerve components to fit the segmentation hypothesis (Northcutt 1989). However, consideration of the lateral line nerves as branches of the trigeminal and facial nerves still universally pervades the literature on early vertebrate fossils, and this convention is followed in this thesis except in chapter 2, which uses the terminology more common in the electroreception literature.

The functional organ of the lateral line system is the neuromast (Coombs et al. 1988; Webb 2013). The sensory epithelium of a neuromast consists of hair cells with supporting and mantle cells. Overlying this epithelium is a gelatinous cap (the cupula) into which ciliary bundles project. These bundles are arranged in lines from shortest to tallest along an axis that defines the polarity of sensitivity of the neuromast. Neuromasts either sit in canals, or lie externally as superficial neuromasts which can be arranged into pit lines (Coombs et al. 1988). Canals enclosed in bone are connected to the surface through tubules. Vibrations are transmitted from the external water via the canal fluid to the cupula and finally the hair cells (van Netten and Kroese 1988).

The lateral line canals of the head have a conservative arrangement: in teleosts sensory canals are associated with particular dermal bones (Webb 1989). Sensory canals display a wide variety of morphologies, including narrow and wide morphologies, and tubules that can be simple or highly branched (Webb 2013).

Canal neuromasts begin development as superficial neuromasts during development, and sink into the dermis and become enclosed in canals later (Webb 2013). Reduction of cranial lateral line canals to form grooves or lines of superficial neuromasts has been considered a form of paedomorphosis (Webb 1989). Within teleosts groups, there is often a trend towards parallel reduction of canals to form replacement pit lines (Nelson 1972). In early vertebrates, terminology for each lateral line canal

and groove follows the terminology for the presumed homologue in living taxa, regardless if these are canals, grooves or pit lines. For example the anterior, middle and posterior pit-lines are preserved as shallow grooves in most placoderms and early osteichthyans. An extreme example is the posterior “pit line” of ptyctodontid placoderms, which is fully enclosed in a bony canal.

Vertebrate electrosensory systems have a number of similarities with the lateral line system.

Electroreceptors develop from the periphery of lateral line placodes (Northcutt et al. 1995; Modrell et al. 2011; Gillis et al. 2012). The sensory epithelium is highly similar to that of lateral line mechanoreceptors: sensory cells are interspersed with supporting cells and the membrane is covered in a gelatinous substance (Jørgensen 1989). The sensory cells have an apical cilium (Jørgensen 2005). The base of the receptor epithelium connects to afferent nerve fibres via ribbon synapses (Bodznick and Montgomery 2005).

The typical morphology of a vertebrate electrosensory organ is a canal filled with a high-conductance jelly, with a widened chamber (the ampulla) at the base (Jørgensen 2005). The morphology of ampullary electroreceptors is similar to some mechanosensory pit organs, and electroreceptors may have evolved from superficial neuromasts (Coombs et al. 1988). Based on morphological resemblance, pit-lines of the lungfish *Neoceratodus* have actually been suggested to carry electroreceptors (Kemp 2017), although this has not been confirmed experimentally.

Electroreceptors of the ancestral vertebrate likely detected direct current (DC) and low frequency alternating current (AC) electric fields (Bodznick and Montgomery 2005). The biologically relevant natural stimuli detected by electroreceptors are dipole fields produced by other organisms and larger scale fields produced when the animal or ocean currents pass through the Earth’s magnetic field (Kalmijn 1974). Natural electric fields surrounding prey items are produced by ion leakage across mucous membranes, and as a result stronger fields are generated by osmoregulators such as teleosts compared with osmoconformers such as chondrichthyans (Bedore and Kajiura 2013).

Electroreceptor morphology is introduced in far greater depth in chapter 2, followed by new information from CT scans investigating putative electroreceptors in early vertebrate fossils.

References

- Ahlberg, P. E., Trinajstić, K., Johanson, Z. and Long, J. A. (2009). Pelvic claspers confirm chondrichthyan-like internal fertilization in arthrodires. *Nature* **460**, 888.
- Alroy, J. (2002). Stratigraphy in phylogeny reconstruction—reply to Smith (2000). *Journal of Paleontology* **76**, 587–589.
- Andreev, P., Coates, M. I., Karatajūtė-Talimaa, V., Shelton, R. M., Cooper, P. R., Wang, N.-Z. and Sansom, I. J. (2016). The systematics of the Mongolepidida (Chondrichthyes) and the Ordovician origins of the clade. *PeerJ* **4**, e1850.
- Baker, C. V. H., Modrell, M. S. and Gillis, J. A. (2013). The evolution and development of vertebrate lateral line electroreceptors. *Journal of Experimental Biology* **216**, 2515–2522.
- Bapst, D. W., Wright, A. M., Matzke, N. J. and Lloyd, G. T. (2016). Topology, divergence dates, and macroevolutionary inferences vary between different tip-dating approaches applied to fossil theropods (Dinosauria). *Biology Letters* **12**, 20160237.
- Baden, A. M. and Young, G. C. (2001). A primitive actinopterygian neurocranium from the Early Devonian of southeastern Australia. *Journal of Vertebrate Paleontology* **21**, 754–766.
- Baden, A. M., Young, G. C., Coates, M. I. and Ritchie, A. (2000). The most primitive osteichthyan braincase? *Nature* **403**, 185–188.
- Beck, R. M. D. and Lee, M. S. Y. (2014). Ancient dates or accelerated rates? Morphological clocks and the antiquity of placental mammals. *Proceedings of the Royal Society B* **281**, 20141278.
- Bedore, C. N. and Kajiura, S. M. (2013). Bioelectric fields of marine organisms: voltage and frequency contributions to detectability by electroreceptive predators. *Physiological and Biochemical Zoology* **86**, 298–311.

- Bellono, N. W., Leitch, D. B. and Julius, D. (2017). Molecular basis of ancestral vertebrate electroreception. *Nature* **543**, 391–396.
- Blackburn, D. G. (2015). Evolution of vertebrate viviparity and specializations for fetal nutrition: a quantitative and qualitative analysis. *Journal of Morphology* **276**, 961–990.
- Bodznick, D. and Montgomery, J. C. (2005). The physiology of low-frequency electrosensory systems. In *Electroreception* (ed. T. H. Bullock, C. D. Hopkins, A. N. Popper and R. R. Fay), pp. 132–153. Springer, New York.
- Botella, H., Blom, H., Dorka, M., Ahlberg, P. E. and Janvier, P. (2007). Jaws and teeth of the earliest bony fishes. *Nature* **448**, 583.
- Brazeau, M. D. (2009). The braincase and jaws of a Devonian ‘acanthodian’ and modern gnathostome origins. *Nature* **457**, 305–308.
- Brazeau, M. D. and de Winter, V. (2015). The hyoid arch and braincase anatomy of *Acanthodes* support chondrichthyan affinity of ‘acanthodians’. *Proceedings of the Royal Society B* **282**, 20152210.
- Brazeau, M. D. and Friedman, M. (2014). The characters of Palaeozoic jawed vertebrates. *Zoological Journal of the Linnean Society* **170**, 779–821.
- Brazeau, M. D. and Friedman, M. (2015). The origin and early phylogenetic history of jawed vertebrates. *Nature* **520**, 490–497.
- Brazeau, M. D., Friedman, M., Jerve, A. and Atwood, R. C. (2017). A three-dimensional placoderm (stem-group gnathostome) pharyngeal skeleton and its implications for primitive gnathostome pharyngeal architecture. *Journal of Morphology* **278**, 1120–1128.
- Brundin, L. (1966). *Transantarctic relationships and their significance, as evidenced by chironomid midges*. Almqvist & Wiksell, Stockholm.
- Bullock, T. H., Bodznick, D. A. and Northcutt, R. G. (1983). The phylogenetic distribution of electroreception: evidence for convergent evolution of a primitive vertebrate sense modality. *Brain Research Reviews* **6**, 25–46.

- Burrow, C. J. (2011). A partial articulated acanthodian from the Silurian of New Brunswick, Canada. *Canadian Journal of Earth Sciences* **48**, 1329–1341.
- Burrow, C. J., Newman, M. J., Davidson, R. G. and den Blaauwen, J. L. (2013). Redescription of *Parexus recurvus*, an Early Devonian acanthodian from the Midland Valley of Scotland. *Alcheringa: An Australasian Journal of Palaeontology* **37**, 392–414.
- Burrow, C. J. and Rudkin, D. (2014). Oldest near-complete acanthodian: the first vertebrate from the Silurian Bertie Formation Konservat-Lagerstätte, Ontario. *PLoS one* **9**, e104171.
- Burrow, C. J. and Young, G. C. (1999). An articulated teleostome fish from the Late Silurian (Ludlow) of Victoria, Australia. *Records of the Western Australian Museum Supplement* **57**, 1–14.
- Carr, R. K. and Jackson, G. L. (2010). The vertebrate fauna of the Cleveland Member (Famennian) of the Ohio Shale. In *Guide to the Geology and Paleontology of the Cleveland Member of the Ohio Shale. Ohio Geological Survey Guidebook 22* (ed. J. T. Hannibal).
- Chang, M.-M. (1982). *The braincase of Youngolepis, a Lower Devonian crossopterygian from Yunnan, south-western China*. Swedish Museum of Natural History, Stockholm.
- Chang, M.-M. (1995). *Diabolepis* and its bearing on the relationships between porolepiforms and dipnoans. *Bulletin du Muséum national d'histoire naturelle. Section C, Sciences de la terre, paléontologie, géologie, minéralogie* **17**, 235–268.
- Clément, G. and Janvier, P. (2004). *Powichthys spitsbergensis* sp. nov., a new member of the Dipnomorpha (Sarcopterygii, lobe-finned fishes) from the Lower Devonian of Spitsbergen, with remarks on basal dipnomorph anatomy. *Fossils and Strata* **50**, 92-112.
- Close, R. A., Friedman, M., Lloyd, G. T. and Benson, R. B. (2015). Evidence for a mid-Jurassic adaptive radiation in mammals. *Current Biology* **25**, 2137–2142.
- Coombs, S., Janssen, J. and Webb, J. F. (1988). Diversity of lateral line systems: evolutionary and functional considerations. In *Sensory biology of aquatic animals* (ed. Atema, R. R. Fay, A. N. Popper and W. N. Tavolga), pp. 553–593. Springer, New York.

- Davis, S. P., Finarelli, J. A. and Coates, M. I. (2012). *Acanthodes* and shark-like conditions in the last common ancestor of modern gnathostomes. *Nature* **486**, 247–250.
- Dunkle, D. H. and Schaeffer, B. (1973). *Tegeolepis clarki* (Newberry), a palaeonisciform from the Upper Devonian Ohio shale. *Palaeontographica Abteilung A* **143**, 151–158.
- Dupret, V., Sanchez, S., Goujet, D., Tafforeau, P. and Ahlberg, P. E. (2014). A primitive placoderm sheds light on the origin of the jawed vertebrate face. *Nature* **507**, 500–503.
- Farris, J. (1983). The logical basis of phylogenetic analysis. In *Advances in Cladistics, Vol. 2* (ed. P. N. I and V. A. Funk), pp. 7–36. Columbia University Press, New York.
- Felsenstein, J. (1973). Maximum-likelihood estimation of evolutionary trees from continuous characters. *American Journal of Human Genetics* **25**, 471–492.
- Fettiplace, R. and Fuchs, P. A. (1999). Mechanisms of hair cell tuning. *Annual Review of Physiology* **61**, 809–834.
- Fisher, D. C. (2008). Stratocladistics: integrating temporal data and character data in phylogenetic inference. *Annual Review of Ecology, Evolution, and Systematics* **39**, 365–385.
- Fox, D. L., Fisher, D. C. and Leighton, L. R. (1999). Reconstructing phylogeny with and without temporal data. *Science* **284**, 1816–1819.
- Friedman, M. (2007). *Styloichthys* as the oldest coelacanth: implications for early osteichthyan interrelationships. *Journal of Systematic Palaeontology* **5**, 289–343.
- Gagnier, P., Hanke, G. and Wilson, M. (1999). *Tetanopsyrus lindoei* gen. et sp. nov., an Early Devonian acanthodian from the Northwest Territories, Canada. *Acta Geologica Polonica* **49**, 81–96.
- Gai, Z., Donoghue, P. C., Zhu, M., Janvier, P. and Stampanoni, M. (2011). Fossil jawless fish from China foreshadows early jawed vertebrate anatomy. *Nature* **476**, 324–327.
- Gardiner, B. G. (1984). The relationships of the paleoniscid fishes. a review based on new specimens of *Mimia* and *Moythomasia* from the upper Devonian of Western Australia. *Bulletin of the British Museum (Natural History) Geology* **37**, 173–248.

- Gauthier, J., Kluge, A. G. and Rowe, T. (1988). Amniote phylogeny and the importance of fossils. *Cladistics* **4**, 105–209.
- Gavryushkina, A., Heath, T. A., Ksepka, D. T., Stadler, T., Welch, D. and Drummond, A. J. (2017). Bayesian total evidence dating reveals the recent crown radiation of penguins. *Systematic Biology* **66**, 57–73.
- Gavryushkina, A., Welch, D., Stadler, T. and Drummond, A. J. (2014). Bayesian inference of sampled ancestor trees for epidemiology and fossil calibration. *PLoS Computational Biology* **10**, e1003919.
- Geiger, D. L., Fitzhugh, K. and Thacker, C. E. (2001). Timeless characters: a response to Vermeij (1999). *Paleobiology* **27**, 177–178.
- Giles, S., Coates, M. I., Garwood, R. J., Brazeau, M. D., Atwood, R., Johanson, Z. and Friedman, M. (2015a). Endoskeletal structure in *Cheirolepis* (Osteichthyes, Actinopterygii), An early ray-finned fish. *Palaeontology* **58**, 849–870.
- Giles, S., Darras, L., Clément, G., Blicek, A. and Friedman, M. (2015b). An exceptionally preserved Late Devonian actinopterygian provides a new model for primitive cranial anatomy in ray-finned fishes. *Proceedings of the Royal Society B* **282**, 20151485.
- Giles, S., Friedman, M. and Brazeau, M. D. (2015c). Osteichthyan-like cranial conditions in an Early Devonian stem gnathostome. *Nature* **520**, 82–85.
- Gillis, J. A., Modrell, M. S., Northcutt, R. G., Catania, K. C., Luer, C. A. and Baker, C. V. H. (2012). Electrosensory ampullary organs are derived from lateral line placodes in cartilaginous fishes. *Development* **139**, 3142–3146.
- Gingerich, P. D. (1979). The stratophenetic approach to phylogeny reconstruction in vertebrate paleontology. *Phylogenetic Analysis and Paleontology*. Columbia University Press, New York, 41–77.
- Goujet, D. (1982). Les affinités des placodermes, une revue des hypothèses actuelles. *Geobios* **15**, 27–38.

- Goujet, D. (1984a). *Les poissons placodermes du Spitzberg: Arthrodiros Dolichothoraci de la Formation de Wood Bay (Dévonien inférieur). Cahiers de Paléontologie, Section Vertébrés.* CNRS, Paris.
- Goujet, D. (1984b). Placoderm interrelationships: a new interpretation, with a short review of placoderm classifications. In *Proceedings of the Linnean Society of New South Wales*, vol. 107, pp. 211–243.
- Goujet, D. (2001). Placoderms and basal gnathostome apomorphies. In *Major Events in Early Vertebrate Evolution* (ed. P. E. Ahlberg), pp. 209–222. Taylor and Francis, London and New York.
- Gross, W. (1961). *Lunaspis broilii* und *Lunaspis heroldi* aus dem Hunsrückschiefer (Unterdevons, Rheinland). *Notizblatt Hessisches Landesamtes für Bodenforschung zu Wiesbaden* **89**, 17–43.
- Gross, W. (1963). *Gemuendina stuerzi* Traquair. Neuuntersuchung. *Sonderdruck aus dem Notizblatt des Hessischen Landesamtes für Bodenforschung zu Wiesbaden* **91**, 36–73.
- Gross, W. (1968). Fragliche actinopterygier-schuppen aus dem silur gotlands. *Lethaia* **1**, 184–218.
- Gross, W. (1969). *Lophosteus superbis* Pander, ein Teleostome aus dem Silur Oesels. *Lethaia* **2**, 15–47.
- Hamilton, R. F. M. and Trewin, N. H. (1988). Environmental controls on fish faunas of the Middle Devonian Orcadian Basin. *Memoir - Canadian Society of Petroleum Geologists* **14**, 589–600.
- Hanke, G. F. (2008). *Promesacanthus eppleri* n. gen., n. sp., a mesacanthid (Acanthodii, Acanthodiformes) from the Lower Devonian of northern Canada. *Geodiversitas* **30**, 287–302.
- Hanke, G. F. and Wilson, M. V. (2006). Anatomy of the Early Devonian acanthodian *Brochoadmones milesi* based on nearly complete body fossils, with comments on the evolution and development of paired fins. *Journal of Vertebrate Paleontology* **26**, 526–537.
- Hanke, G. F., Wilson, M. V. and Lindoe, L. A. (2001). New species of Silurian acanthodians from the Mackenzie Mountains, Canada. *Canadian Journal of Earth Sciences* **38**, 1517–1529.

- Hanke, G. F. and Wilson, M. V. H. (2010). The putative stem-group chondrichthyans *Kathemacanthus* and *Seretolepis* from the Lower Devonian MOTH locality, Mackenzie Mountains, Canada. In *Morphology, Phylogeny, and Paleobiogeography of Fossil Fishes, Honoring Meemann Chang* (ed. D. K. Elliott, J. G. Maisey, X. Yu and D. Miao), pp. 159–182. Verlag Dr. Friedrich Pfeil, München.
- Harris, J. E. (1938). The Dorsal Spine of Cladoselache. *Scientific Publications of the Cleveland Museum of Natural History* **8**, 1–6.
- Heath, T. A., Huelsenbeck, J. P. and Stadler, T. (2014). The fossilized birth–death process for coherent calibration of divergence-time estimates. *Proceedings of the National Academy of Sciences* **111**, E2957–E2966.
- Heimberg, A. M., Cowper-Sal, R., Sémon, M., Donoghue, P. C. and Peterson, K. J. (2010). microRNAs reveal the interrelationships of hagfish, lampreys, and gnathostomes and the nature of the ancestral vertebrate. *Proceedings of the National Academy of Sciences* **107**, 19379–19383.
- Hennig, W. (1966). *Phylogenetic systematics*. University of Illinois Press.
- Heyning, J. E. and Thacker, C. (1999). Phylogenies, temporal data, and negative evidence. *Science* **285**, 1179–1179.
- Huelsenbeck, J. P., Bollback, J. P. and Levine, A. M. (2002). Inferring the root of a phylogenetic tree. *Systematic Biology* **51**, 32–43.
- Huelsenbeck, J. P., Ronquist, F., Nielsen, R. and Bollback, J. P. (2001). Bayesian inference and its impact on evolutionary biology. *Science* **294**, 2310–2314.
- IUCN. (2017). The IUCN Red List of Threatened Species. Version 2017-3.
- Janvier, P. (1981). The phylogeny of Craniata, with particular reference to the significance of fossil 'agnathans'. *Journal of Vertebrate Paleontology* **1**, 121–159.
- Janvier, P. (1985). *Les Céphalaspides du Spitsberg. Anatomie, phylogénie et systématique des Ostéostracés siluro-dévonien. Révision des Ostéostracés de la formation de Wood Bay (Dévonien inférieur du Spitsberg)*. *Cahiers de Paléontologie, Section Vertébrés*. CNRS, Paris.

- Janvier, P. (1996). *Early vertebrates*. Clarendon Press, Oxford.
- Janvier, P. (2015). Facts and fancies about early fossil chordates and vertebrates. *Nature* **520**, 483–489.
- Janvier, P., Arsenault, M. and Desbiens, S. (2004). Calcified cartilage in the paired fins of the osteostracan *Escuminaspis laticeps* (Traquair 1880), from the Late Devonian of Miguasha (Québec, Canada), with a consideration of the early evolution of the pectoral fin endoskeleton in vertebrates. *Journal of Vertebrate Paleontology* **24**, 773–779.
- Jarvik, E. (1942). On the structure of the snout of crossopterygians and lower gnathostomes in general. *Zoologiska bidrag från Uppsala* **21**, 235–675.
- Jarvik, E. (1972). Middle and upper devonian porolepiformes from East Greenland with special reference to *Glyptolepis groenlandica* N. Sp.: and a discussion on the structure of the head in the porolepiformes. *Palaeontographica Abteilung A Palaeozoologie-Stratigraphie* **167**, 180–214.
- Jarvik, E. (1977). The systematic position of acanthodian fishes. In *Problems in vertebrate evolution* (ed. S. M. Andrews, R. S. Miles and A. D. Walker), pp. 199–224. Academic, London.
- Jarvik, E. (1980). *Basic structure and evolution of vertebrates*. Academic Press, London.
- Johanson, Z. (2002). Vascularization of the osteostracan and antiarch (Placodermi) pectoral fin: similarities, and implications for placoderm relationships. *Lethaia* **35**, 169–186.
- Jørgensen, J. M. (1989). Evolution of octavolateralis sensory cells. In *The Mechanosensory Lateral Line, Neurobiology and Evolution* (ed. S. Coombs, P. Görner and H. Münz), pp. 115–145. Springer, New York.
- Jørgensen, J. M. (2005). Morphology of electroreceptive sensory organs. In *Electroreception* (ed. T. H. Bullock, C. D. Hopkins, A. N. Popper and R. R. Fay), pp. 47–67. Springer, New York.
- Kalmijn, A. J. (1974). The detection of electric fields from inanimate and animate sources other than electric organs. In *Electroreceptors and Other Specialized Receptors in Lower Vertebrates* (ed. A. Fessard), pp. 147–200. Springer, New York.

- Karatajute-Talimaa, V. and Predtechenskyj, N. (1995). The distribution of the vertebrates in the Late Ordovician and Early Silurian palaeobasins of the Siberian Platform. *Bulletin du Muséum national d'histoire naturelle. Section C, Sciences de la terre, paléontologie, géologie, minéralogie* **17**, 39–55.
- Karatujute-Talimaa, V., Novitskaya, L. I., Rozman, K. S. and Sodov, Z. (1990). *Mongolepis*—a new lower Silurian genus of elasmobranchs from Mongolia. *Paleontologicheskii Zhurnal* **1990**, 76–86.
- Kemp, A. (2017). Cranial nerves in the Australian lungfish, *Neoceratodus forsteri*, and in fossil relatives (Osteichthyes: Dipnoi). *Tissue and Cell* **49**, 45–55.
- Kemp, T. S. (1988). Haemothermia or Archosauria? The interrelationships of mammals, birds and crocodiles. *Zoological Journal of the Linnean Society* **92**, 67–104.
- Lee, M. S., Cau, A., Naish, D. and Dyke, G. J. (2014a). Dinosaur evolution. Sustained miniaturization and anatomical innovation in the dinosaurian ancestors of birds. *Science* **345**, 562–6.
- Lee, M. S. Y., Cau, A., Naish, D. and Dyke, G. J. (2014b). Morphological clocks in paleontology, and a mid-Cretaceous origin of crown Aves. *Systematic Biology* **63**, 442–449.
- Lewis, P. O. (2001). A likelihood approach to estimating phylogeny from discrete morphological character data. *Systematic Biology* **50**, 913–925.
- Long, J. A. (1984). New phyllolepid fish from Victoria and the relationships of the group. In *Proceedings of the Linnean Society of New South Wales*, vol. 107, pp. 263–308.
- Long, J. A. (1988). New palaeoniscoid fishes from the Late Devonian and Early Carboniferous of Victoria. *Memoirs of the Association of Australasian Palaeontologists* **7**, 1–64.
- Long, J. A. (1999). A new genus of fossil coelacanth (Osteichthyes: Coelacanthiformes) from the Middle Devonian of Southeastern Australia. *Records of the Western Australian Museum Supplement* **57**, 37–53.
- Long, J. A., Barwick, R. E. and Campbell, K. S. W. (1997). Osteology and functional morphology of the osteolepiform fish *Gogonasus andrewsae* Long, 1985, from the Upper Devonian Gogo

- Formation, Western Australia. *Records of the Western Australian Museum Supplement* **53**, 1–89.
- Long, J. A., Mark-Kurik, E., Johanson, Z., Lee, M. S., Young, G. C., Min, Z., Ahlberg, P. E., Newman, M., Jones, R. and Den Blaauwen, J. (2015). Copulation in antiarch placoderms and the origin of gnathostome internal fertilization. *Nature* **517**, 196–199.
- Long, J. A. and Trinajstic, K. (2010). The Late Devonian Gogo Formation lagerstätte of Western Australia: exceptional early vertebrate preservation and diversity. *Annual Review of Earth and Planetary Sciences* **38**, 255–279.
- Long, J. A., Trinajstic, K. and Johanson, Z. (2009). Devonian arthrodire embryos and the origin of internal fertilization in vertebrates. *Nature* **457**, 1124.
- Long, J. A., Trinajstic, K., Young, G. C. and Senden, T. (2008). Live birth in the Devonian period. *Nature* **453**, 650–652.
- Løvtrup, S. (1976). *The phylogeny of Vertebrata*. Wiley, London.
- Maisch, M. W. (1998). *Wildungenichthys grossi* n. gen., n. sp.—a new selenosteid arthrodire (Placodermi, Arthrodira) from the Kellwasserkalk (late Frasnian, Upper Devonian) of Bad Wildungen (Hessen, W-Germany). *Palaeontologische Zeitschrift* **72**, 373–382.
- Maisey, J., Miller, R. and Turner, S. (2009). The braincase of the chondrichthyan *Doliodus* from the Lower Devonian Campbellton formation of New Brunswick, Canada. *Acta Zoologica* **90**, 109–122.
- Maisey, J. G. (1986). Heads and tails: a chordate phylogeny. *Cladistics* **2**, 201–256.
- Maisey, J. G. (2001). A primitive chondrichthyan braincase from the Middle Devonian of Bolivia. In *Major events in early vertebrate evolution* (ed. P. Ahlberg), pp. 263–288. Taylor and Francis, London and New York.
- Maisey, J. G. (2005). Braincase of the Upper Devonian shark *Cladodoides wildungensis* (Chondrichthyes, Elasmobranchii), with observations on the braincase in early chondrichthyans. *Bulletin of the American Museum of Natural History* **288**, 1–103.

- Maisey, J. G. (2007). The braincase in Paleozoic symmoriiform and cladoselachian sharks. *Bulletin of the American Museum of Natural History* **307**, 1–122.
- Marcot, J. D. and Fox, D. L. (2008). StrataPhy: a new computer program for stratocladistic analysis. *Palaeontologia Electronica* **11**, 5A–16.
- Matzke, N. J. and Wright, A. (2016). Inferring node dates from tip dates in fossil Canidae: the importance of tree priors. *Biology Letters* **12**, 20160328.
- Miles, R. S. (1973a). Articulated acanthodian fishes from the old red sandstone of England: with a review of the structure and evolution of the acanthodian shoulder-girdle. *Bulletin of the British Museum (Natural History) Geology* **24**, 113–213.
- Miles, R. S. (1973b). Relationships of acanthodians. In *Interrelationships of fishes* (ed. P. H. Greenwood, R. S. Miles and C. Patterson), pp. 63–103. Zoological Journal of the Linnean Society, London.
- Miles, R. S. and Young, G. C. (1977). Placoderm interrelationships reconsidered in the light of new ptyctodontids from Gogo, Western Australia. *Linnean Society Symposium Series* **4**, 123–198.
- Miller, R. F., Cloutier, R. and Turner, S. (2003). The oldest articulated chondrichthyan from the Early Devonian period. *Nature* **425**, 501–504.
- Modrell, M. S., Bemis, W. E., Northcutt, R. G., Davis, M. C. and Baker, C. V. H. (2011). Electrosensory ampullary organs are derived from lateral line placodes in bony fishes. *Nature Communications* **2**, 496.
- Nelson, G. J. (1969). Origin and diversification of teleostean fishes. *Annals of the New York Academy of Sciences* **167**, 18–30.
- Nelson, G. J. (1972). Cephalic sensory canals, pitlines, and the classification of esocoid fishes, with notes on galaxiid and other teleosts. *American Museum Novitates* **2492**, 1–37.
- Nicoll, R. S. (1977). Conodont apparatuses in Upper Devonian palaeoniscoid fish from the Canning Basin, Western Australia. *Bureau of Mineral Resources Journal of Australian Geology and Geophysics* **2**, 217–228.

- Northcutt, R. G. (1989). The phylogenetic distribution and innervation of craniate mechanoreceptive lateral lines. In *The mechanosensory lateral line* (ed. S. Coombs, P. Görner and H. Münz), pp. 17–78. Springer, New York.
- Northcutt, R. G. (2008). Historical hypotheses regarding segmentation of the vertebrate head. *Integrative and Comparative Biology* **48**, 611–619.
- Northcutt, R. G., Brändle, K. and Fritzschn, B. (1995). Electroreceptors and mechanosensory lateral line organs arise from single placodes in axolotls. *Developmental Biology* **168**, 358–373.
- Ørvig, T. (1962). Y at-il une relation directe entre les arthrodires ptyctodontides et les holocephales. *Colloques Internationaux du Centre National de la Recherche Scientifique* **104**, 49–61.
- Ota, K. G., Fujimoto, S., Oisi, Y. and Kuratani, S. (2011). Identification of vertebra-like elements and their possible differentiation from sclerotomes in the hagfish. *Nature Communications* **2**, 373.
- Ota, K. G., Fujimoto, S., Oisi, Y. and Kuratani, S. (2013). Late development of hagfish vertebral elements. *Journal of Experimental Zoology Part B: Molecular and Developmental Evolution* **320**, 129–139.
- Pan, J. (1986). Notes on Silurian vertebrates of China. *Bulletin of the Chinese Academy of Geological Sciences* **15**, 227–249.
- Patterson, C. (1981). Significance of fossils in determining evolutionary relationships. *Annual Review of Ecology and Systematics* **12**, 195–223.
- Platnick, N. I. (1979). Philosophy and the transformation of cladistics. *Systematic Zoology* **28**, 537–546.
- Prichonnet, G., Di Vergilio, M. and Chidiac, Y. (1996). Stratigraphical, sedimentological and paleontological context of the Escuminac Formation: paleoenvironmental hypotheses. In *Devonian fishes and plants of Miguasha, Quebec, Canada* (ed. H.-P. Schultze and R. Cloutier), pp. 23–36. Verlag Dr. Friedrich Pfeil, München.

- Pyron, R. A. (2011). Divergence time estimation using fossils as terminal taxa and the origins of Lissamphibia. . *Systematic Biology* **60**, 466–481.
- Qu, Q. M., Zhu, M. and Zhao, W. J. (2010). Silurian atmospheric O₂ changes and the early radiation of gnathostomes. *Palaeoworld* **19**, 146–159.
- Ronquist, F., Klopfstein, S., Vilhelmsen, L., Schulmeister, S., Murray, D. L. and Rasnitsyn, A. P. (2012). A total-evidence approach to dating with fossils, applied to the early radiation of the Hymenoptera. *Systematic Biology* **61**, 973–999.
- Rosen, D. E., Forey, P. L., Gardiner, B. G. and Patterson, C. (1981). Lungfishes, tetrapods, paleontology, and plesiomorphy. *Bulletin of the American Museum of Natural History* **167**, 159–267.
- Sansom, I. J., Davies, N. S., Coates, M. I., Nicoll, R. S. and Ritchie, A. (2012). Chondrichthyan - like scales from the Middle Ordovician of Australia. *Palaeontology* **55**, 243–247.
- Sansom, I. J., Smith, M. M. and Smith, M. P. (2001). The Ordovician radiation of vertebrates. In *Major Events in Early Vertebrate Evolution* (ed. P. E. Ahlberg), pp. 156–171. Taylor & Francis, London.
- Sansom, R. S., Freedman, K., Gabbott, S. E., Aldridge, R. J. and Purnell, M. A. (2010). Taphonomy and affinity of an enigmatic Silurian vertebrate, *Jamoytius kerwoodi* White. *Palaeontology* **53**, 1393–1409.
- Schaeffer, B., Hecht, M. K. and Eldredge, N. (1972). Phylogeny and paleontology. In *Evolutionary biology* (ed. T. Donzhansky, M. K. Hecht and W. C. Steere), pp. 31–46. Appleton-Century-Crofts, New York.
- Schultze, H.-P. (1992). Early Devonian actinopterygians (Osteichthyes, Pisces) from Siberia. In *Fossil Fishes as Living Animals* (ed. E. Mark-Kurik), pp. 233–242. Academy of Sciences of Estonia, Tallinn.

- Schultze, H.-P. (1996). The vertebrates of the Escuminac Formation. In *Devonian fishes and plants of Miguasha, Quebec, Canada* (ed. H.-P. Schultze and R. Cloutier), pp. 120–122. Verlag Dr. Friedrich Pfeil, München.
- Smith, M. M. and Sansom, I. J. (1997). Exoskeletal micro-remains of an Ordovician fish from the Harding Sandstone of Colorado. *Palaeontology* **40**, 645–658.
- Stadler, T. (2010). Sampling-through-time in birth–death trees. *Journal of Theoretical Biology* **267**, 396–404.
- Stensiö, E. A. (1927). The Downtonian and Devonian vertebrates of Spitsbergen. I, Family Cephalaspidae. *Skrifter om Svalbard og Ishavet* **12**, 1–391.
- Stensiö, E. A. (1937). *On the Devonian coelacanthids of Germany with special reference to the dermal skeleton*. Almqvist & Wiksell, Stockholm.
- Stensiö, E. A. (1963a). *Anatomical studies on the arthrodiran head*. Almqvist & Wiksell, Stockholm.
- Stensiö, E. A. (1963b). *The Brain and the Cranial Nerves in Fossil, Lower Craniate Vertebrates*. Universitetsforlaget, Oslo.
- Stensiö, E. A. (1969). Elasmobranchiomorphi Placodermata Arthrodiros. In *Traité de paléontologie*, vol. 4 (ed. J. Piveteau), pp. 71–692. Masson, Paris.
- Thomson, K. S. (1965). The endocranium and associated structures in the Middle Devonian rhipidistian fish *Osteolepis*. *Proceedings of the Linnean Society of London* **176**, 181–195.
- Thorsteinsson, R. (1973). Dermal elements of a new lower vertebrate from Middle Silurian (Upper Wenlockian) Rocks of the Canadian Arctic Archipelago. *Palaeontographica Abteilung A*, 51–57.
- Tông-Dzuy, T., Phuong, T. H., Boucot, A. J., Goujet, D. and Janvier, P. (1997). Vertébrés siluriens du Viêt-nam central. *Comptes rendus de l'Académie des sciences. Série 2. Sciences de la terre et des planètes* **324**, 1023–1030.
- Trewin, N. H. (1985). Mass mortalities of Devonian fish—the Achanarras Fish Bed, Caithness. *Geology Today* **1**, 45–49.

- Trinajstić, K., Marshall, C., Long, J. and Bifield, K. (2007). Exceptional preservation of nerve and muscle tissues in Late Devonian placoderm fish and their evolutionary implications. *Biology Letters* **3**, 197–200.
- Trinajstić, K., Sanchez, S., Dupret, V., Tafforeau, P., Long, J., Young, G., Senden, T., Boisvert, C., Power, N. and Ahlberg, P. E. (2013). Fossil musculature of the most primitive jawed vertebrates. *Science* **341**, 160–164.
- van Netten, S. M. and Kroese, A. B. A. (1988). Dynamic behaviour and micromechanical properties of the cupula. In *The Mechanosensory Lateral Line, Neurobiology and Evolution* (ed. S. Coombs, P. Görner and H. Münz), pp. 247–263. Springer, New York.
- Watson, D. M. S. (1937). The acanthodian fishes. *Philosophical Transactions of the Royal Society of London. Series B, Biological Sciences*, 49–146.
- Webb, J. F. (1989). Gross morphology and evolution of the mechanoreceptive lateral-line system in teleost fishes. *Brain Behavior and Evolution* **33**, 34–43.
- Webb, J. F. (2013). Morphological diversity, development, and evolution of the mechanosensory lateral line system. In *The Lateral Line System* (ed. S. Coombs, H. Bleckmann, R. R. Fay and A. N. Popper), pp. 17–72. Springer, New York.
- Williams, M. E. (1998). A new specimen of *Tamiobatis vetustus* (Chondrichthyes, Ctenacanthoidea) from the late Devonian Cleveland Shale of Ohio. *Journal of Vertebrate Paleontology* **18**, 251–260.
- Young, G. C. (1979). New information on the structure and relationships of *Buchanosteus* (Placodermi: Euarthrodira) from the Early Devonian of New South Wales. *Zoological Journal of the Linnean Society* **66**, 309–352.
- Young, G. C. (1980). A new Early Devonian placoderm from New South Wales, Australia, with a discussion of placoderm phylogeny. *Palaeontographica Abteilung A Palaeozoologie-Stratigraphie* **167**, 10–76.

- Young, G. C. (1991). The first armoured agnathan vertebrates from the Devonian of Australia. In *Early Vertebrates and Related Problems Of Evolutionary Biology* (ed. M.-M. Chang, Y.-H. Liu and G.-R. Zhang), pp. 41–65. Science Press, Beijing.
- Young, G. C. (1997). Ordovician microvertebrate remains from the Amadeus Basin, central Australia. *Journal of Vertebrate Paleontology* **17**, 1–25.
- Young, G. C. (2008). The relationships of antiarchs (Devonian placoderm fishes)—evidence supporting placoderm monophyly. *Journal of Vertebrate Paleontology* **28**, 626–636.
- Young, G. C. (2010). Placoderms (armored fish): dominant vertebrates of the Devonian period. *Annual Review of Earth and Planetary Sciences* **38**, 523–550.
- Young, G. C. (2011). Wee Jasper-Lake Burrinjuck fossil fish sites: scientific background to national heritage nomination. *Proceedings of the Linnean Society of New South Wales* **132**, 83–107.
- Young, G. C., Lelièvre, H. and Goujet, D. (2001). Primitive jaw structure in an articulated brachythoracid arthrodire (placoderm fish; Early Devonian) from Southeastern Australia. *Journal of Vertebrate Paleontology* **21**, 670–678.
- Yu, X. (1998). A new porolepiform-like fish, *Psarolepis romeri*, gen. et sp. nov. (Sarcopterygii, Osteichthyes) from the Lower Devonian of Yunnan, China. *Journal of Vertebrate Paleontology* **18**, 261–274.
- Zhang, G.-R., Wang, S.-T., Wang, J.-Q., Wang, N.-Z. and Zhu, M. (2010). A basal antiarch (placoderm fish) from the Silurian of Qujing, Yunnan, China. *Palaeoworld* **19**, 129–135.
- Zhang, M. (1980). Preliminary note on a Lower Devonian antiarch from Yunnan, China. *Vertebrata Palasiatica* **18**, 179–&.
- Zhao, W. J., Zhu, M., Liu, S., Pan, Z. H. and Jia, L. T. (2016). A new look at the Silurian fish-bearing strata around the Shanmen reservoir in Lixian, Hunan province. *Journal of Stratigraphy* **40**, 341–350.

- Zhu, M. (1996). The phylogeny of the Antiarcha (Placodermi, Pisces), with the description of early Devonian antiarchs from Qujing, Yunnan, China. *Bulletin du Muséum national d'histoire naturelle. Section C, Sciences de la terre, paléontologie, géologie, minéralogie* **18**, 233–347.
- Zhu, M., Ahlberg, P. E., Pan, Z., Zhu, Y., Qiao, T., Zhao, W., Jia, L. and Lu, J. (2016). A Silurian maxillate placoderm illuminates jaw evolution. *Science* **354**, 334–336.
- Zhu, M. and Janvier, P. (1998). The histological structure of the endoskeleton in galeaspids (Galeaspida, Vertebrata). *Journal of Vertebrate Paleontology* **18**, 650–654.
- Zhu, M. and Schultze, H. P. (1997). The oldest sarcopterygian fish. *Lethaia* **30**, 293–304.
- Zhu, M. and Yu, X. (2002). A primitive fish close to the common ancestor of tetrapods and lungfish. *Nature* **418**, 767–770.
- Zhu, M., Yu, X., Ahlberg, P. E., Choo, B., Lu, J., Qiao, T., Qu, Q., Zhao, W., Jia, L., Blom, H. and Zhu, Y.-A. (2013). A Silurian placoderm with osteichthyan-like marginal jaw bones. *Nature* **502**, 188–193.
- Zhu, M., Yu, X., Choo, B., Qu, Q., Jia, L., Zhao, W., Qiao, T. and Lu, J. (2012a). Fossil fishes from China provide first evidence of dermal pelvic girdles in osteichthyans. *PloS one* **7**, e35103.
- Zhu, M., Yu, X., Choo, B., Wang, J. and Jia, L. (2012b). An antiarch placoderm shows that pelvic girdles arose at the root of jawed vertebrates. *Biology Letters* **8**, 453–456.
- Zhu, M., Yu, X. and Janvier, P. (1999). A primitive fossil fish sheds light on the origin of bony fishes. *Nature* **397**, 607–610.
- Zhu, M., Zhao, W., Jia, L., Lu, J., Qiao, T. and Qu, Q. (2009). The oldest articulated osteichthyan reveals mosaic gnathostome characters. *Nature* **458**, 469–474.

Chapter 2

Electroreception in early vertebrates: survey, evidence and new information

Benedict King¹, Yuzhi Hu^{2,3}, John A. Long¹

¹College of Science and Engineering, Flinders University, PO Box 2100, Adelaide, South Australia 5001, Australia. ²Department of Applied Mathematics, Research School of Physics and Engineering, Oliphant Building 60, Australian National University, Canberra, ACT, 2601, Australia. ³Research School of Earth Sciences, Building 142 Mills Road, Australian National University, Canberra, ACT, 2601, Australia

Context

The aim of this chapter is to determine if fossils of early vertebrates show evidence for the presence of electrosensory systems. This chapter reviews the structures in early vertebrate fossils that have been previously suggested to be involved in electroreception, and provides new evidence based on CT scans and digital rendering.

Statement of authorship

JAL conceived the project. BK performed all digital segmentations, collected data in museums, produced illustrations and figures and wrote the paper. YH provided specimens from ANU, wrote sections pertaining to ANU CT scanning and provided image for figure 14A.

Abstract

Electroreception is widespread in living vertebrates, and is often considered a primitive vertebrate character. However, the early evolution of electroreception remains unclear. A variety of structures in early vertebrate fossils have been put forward as potential electroreceptors, but these need to be reassessed in light of the now substantial literature on electroreceptors in living vertebrates. Here we review the evidence for all putative electroreceptors in early vertebrates, and provide new information from CT scans. In the jawless osteostracans, the pore canal system in the dermal skeleton and the lateral and dorsal fields do not resemble electroreceptors in living species. Nevertheless the presence of a recurrent ramus of the anterior lateral line nerve in osteostracans suggests electroreceptors were present, by comparison with lampreys. In placoderms, cutaneous sense organs on arthrodire cheek plates are possible electroreceptors. CT data shows that the orientation of these pits is anomalous for electroreceptors, and intimately associated with bone growth. A newly identified type of cheek pit, for which the term “Young’s apparatus” is introduced, is known so far only from two arthrodire specimens. It is closely associated with the underlying jaw joint, but its precise function is unknown. In osteichthyans, the “pore-group” clusters of early sarcopterygians may have housed electroreceptors. CT data from Devonian lungfish support this interpretation, showing internal morphology consistent with electroreceptors, and innervation via the rostral tubuli underlying the dermal bone of the snout. The early osteichthyan *Ligulalepis* has pit structures which may be electroreceptors, and they were possibly innervated by lateral line nerves. Specialised electroreceptor systems, including elaborated “pore-group” pits in Devonian lungfishes and rostral organs in the earliest coelacanths, show that electroreception was already elaborated in early vertebrates. Finally, fossil data does not

support the hypothesis that vertebrate hard tissues initially evolved to shield electroreceptors.

Introduction

Electroreception, the ability to detect electric fields, is the most recently discovered of the major sensory modalities. Lissmann (1951) and Lissmann and Machin (1958) discovered that African knifefish (*Gymnarchus*) could detect perturbations in electric fields produced by their electric organs, allowing them to navigate their environment. Detecting electric fields produced by an electric organ is known as active electroreception. Later, sensitivity to external electric fields without use of an electric organ was demonstrated in sharks and rays (Murray 1960; Murray 1962; Bennett 1971). Experiments on the catshark *Scyliorhinus canicula* showed that passive electroreception functions in the detection of naturally-occurring electric fields surrounding prey items (Kalmijn 1971).

Passive electroreception was subsequently discovered in a broad range of vertebrates including basal actinopterygians (ray-finned fish), lungfishes, coelacanths, amphibians, chimaeras (relatives of sharks and rays) and the jawless lampreys (Jørgensen et al. 1972; Roth 1973; Fields and Lange 1980; Teeter et al. 1980; Bodznick and Northcutt 1981; Münz et al. 1982; Watt et al. 1999). The presence of electroreception is distributed widely in phylogeny (Fig. 1) and is often regarded as a plesiomorphic feature of vertebrates (Bullock et al. 1983). In addition to the phylogenetic distribution, shared features of electrosensory systems (excluding those of teleost fishes) have been used to support their homology: activation by cathodal (outside negative) stimuli, innervation by the anterior lateral line nerve (ALLN: superficial ophthalmic, buccal, otic and mandibularis externus lateral line nerves) and projections to the dorsal octavolateralis nucleus (DON) in the medulla region of the hindbrain (Bullock et al. 1983). These electroreceptors also share a common embryonic

origin, forming on the periphery of lateral line placodes, patches of thickened cranial ectoderm that also give rise to the mechanosensory lateral lines (Northcutt et al. 1995; Modrell et al. 2011; Gillis et al. 2012; Baker et al. 2013). For these reasons, there is a general consensus that the electroreceptors of non-teleosts are homologous, although there are significant morphological differences between groups (see below).

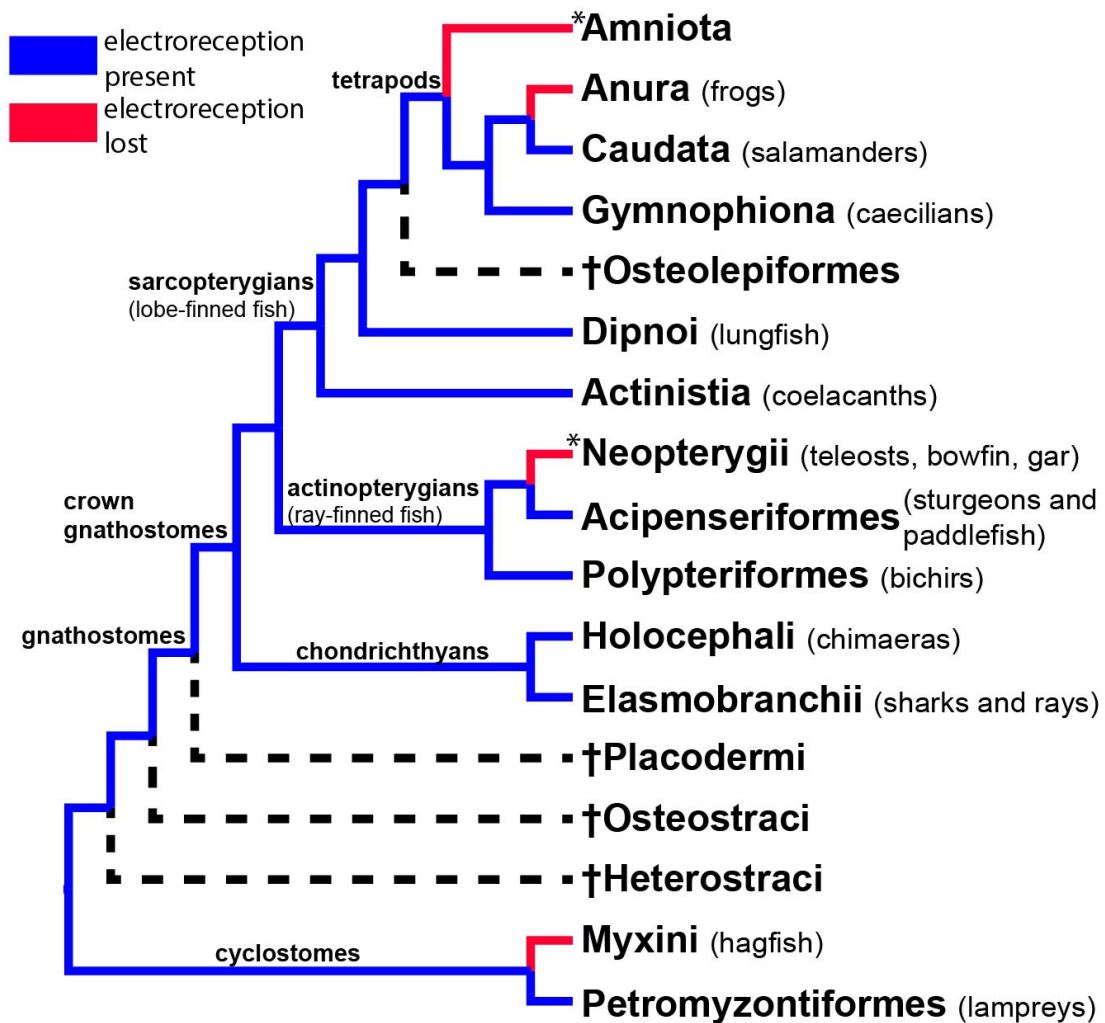


Figure 1. Vertebrate phylogeny showing presence and absence of electroreception, and the position of key fossil taxa discussed during this review. Electroreception is inferred to be a primitive vertebrate feature as it is present across the phylogeny (blue branches). It has been lost four times (red branches). The asterisks indicate clades within which electroreception has evolved secondarily following loss (i.e. within teleosts and mammals). Key fossil groups that will be discussed in this review are shown on dotted black

branches. All of these would be inferred to have had electroreception, or to have lost it, based on their relationships to living taxa with electroreception.

Electroreception has apparently been lost in hagfish, neopterygian fish (including teleosts), anurans (frogs) and amniotes (Fig. 1). However, it has subsequently been re-gained at least twice in teleosts (in subgroups of Osteoglossomorpha and Ostariophysii) (Alves-Gomes 2001) and twice in mammals (dolphins and monotremes) (Proske et al. 1998; Czech-Damal et al. 2012). The electroreceptors of teleosts are not considered homologous with those of non-teleost fishes (Bullock et al. 1983; Baker et al. 2013). This review will focus mainly on the vertebrate “ancestral-type” of electroreceptor (i.e. those of non-teleosts).

Lampreys and gnathostomes, in possessing electroreceptors that are thought to be homologous, form an extant phylogenetic bracket (Witmer 1995). Fossil stem gnathostomes (closer to extant gnathostomes than to extant agnathans) fall within this bracket. The jawless arandaspids, anaspids, thelodonts, heterostracans, galeaspids, pituriaspids and osteostracans are considered stem gnathostomes (Janvier 1996; Donoghue et al. 2000; Sansom et al. 2010), as are the jawed placoderms (Young 1986; Goujet 2001; Brazeau 2009). All of these groups can therefore be assumed to have had electroreception, or to have secondarily lost it. The purpose of this review is to re-examine the putative electroreceptors in fossil stem and early crown gnathostomes. CT scan data is presented on ‘cutaneous sense organs’, putative electoreceptor pits on the cheeks of arthrodire placoderms, lungfish “pore-group” pits and newly identified pits on the skull of the enigmatic early osteichthyan “*Ligulalepis*”.

Materials and methods

Material selected

We selected a number of placoderm cheek plates for scanning (Table 1). Two lungfish datasets from Campbell et al. (2010) were reanalysed and a new specimen of “*Ligulalepis*” was scanned.

Species name	Specimen number	Part scanned	Place scanned	voxel size (microns)
<i>Torosteus tuberculatus</i>	MV P230808	suborbital	Australian synchrotron	6.122
<i>Torosteus tuberculatus</i>	MV P230808	postsuborbital	Australian synchrotron	6.122
<i>Parabuchanosteus murrumbidgeensis</i>	ANU V1686	suborbital	Australian synchrotron	6.122
<i>Kimberleyichthys bispicatus</i>	ANU V1037	postsuborbital	Australian synchrotron	6.122
<i>Eastmanosteus calliaspis</i>	MV P231104	postsuborbital	Australian synchrotron	6.122
<i>Camuropiscis</i> sp.	SAM P53772	suborbital	CT Lab, ANU	11.9728
torosteid sp.	SAM P50606	postsuborbital	CT Lab, ANU	11.9728
arthrodire sp.	ANU V79	suborbital- postsuborbital	CT Lab, ANU	23.9784
‘buchanosteid’ sp.	ANU V244	Whole specimen	CT Lab, ANU	20.5714
<i>Speonesydrion iani</i>	ANU 49340	snout region of skull	CT Lab, ANU	16.8
<i>Chirodipterus australis</i>	ANU V1710 (ANU 25743 in Campbell et al. 2010)	snout region of skull	CT Lab, ANU	26.88
“ <i>Ligulalepis</i> ”	ANU V3628	Skull and braincase	Adelaide Microscopy	8.5

Table 1: Material scanned for this study

Synchrotron radiation X-ray tomographic microscopy

Some specimens (Table 1) were scanned at the medical imaging beamline of the Australian Synchrotron, Victoria, Australia (<http://www.synchrotron.org.au/index.php/home>). Scans

used a monochromatic beam with a photon energy of 30keV, sample to detector distance of 325mm and an nRuby detector. A total of 1800 projections over 180 degrees were taken. Raw data was processed using the X-TRACT software. The images from the overlapping 3mm slices were concatenated for segmentation. 3-D segmentation of the bone and internal canals was performed using MIMICS 17.0 and 18.0. Additional renderings were performed in Blender (blender.org) and Drishti (Limaye 2012).

Micro-CT scanning

All CT scans (with the exception of ANU V3628) were done on instruments developed and built at the ANU CT Lab (<https://ctlab.anu.edu.au/>), Department of Applied Mathematics, Research School of Physics and Engineering, Australian National University. ANU V244 was scanned in 2011; see Hu et al. (2017) for information. ANU 49340 was scanned in 2004, and ANU V1710 in 2005. For more information about these specimens, see Campbell et al. (2010). For further technical information about the CT Scanner, see Sakellariou et al. (2004). ANU V79 was scanned on double helix HeliScan CT Scanner. A 3mm aluminium filter was used, with specimen distance 128 mm from the source, and detector position 672 mm from the source. Accelerating voltage of the electron beam generating the Bremsstrahlung radiation was 110kV with a current of 120 μ A. Reconstruction was based on 3600 radiographic projections formed on a 2840 \times 2872 Pixium Flat Panel camera. SAM P53772 and SAM P50606 were scanned together in a 25 mm jar on a double helix HeliScan CT Scanner. A 2.2mm aluminium filter was used, with specimen distance 18.5 mm from the source, and detector position 300 mm from the source. Accelerating voltage of the electron beam generating the Bremsstrahlung radiation was 100kV with a current of 80 μ A. Reconstruction was based on 3600 radiographic projections formed on a 1536 \times 2048 Varian Flat Panel camera.

ANU V3628 was scanned at Adelaide Microscopy on a skyscan 1076. Specimen to source distance was 121 mm, camera to source distance was 161 mm. Source voltage was 100kV, and current 100 μ A. 393 projections were taken on a Hamamatsu Orca-HRF camera.

Data availability

3D pdf files of segmented models and a ply file of specimen V79 are available on the Dryad digital repository (doi:10.5061/dryad.hf124). Raw scan data from the Australian synchrotron are available via e-researchSA (doi:10.4226/86/5a05055b47a98). Netcdf data of specimens ANU V79, ANU 49340, ANU 25743, SAM P53772 and SAM P50606 are available via e-researchSA (<https://doi.org/10.4226/86/5a05055b47a98>).

Anatomical abbreviations

acc.cu.so, accessory cutaneous sense organs; **AMV**, anterior median ventral plate; **aup**, autopalatine section of palatoquadrate; **cu.so**, cutaneous sense organ; **hc**, horizontal sensory canal; **ioc**, infraorbital sensory canal; **orb**, orbit; **ot.lat**, otic lateralis nerve branches; **pq**, palatoquadrate; **pr.sm**, submarginal process of the postsuborbital plate; **psoc**, post-suborbital sensory canal; **soc**, supraorbital sensory canal; **soph**, superficial ophthalmic nerve; **sorc**, supraoral sensory canal; **ST**, supratemporal bone

Institutional abbreviations

AM, Australian Museum (Sydney, Australia); **ANU**, Australian National University (Canberra, Australia); **MV**, Museum Victoria (Melbourne, Australia); **NHMUK**, Natural History Museum (London, UK); **NMS**, National Museums Scotland (Edinburgh, UK); **SAM**, South Australia Museum (Adelaide, Australia).

Survey of electroreceptors in extant vertebrates

Electroreceptor structure and morphology in each group of vertebrates has been reviewed elsewhere (Jørgensen 2005; Baker et al. 2013). This section will focus on aspects of electroreception that are important for the recognition of electroreception in fossils: gross morphology, innervation and distribution.

Morphology of electroreceptors in living groups

Adult lamprey electroreceptors are called “end buds” (Ronan and Bodznick 1986). These are goblet shaped organs, 25–60µm in diameter, found in groups of 2–8 in the epidermis over the head and trunk on the surface of the skin. End buds are absent in larval lampreys (ammocetes), although ammocetes are known to be electroreceptive (Ronan 1988). Likely candidates for larval electroreceptors are multivillous cells found scattered throughout the epidermis in both ammocetes and adults (Whitear and Lane 1983). End buds are indistinguishable from the surrounding epidermis unless stained (Ronan and Bodznick 1986) and have no potential for preservation in the fossil record, even in lamprey fossils with good soft tissue preservation (Bardack and Zangerl 1968; Chang et al. 2006; Gess et al. 2006). In elasmobranchs (sharks and rays), electroreceptors are called ampullae of Lorenzini (Fig. 2). These are jelly-filled canals, approximately 1mm in diameter, ending in small sacs known as ampullae (Lorenzini 1678). A series of experiments showed these to be electroreceptors (Murray 1960; Murray 1962; Dijkgraaf and Kalmijn 1963). Elasmobranch ampullae are grouped into clusters surrounded by connective tissue beneath the dermis, with long subdermal canals penetrating the dermis and opening into pores on the external surface

(Tricas and Sisneros 2004; Wueringer and Tibbetts 2008). The ampullae have a range of morphologies, from simple tubes with an enlarged chamber at the base (e.g. in *Torpedo* rays) to “lobular” or “alveolate” ampullae with diverticulae emanating from a central chamber (Jørgensen 2005). The total number of ampullary organs varies between species, from the 148 to over 2000 (Bodznick and Boord 1986).

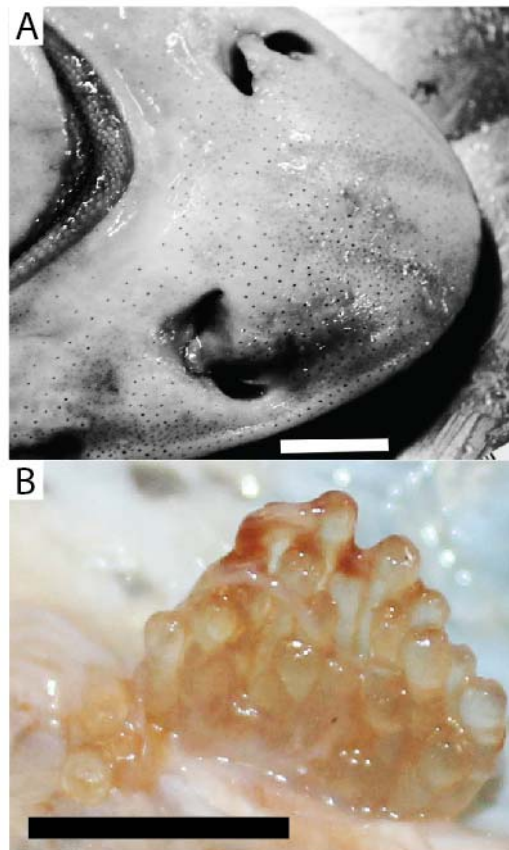


Figure 2. Ampullae of Lorenzini in the shark *Mustelus antarcticus*. A) Pores on the ventral snout area. B) Ampullae. Author provided. Scale bars represent 20mm (A) and 10mm (B).

The other major lineage of cartilaginous fish, the chimaeras or Holocephali, also have electroreceptors (Fields and Lange 1980). In the spotted ratfish *Hydrolagus colliei*, ampullae are largely similar to those in elasmobranchs (Fields et al. 1993): alveolate and grouped in connective tissue capsules. The density of pores falls within the lower end of the range seen in elasmobranchs (Lisney 2010). In addition to “macro-ampullae”, Holocephali have “micro-

ampullae”, with pores of 80–100 μm in diameter on the surface of the rostrum (Andres and Von Düring 1988).

In actinopterygians (ray-finned fish), electroreceptors are present in the two earliest diverging lineages: polypteriforms (bichirs and reedfish), and acipenseriforms (paddlefish and sturgeons) (Jørgensen et al. 1972; Roth 1973). Ampullae of polypteriforms are superficial structures with short canals (Roth and Tschardtke 1976; Jørgensen 1982), particularly in *Polypterus* where they are confined to the epidermis of the skin. In sturgeons, electroreceptors are also superficial structures, although ampullae are sunken into the dermis (Jørgensen 1980; Teeter et al. 1980). Canals in sturgeons have a diameter of 30–40 μm at the surface, widening basally to 60–70 μm . Ampullae are clustered into groups of 4–85, and pairs of ampullae sometimes share common pores (Weisel 1978).

Within sarcopterygians (lobe-finned fishes), the electroreceptors of lungfishes are superficial tube-like structures embedded in the epidermis with ampullae at the base (Roth and Tschardtke 1976; Jørgensen 2011). The electroreceptors of both caecilian and urodele amphibians are likewise simple structures confined to the epidermis (Hetherington and Wake 1979; Istenič and Bulog 1984).

Coelacanth, the sister group to other living sarcopterygians, have an electroreceptor system with a unique morphology, called the rostral organ. This is a subdermal chamber enclosed in the ethmoid region of the braincase, and connected to the outside by three pairs of jelly-filled canals (Millot and Anthony 1965; Bemis and Hetherington 1982). This highly specialised system is sensitive only in a small region directly in front of the mouth, and is thought to function solely in the feeding strike (Berquist et al. 2015).

Structural differences between marine and freshwater ampullary electroreceptors.

The morphology of electroreceptors differs between marine and freshwater species, with long canals characterising marine species and short canals characterising freshwater species (Kramer 1996). Long canals characterise the majority of chondrichthyans, but short ampullary canals are known in the freshwater rays *Potamotrygon* and *Himantura* (Szabo et al. 1972; Raschi et al. 1997). This difference also occurs in the electroreceptors of catfish, although teleost electroreceptors are likely not homologous to vertebrate ancestral-type electroreceptors (Bullock et al. 1983; Baker et al. 2013). Marine catfish *Plotosus* have long canals that penetrate deep into the dermis (Obara 1976). A freshwater member of the same genus has short canals (Whitehead et al. 2003). Euryhaline populations of the catfish *Arius graeffi* have intermediate canal length between marine and freshwater catfish (Whitehead et al. 1999) and freshwater populations of the same species have short canals (Whitehead et al. 2000).

The difference in electroreceptor morphology between marine and freshwater species has been attributed to the biophysical properties of these two media (Szabo et al. 1972; Kalmijn 1974; Fig. 3). In saltwater, skin resistance is low and the body fluids are less conductive than the surrounding water, so voltage gradients extend throughout the body in marine vertebrates (Fig. 3A). There is little voltage difference across the skin so marine vertebrates require long canals filled with a highly conductive jelly to produce sufficient voltage differences across the receptor membrane. The long canals effectively focus the voltage difference between the canal pore and the body fluids surrounding the ampulla onto the receptor membrane. Freshwater species have a higher skin resistance and relatively conductive body fluids, and therefore the voltage difference across the skin is sufficient for detection (Fig 3), without requiring long canals. Szabo et al. (1972) suggested that short

canals in freshwater species are an adaptation to minimise loss of ions by outward diffusion from the canal jelly.

The morphological difference between electroreceptors of living freshwater and saltwater species is consistent across multiple groups, and is associated with the biophysical properties of the water. Therefore, similar morphological differences should be applicable in fossils from freshwater and marine deposits, if preservation allows.

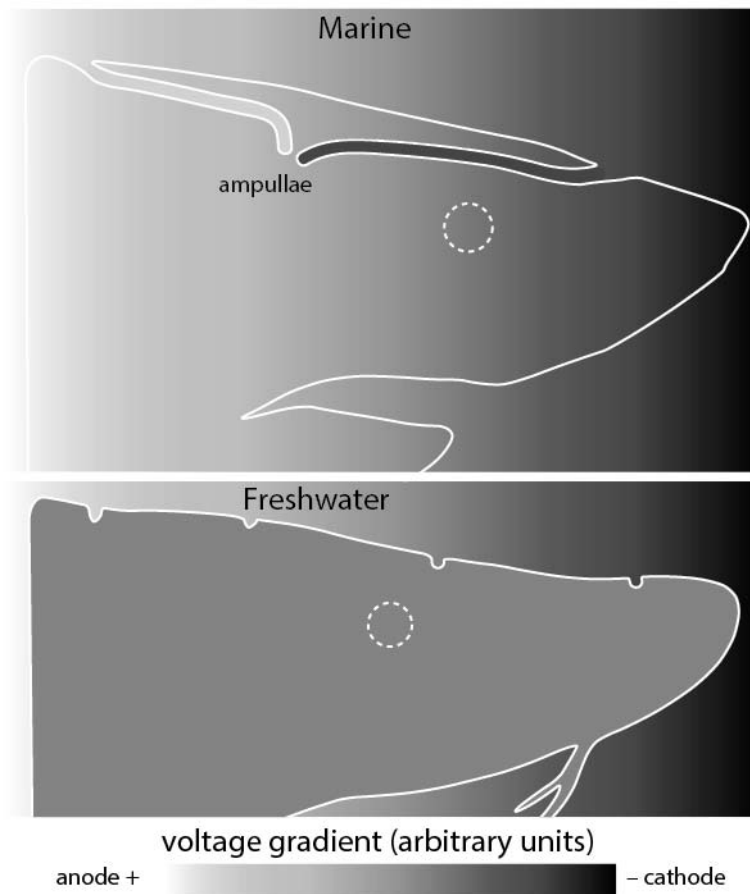


Figure 3. Marine species have long ampullary canals to obtain sufficient voltage difference across the receptor membrane in the ampullae, whereas freshwater species have sufficient voltage difference across the skin and only require short canals. The background gradient represents an imposed electric field. In marine species (represented by a shark), skin resistance is low and voltage gradients extend through the body. Long canals with high resistance walls allow the voltage at the pore opening to extend to the ampulla, where there is sufficient voltage difference with the surrounding tissues to allow detection. In freshwater species (represented by a sturgeon), skin resistance is high, so that voltage gradients do not extend through the body. The inside of the fish is instead relatively isopotential (apparent reverse gradient in the figure is an optical illusion). The voltage difference across the skin is sufficient that

only short canals are required. Based on similar figures in Kramer (1996) and Kalmijn (1974).

Distribution of electroreceptors

In the majority of non-teleosts with electroreceptors, they are confined to the head.

However in lampreys, they are also distributed widely over the body and externally on the branchial region (Bodznick and Preston 1983). Trunk electroreceptors are also found in lungfishes (Northcutt 1986b), and ampullary organs are found on the pectoral fins of rays and skates (Raschi 1978).

In chondrichthyans, each ampullary organ is most sensitive to voltage gradients that are parallel to canal direction (Murray 1962). In many species, ampullary canals radiate in many directions, to enable sensitivity to electric fields in various orientations (Kramer 1996; Tricas 2001).

Ampullary pores are generally most densely distributed at the anterior end of the snout in sharks (e.g. Norris 1929; Kajiura 2001; Winther-Janson et al. 2012). Whether pores are primarily found on the dorsal or ventral surface appears to depend on ecology (Raschi 1986).

Pores primarily on the dorsal surface are indicative of a vertical ambush predatory lifestyle (Theiss et al. 2011; Moore and McCarthy 2014), whereas pores primarily on the ventral surface is characteristic of species that feed on bottom-dwelling prey (Raschi 1978; Raschi 1986). Pelagic forms have more evenly distributed pores (Raschi 1986; Kajiura 2001). In holocephalans, the highest pore densities are also on the snout anterior to the eyes (Fields et al. 1993), and the same is true in general for osteichthyans (Northcutt 1986a).

Some electroreceptive species have evolved specialised morphologies associated with enhanced electroreceptive abilities. The elongate snouts of rhinochimaerid holocephalans have increased density of electroreceptive pores on their ventral surface (Lisney 2010), as do the wide heads of hammerhead sharks (Kajiura 2001). The elongate bill of the American

paddlefish acts as an electroreceptive antenna aiding capture of plankton in murky water (Wilkins et al. 1997).

Ampullary electroreceptors develop from the periphery of lateral line placodes (Northcutt et al. 1995; Modrell et al. 2011; Gillis et al. 2012). This is reflected in the distribution of pores in the adult: ampullary organs occur in fields alongside the latero-sensory canals (e.g. Norris 1929; Fields et al. 1993).

Innervation of electroreceptors

Non-teleost electroreceptors are innervated by branches of the anterior lateral line nerve (ALLN) which project to the dorsal octavolateralis nucleus (DON) in the medulla (Bullock et al. 1983). In marine chondrichthyans, in which the ampullary bulbs are clustered into a number of discrete capsules, each capsule is innervated by a branch of the ALLN: the superficial ophthalmic, outer buccal, inner buccal, hyomandibular and mandibular branches (Raschi 1986).

The dorsal octavolateralis nucleus in the medulla is thought to be exclusively involved in electroreception (Bodznick and Northcutt 1980; Bodznick and Northcutt 1981; Bullock et al. 1983). However, presence of such a nucleus cannot be ascertained in fossil endocasts. In fact, the dorsal hindbrain has a particularly poor fit to the endocast in the lungfish *Neoceratodus* (Clement et al. 2015).

In lampreys and lungfishes, which possess trunk electroreceptors, these are innervated by a recurrent ramus of the ALLN (Bodznick and Preston 1983; Northcutt 1986b). This nerve courses around the otic capsule and runs posteriorly to join the posterior lateral line nerve, which innervates trunk mechanoreceptors. Since this nerve exclusively innervates trunk electroreceptors (it is not found in taxa that lack electroreception), its presence in a fossil would likely indicate the presence of electroreception.

Criteria for recognising electroreceptors in fossils

The above review of the morphology, distribution and innervation of non-teleost electroreceptors allows a number of criteria for their recognition in fossils to be put forward.

1. Morphologically, electroreceptors are canals with a diameter between 100 and 1500 microns. The canal endings may be expanded to form bulb-like ampullae (Jørgensen 2005). Electroreceptors of modern fishes are not enclosed in bone, so will only appear in fossils under special circumstances.
2. Most densely distributed on the head, particularly around the snout and mouth (Norris 1929; Northcutt 1986a; Fields et al. 1993)
3. Distribution in fields surrounding the lateral line canals (Norris 1929; Fields et al. 1993)
4. Long canals in marine species, with ampullae grouped together. Short canals in freshwater species (Szabo et al. 1972).
5. When long canals are present, there are usually many with differing orientations (Tricas 2001).
6. Innervation by branches of the anterior lateral line nerve (ALLN) (Bullock et al. 1983).
7. A recurrent ramus of the ALLN would indicate presence of trunk electroreceptors (Northcutt 1986b).

Jawless stem gnathostomes

There are a number of jawless fish groups that may be more closely related to crown gnathostomes than extant jawless fishes (Janvier 1996; Donoghue et al. 2000; Sansom et al. 2010). These are the arandaspids, anaspids, thelodonts, heterostracans, galeaspids,

pituriaspids and osteostracans (Fig. 1). Of these groups, only osteostracans have morphological structures that have been suggested to represent electroreceptors (Bohlin 1941; Thomson 1977; Janvier 1985). Their bones contain a network of canals linked to the exterior via pores termed the “pore-canal system” (Denison 1964; Fig. 4A), which has been suggested to house electroreceptors (Thomson 1977). Importantly, osteostracans also have shallow depressed areas along the edges of the head shield and posterior to the pineal opening (dorsal and lateral fields, fig. 4B), for which a number of functions have been suggested including both detection and generation of electric fields (Stensiö 1927; Bohlin 1941). In heterostracans, Ørvig (1989) came to the conclusion that electroreceptors must be absent, as no trace of them could be found in the dermal skeleton.

The pore canal system in osteostracans

The pore-canal system of osteostracans is a polygonal network of “mesh canals” in the middle layer of the exoskeleton connecting to the outside through “pore canals” (Denison 1966; Sire et al. 2009; Fig. 4A). The mesh canals are divided into dorsal and ventral halves by a thin, perforated bony septum in *Tremataspis* (Denison 1947; Denison 1966).

In a detailed treatment of the pore canal system in sarcopterygians (lobe-finned fish), Thomson (1977) extrapolated the proposed electroreceptive function of this system to osteostracans (see below for full discussion of sarcopterygian pore canal system). Stensiö (1927) initially suggested that the osteostracan pore canal system housed mucous canals. However, the pore canal system is connected to, and in cross-section indistinguishable from, the lateral line canals (Denison 1947). A mechanoreceptive function was therefore proposed. A mechanoreceptive function was further supported on the basis of synchrotron x-ray microtomography (Qu et al. 2015). The mesh canals in *Oeselaspis*, which lack a horizontal dividing septum, connect to the outside via “polyp-like” structures resembling the

nerve supply of neuromasts. In the divided mesh canals of *Tremataspis*, the upper portion was suggested to house epithelial invaginations, perhaps representing a more sophisticated version of the same sensory system (Qu et al. 2015).

The argument for an electroreceptive function in osteostracans rests on extrapolation from the pore canal system in sarcopterygians (Thomson 1977), but the two systems are unlikely to be homologous (Meinke 1984). The sarcopterygian pore canal system is within a dentinous layer. In osteostracans it underlies the dentine layer, although it occurs in a lamellar layer resembling elasmodine, a hard tissue with plywood-like structure which is putatively a form of dentine (Sire et al. 2009). Furthermore, the pore canal system in sarcopterygians may not be involved in electroreception (New 1997, and see discussion below).

Denison (1964) suggested that the “intercostal grooves” of heterostracans (separating dentine ridges or tubercles) were homologous to the pore canal system of osteostracans. No electroreceptive function has been suggested for this system in heterostracans.

Some tremataspid osteostracans have “porous fields”, clusters of microscopic pits that occur between tubercles (Afanassieva 2004; Märss et al. 2014). Some tremataspid osteostracans have “porous fields”, clusters of microscopic pits that occur between tubercles. However these have not been suggested to be electroreceptors, and they are smaller than any known electroreceptors.

Dorsal and lateral fields in osteostracans

The dorsal and lateral fields (Fig. 4B) were first suggested to be electric organs (i.e. for generating electric fields or shocking prey) by Stensiö (1927). Due to their superficial position he argued that they were unlikely to be derived from muscle (electric organs of modern species are derived from muscle). These “fields” are connected to the labyrinth

(inner ear cavity) by large canals (termed sinus expansions of the labyrinth or s.e.l.)(Fig. 4B). These were thought to provide nerves (Stensiö 1927). Electroreception was unknown at the time, but electric organs for stunning prey were well known. Living species with electric organs mostly also possess electroreceptors, although stargazers (Uranoscopidae) are an exception to this rule, having electric organs but no electroreceptors (Baron 2009). The electric organ interpretation was challenged based on comparison with electric organs in living species (Bohlin 1941; Wängsjö 1952), as the volume of the fields was too small and the nerves disproportionately large to support their interpretation as electric organs. Wängsjö (1952) instead interpreted the lateral and dorsal fields as housing lateral line organs, and suggested that the well-developed cerebellum of osteostracans was associated with this.

Bohlin (1941) compared the dorsal and lateral fields of osteostracans with the ampullae of Lorenzini of elasmobranchs, at that time thought to be thermoreceptors (Sand 1938). Bohlin (1956) dismissed this idea, and suggested the fields were specialised hearing organs or mechanoreceptors. In this hypothesis, the canals connecting the fields to the labyrinth would have been filled with endolymph, and the roof of the cavity, formed from a mosaic of small plates, would have acted as a membrane to transmit vibrations to the ear via the canals. This idea was first put forward by Watson (1954), who argued that the canals leading to the lateral fields were far too wide to carry nerves, being much wider than the entry foramina for nerves VII and VIII into the labyrinth. Jarvik (1965) reinforced this interpretation of the lateral fields. Additionally, he identified one dorsal and five ventral protruberences in the labyrinth of lampreys, which might be vestiges of the s.e.l. canals in osteostracans.

Northcutt (1985) also considered the electric organ hypothesis unlikely, as the electric organs of modern species are innervated by postotic branchiomic nerves and have associated expanded brain stem areas. He agreed with Jarvik (1965), arguing that the fields

could be evaginations of the labyrinth homologous with the ciliated dorsal and lateral chambers of the lamprey labyrinth.

Despite these arguments, the morphology and innervation of the lateral fields is consistent with the electric organs of certain catfish (Janvier 1985). *Malapterurus* catfish have thin electric organs, which may be derived from muscle despite their superficial position (Johnels 1956). Both an electric organ and a vibration sensor remain plausible possibilities for the function of the lateral and dorsal fields. They are unlikely to have housed electroreceptors.

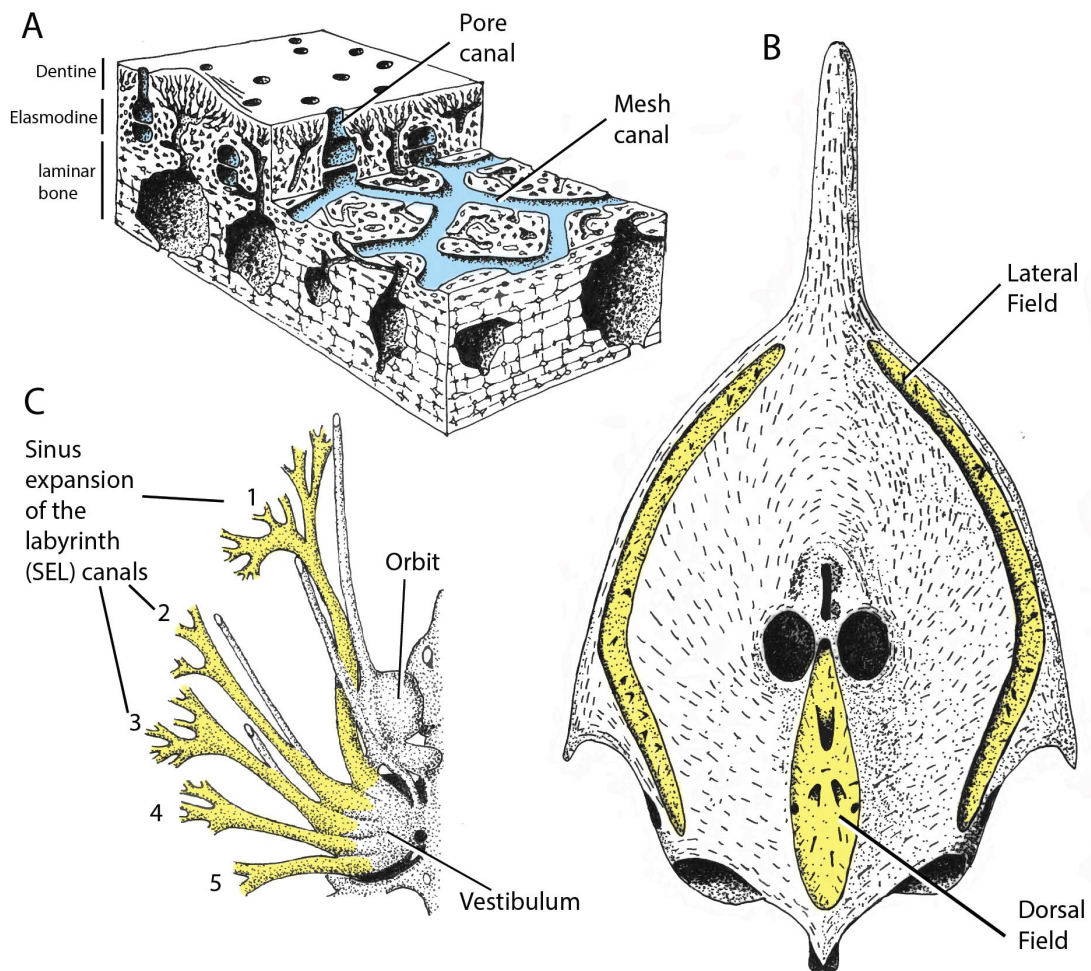


Figure 4. Structures in osteostracans that have been suggested to be electroreceptors or electric organs. A) Dermal bone structure in *Tremataspis*, showing the pore canal system (highlighted in blue). B) Dorsal surface of the head in *B. puella*. Lateral fields, shallow troughs in the dermal bone, are highlighted in yellow. C) Ventral view of the internal cavities of the neurocranium in *Belonaspis puella*. Sinus expansions of the labyrinth, canals

that connect the inner ear to the lateral fields, are highlighted in yellow. A redrawn based on Denison (1947). B–C redrawn based on Janvier (1985).

Ramus recurrens of the anterior lateral line nerve in osteostracans

Janvier (1974) interpreted a groove over the labyrinth cavity in the wax model from Stensiö (1927) as a possible ramus recurrens, connecting the preotic and postotic ganglia. A small canal in *Benneviaspis*, piercing the labyrinth cavity antero-dorsal to the acoustic and facial nerves, is thought to have carried the ramus recurrens (Janvier 1985); it likely rejoined the postotic ganglion via the glossopharyngeal canal. As discussed above, the ramus recurrens is thought to be exclusively involved in innervation of trunk electroreceptors. This would indicate that osteostracans had electroreceptors, despite lack of convincing evidence for preservation of the electroreceptors themselves.

Placoderms

Placoderm 'cutaneous sense organ' pits

In some arthrodire placoderms, large (approx. 1mm) isolated pits in the cheek plates, called cutaneous sense organs (cu.so), are putative electroreceptors (Ørvig 1960; Fig. 5). They were compared to the clusters of ampullae of Lorenzini of elasmobranchs, a short time before they were shown to be electroreceptors in sharks (Murray 1960; Murray 1962).

Within arthrodires, cutaneous sensory organ pits are most commonly found on the suborbital and postsuborbital plates of eubrachythoracid arthrodires: the suborbital and postsuborbital plates of *Coccosteus* (Stensiö 1963; Fig. 5B), *Watsonosteus* (Miles and Westoll 1962), *Goodradigbeeon* (White 1978), *Torosteus* (Gardiner and Miles 1990) and *Plourdosteus* (Ørvig 1960) and the postsuborbital plate of *Harrytoombsia* (Miles and Dennis 1979), *Mcnamaraspis* (Long 1995), *Simosteus* (Dennis and Miles 1982), *Compagopiscis* (Gardiner

and Miles 1994), *Dickosteus* (Miles and Westoll 1962) and *Kimberleyichthyes* (Dennis-Bryan and Miles 1983). These pits therefore appear to have been a widespread feature in coccosteomorph (*sensu* Carr and Hlavin (2010)) arthrodires, although they are absent in *Incisoscutum*, *Camuropiscis*, *Tubonasus*, *Latocamurus* and *Rolfosteus* (Dennis and Miles 1979b; Dennis and Miles 1979a; Long 1988a). The latter taxa are deeply nested within coccosteomorphs (Zhu and Zhu 2013), suggesting secondary loss.

These pits are not so well known in the dunkleosteoid and aspinothoracid (*sensu* Zhu and Zhu (2013)) eubrachythoracid arthrodires. However, postsuborbital pits are known in *Eastmanosteus calliaspis* (Dennis-Bryan 1987). Miles (1966) described a number of pits in *Rhachioosteus*, which has recently been placed within the Dunkleosteoidea (Zhu et al. 2015), but these appear to be unrelated to the cheek plate “cu.so pits” of other arthrodires, and may simply be due to the bone structure becoming more open and porous toward the edge of plates, as in many other placoderms (pers. obs.).

In more basal brachythoracid arthrodires, pits are found on the suborbital plates of *Parabuchanosteus* (White and Toombs 1972; Young 1979), *Gemuendenaspis* (Miles 1962), *Atlantidosteus* (Young 2003; Fig. 5D) and *Urvaspis* (Long et al. 2014). *Atlantidosteus*, has a large cutaneous sense organ and a group of smaller pits at the confluence of the supraoral and infraorbital sensory lines (Young 2003; Fig. 5D).

In non-brachythoracid arthrodires, preservation of cheek plates is relatively rare. Cutaneous sense organ pits are absent in *Holonema* (Miles 1971) and *Dicksonosteus* (Goujet 1975). However a pit is found on the suborbital plate of *Wuttagoonaspis* (Ritchie 1973; Miles and Young 1977; Young and Goujet 2003), which occupies a very basal position in arthrodire phylogeny (Dupret et al. 2009; Dupret et al. 2017b).

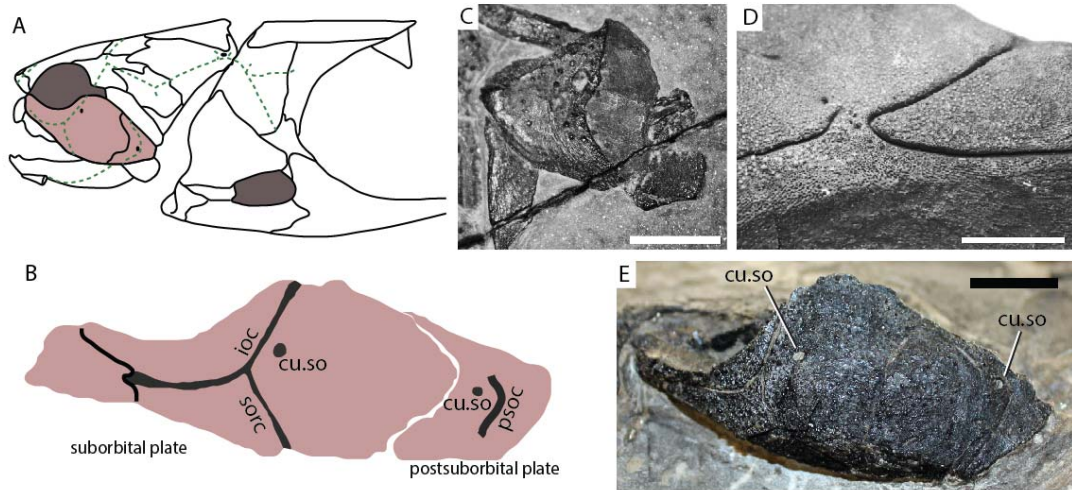


Figure 5. Placoderm cutaneous sense organs. A) Diagram of *Torosteus tuberculatus* skeleton in left lateral view, with the suborbital and postsuborbital plates highlighted in red. B) Diagram of the suborbital and postsuborbital plates of *Torosteus tuberculatus*, showing positions of the anterior and posterior cu.so pits. C) *Dickosteus threiplandi* postsuborbital plate with cu.so pits (NMS 1859.33.620). D) *Atlantidosteus pacifica* suborbital plate with multiple small cu.so pits (ANU V1033). E) *Coccosteus cuspidatus* suborbital and postsuborbital plates, with cu.so pits (NHMUK P44544). A and B redrawn based on Gardiner and Miles (1990). All scale bars represent 10mm. Abbreviations: cu.so, cutaneous sense organ; ioc, infraorbital canal; psoc, postsuborbital canal; sorc, supraoral canal.

Outside the arthrodiros, cutaneous sensory organs are known from the skull roofs of the acanthothoracid placoderms *Romundina* and *Brindabellaspis*, situated behind the orbit near the confluence of the main lateral line canal and the infraorbital canal (Ørvig 1975; Young 1980). Dupret et al. (2017a) describe two pairs of sensory pits behind the orbit of a different specimen of *Romundina*. Both pits in *Romundina* are innervated by a nerve that emerges from the confluence of the trigeminal and facial nerves behind the orbit (Dupret et al. 2017a). The petalichthyid placoderm *Eurycaraspis* possesses a group of three foramina towards the posterior of the skull roof, near the confluence of the main lateral line canal and the posterior pit line (Liu 1991). Ørvig (1971) described multiple cutaneous sensory organs surrounding sensory lines in skull bones of the ptyctodontid *Ctenurella*, but material from Gogo, preserved in three dimensions, shows no evidence for the presence of sensory pits

(Long 1997; Trinajstić et al. 2012). As with *Rhachioosteus* these “pits” in ptyctodontids are likely to simply be open bone structure around the edges of plates. Cutaneous sensory organs have been described in the yunnanolepid antiarch *Phymolepis* on the suborbital plate (Young and Zhang 1996). Cutaneous sense organ pits are therefore known from three major placoderm groups (arthrodires, antiarchs and acanthothoracids).

New information on placoderm sensory pits

The morphology of cutaneous sense organ (cu.so) pits, as shown by CT scans, varies from deep pits to shallow grooves (Fig. 6). The postsuborbital plate of *Eastmanosteus callispis* has a deep, vertical, funnel-shaped pit (Fig. 6A), whereas the postsuborbital plates of *Torosteus* and *Kimberleyichthys* have cutaneous sense organs that form grooves, with that in *Kimberleyichthys* being particularly elongate (Fig. 6D-E). The suborbital of *Parabuchanosteus* has a shallow, rounded vertical pit (Fig. 6B). The suborbital plate of *Torosteus* has a pit that is inclined at a slight angle, and is intermediate between the vertical pits and groove-like pits (Fig. 6C). The groove-like pits have the appearance of being blind-ending tubes projecting almost horizontally.

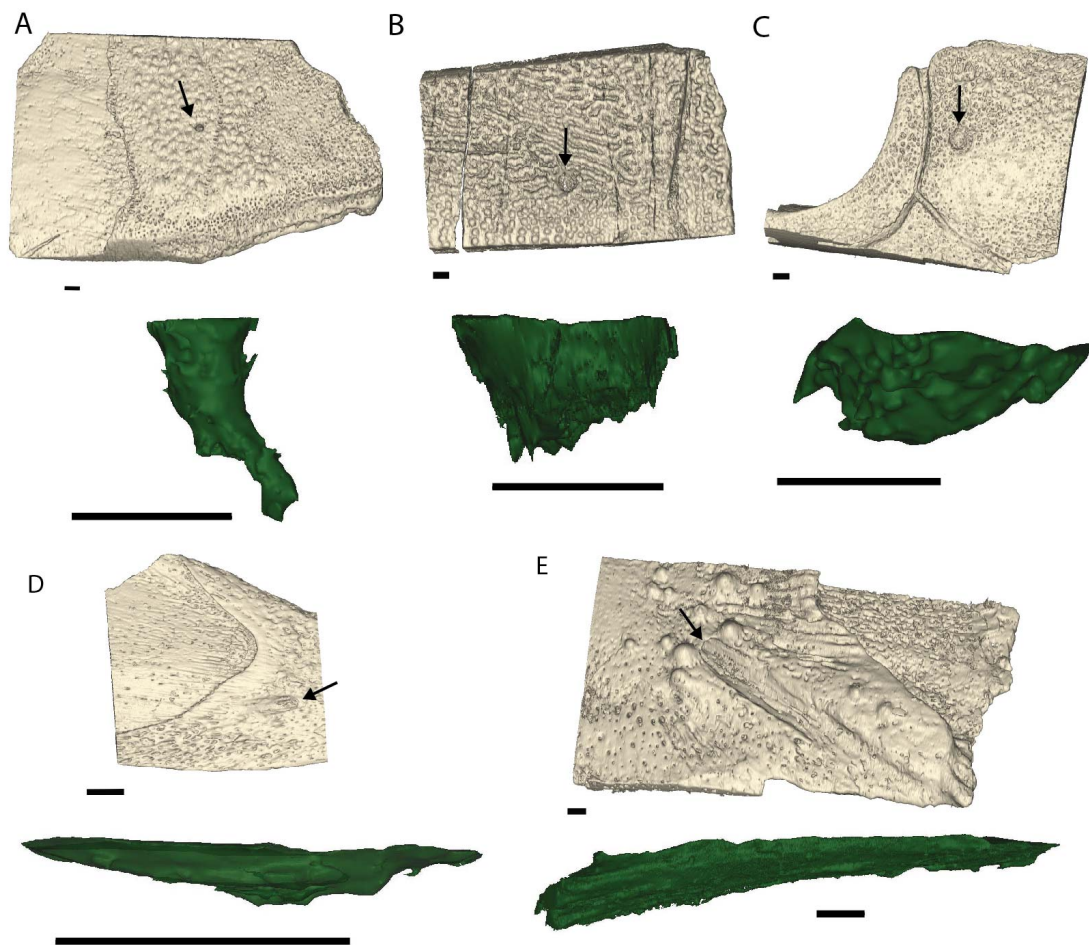


Figure 6. Internal shape of placoderm cutaneous sensory organs. The pits can be deep funnel-shaped pits (A), rounded pits (B–C), or grooves (D–E). A) *Eastmanosteus calliaspis* postsuborbital plate (MV P231104). B) *Parabuchanosteus murrumbidgeensis* suborbital plate (ANU V1686). C) *Torosteus tuberculatus* suborbital plate (MV P230808). D) *Torosteus tuberculatus* postsuborbital plate (MV P230808). E) *Kimberleyichthys bispicatus* postsuborbital plate (ANU V1686). All scale bars represent 1mm.

The CT scans allow the spatial relationship of these pits with the underlying structure of the dermal bone to be investigated (Fig. 7). Placoderm dermal bones typically have a three layer structure, with basal laminar and middle cancellar layers overlain by a superficial layer of either semidentine tubercles or laminar bone (Giles et al. 2013). These layers are easily distinguished from each other when the internal vascular canals are segmented and viewed in three dimensions (Fig. 7). The cutaneous sense organs (dark green, Fig. 6-7) are mostly confined to the superficial layer, although in all cases they dip into the middle layer (Fig. 7).

The depth of the pit therefore seems to depend on the depth of the superficial layer. In *Eastmanosteus*, which has a very deep pit, the superficial layer is also very deep (Fig. 7A-B). The orientation of the pits also follows the orientation of the canals in the superficial layer. In the *Kimberleyichthys* and *Toroosteus* postsuborbitals, in which the pits form elongate grooves, canals within the superficial layer are orientated almost parallel to the surface, and radiate out from the growth centre of the plate (Fig 7E-G). The groove-like cutaneous sense organs run parallel to these superficial layer canals, and appear to project away from the growth centre of the plate (Fig. 7G). In the *Eastmanosteus* postsuborbital plate, the canals in the superficial layer are vertical, and therefore so is the pit (Fig. 7B). In the *Toroosteus* suborbital, the pit is again parallel to the canals in the superficial layer, this time at a slight angle to the vertical (Fig. 7D).

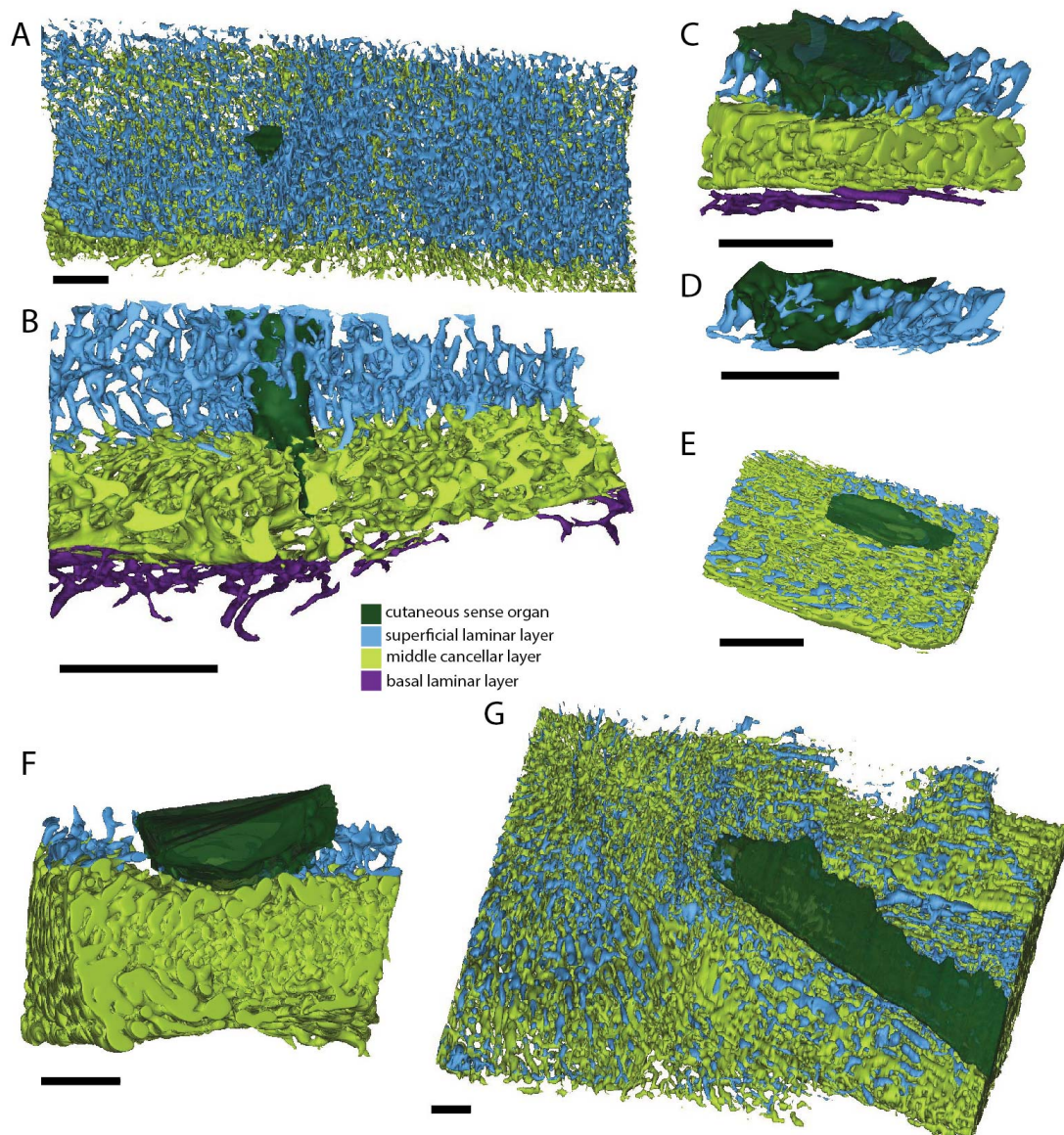


Figure 7. Relationship of cutaneous sense organs with the underlying bone structure. Spaces within the basal laminar (purple), middle cancellar (green) and superficial laminar (blue) layers are coloured separately. The cutaneous sense organs (dark green) are found in the superficial layer. When canals in the superficial layer are predominantly vertical, the pits are also vertical (A–D). The groove-like pits occur when the canals in the superficial layer are near horizontal (E–G). The groove-like pits also follow the direction of the superficial layer canals, radiating out from the growth centre of the plate (G). A–B) *Eastmanosteus calliaspis* postsuborbital plate (MVP231104). C–D) *Torosteus tuberculatus* suborbital plate (MV P230808). E) *Torosteus tuberculatus* postsuborbital plate (MV P230808). F–G) *Kimberleyichthys bispicatus* postsuborbital plate (ANU V1686).

The unusual morphology of the arthropod *Wuttagoonaspis*, which has an elongate suborbital plate facing dorsally and firmly united with the skull roof, makes its cutaneous sense organs an interesting case study (Fig. 8). The cu.so can be studied in specimens which preserve the suborbital plates as natural moulds, thus revealing the internal morphology of the pit in positive relief (Fig. 8B). The cu.so is an elongate groove, but the angle and length of the groove varies considerably between specimens. The specimen shown in figure 8B (AMF 53628) is the most extreme example: other specimens have shorter grooves. The cu.so is always orientated posteriorly, consistent with an elongate suborbital plate with the growth centre (assumed to lie near the confluence of the infraorbital and supraoral sensory lines) placed at the extreme anterior end of the bone.

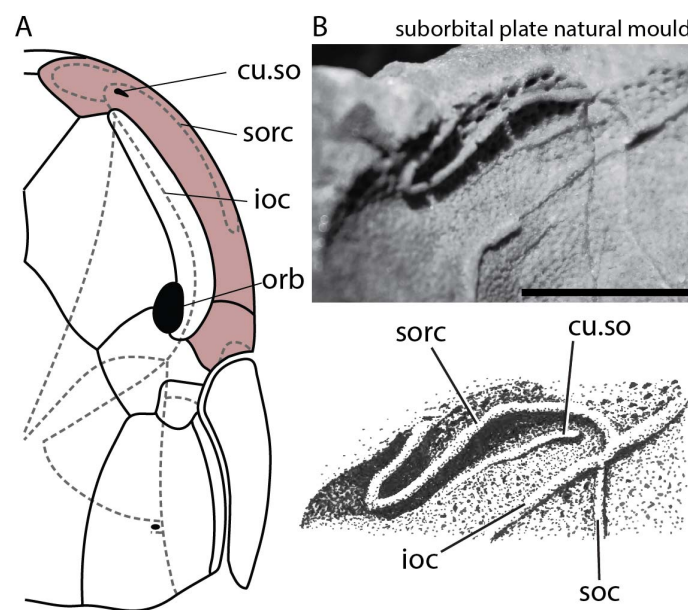


Figure 8. Posteriorly orientated cutaneous sense organs in the unusual anteriorly positioned suborbital plate of *Wuttagoonaspis*. A) Dorsal view of the right side of the skull of *Wuttagoonaspis fletcheri*. Suborbital and postsuborbital plates highlighted in red. Note the anterior position of the junction between the infraorbital and supraoral canals (and presumably therefore the growth centre). B) Natural mould of the anterior dorsal right part of the skull, showing sensory canals and cu.so in positive relief. The cu.so in this specimen (AM F53628) is a particularly long groove, orientated posteriorly away from the presumed growth centre at the extreme anterior part of the plate. A is redrawn based on Miles and Young (1977). Scale bar represents 10mm. Abbreviations: cu.so, cutaneous sense organ; ioc, infraorbital sensory canal; orb, orbit; soc, supraorbital canal; sorc, supraoral canal.

Since cu.so pits appear to be confined to the superficial layer of the dermal bone in eubrachythoracid arthroidres, it raises the question of whether the absence of pits in some taxa simply reflects a very shallow or absent superficial layer. Scans of arthrodire cheek plates that lack pits (Fig. 9), demonstrate that this is not the case.

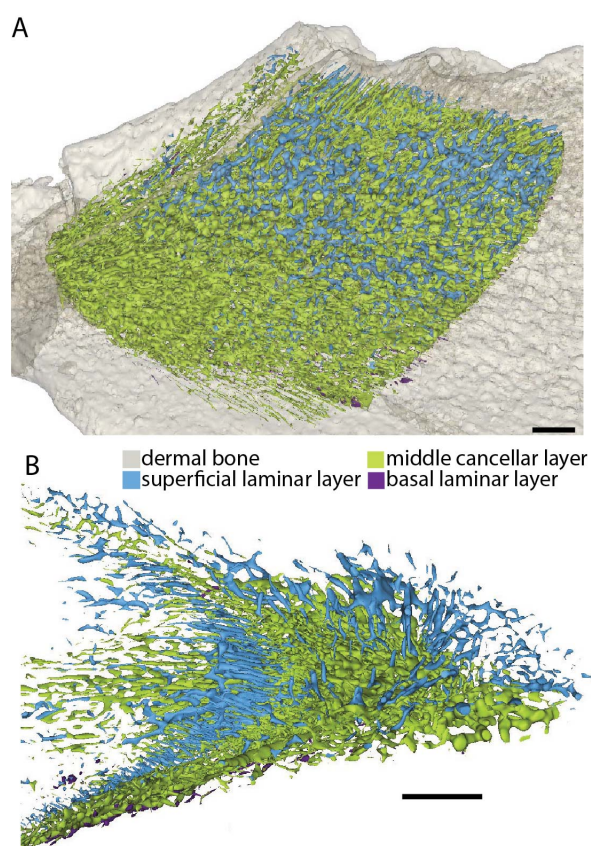


Figure 9. Plates without cutaneous sense organs still have thick superficial laminar layers. A) *Camuropiscis* sp. suborbital plate (SAM P53772). B) *torosteid* sp. postsuborbital plate (SAM P50606). The internal spaces within the superficial laminar layer are shown in blue. This layer was still substantial in these plates that lack cutaneous sense organs, suggesting that lack of these structures is not simply a result of a thin or absent superficial layer. Both scale bars represent 10mm.

Were cutaneous sense organs electroreceptors?

Cutaneous sense organs of placoderms do not demonstrate any of the criteria outlined above that would allow a positive identification of electroreceptors. The diameter of cu.so pits is consistent with the size of a single ampullary canal, rather than a capsule containing multiple canals as suggested by Ørving (1960). The low number of cu.so pits stands in contrast to the generally hundreds of ampullary organs in extant vertebrates. There is no expanded ampullary bulb at the base of the cu.so pits.

The CT scans reveal that the orientation of the pits is influenced by growth. The depth of the superficial layer of exoskeleton determines the depth of the cu.so. Vertical pits occur when the superficial layers are also vertical, which may be indicative of rapid growth (de Boef and Larsson 2007; Giles et al. 2013). The groove-like pits may occur in slow growing plates, with their orientation determined by the relative position of the cu.so to the growth centre. The intimate association of the cu.so pits with the growth of the plate suggests that they are not directional sense organs. In particular, the posteriorly orientated, dorsal cu.so of *Wuttagoonaspis* is inconsistent with electroreceptors in living species, in which they are most densely distributed around the snout and mouth.

Finally, the presence of long cu.so grooves in the presumed freshwater *Wuttagoonaspis* is also inconsistent with an electroreceptor identity. As discussed above, in living freshwater electroreceptive species, ampullae lie at the base of very short canals. The 10mm groove in *Wuttagoonaspis* is therefore unlikely to represent an electroreceptor. The combination of the low number, orientation, association with bone growth and presence of long canals in freshwater species all suggest that cutaneous sense organs are not electroreceptors.

However, the presence of nerve canals joining the cutaneous sense organs in *Romundina* and some bichanosteid arthrodires (see below) might suggest a sensory function, although only in *Romundina* can these canals be traced back to cranial nerves (Dupret et al. 2017a).

They may have housed an adirectional pressure detector, but their function cannot be determined with confidence.

The “Young’s apparatus”: a new pit structure on ‘buchanosteid’ cheek plates

A distinct type of pit structure is found on the suborbital-postsuborbital complex of two specimens from Taemas-Wee Jasper: an isolated arthrodire suborbital-postsuborbital (ANU V79; Fig. 10, 11B), and the ‘buchanosteid’ ANUV244 (Young et al. 2001; Hu et al. 2017; Fig. 11A). This structure is distinct from the cutaneous sense organs in being larger, having a more complex shape and penetrating almost the entire thickness of the bone. Here we erect the name “Young’s apparatus” for these unusual structures, in honour of Gavin C. Young, the world’s leading authority on buchanosteid placoderms and Taemas-Wee Jasper fossils. The Young’s apparatus was labeled as a “sensory sulcus” in ANU V244 by Hu et al. (2017). ANU V79 was initially suggested to belong to a heterostiid (Young 2011), but the suborbital plate of the recently described heterostiid *Herasmius dayi* (Schultze and Cumbaa 2017) has very different proportions from V79. V79 has several features in common with ANU V244, suggesting it may instead be a ‘buchanosteid’. These features include a horizontal canal, a supraoral canal that does not contact the infraorbital canal, no clear suture between the postsuborbital and suborbital plates, presence of two cutaneous sense organ pits and a strongly curved ventral margin. On the posterior part of the plate, on the visceral surface, is a dermal process (Fig. 10, pr.sm). A similar process occurs in ANU V244, where it is associated with a possible interhyal element (but see below for an alternative interpretation), and braces the submarginal plate (Hu et al. 2017). The dermal process and Young’s apparatus are only known in these two specimens, while they are absent in *Parabuchanosteus* (Young 1979), suggesting V79 and V244 belong to a subgroup of ‘buchanosteids’. Although the orbital area of V79 is broken, the curvature of the preserved

portion suggests small orbits, such that V79 has an unusual morphology relative to other 'buchanosteids', possibly an allometric difference due to the large size of this specimen.

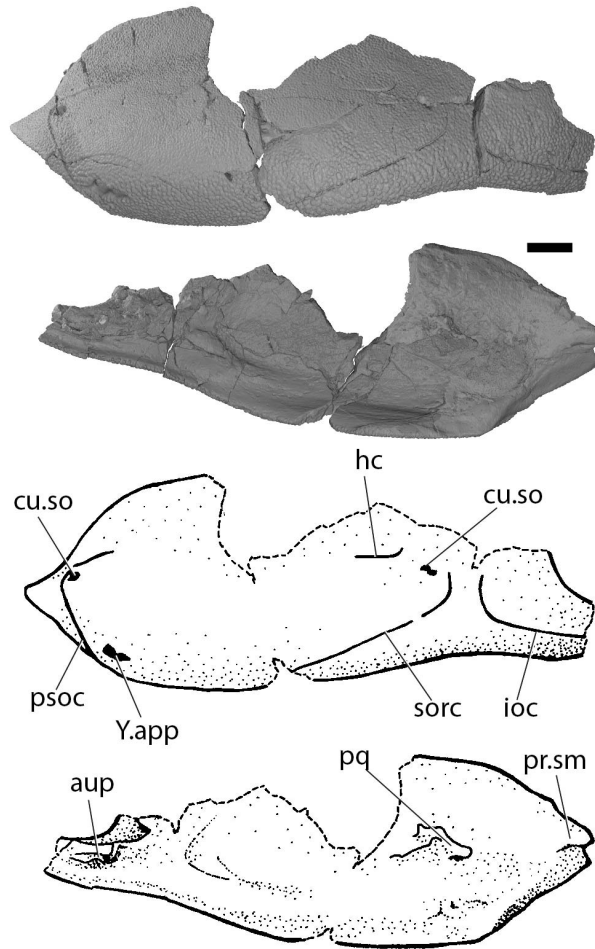


Figure 10. Arthrodire suborbital plate ANU V79. A) specimen in lateral view B) specimen in visceral view. Specimen imaged in Blender. C–D) Line drawings of A and B showing key features. Scale bar represents 10mm. Abbreviations: aup, autopalatine part of palatoquadrate; cu.so, cutaneous sense organ; hc, horizontal sensory canal; ioc, infraorbital sensory canal; pq, part of palatoquadrate; pr.sm, submarginal process; psoc, postsuborbital sensory canal; sorc, supraoral sensory canal; Y.app, Young's apparatus.

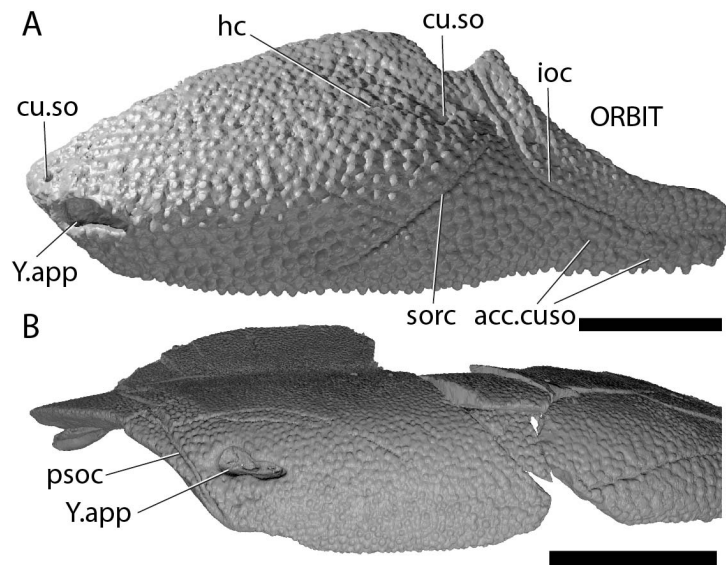


Figure 11. The Young's apparatus in two "buchanosteid" suborbital-postsuborbital plates. This unusual structure has so far only been found in these two specimens. A) ANU V244. B) ANU V79 in posterior ventral view. Scale bars represent 5mm (A) and 20mm (B). Abbreviations: acc.cu.so, accessory cutaneous sense organs; cu.so, cutaneous sense organ; hc, horizontal sensory canal; ioc, infraorbital sensory canal; psoc, postsuborbital sensory canal; sorc, supraoral canal; Y.app, Young's apparatus.

Externally the Young's apparatus is an elongate pit with a constriction, giving it a peanut-like shape (Fig. 11). In both V79 and V244 there are two recesses at the base of the apparatus, at the anterior and the middle, which connect to canals in the underlying bone (Fig. 12B; Fig. 13A–C).

The Young's apparatus in V244 is closely associated positionally with the quadrate and jaw joint (Fig. 12). Hu et al. (2017) identified a separate interhyal element sat behind the quadrate in ANU V244. Revisiting the scans shows that the quadrate and interhyal are continuous, although there is constriction in the quadrate behind the mandibular joint. Posterior to this constriction the "interhyal" portion of the quadrate enters a tunnel in the dermal bone that is continuous with the submarginal process, as described by Hu et al. (2017). The Young's apparatus sits directly above the mandibular joint (Fig. 12A,C). Various canals from the base of the apparatus and the posterior cu.so run around the quadrate or

run at the interface of the quadrate and the dermal bone (Fig. 12A). One canal from Young's apparatus pierces the constricted portion of the quadrate behind the mandibular joint (Fig. 12A).

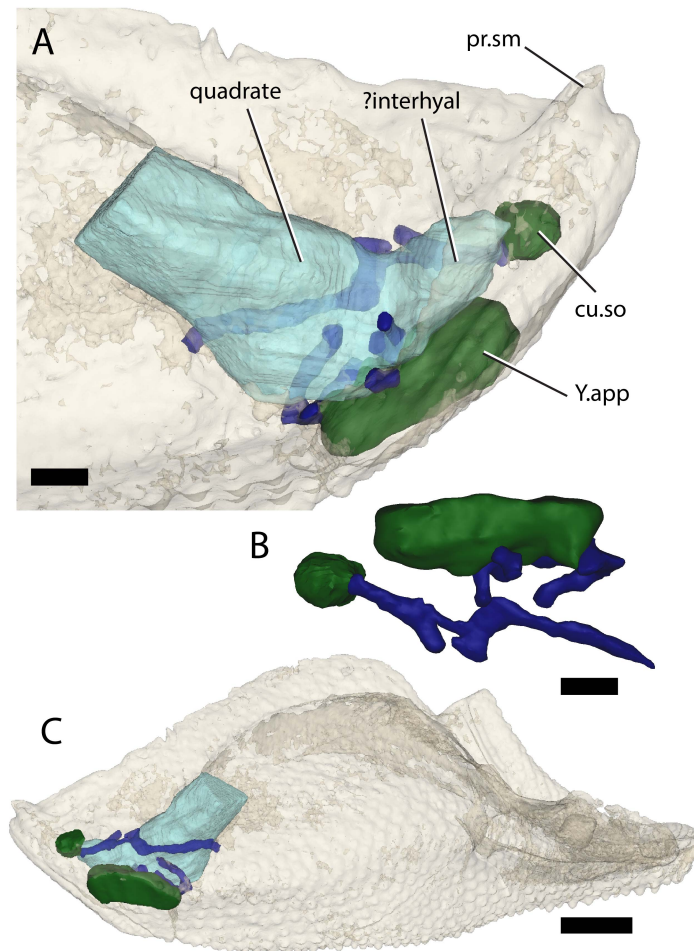


Figure 12. Internal structure of the Young's apparatus in V244, showing the close association with the quadrate. Dermal bone in beige, transparent. Quadrate in turquoise, transparent. Young's apparatus and posterior cutaneous sense organ in dark green (opaque). Canals in navy blue (opaque). A) Visceral view of the posterior part of the suborbital-postsuborbital complex. B) The Young's apparatus and posterior cu.so, with connecting canals, ventral view. C) Lateral view of the plate, showing the positions of the structures discussed. Scale bars represent 1mm (A,B) and 3mm (C). Abbreviations: cu.so, cutaneous sense organs; pr.sm, submarginal process; Y.app, Young's apparatus.

The Young's apparatus in V79 can be interpreted in light of the information from the quadrate of V244. Although the quadrate is not preserved in V79, the bone directly below the apparatus is highly cancellar (Fig. 13A, B, D), and is likely the point of contact of the

perichondral bone of the quadrate with the dermal bone. A small portion of the quadrate may be present below the Young's apparatus (Fig. 13 A, B), an interpretation supported by the canals that pierce this space (Fig. 13B, arrows). Long canals, curving in a similar shape to the postsuborbital sensory line, connect the Young's apparatus and the posterior cu.so (Fig. 13E). Above the posterior cu.so are two smaller pits (Fig. 13E, acc.cu.so). One of these is continuous with the postsuborbital sensory canal.

The Young's apparatus crosses almost the entire thickness of the plate in V79 and V244. The histology of V79 is different to the eubrachythoracid arthrodires shown in figure 5: rather than a laminar layer, the superficial layer consists of stacked tubercle generations, as reported for some buchanosteids (Burrow and Turner 1998; Giles et al. 2013). The cutaneous sense organs penetrate approximately half the thickness of the plate, but still appear to penetrate deeper than the oldest generation of overgrown tubercles (Fig. 13F).

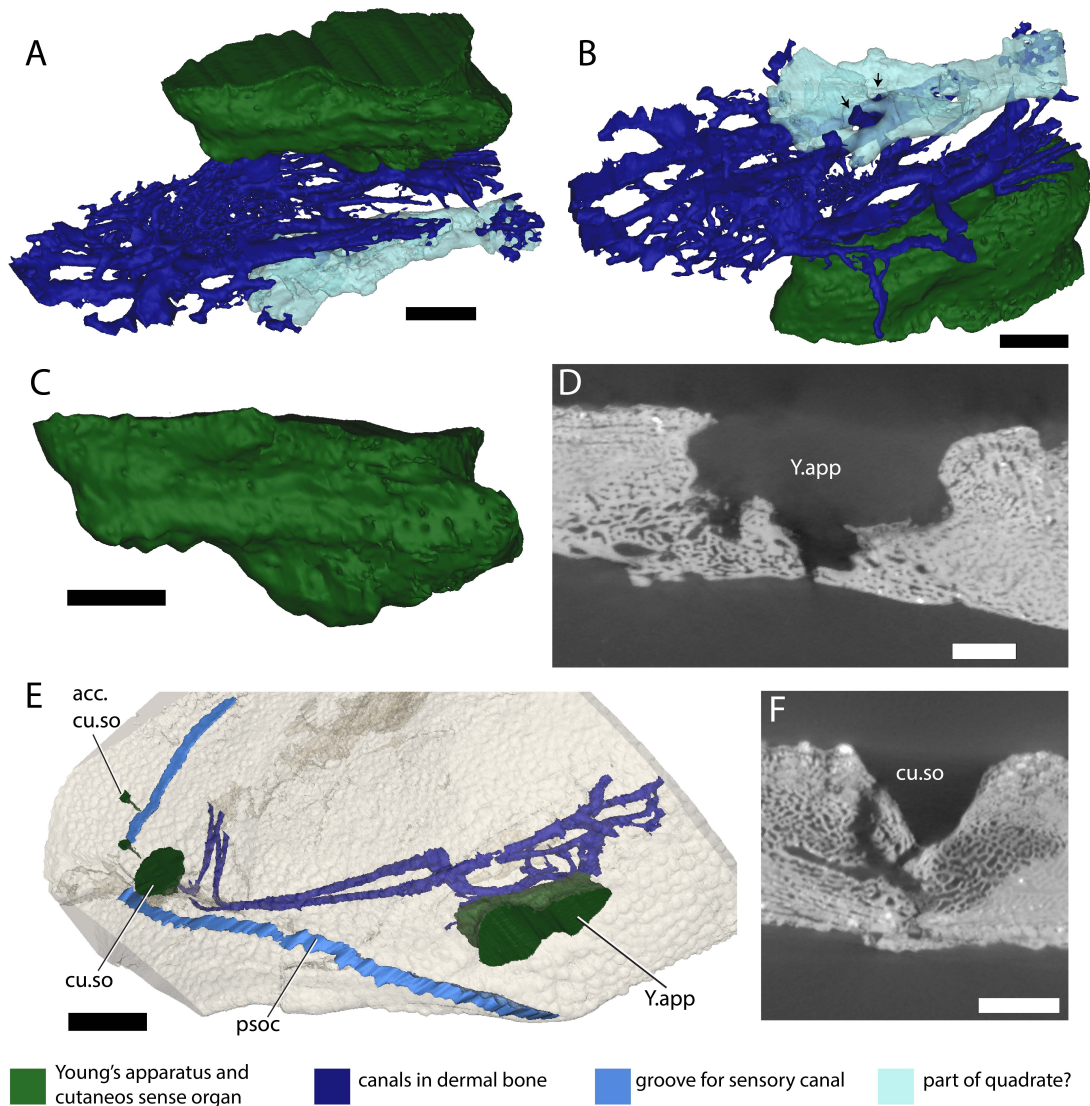


Figure 13. ANU V79 internal structure of Young's apparatus and cutaneous sense organs. A–B) The Young's apparatus (dark green) sits above a region of highly cancellar bone with many canals (navy blue). A space within the bone may represent part of the quadrate (turquoise), and canals pierce this space (B, arrows). C) The Young's apparatus (posterior to the right). Canals join to the ventral recesses in the centre and anterior of the pit. There is also a posteriorly directed recess. D) Cross section of the Young's apparatus. E) lateral view of the postsuborbital plate showing Young's apparatus, posterior cu.so and their connections. Bone in transparent beige, postsuborbital sensory canal in light blue. Canals (navy blue) connect the Young's apparatus with the posterior cutaneous sense organ. Two smaller pits are present dorsal to the cu.so (acc.cu.so). F) Cross section of the posterior cutaneous sense organ. Stacked tubercle generations are visible in the upper part of the bone. All scale bars represent 1mm. Abbreviations: acc.cu.so, accessory cutaneous sense organs; cu.so, cutaneous sense organs; psoc, postsuborbital sensory canal; Y.app, Young's apparatus.

The Young's apparatus lacks an obvious analogue in living fish, hindering functional interpretations, but the large canals (perhaps for nerves) joining the base, principally in two positions, might suggest a sensory function. Possible comparisons are with various specialised mechanoreceptor systems, such as the vesicles of Savi of various dorsoventrally flattened elasmobranchs (Barry and Bennett 1989), or the submandibular organ of *Potamotrygon* (Szabo et al. 1972). Structurally vesicles of Savi are pits with neuromast organs sitting in depressions at their base, and by comparison the two depressions at the base of the Young's apparatus may have held neuromast organs. The position of the Young's apparatus on the skull suggests that possible functional roles may have been to detect movement of the cheek relative to the skull roof or movement of the cranial-thoracic joint, through pressure changes on the apparatus that occur during joint movement. As with other structures reviewed for placoderms, the position of the Young's apparatus makes an electroreceptor interpretation difficult to support.

Ventral sulci in arthrodires

The interolateral plates of many arthrodires possess a ventral sulcus (Fig. 14), a transverse groove on the ventral lamina. Ventral sulci are present in most basal arthrodires, but are only known in coccosteids within the eubranchyothoracids (Zhu et al. 2015: character 121). Miles (1965) suggested these may contain neuromasts or cutaneous sense organs analogous with cu.so pits of arthrodire cheek plates. However, as discussed above, there is little evidence to support an electroreceptor identity for cu.so pits. In addition, the position of these sulci (posterior to the branchial chamber on the ventral surface), would be highly unusual for a group of electroreceptors. We consider it highly unlikely that the ventral sulci of arthrodires contained electroreceptors.

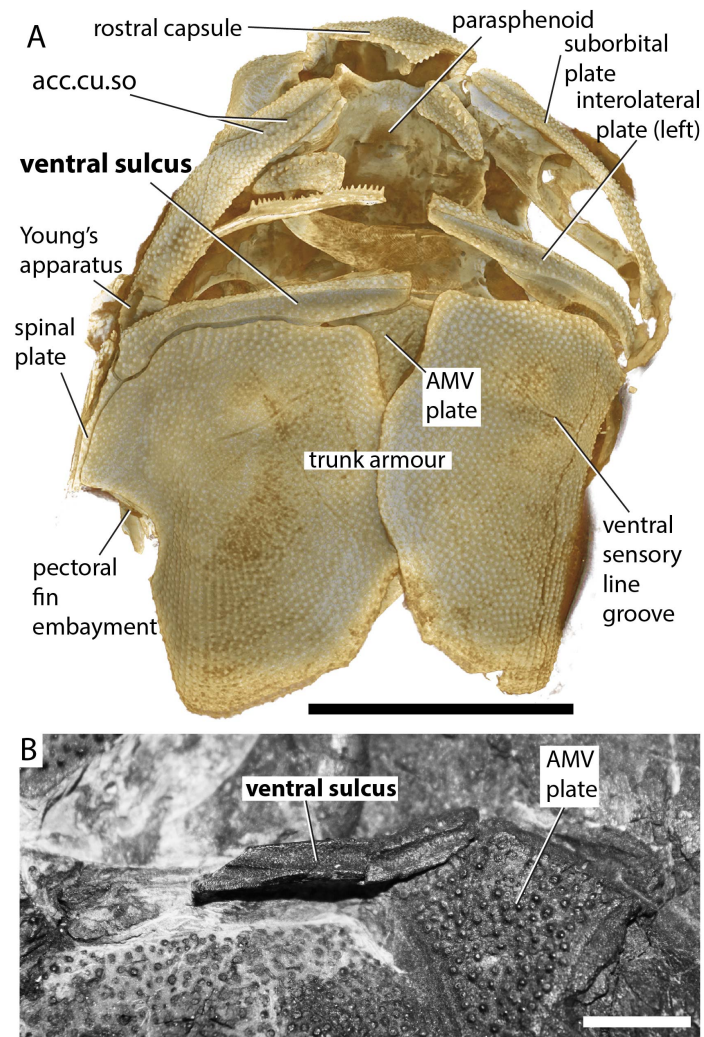


Figure 14. Ventral sulci on the interlateral plates of arthrodires. A) “bucanosteid” ANU V244 in ventral view, adapted from Hu, *et al.* (2017). Imaged using Drishti. B) *Dickosteus threiplandi*, (NMS 2003.21.1). Close-up of sulcus on right interlateral plate, ventral view. Scale bars represent 5mm (A) and 10mm (B).

Chang’s apparatus in yunnanolepid antiarchs

The yunnanolepidid antiarchs *Yunnanolepis* and *Phymolepis* have a pore and cavity on the trunk shield called the Chang’s apparatus (Zhu 1996). The Chang’s apparatus occurs at the junction of the anterior ventrolateral plate and the anterior dorsolateral plates, on a vertical ridge at the anterior edge of the trunk armour; internally it forms a blind-ending tube. A small anterior lateral plate covers the opening for the Chang’s apparatus in *Phymolepis*, so

that the opening is obscured in lateral view. Zhu (1996) suggested that the Chang's apparatus housed ampullary electroreceptors, or that it was glandular and performed a role in mucus secretion. The function of the Chang's apparatus remains open to interpretation, although the position of this apparatus is not consistent with an electroreceptor identification.

Osteichthyans (bony fish)

The pore canal system and cosmine

The dermal skeleton of many early sarcopterygians is characterised by cosmine, a covering of dentine and enamel containing a pore canal system (Ørvig 1969; Thomson 1975; Meinke 1984). The pore canal system involves a horizontal network of mesh canals in the dentinous layer, with vertical pore canals opening to the surface (Fig. 15A, B). Thomson (1977) suggested an electroreceptive function for the pore canal system, based on a detailed study of cosmine in *Ectosteorhachis* (Thomson 1975). He argued that since sensory lines are well-developed in the fossils, the pore canal system was unlikely to also have housed neuromasts. While the structure of the pore-canal system was acknowledged to be significantly different from that of the ampullae of Lorenzini, the size and spacing of electroreceptors in freshwater teleosts was considered comparable. Furthermore, it was suggested that the pore canal system housed tonic electroreceptors (=ampullary receptors, sensitive to low frequency AC and DC fields), while the larger "pore-group" receptors of osteolepids and other sarcopterygians (discussed in the next section) housed phasic electroreceptors (=tuberous receptors, sensitive to high frequency AC fields used for communication). In modern mormyrids, tuberous receptors are indeed larger than the ampullary organs (Bennett 1971), but the identification of tuberous receptors in osteolepids remains largely speculative.

Against the idea of the pore canal system being electroreceptive is the fact that the pores are more densely spaced posteriorly (Thomson 1977), in the direct opposition to the pattern seen in all modern electroreceptive vertebrates (Borgen 1992). In addition, as pointed out by New (1997), connections between adjacent ampullae, as seen in the pore canal system, would nullify the spatial resolution of the system. This is because each canal would no longer be insulated from the rest, so that the whole network would become isopotential.

Studies on the living lungfish *Neoceratodus* do not support an electroreceptive function for the pore canal system (Bemis and Northcutt 1992). Although *Neoceratodus* lacks cosmine, Bemis and Northcutt (1992) described a rich array of cutaneous blood vessels in the epidermis of the snout, supplying dermal papillae (capillary loops in connective tissue).

Similar capillary loops were found in the hypermineralised tooth plates of *Neoceratodus*. On this basis, they argued that dermal papillae are vestigial organs involved in the deposition of dentine. Under this hypothesis this process is halted in an early stage of development in modern lungfish, before the deposition of mineralised tissues (Bemis and Northcutt 1992).

The hypothesis that the pore canal system is involved in deposition of mineralised tissue perhaps fits better with certain observations on cosmine development. Cosmine bears no developmental relation to the underlying dermal bone and is uninterrupted across sutures between bones. This causes problems with growth and it is generally thought that cosmine went through cycles of growth and redeposition (Westoll 1936; Gross 1956; Fig. 15C).

Resorption may start at the cosmine pores (Borgen 1989). Based on the incomplete covering of cosmine in larger individuals of *Ectosteorhachis* (see also Figure 15C for *Megalichthys*) it was suggested that cosmine acts as a store for excess phosphates that could be mobilised at certain times, perhaps during the breeding season (Thomson 1975). If this is the case then an efficient system for deposition and resorption as proposed by Bemis and Northcutt would

be expected, and the pore canal system may be associated with this function. Overall, the pore canal system appears unlikely to have housed electroreceptors.

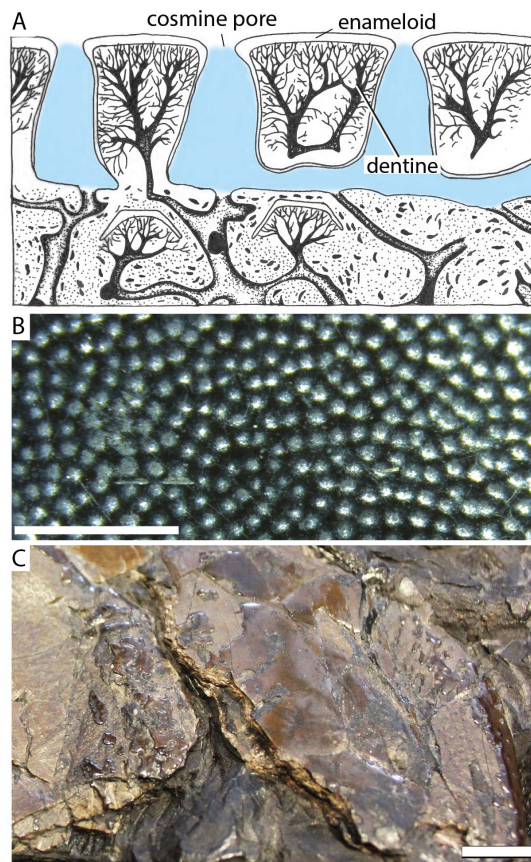


Figure 15. Cosmine and cosmine resorption. A) Cross-sectional structure of cosmine, after Ørvig (1969). The pore canal system is highlighted in blue. A horizontal mesh of canals in the dentine layer joins to the surface via pore canals. B) Cosmine pores on the skull of *Megalichthys hibberti* (NMS 1957.1.5688). C) Incomplete covering of cosmine on the right squamosal and right hand side of the postparietal shield in *Megalichthys hibberti* (NHMUK P11554). Scale bars represent 2mm (B) and 10mm (C).

Rostral tubuli in lungfish

The rostral and symphyseal tubuli of fossil lungfish (Fig. 16) were first identified by Thomson and Campbell (1971) in *Dipnorhynchus*. Rostral tubuli occur in the snout and mandible, and consist of a series of mineralised, branching tubules forming a plexus beneath the dermal exoskeleton. (Thomson and Campbell 1971; Fig. 16A–B). They connect with the pore canal

system and also extend internally to open into the nasal capsule or meckelian cavity (Miles 1977; Cheng 1989). Recently rostral tubuli have also been found in the non-dipnoan taxa *Gogonasus* and *Qingmenodus* (Holland 2014; Lu et al. 2016).

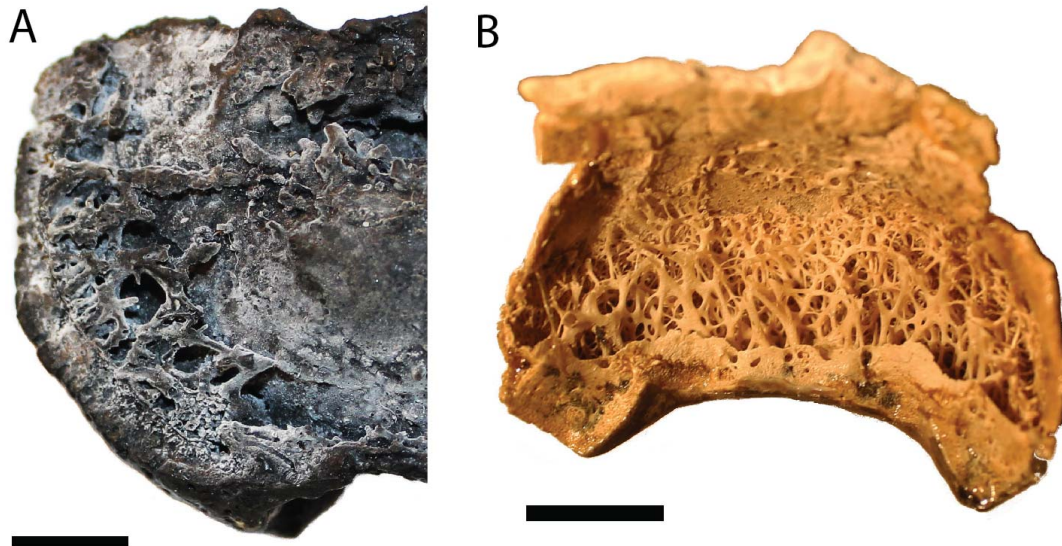


Figure 16. Rostral tubuli on the snout of Devonian lungfish. A) *Dipnorhynchus kurikae*, anterior part of skull in left lateral view (ANU V48676). Dorsal covering of dermal bones abraded, revealing rostral tubuli in the anterior part of the snout. Note the sharp discontinuity between the rostral tubuli and the dermal bone on the anterior margin. B) *Chirodipterus australis*, inside of dermal snout bones in posteroventral view, showing rostral tubuli (NHMUK P50101). Both scale bars represent 10mm.

Although it has been proposed that rostral tubuli housed ampullae of Lorenzini (Thomson and Campbell 1971; Campbell and Barwick 1986), the branching structure of the tubules, forming a plexus, does not fit this hypothesis. Alternatively, Cheng (1989) proposed that the tubuli were a part of the lateral line system, in part because they have a similar histological structure to the lateral line canals. However, the rostral tubuli appear to carry nerves: specifically the profundus, superficial ophthalmic and buccal nerves (Miles 1977; Challands 2015). Campbell et al. (2010) also argued that rostral tubuli carried nerves, as they connect with the lateral line canals, and some tubules open through the dorsal wall of the nasal cavity as found for nerve bundles in *Neoceratodus* (Bartsch 1993). Although it is unlikely that

the rostral tubuli themselves housed electroreceptors, they may have supplied nerves to electroreceptors (see below).

An alternative view is that the rostral tubuli carried lymphatic vessels (Bemis and Northcutt 1992; Kemp 2014; Kemp 2017). The snout of *Neoceratodus*, the Australian lungfish, has unmineralised tubules that form a double plexus in the dermis which may be comparable to rostral tubuli, first interpreted as blood vessels (Bemis and Northcutt 1992), but later found to be lymphatics (Kemp 2014; Kemp 2017). At present it is difficult to reconcile the data from living lungfish (suggesting rostral tubuli are lymphatics) and fossil lungfish (suggesting they are nerves). However, given the clear connections with the neurocranium and sensory line canals (Campbell et al. 2010; Challands 2015), we assume that at least part of the rostral tubuli carried nerves for our interpretation of the “pore-group” pits (see below).

‘Pore-group’ clusters in sarcopterygians

A more likely candidate for electroreceptors in sarcopterygians are the ‘pore-groups’, first identified by Jarvik (1948), who compared them to ampullae of Lorenzini. He identified clusters of pits near sensory canals or pit-lines on the lower jaw, lachrymal, jugal, postorbital, squamosal, fronto-ethmoidal shield and the branchiostegal rays of the osteolepid tetrapodomorph fishes *Osteolepis*, *Gyroptychius* and *Thursius* (fig. 17A–B). The pores are intermediate in size between those of the sensory canals and the cosmine pores, and fine canals lead from their bases (Jarvik 1948). Similar pores have been found in a number of basal tetrapodomorph fishes, including *Kenichthys* (Chang and Zhu 1993), *Tungsenia* (Lu et al. 2012), the canowindrid *Koharalepis* (Young et al. 1992; Fig. 17D) and the megalichthyids *Megalichthys* (Bjerring 1972; Fig. 17C), *Mahalalepis* (Young et al. 1992) and *Cladarosymblema* (Fox et al. 1995). Pore group clusters resembling those of osteolepiforms have also been found in the early Devonian *Powichthys* (Jessen 1975), and *Youngolepis*

(Zhang and Yu 1981), which are basal dipnomorphs, the lineage that includes lungfish (Lu et al. 2012) .

Pore group clusters are good candidates for electroreceptors. They occur close to sensory lines and are particularly densely distributed around the snout (Fig. 17A). They occur in fossil sarcopterygians with cosmine. Cosmine, with its covering layer of enamel, may allow superficial structures that do not typically leave an impression in dermal bone to be preserved. The pit clusters, including the variability in the size of the pits, resemble the electroreceptor pit clusters in the paddlefish *Polyodon* (Jørgensen et al. 1972; Fig. 17E). The internal structure of the pore-group clusters has been investigated in the tetrapodomorph *Megalichthys* using serial grinding techniques (Bjerring 1972). This revealed that the pore group on the supratemporal bone is connected to a dorsally branching canal that pierces the ventral surface of the bone (Fig. 17F). The canal at the base of the pore groups lies in close proximity to canals at the base of the sensory canal (Fig. 17F: ot.lat), and on this basis was inferred to have carried a branch of the otic lateral line nerve (Bjerring 1972). Although Bjerring's suggestion was that the pore-groups might supply thermoreceptors, the available evidence suggests that pore-groups may be electroreceptors. The results from serial grinding of *Megalichthys* are consistent with results from CT scanning pore-group pits in lungfish, presented in the next section, which provide additional evidence that pore-group pits are electroreceptors.

The cosmine-coated osteolepiform *Gogonasmus* does not have pit clusters (Long et al. 1997), and it was suggested that this may be due to water salinity, although this interpretation does not fit with comparisons of marine and freshwater species in extant taxa (see above). Presence of pore-groups in *Powichthys* and *Youngolepis* shows that these clusters can be found in marine species. *Gogonasmus* also has a cavity in the neurocranium that has been

compared to the rostral organ of coelacanth (Holland 2014), but this lacks connections to the surface.

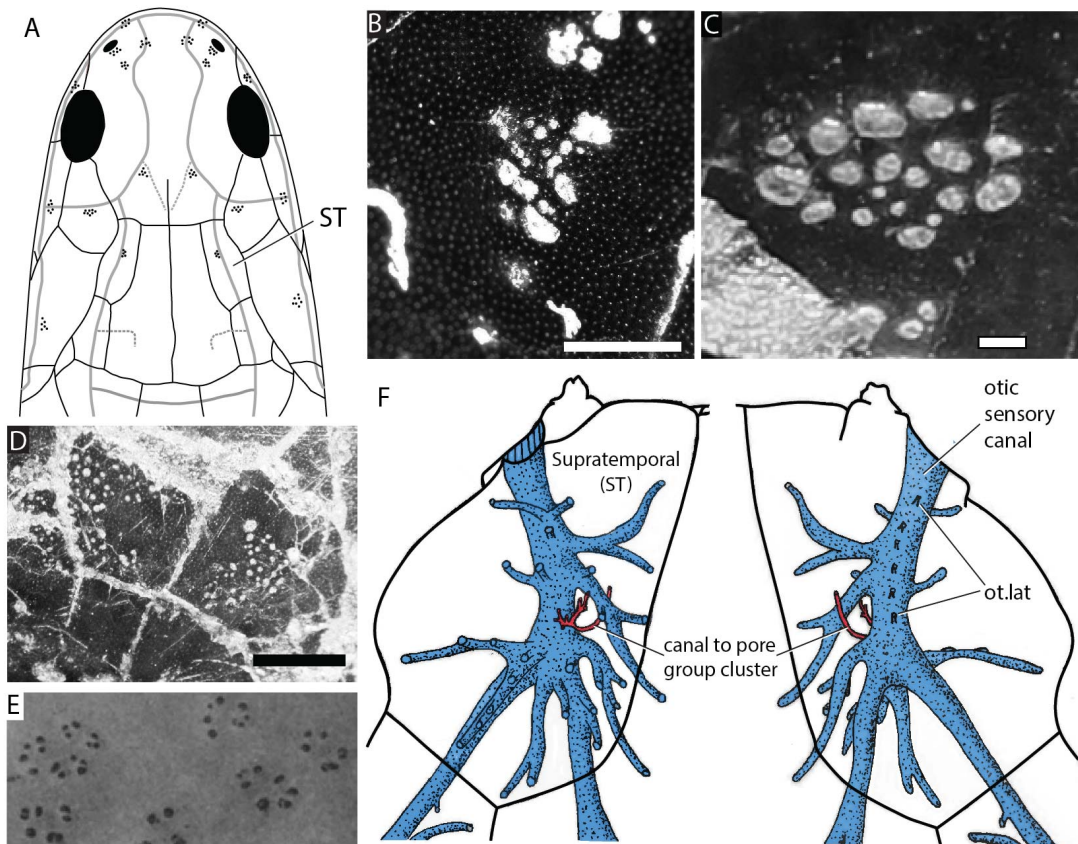


Figure 17. Pore group clusters in fossil sarcopterygians, compared with the electroreceptor clusters of the extant paddlefish. A) Diagram of dorsal skull roof of a generalised osteolepidid, after Jarvik (1948), showing locations of pore group clusters. These are closely associated with sensory lines. B) Pore group cluster on snout region of *Gyroptychius milleri* (NMS 1895.185.25). C) Pore group cluster in *Megalichthys intermedius* (NHMUK P3303). D) Pore group clusters in *Koharalepis* (AM F54325). E) Electroreceptor pore cluster in the skin of the paddlefish *Polyodon spathula*, reused with permission from Jørgensen, *et al.* (1972). F) Dorsal (left) and ventral (right) view of canals within the supratemporal bone of the tetrapodomorph *Megalichthys*. The sensory canal is in blue, and the dorsally branching canal at the base of the pore group cluster in red. Redrawn and adapted from Bjerring (1972). Scale bars represent 1mm (B, C) and 10mm (D). Abbreviations: ot.lat, branches of the otic lateralis nerve; ST, supratemporal bone.

New information on lungfish “pore-group” pits

“Pore group” pits are also known from the skulls of lungfish where they are often so numerous on the snout that they do not form obvious clusters (Jarvik 1950; Ørving 1961; Bemis and Northcutt 1992). In some specimens of *Chirodipterus*, many of the pores on the snout appear to occur in pairs (Campbell et al. 2010). In *Rhinodipterus* pore clusters are found on the jaw and gular bones in addition to the skull (Ørving 1961), and clusters of pits occur on the operculum of the lungfishes *Howdipterus* and *Barwickia* (Long 1992).

The “pore-group” pits are intermediate in size between the cosmine pores and the lateral line pores and are densely distributed on the snout alongside the lateral line pores (Ørving 1961; Bemis and Northcutt 1992; Fig. 18). The pores are variable in size: those on the downturned tip of the snout are larger than those further dorsally (Ørving 1961; Gross 1965; Bemis and Northcutt 1992; Fig. 18C). The smaller cosmine pores are less abundant or absent anteriorly (Bemis and Northcutt 1992). The size, distribution and number of “pore-group” pits in fossil lungfish are consistent with their identification as electroreceptors (Bemis and Northcutt 1992). In extant lungfishes, electroreceptor pores also increase in size at the tip of the snout (Kemp 2014).

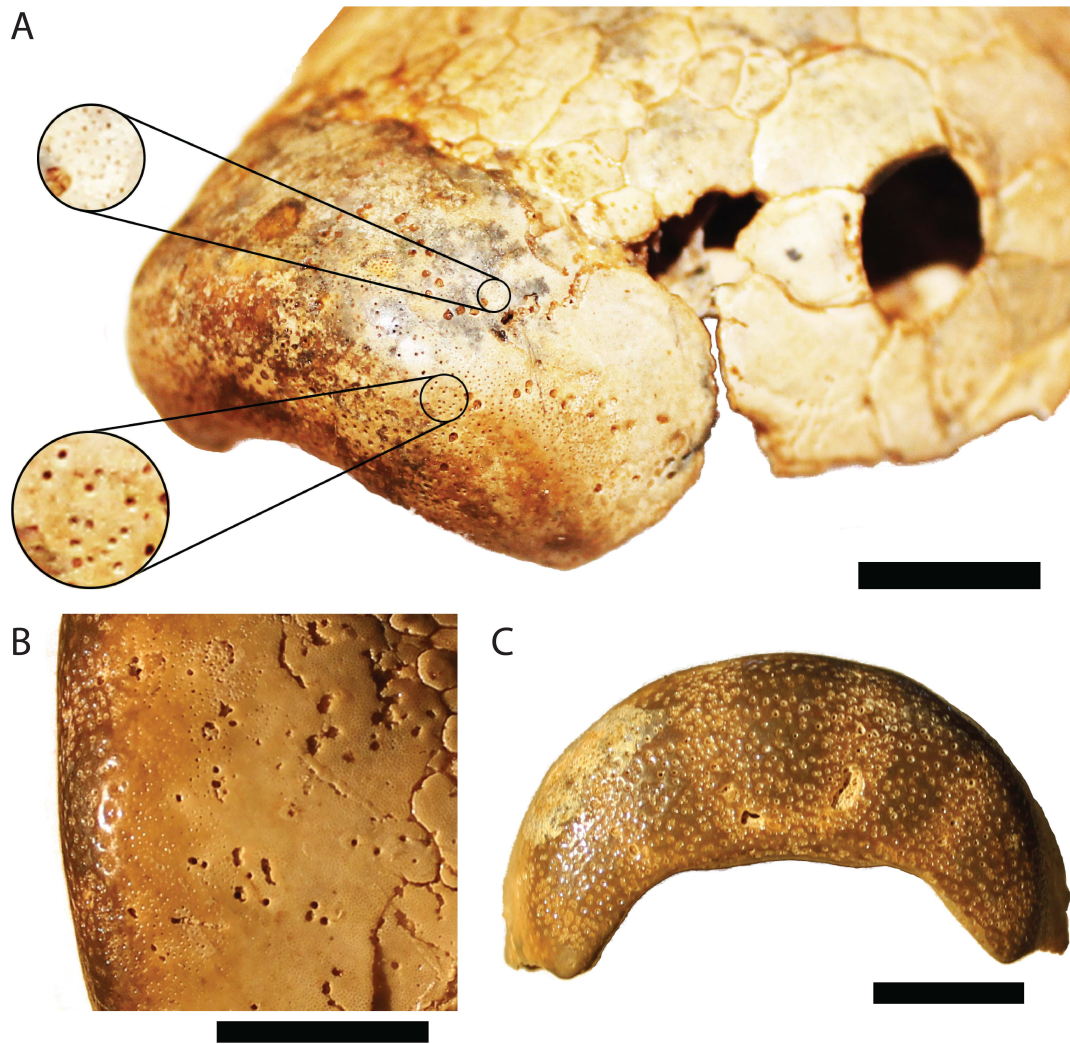


Figure 18. Numerous pore-group pits on the snouts of Devonian lungfishes. A) *Chirodipterus australis*, skull in left antero-dorsal view (ANU 21634a). Pores on the snout are densely distributed around the lateral line pores, and some appear paired. B) *Chirodipterus australis* in dorso-lateral view, showing pore-groups clustered around sensory line canals (NHMUK P50101). C) Same specimen as B, anterior view showing enlarged pores, with highest density around the sensory lines. All scale bars represent 10mm.

CT scans reveal new information on the internal structure of the “pore-group” pits in the lungfish *Speonesydrion* (Figs. 19–21). As with other fossil lungfish snouts, cosmine pores are numerous at the posterior of the specimen but are rare or absent anteriorly. Pore-group pits are most densely distributed around the lateral line pores anteriorly (Fig. 19).

Internally, the structure of the dermal bone is as reported by Cheng (1989) for the snout *Chirodipterus*: the cosmine layer is underlain by cancellar bone, and a basal laminar layer is absent. There is a sharp discontinuity between the underlying rostral tubuli and the dermal bone, as previously reported (Cheng 1989; Campbell and Barwick 2000; Campbell et al. 2010).

The shape of the pore-group pits is suggestive of an electroreceptive function. The external part of the pore-group pits, within the cosmine layer of the dermal bones, resembles that of the smaller cosmine pores. They are constricted dorsally, appearing triangular in cross-section. The “pore group” pits differ from the cosmine pores in that each one continues in the upper part of the cancellar bone (Gross 1965; Schultze 2016; Fig. 20A,D). The combination of the dorsally constricted part in the cosmine and the canal in the cancellar bone gives the “pore-group” pits the overall shape of an arrow (Fig. 20, 21). The pore-group pits show evidence for ampullae at the base: some of the clearer examples for *Speonesydrion* are shown in figure 21A. These ampullae sit in the cancellar bone layer. The depth from the surface to the base of the ampullae is approximately 500–720 microns (n=7 pits). The diameter of the canals in the constricted part above the ampullae is 170–280 microns on the anterior part and 110–250 microns posteriorly. *Chirodipterus* also shows evidence for ampullae, giving the pits a flask-shape (Fig. 21B). The flask shape of the pores in *Speonesydrion*, *Chirodipterus* and *Griphognathus* is also clearly visible in figures 8, 13, 15 and 17 of Campbell et al. (2010).

Canals connect the rostral tubuli with clusters of pore-group pits (Fig. 20B–D, 21B). Clusters of pits are supplied by an upwardly branching system of canals emanating from a single opening of a rostral tubule. These clusters vary in number: clusters with between two and six pits have been observed but larger clusters may exist. In *Chirodipterus*, many of the pores are paired (Campbell et al. 2010; Fig. 18A), but pore groups are not universally paired in

Chirodipterus or *Speonesydrion* (Fig. 18B, 19). As previously reported (Campbell et al. 2010), some of the rostral tubuli cross the discontinuity between the dermal bone and the underlying neurocranium. The upwardly branching system of canals at the base of the pore-group pits may have housed a nerve supply from the rostral tubuli, although it should be noted that these have also been suggested to carry vessels (see above).

In summary, the morphological evidence presented here supports the identification (based on size and distribution) by Bemis and Northcutt (1992) that the pore-group pits are electroreceptors. They meet the criteria listed above for the identification of electroreceptors in fossils: the size, distribution (concentrated on the snout and around lateral line canals) and the possible presence of ampullae are all consistent with an electroreceptor identification. As noted by Campbell et al. (2010), the pore-group pits have differing orientations, as do the electroreceptors of modern species. Rostral tubuli communicate with the lateral lines and presumably carried nerves (Miles 1977; Campbell et al. 2010; Challands 2015, but see discussion on rostral tubuli above), and it is likely that lateral line nerves also innervated the pore-group clusters via the rostral tubuli. Finally, although the depth and diameter of the pore group pits is larger than the values reported for living lungfish (Roth and Tschardt 1976; Kemp 2014), this might be expected given that the fossils dealt with here are marine species (see above for explanation of differences between electroreceptors in marine and freshwater species).

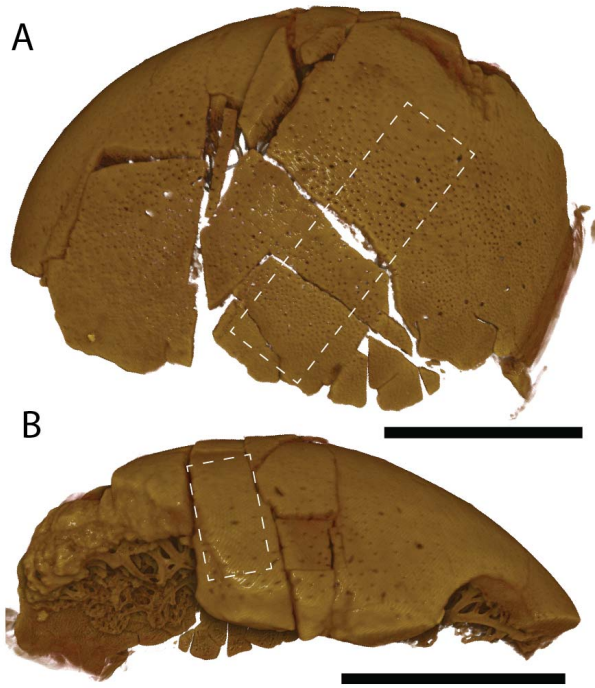


Figure 19. The snout of the lungfish *Speonesydrion iani* showing pore groups. A) Dorsal view of specimen ANU 49340. B) anterior view of same specimen. Areas with dashed white borders indicate the segmented regions (see figure 20). Images from Drishti. Both scale bars represent 10mm.

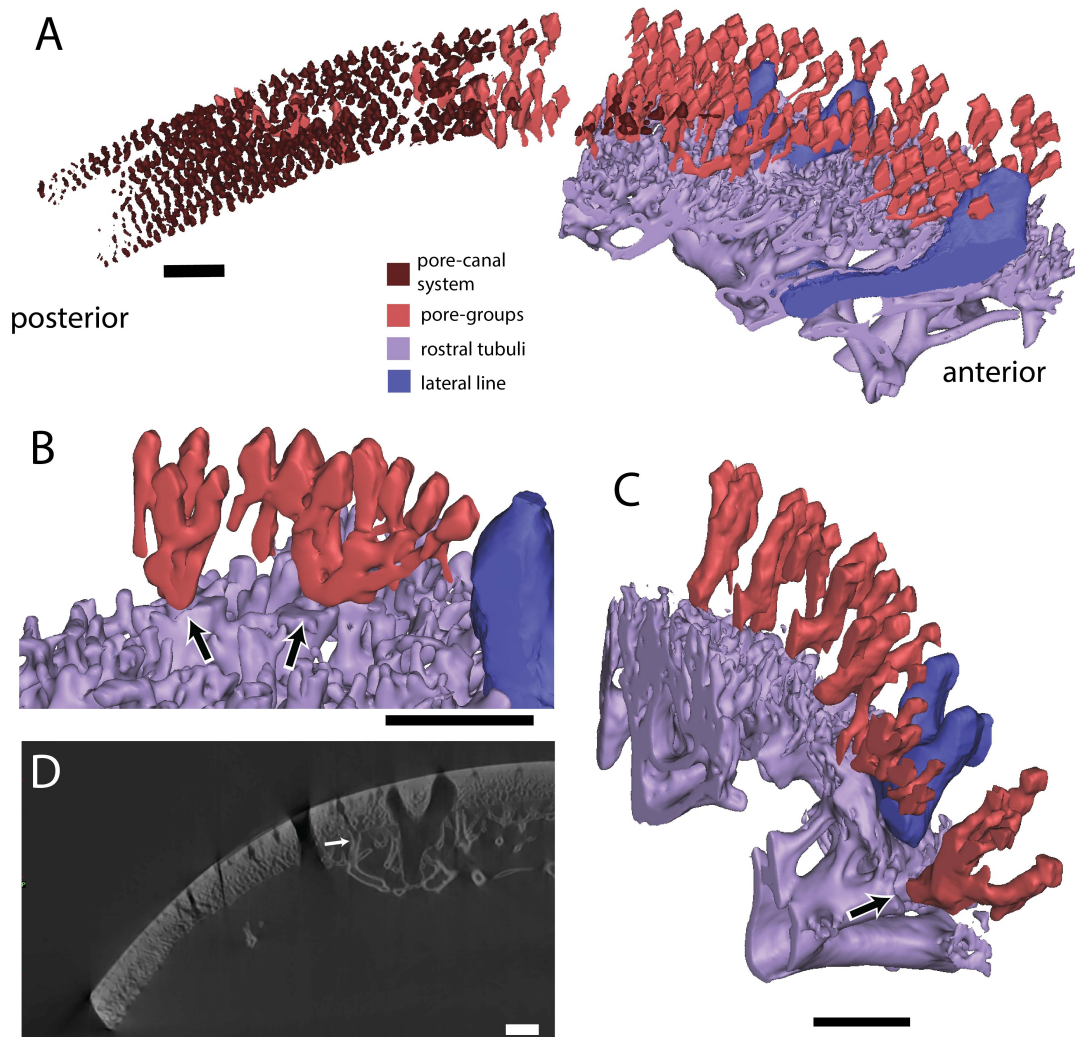


Figure 20. Internal structure of pore-group pits in the lungfish *Speonesydrion iani*, and their connections to rostral tubuli. A) Internal model of a dorsal region of the snout (outlined in figure 19A). Cosmine pores (burgundy colour) become less common anteriorly, while pore-group pits (light red) become more common. Rostral tubuli are in lavender colour and sensory lines and pores in blue. B) Two individual clusters of pore-group pits from figure A, showing their connections to a single opening of the rostral tubuli (arrow). C) Internal model of a region of the anterior part of the snout (outlined in figure 19B). Connection of a cluster of pore-group pits to an opening of the rostral tubuli is indicated with an arrow. D) Cross-section of the dorsal part of the snout (through figure A). Connection of the rostral tubuli to canals joining the base of a pore-group cluster is indicated with an arrow (equivalent to right-hand arrow in figure B). Specimen ANU 49340, imaged in Mimics. All scale bars represent 1mm.

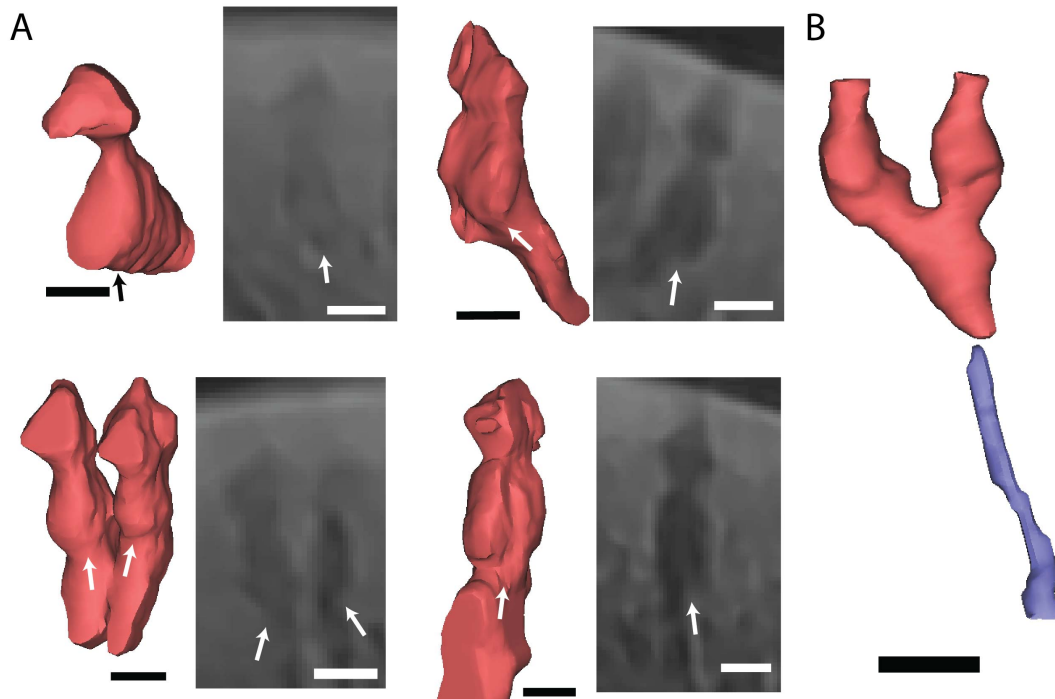


Figure 21. Possible ampullae at the base of pore-group pits in fossil lungfish.
 A) *Speonesydrion iani*, ANU 49340. Pore-group pits from anterior region of snout (outlined region in figure 19B). Arrows indicate possible ampullae with canals continuing in the underlying bone. B) *Chirodipterus australis* (ANU V1710). Pair of pore-group pits indicating flask-like shape (possible ampullae) and connections to underlying rostral tubule (lavender colour). Scale bars represent 200 μm (A) and 500 μm (B).

The rostral organ in coelacanths

The presence of a rostral organ in fossil coelacanths can be inferred from the presence of large foramina in the skull bones, similar to the pores for the rostral organ in the extant *Latimeria* (Forey 1998; Fig. 22A). These are present in coelacanths of Devonian age: *Miguashaia*, *Gavinia*, *Euporosteus* and *Diplocercides* (Cloutier 1996; Forey 1998; Long 1999; Fig. 22B). These taxa are the earliest coelacanths known from relatively complete remains, and they are also the most basal taxa in coelacanth phylogeny (Zhu et al. 2012). In addition to openings through the dermal bones, *Euporosteus* also preserves the anterior portion of the neurocranium, in which a median cavity for the rostral organ has been reconstructed (Jarvik 1942), and rostral organ pores are visible on the external surface (Jarvik 1942; Forey

1998; Fig. 22B). Although the anterior part of the neurocranium of *Diplocercides* (= *Nesides*) is incomplete, there is a notch which has been interpreted as the opening for the posterior inferior rostral organ tube (Jarvik 1980; Forey 1998). In contrast to modern coelacanth in which the anterior rostral organ pore passes through the median rostral bone and the posterior pores lie ventral to the posterior tectal (Forey 1998), those in early fossil coelacanth pass through the premaxilla and preorbital respectively (Cloutier 1996; Forey 1998; Long 1999). However, although the association of rostral organ pores with particular dermal bones has changed, the number and position of these rostral organ pores has apparently remained constant for nearly 400 million years of evolution, and a rostral organ was present in the earliest recognizable coelacanth.

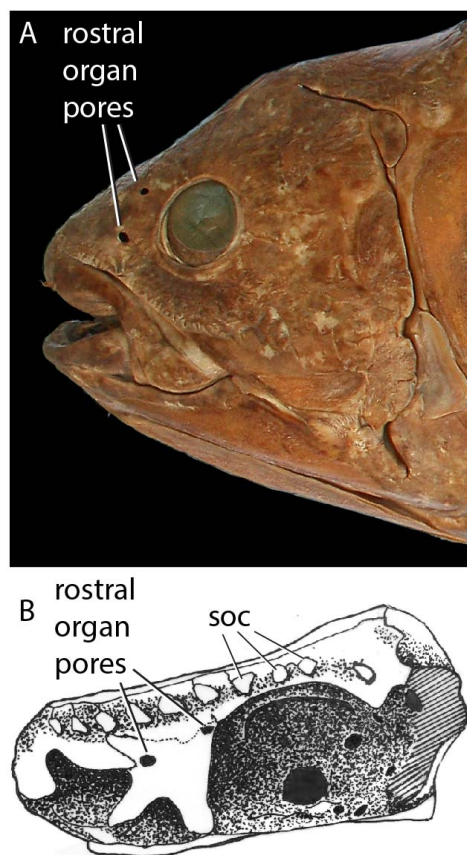


Figure 22. The rostral organ in living and fossil coelacanth. A) Head of *Latimeria chalumnae* showing the two posterior openings for the rostral organ. B) Drawing of the ethmosphenoid of *Euporosteus eifeliensis* in left lateral view, showing openings for the rostral organ. A) From the Digital Fish Library (www.digitalfishlibrary.org), with permission. B) Redrawn after Forey (1998).

Early actinopterygians and a possible stem osteichthyan

In early actinopterygians, potential electroreceptor pits have been identified on skull bones in *Howqualepis* (Long 1988b). The enigmatic early osteichthyan "*Ligulalepis*" (Basden et al. 2000; Basden and Young 2001) has similar structures above the orbits (Fig. 23). The phylogenetic position of *Ligulalepis* is uncertain, and it may be a stem osteichthyan rather than an actinopterygian (Friedman 2007; Friedman and Brazeau 2010). Here it is discussed alongside *Howqualepis* for convenience and due to the similarity of the structures under discussion.

In *Ligulalepis*, the pits are found on both sides of the skull above the orbits (Fig. 23A), although the distribution is not strictly symmetrical. There are two main groups: a line alongside the supraorbital sensory canal, and a second group around the intersection of the otic and infraorbital sensory canals (Fig. 23A). The size and shape of individual pits are variable. In "*Ligulalepis*" some of the pits, particularly the posterior group, have very small openings, so they are barely visible in dorsal view. The pits fully penetrate the bone (Fig. 23B) and their bases are expanded, (Fig. 23D), which may hint at the presence of ampullae. Two of the pits on the left hand side have connecting canals at their base (Fig. 23C). One connects to a branch of the otic nerve that also innervates the sensory line (Fig. 23C, arrow 1). The other (arrow 2) runs mesially, and although it cannot be followed through, it may arise at the base of the superficial ophthalmic nerve. It is therefore likely that lateral line nerves innervate these pits.

The pits of *Howqualepis* also vary in size (Fig. 23E) and in distribution between specimens (Long 1988b). They do not appear to have expanded bases (Fig. 23E), but the nature of the material (latex peels from natural moulds) makes this hard to judge.

The distribution of the pits in both *Howqualepis* and *Ligulalepis* alongside sensory line canals, the expanded bases of the pits in *Ligulalepis* and the likely innervation by lateral line nerves suggest that they may house electroreceptors. This was originally suggested for *Howqualepis* by comparison with the sturgeon *Scaphirhynchus* (Weisel 1978; Long 1988b). A caveat is that these structures are mainly present on the dorsal skull roof, and are not found on the anterior part of the snout, although this is incomplete ventrally and no lower jaw is known for “*Ligulalepis*”.

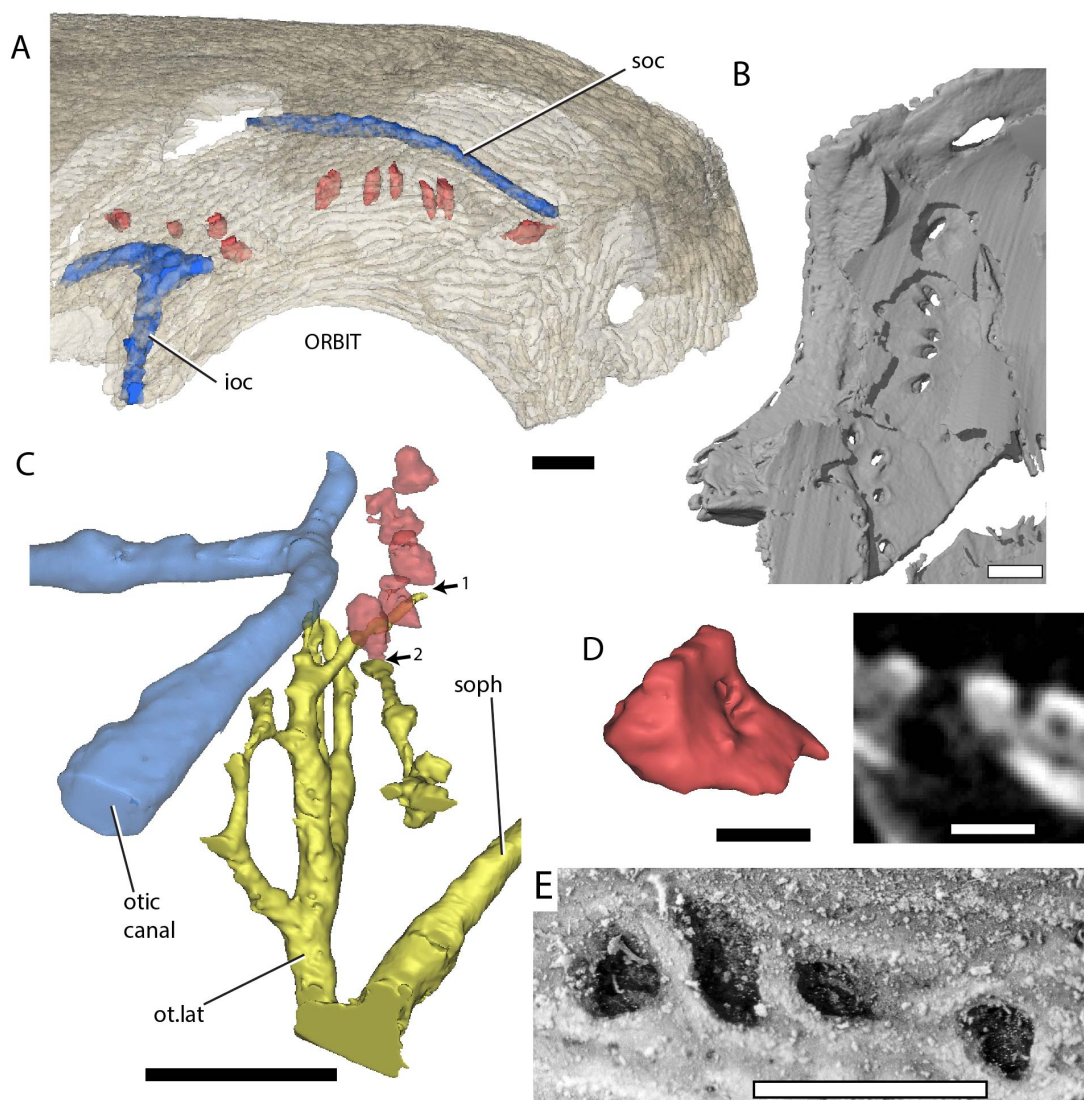


Figure 23. Possible electrosensory pits in the early osteichthyan “*Ligulalepis*” and the early actinopterygian *Howqualepis*. A) Right lateral view of the skull of “*Ligulalepis*” (ANU V3628). Dermal bone transparent, showing an irregular series of pores above the orbit (in red) alongside sensory line canals (blue). B)

Visceral view of dermal skull roof, showing openings on the right hand side of the skull. C) Internal structure above the orbit on the left side of the skull, in posterior-mesial view. One of the pit structures is connected via a canal at its base (arrow number 1) to a branch of the otic nerve, which innervates the sensory canals. The most posterior pit also has a canal at its base (arrow 2). Although this is incomplete ventrally, it may be a dorsal branch of the superficial ophthalmic nerve. D) Internal model and cross section of a pit from the left-hand side of the skull, anterior view, showing the expanded base. E) Series of pits above the orbit in the actinopterygian *Howqualepis rostridens* (latex peel of NMV P160780, whitened with ammonium chloride). Scale bars represent 1mm (A-C, E) and 200 μ m (D). Abbreviations: ioc, infraorbital sensory canal; soc, supraorbital sensory canal; soph, superficial ophthalmic nerve.

Early tetrapods

Possible electroreceptors are known from the Permian seymouriamorph *Discosauriscus* which possesses “foraminate pits” of approximately 1mm diameter (Klembara 1994; Fig. 24). The foraminate pits are depressions with foramina at their base (Fig. 24B). They are found alongside sensory line canals on the skull (Fig. 24A), and the position of these structures has led to comparisons with the pore-group clusters of non-tetrapod sarcopterygians (Klembara 1994), which are sometimes found in shallow depressions (Bjerring 1972). This shows the possible existence of electroreception on the amniote stem, given the possible phylogenetic position of seymouriamorphs as stem amniotes (Ruta et al. 2003).

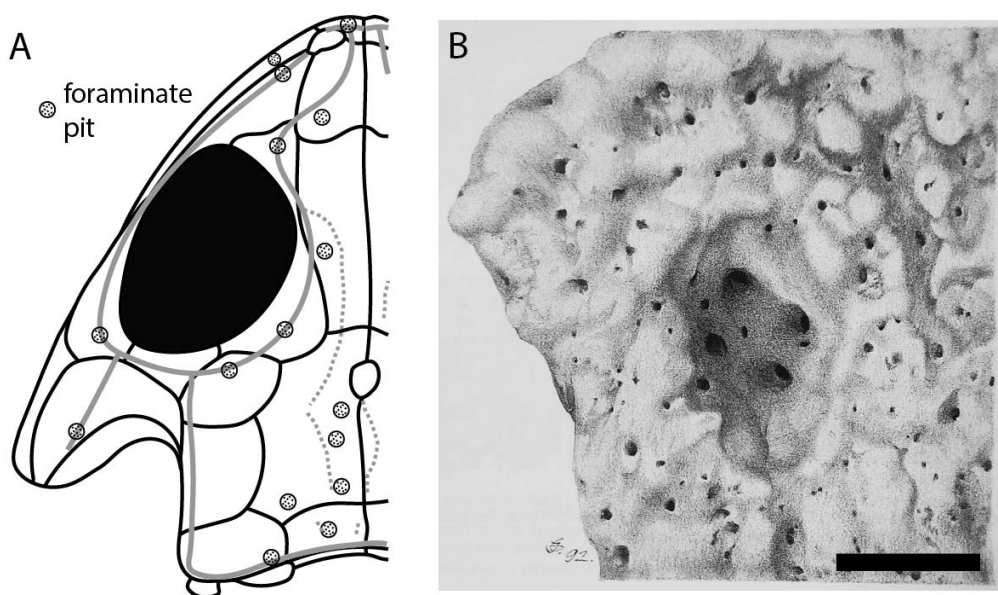


Figure 24. Foraminate pits in the seymouriamorph tetrapod *Discosauriscus austriacus*. A) Skull roof diagram, showing the position of the foraminate pits. Note the similarity to the positions of sarcopterygian “pore-group” clusters (Fig. 17A). Redrawn after Klembara (1994). B) Illustration of foraminate pit from the right parietal, from Klembara (1994), with permission. Scale bar represents 1mm.

Discussion

Preservation of electroreceptors in early vertebrate fossils

Many of the putative electroreceptors in early vertebrate fossils do not meet the criteria set out above for the recognition of electroreceptors in fossils. Osteostracan lateral fields, the pore canal system of osteostracans and sarcopterygians, placoderm cutaneous sense organs and ventral sulci and rostral tubuli in lungfish all fail to meet the criteria for the identification of electroreceptors. However, pore group clusters in cosmine-covered sarcopterygians are likely candidates for electroreceptors. The possible presence of a ramus recurrens of the anterior lateral line nerve in osteostracans also suggests the presence of electroreception. The rarity of evidence for electroreception in fossils is perhaps not surprising. With the exception of the highly specialised coelacanth, no living vertebrate has electroreceptors that leave impressions in bones. Fossil evidence for electroreception comes from the presence of a nerve in osteostracans that is thought to exclusively innervate trunk electroreceptors, and pore group clusters in sarcopterygians with cosmine. The enamel coating of cosmine may allow for preservation of superficial structures that are not usually fossilised.

There are a limited number of conclusions that can be ascertained from this evidence.

Presence of trunk electroreceptors in lampreys and osteostracans suggest that electroreceptors were initially spread out over the whole body, becoming restricted to the head in gnathostomes (and probably reversed in lungfish). The widespread presence of pore group clusters among early sarcopterygians with cosmine shows that electroreception was

possibly widely distributed at least in sarcopterygians. There is no reason to believe that electroreception was not present in many groups of early vertebrates, but the lack of preservation potential for electroreceptors means it is difficult to reach firm conclusions.

The origin of electroreception

The “new head hypothesis” of Gans and Northcutt (1983) argues that all vertebrate synapomorphies are produced by neural crest, cranial placodes and muscularised hypomere and are involved either directly or indirectly in active predation. A central role for electroreception was postulated as part of this hypothesis (Northcutt and Gans 1983). The origin of electroreception is hypothesised to have been involved in the rapid evolution of vertebrate special sensory systems that occurred after the origin of neural crest and cranial placodes. Even the origin of hard tissues could perhaps initially be associated with electroreception (Northcutt and Gans 1983). Under this hypothesis, the initial function of enamel and dentine was as a material of high electrical resistance to shield the electroreceptors, analogous to the tight junctions and desmosomes in the canal walls in modern species. In addition, the original function of the bone underlying the dentine and enamel would simply be as a support to prevent breakage of the enamel and dentine. Electroreception was suggested to be the most important sense in the origin of the new head and the first to evolve, as electrical cues are almost always generated by living organisms and therefore even a rudimentary form of electroreception could be used to detect prey (Gans 1989).

However, fossil evidence discovered since the formation of the new head hypothesis does not support the idea that electroreceptors had a special role. First, the early Cambrian chordates *Haikouichthys* and *Mettaspriggina* have features including paired nasal sacs and eyes that show that other special sensory systems were in place, and neural crest and

cranial placodes were present (Shu et al. 2003; Morris and Caron 2014). However they lack mineralised tissue and so if they had electroreceptors these were not shielded by enamel and dentine.

Second, tight junctions, which make the canals of the ampullary organs of extant gnathostomes resistant to the flow of ions, are also present in the gills of lampreys (Chasiotis et al. 2012). Tight junctions are also present in tunicates (Georges 1979), suggesting they are a chordate feature that predates the origin of vertebrates. This raises the question of why a novel hard tissue would evolve only to be replaced later by a pre-existing structure.

Third, the idea that vertebrate hard tissues evolved as part of the electrosensory system rests on the pore canal system of sarcopterygians and osteostracans being electroreceptive, which appears unlikely (Bemis and Northcutt 1992). There is also no evidence for the pore canal system being a plesiomorphic vertebrate feature, being mostly absent in jawless vertebrates aside from osteostracans.

Electroreception and the early radiation of jawed vertebrates

The lack of preservation of electroreceptors in the majority of early vertebrate groups hinders attempts to understand its evolutionary importance. However, the pore-group clusters of early sarcopterygians, here interpreted as housing electroreceptors, show variation between taxa. Devonian lungfish have a highly elaborated system of pore-groups on their snouts (Ørvig 1961; Bemis and Northcutt 1992).

The rostral organ of coelacanths is a highly specialized system of electroreception (Berquist et al., 2015) and was present in early coelacanths (Cloutier 1996; Forey 1998; Long 1999). It seems clear therefore that highly adapted electroreceptor systems were present in Devonian sarcopterygians (e.g. coelacanths, lungfish).

Conclusions

1. Character state optimisation suggests that electroreception should be a widespread feature of early vertebrates. However, preservation potential of electroreceptors is low because in extant taxa they rarely leave impressions in dermal bones.
2. Many putative electroreceptors in early vertebrates, including the pore canals system of osteostracans and sarcopterygians and the rostral tubuli of lungfish, do not resemble electroreceptors in living species in morphology or distribution.
3. Osteostracans have a ramus recurrens of the anterior lateral line nerve, which suggests that trunk electroreceptors were present by comparison with lampreys and lungfish.
4. CT scans of placoderm cutaneous sense organ pits (cu.so) show that the orientation and length of these structures is intimately associated with dermal bone growth. These structures also do not appear to be electroreceptors.
5. A novel structure on the cheek plates of two “buchanosteid” placoderms is identified and termed the Young’s apparatus. This unusual structure is unlikely to have housed electroreceptors however.
6. Clusters of pits on the skulls of cosmine-covered sarcopterygians (“pore-group” pits) are likely to be electroreceptors. CT scans of fossil lungfish provide additional support for this identification.
7. The enigmatic early osteichthyan *Ligulalepis* has pit structures alongside the sensory lines which may be electroreceptors, a hypothesis supported by probable innervation from lateral line nerves. Similar structures are present in the early actinopterygian *Howqualepis*.
8. Devonian lungfish have a highly developed system of “pore-group” pits on their snouts, and the first coelacanths had rostral organs.

9. The hypothesis that vertebrate hard tissues developed initially as part of an electrosensory system is not supported by fossil evidence.

Acknowledgements

For access to collections we thank Ross Pogson, Gavin Young, Stig Walsh, Emma Bernard and the late Dave Pickering. We thank Michael Turner, Tim Senden, Vincent Dupret, Kate Trinajstic, Ruth Williams and Anton Maksimenko for help with scanning; Tim Senden for access to lungfish scans and library staff of Flinders University for tracking down copies of obscure references. We thank Grant gully for assistance with data archiving. Steve McLoughlin, Benjamin Kear, Kate Trinajstic and Henning Blom provided detailed reviews of a much earlier version of this manuscript, which were helpful in extending it to its current form. We are grateful to Gavin Young, Jing Lu and Alice Clement for providing helpful comments and discussions related to this manuscript. Tom Challands and Henning Blom provided helpful reviews which improved the manuscript. Travel to the UK to visit collections was partly funded by a Flinders University Elaine Martin travel grant. This work is supported by Australian Research Council grant DP 14014161.

References

- Afanassieva, O. B. (2004). Microrelief on the exoskeleton of some early osteostracans (Agnatha): preliminary analysis of its significance. *The Gross Symposium, Vol. 2*, 14–21.
- Alves-Gomes, J. A. (2001). The evolution of electroreception and bioelectrogenesis in teleost fish: a phylogenetic perspective. *Journal of Fish Biology* **58**, 1489–1511.

- Andres, K. H. and Von Düring, M. (1988). Comparative anatomy of vertebrate electroreceptors. *Progress in Brain Research* **74**, 113–131.
- Baker, C. V. H., Modrell, M. S. and Gillis, J. A. (2013). The evolution and development of vertebrate lateral line electroreceptors. *Journal of Experimental Biology* **216**, 2515–2522.
- Bardack, D. and Zangerl, R. (1968). First fossil lamprey: a record from the Pennsylvanian of Illinois. *Science* **162**, 1265–1267.
- Baron, V. D. (2009). Electric discharges of two species of stargazers from the South China Sea (Uranoscopidae, Perciformes). *Journal of Ichthyology* **49**, 1065–1072.
- Barry, M. A. and Bennett, M. V. L. (1989). Specialized lateral line receptor systems in elasmobranchs: the spiracular organs and vesicles of Savi. In *The Mechanosensory Lateral Line* (ed. S. Coombs, P. Görner and H. Münz), pp. 591–606. Springer.
- Bartsch, P. (1993). Development of the snout of the Australian lungfish *Neoceratodus forsteri* (Krefft, 1870), with special reference to cranial nerves. *Acta Zoologica* **74**, 15–29.
- Basden, A. M. and Young, G. C. (2001). A primitive actinopterygian neurocranium from the Early Devonian of southeastern Australia. *Journal of Vertebrate Paleontology* **21**, 754–766.
- Basden, A. M., Young, G. C., Coates, M. I. and Ritchie, A. (2000). The most primitive osteichthyan braincase? *Nature* **403**, 185–188.

- Bemis, W. E. and Hetherington, T. E. (1982). The rostral organ of *Latimeria chalumnae*: Morphological evidence of an electroreceptive function. *Copeia* **1982**, 467–471.
- Bemis, W. E. and Northcutt, R. G. (1992). Skin and blood vessels of the snout of the Australian lungfish, *Neoceratodus forsteri*, and their significance for interpreting the cosmopolitan of Devonian lungfishes. *Acta Zoologica* **73**, 115–139.
- Bennett, M. V. L. (1971). Electroreception. *Fish Physiology* **5**, 493–574.
- Berquist, R. M., Galinsky, V. L., Kajiura, S. M. and Frank, L. R. (2015). The coelacanth rostral organ is a unique low-resolution electro-detector that facilitates the feeding strike. *Scientific reports* **5**, 8962.
- Bjerring, H. C. (1972). Morphological observations on the exoskeletal skull roof of an osteolepiform from the Carboniferous of Scotland. *Acta Zoologica* **53**, 73–92.
- Bodznick, D. and Boord, R. (1986). Electroreception in Chondrichthyes. Central anatomy and physiology. In *Electroreception* (ed. T. H. Bullock and W. Heiligenberg), pp. 225–257. John Wiley & Sons, New York.
- Bodznick, D. and Northcutt, R. G. (1980). Segregation of electro- and mechanoreceptive inputs to the elasmobranch medulla. *Brain Research* **195**, 313–321.
- Bodznick, D. and Northcutt, R. G. (1981). Electroreception in lampreys: evidence that the earliest vertebrates were electroreceptive. *Science* **212**, 465–467.
- Bodznick, D. and Preston, D. G. (1983). Physiological characterization of electroreceptors in the lampreys *Ichthyomyzon unicuspis* and *Petromyzon marinus*. *Journal of Comparative Physiology* **152**, 209–217.

- Bohlin, B. (1941). The dorsal and lateral cephalic fields in the Osteostraci. *Zoologiska bidrag från Uppsala* **20**, 543–554.
- Bohlin, B. (1956). The dorsal and lateral sensory fields in the Osteostraci parts of the internal ear? *Zoologiska bidrag från Uppsala* **31**, 205–209.
- Borgen, U. (1989). Cosmine resorption structures on three osteolepid jaws and their biological significance. *Lethaia* **22**, 413–424.
- Borgen, U. (1992). The function of the pore canal system. In *Fossil Fishes as Living Animals* (ed. E. Mark-Kurik), pp. 141–151. Academy of Sciences of Estonia, Tallinn.
- Brazeau, M. D. (2009). The braincase and jaws of a Devonian ‘acanthodian’ and modern gnathostome origins. *Nature* **457**, 305–308.
- Bullock, T. H., Bodznick, D. A. and Northcutt, R. G. (1983). The phylogenetic distribution of electroreception: evidence for convergent evolution of a primitive vertebrate sense modality. *Brain Research Reviews* **6**, 25–46.
- Burrow, C. and Turner, S. (1998). Devonian placoderm scales from Australia. *Journal of Vertebrate Paleontology* **18**, 677–695.
- Campbell, K. S. W. and Barwick, R. E. (1986). Paleozoic lungfishes—a review. *Journal of Morphology Supplement* **1**, 93–131.
- Campbell, K. S. W. and Barwick, R. E. (2000). The braincase, mandible and dental structures of the Early Devonian lungfish *Dipnorhynchus kurikae* from Wee Jasper, New South Wales. *Records of the Australian Museum* **52**, 103–128.
- Campbell, K. S. W., Barwick, R. E. and Senden, T. (2010). Perforations and tubules in the snout region of Devonian dipnoans. In *Morphology, Phylogeny and*

- Paleobiogeography of Fossil Fishes* (ed. D. K. Elliott, J. G. Maisey, X. Yu and D. Miao), pp. 325–361. Verlag Dr. Friedrich Pfeil, München.
- Carr, R. K. and Hlavin, W. J. (2010). Two new species of *Dunkleosteus* Lehman, 1956, from the Ohio Shale Formation (USA, Famennian) and the Kettle Point Formation (Canada, Upper Devonian), and a cladistic analysis of the Eubranchyothoraci (Placodermi, Arthrodira). *Zoological Journal of the Linnean Society* **159**, 195–222.
- Challands, T. J. (2015). The cranial endocast of the Middle Devonian dipnoan *Dipterus valenciennesi* and a fossilized dipnoan otoconial mass. *Papers in Palaeontology* **1**, 289–317.
- Chang, M.-m., Zhang, J. and Miao, D. (2006). A lamprey from the Cretaceous Jehol biota of China. *Nature* **441**, 972–974.
- Chang, M.-M. and Zhu, M. (1993). A new Middle Devonian osteolepidid from Qujing, Yunnan. *Memoirs of the Association of Australasian Palaeontologists* **15**, 183–198.
- Chasiotis, H., Kolosov, D., Bui, P. and Kelly, S. P. (2012). Tight junctions, tight junction proteins and paracellular permeability across the gill epithelium of fishes: a review. *Respiratory Physiology & Neurobiology* **184**, 269–281.
- Cheng, H. (1989). On the tubuli in Devonian lungfishes. *Alcheringa* **13**, 153–166.
- Clement, A. M., Nysjö, J., Strand, R. and Ahlberg, P. E. (2015). Brain–Endocast Relationship in the Australian Lungfish, *Neoceratodus forsteri*, Elucidated from Tomographic Data (Sarcopterygii: Dipnoi). *PloS one* **10**, e0141277.

- Cloutier, R. (1996). The primitive actinistian *Miguashaia bureaui* Schultze (Sarcopterygii). In *Devonian Fishes and Plants of Miguasha, Quebec, Canada* (ed. H.-P. Schultze and R. Cloutier), pp. 227–247. Verlag Dr. Friedrich Pfeil, München.
- Czech-Damal, N. U., Liebschner, A., Miersch, L., Klauer, G., Hanke, F. D., Marshall, C., Dehnhardt, G. and Hanke, W. (2012). Electroreception in the Guiana dolphin (*Sotalia guianensis*). *Proceedings of the Royal Society of London B* **279**, 663–668.
- de Boef, M. and Larsson, H. C. E. (2007). Bone microstructure: quantifying bone vascular orientation. *Canadian Journal of Zoology* **85**, 63–70.
- Denison, R. H. (1947). The exoskeleton of *Tremataspis*. *American Journal of Science* **245**, 337–365.
- Denison, R. H. (1964). The Cyathaspididae: a family of Silurian and Devonian jawless vertebrates. *Fieldiana, Geology* **13**, 309–473.
- Denison, R. H. (1966). The origin of the lateral-line sensory system. *American Zoologist* **6**, 368–370.
- Dennis, K. and Miles, R. S. (1979a). Eubrachythoracid arthrodires with tubular rostral plates from Gogo, Western Australia. *Zoological Journal of the Linnean Society* **67**, 297–328.
- Dennis, K. and Miles, R. S. (1979b). A second eubrachythoracid arthrodire from Gogo, Western Australia. *Zoological Journal of the Linnean Society* **67**, 1–29.

- Dennis, K. and Miles, R. S. (1982). A eubrachythoracid arthrodire with a snubnose from Gogo, Western Australia. *Zoological Journal of the Linnean Society* **75**, 153–166.
- Dennis-Bryan, K. (1987). A new species of eastmanosteid arthrodire (Pisces: Placodermi) from Gogo, Western Australia. *Zoological Journal of the Linnean Society* **90**, 1–64.
- Dennis-Bryan, K. and Miles, R. S. (1983). Further eubrachythoracid arthrodires from Gogo, Western Australia. *Zoological Journal of the Linnean Society* **77**, 145–173.
- Dijkgraaf, S. and Kalmijn, A. J. (1963). Untersuchungen über die Funktion der Lorenzinischen Ampullen an Haifischen. *Journal of Comparative Physiology A* **47**, 438–456.
- Donoghue, P. C., Forey, P. L. and Aldridge, R. J. (2000). Conodont affinity and chordate phylogeny. *Biological Reviews* **75**, 191–251.
- Dupret, V., Sanchez, S., Goujet, D. and Ahlberg, P. (2017a). The internal cranial anatomy of *Romundina stellina* Øravig, 1975 (Vertebrata, Placodermi, Acanthothoraci) and the origin of jawed vertebrates—Anatomical atlas of a primitive gnathostome. *PloS one* **12**, e0171241.
- Dupret, V., Zhu, M. and Wang, J.-Q. (2017b). Redescription of *Szelepis* Liu, 1981 (Placodermi, Arthrodira) from the Lower Devonian of China. *Journal of Vertebrate Paleontology*, e1312422.
- Dupret, V., Zhu, M. and Wang, J. Q. (2009). The morphology of *Yujiangolepis liujingensis* (Placodermi, Arthrodira) from the Pragian of Guangxi (South

- China) and its phylogenetic significance. *Zoological Journal of the Linnean Society* **157**, 70–82.
- Fields, R. D., Bullock, T. H. and Lange, G. D. (1993). Ampullary sense organs, peripheral, central and behavioral electroreception in chimeras (*Hydrolagus*, Holocephali, Chondrichthyes). *Brain, behavior and evolution* **41**, 269–289.
- Fields, R. D. and Lange, G. D. (1980). Electroreception in the ratfish (*Hydrolagus colliei*). *Science* **207**, 547–548.
- Forey, P. L. (1998). *History of the Coelacanth Fishes*. Chapman and Hall, London.
- Fox, R. C., Campbell, K. S. W., Barwick, R. E. and Long, J. (1995). A new osteolepiform fish from the lower Carboniferous Raymond Formation, Drummond Basin, Queensland. *Memoirs of the Queensland Museum* **38**, 97–221.
- Friedman, M. (2007). *Styloichthys* as the oldest coelacanth: implications for early osteichthyan interrelationships. *Journal of Systematic Palaeontology* **5**, 289–343.
- Friedman, M. and Brazeau, M. D. (2010). A reappraisal of the origin and basal radiation of the Osteichthyes. *Journal of Vertebrate Paleontology* **30**, 36–56.
- Gans, C. (1989). Stages in the origin of vertebrates: analysis by means of scenarios. *Biological Reviews* **64**, 221–268.
- Gans, C. and Northcutt, R. G. (1983). Neural crest and the origin of vertebrates: a new head. *Science* **220**, 268–273.
- Gardiner, B. G. and Miles, R. S. (1990). A new genus of eubrachythoracid arthrodire from Gogo, Western Australia. *Zoological Journal of the Linnean Society* **99**, 159–204.

- Gardiner, B. G. and Miles, R. S. (1994). Eubrachythoracid arthrodires from Gogo, Western Australia. *Zoological Journal of the Linnean Society* **112**, 443–477.
- Georges, D. (1979). Gap and tight junctions in tunicates. Study in conventional and freeze-fracture techniques. *Tissue and Cell* **11**, 781–792.
- Gess, R. W., Coates, M. I. and Rubidge, B. S. (2006). A lamprey from the Devonian period of South Africa. *Nature* **443**, 981–984.
- Giles, S., Rücklin, M. and Donoghue, P. C. J. (2013). Histology of “placoderm” dermal skeletons: Implications for the nature of the ancestral gnathostome. *Journal of Morphology* **274**, 627–644.
- Gillis, J. A., Modrell, M. S., Northcutt, R. G., Catania, K. C., Luer, C. A. and Baker, C. V. H. (2012). Electrosensory ampullary organs are derived from lateral line placodes in cartilaginous fishes. *Development* **139**, 3142–3146.
- Goujet, D. (1975). *Dicksonosteus*, un nouvel arthrodire du Dévonien du Spitsberg—Remarques sur le squelette viscéral des Dolichothoraci. *Colloques Internationaux du Centre National de la Recherche Scientifique* **218**, 81–99.
- Goujet, D. (2001). Placoderms and basal gnathostome apomorphies. In *Major Events in Early Vertebrate Evolution* (ed. P. E. Ahlberg), pp. 209–222. Taylor and Francis, London and New York.
- Gross, W. (1956). Über Crossopterygier und Dipnoer aus dem baltischen Oberdevon im Zusammenhang einer vergleichenden Untersuchung des Porenkanalsystems paläozoischer Agnathen und Fische. *Kungliga Svenska Vetenskapsakademiens Handlingar* **5**, 1–140.

- Gross, W. (1965). Über den Vorderschädel von *Ganorhynchus splendens* Gross (Dipnoi, Mitteldevon). *Paläontologische Zeitschrift* **39**, 113.
- Hetherington, T. E. and Wake, M. H. (1979). The lateral line system in larval *Ichthyophis* (Amphibia: Gymnophiona). *Zoomorphologie* **93**, 209–225.
- Holland, T. (2014). The endocranial anatomy of *Gogonasus andrewsae* Long, 1985 revealed through micro CT-scanning. *Earth and Environmental Science Transactions of the Royal Society of Edinburgh* **105**, 9–34.
- Hu, Y., Lu, J. and Young, G. C. (2017). New findings in a 400 million-year-old Devonian placoderm shed light on jaw structure and function in basal gnathostomes. *Scientific reports* **7**, 7813.
- Istenič, L. and Bulog, B. (1984). Some evidence for the ampullary organs in the European cave salamander *Proteus anguinus* (Urodela, Amphibia). *Cell and tissue research* **235**, 393–402.
- Janvier, P. (1974). The sensory line system and its innervation in the Osteostraci (Agnatha, Cephalaspidomorphi). *Zoologica Scripta* **3**, 91–99.
- Janvier, P. (1985). *Les Céphalaspides du Spitsberg. Anatomie, phylogénie et systématique des Ostéostracés siluro-dévonien. Révision des Ostéostracés de la formation de Wood Bay (Dévonien inférieur du Spitsberg)*. Cahiers de Paléontologie, Section Vertébrés. CNRS, Paris.
- Janvier, P. (1996). The dawn of the vertebrates: characters versus common ascent in the rise of current vertebrate phylogenies. *Palaeontology* **39**, 259–287.
- Jarvik, E. (1942). On the structure of the snout of crossopterygians and lower gnathostomes in general. *Zoologiska bidrag från Uppsala* **21**, 235–675.

- Jarvik, E. (1948). On the morphology and taxonomy of the Middle Devonian osteolepid fishes of Scotland. *Kungliga Svenska Vetenskapsakademiens Handlingar* **25**, 1–301.
- Jarvik, E. (1950). Middle Devonian vertebrates from Canning Land and Wegeners Halvö (East Greenland): Part II: Crossopterygii. *Meddelelser om Grønland* **96**, 1–132.
- Jarvik, E. (1965). Die Raspelzunge der Cyclostomen und die pentadactyle Extremität der Tetrapoden als Beweise für monophyletische Herkunft. *Zoologischer Anzeiger* **175**, 101–143.
- Jarvik, E. (1980). *Basic structure and evolution of vertebrates*. Academic Press, London.
- Jessen, H. (1975). A new choanate fish, *Powichthys thorsteinssoni* n.g., n. sp., from the early Lower Devonian of the Canadian Arctic Archipelago. *Colloques Internationaux du Centre National de la Recherche Scientifique* **218**, 214–222.
- Johnels, A. G. (1956). On the origin of the electric organ in *Malapterurus electricus*. *Journal of Cell Science* **3**, 455–463.
- Jørgensen, J. M. (1980). The morphology of the Lorenzian ampullae of the sturgeon *Acipenser ruthenus* (Pisces: Chondrostei). *Acta Zoologica* **61**, 87–92.
- Jørgensen, J. M. (1982). Fine structure of the ampullary organs of the bichir *Polypterus senegalus* Cuvier, 1829 (Pisces: Brachiopterygii) with some notes on the phylogenetic development of electroreceptors. *Acta Zoologica* **63**, 211–217.

- Jørgensen, J. M. (2005). Morphology of electroreceptive sensory organs. In *Electroreception* (ed. T. H. Bullock, C. D. Hopkins, A. N. Popper and R. R. Fay), pp. 47–67. Springer, New York.
- Jørgensen, J. M. (2011). The lateral line system in lungfishes: mechanoreceptive neuromasts and electroreceptive ampullary organs. In *The Biology of Lungfishes* (ed. J. M. Jørgensen and J. Joss), pp. 477–492. CRC Press, Enfield.
- Jørgensen, J. M., Flock, Å. and Wersäll, J. (1972). The Lorenzinian ampullae of *Polyodon spathula*. *Zeitschrift für Zellforschung und Mikroskopische Anatomie* **130**, 362–377.
- Kajiura, S. M. (2001). Head morphology and electrosensory pore distribution of carcharhinid and sphyrnid sharks. *Environmental Biology of Fishes* **61**, 125–133.
- Kalmijn, A. J. (1971). The electric sense of sharks and rays. *Journal of Experimental Biology* **55**, 371–383.
- Kalmijn, A. J. (1974). The detection of electric fields from inanimate and animate sources other than electric organs. In *Electroreceptors and Other Specialized Receptors in Lower Vertebrates* (ed. A. Fessard), pp. 147–200. Springer, New York.
- Kemp, A. (2014). Skin structure in the snout of the Australian lungfish, *Neoceratodus forsteri* (Osteichthyes: Dipnoi). *Tissue and Cell* **46**, 397–408.
- Kemp, A. (2017). Cranial nerves in the Australian lungfish, *Neoceratodus forsteri*, and in fossil relatives (Osteichthyes: Dipnoi). *Tissue and Cell* **49**, 45–55.

- Klembara, J. (1994). Electroreceptors in the Lower Permian tetrapod *Discosauriscus austriacus*. *Palaeontology* **37**, 609–626.
- Kramer, B. (1996). *Electroreception and Communication in Fishes*. Gustav Fischer Verlag, Stuttgart.
- Limaye, A. (2012). Drishti, a volume exploration and presentation tool. *SPIE Developments in X-Ray Tomography* **8506**, 85060X.
- Lisney, T. J. (2010). A review of the sensory biology of chimaeroid fishes (Chondrichthyes; Holocephali). *Reviews in Fish Biology and Fisheries* **20**, 571–590.
- Lissmann, H. W. (1951). Continuous Electrical Signals from the Tail of a Fish, *Gymnarchus niloticus* Cuv. *Nature* **167**, 201–202.
- Lissmann, H. W. and Machin, K. E. (1958). The mechanism of object location in *Gymnarchus niloticus* and similar fish. *Journal of Experimental Biology* **35**, 451–486.
- Liu, Y.-H. (1991). On a new petalichthyid, *Eurycaraspis incilis* gen. et sp. nov., from the middle Devonian of Zhanyi, Yunnan. In *Early Vertebrates and Related Problems of Evolutionary Biology* (ed. M.-M. Chang, Y.-H. Liu and G.-R. Zhang), pp. 139–177. Science Press, Beijing.
- Long, J. A. (1988a). A new camuropiscid arthrodire (Pisces: Placodermi) from Gogo, Western Australia. *Zoological Journal of the Linnean Society* **94**, 233–258.
- Long, J. A. (1988b). New palaeoniscoid fishes from the Late Devonian and Early Carboniferous of Victoria. *Memoirs of the Association of Australasian Palaeontologists* **7**, 1–64.

- Long, J. A. (1992). Cranial anatomy of two new late Devonian lungfishes (Pisces: Dipnoi) from Mount Howitt, Victoria. *Records of the Australian Museum* **44**, 299–318.
- Long, J. A. (1995). A new plourdosteid arthrodire from the Upper Devonian Gogo Formation of Western Australia. *Palaeontology* **38**, 39–62.
- Long, J. A. (1997). Ptyctodontid fishes (Vertebrata, Placodermi) from the Late Devonian Gogo Formation, Western Australia, with a revision of the European genus *Ctenurella* Ørvig, 1960. *Geodiversitas* **19**, 515–555.
- Long, J. A. (1999). A new genus of fossil coelacanth (Osteichthyes: Coelacanthiformes) from the Middle Devonian of Southeastern Australia. *Records of the Western Australian Museum Supplement* **57**, 37–53.
- Long, J. A., Barwick, R. E. and Campbell, K. S. W. (1997). Osteology and functional morphology of the osteolepiform fish *Gogonassus andrewsae* Long, 1985, from the Upper Devonian Gogo Formation, Western Australia. *Records of the Western Australian Museum Supplement* **53**, 1–89.
- Long, J. A., Mark-Kurik, E. and Young, G. C. (2014). Taxonomic revision of buchanosteoid placoderms (Arthrodira) from the Early Devonian of southeastern Australia and Arctic Russia. *Australian Journal of Zoology* **62**, 26–43.
- Lorenzini, S. (1678). *Osservazioni intorno alle Torpedini. vol 1*, Florence.
- Lu, J., Zhu, M., Ahlberg, P. E., Qiao, T., Zhu, Y. a., Zhao, W. and Jia, L. (2016). A Devonian predatory fish provides insights into the early evolution of modern sarcopterygians. *Science Advances* **2**, e1600154.

- Lu, J., Zhu, M., Long, J. A., Zhao, W., Senden, T. J., Jia, L. and Qiao, T. (2012). The earliest known stem-tetrapod from the Lower Devonian of China. *Nature Communications* **3**, 1160.
- Märss, T., Afanassieva, O. B. and Blom, H. (2014). Biodiversity of the Silurian osteostracans of the East Baltic. *Earth and Environmental Science Transactions of the Royal Society of Edinburgh* **105**, 73–148.
- Meinke, D. K. (1984). A review of cosmine: its structure, development, and relationship to other forms of the dermal skeleton in osteichthyans. *Journal of Vertebrate Paleontology* **4**, 457–470.
- Miles, R. S. (1962). III.—*Gemuendenaspis* n. gen., an arthrodiran fish from the Lower Devonian Hunsrückschiefer of Germany. *Transactions of the Royal Society of Edinburgh* **65**, 59–77.
- Miles, R. S. (1965). Ventral thoracic neuromast lines of placoderm fishes. *Nature* **206**, 524–525.
- Miles, R. S. (1966). XV.—The placoderm fish *Rhachiosteus pterygiatus* Gross and its relationships. *Transactions of the Royal Society of Edinburgh* **66**, 377–392.
- Miles, R. S. (1971). The Holonematidae (placoderm fishes), a review based on new specimens of *Holonema* from the Upper Devonian of Western Australia. *Philosophical Transactions of the Royal Society of London B* **263**, 101–234.
- Miles, R. S. (1977). Dipnoan (lungfish) skulls and the relationships of the group: a study based on new species from the Devonian of Australia. *Zoological Journal of the Linnean Society* **61**, 1–328.

- Miles, R. S. and Dennis, K. (1979). A primitive eubrachythoracid arthrodire from Gogo, Western Australia. *Zoological Journal of the Linnean Society* **66**, 31–62.
- Miles, R. S. and Westoll, T. S. (1962). IX.—Two New Genera of coccosteid Arthrodira from the Middle Old Red Sandstone of Scotland, and their stratigraphical distribution. *Transactions of the Royal Society of Edinburgh* **65**, 179–210.
- Miles, R. S. and Young, G. C. (1977). Placoderm interrelationships reconsidered in the light of new ptyctodontids from Gogo, Western Australia. *Linnean Society Symposium Series* **4**, 123–198.
- Millot, J. and Anthony, J. (1965). *Anatomie de Latimeria chalumnae, Tome 2: Système nerveux et organes des sens*. CNRS, Paris.
- Modrell, M. S., Bemis, W. E., Northcutt, R. G., Davis, M. C. and Baker, C. V. H. (2011). Electrosensory ampullary organs are derived from lateral line placodes in bony fishes. *Nature Communications* **2**, 496.
- Moore, D. M. and McCarthy, I. D. (2014). Distribution of ampullary pores on three catshark species (*Apristurus* spp.) suggest a vertical-ambush predatory behaviour. *Aquatic Biology* **21**, 261–265.
- Morris, S. C. and Caron, J.-B. (2014). A primitive fish from the Cambrian of North America. *Nature* **512**, 419–422.
- Münz, H., Claas, B. and Fritzsche, B. (1982). Electrophysiological evidence of electroreception in the axolotl *Siredon mexicanum*. *Neuroscience Letters* **28**, 107–111.
- Murray, R. W. (1960). Electrical sensitivity of the ampullae of Lorenzini. *Nature* **187**, 957.

- Murray, R. W. (1962). The response of the ampullae of Lorenzini of elasmobranchs to electrical stimulation. *Journal of Experimental Biology* **39**, 119–128.
- New, J. G. (1997). The evolution of vertebrate electrosensory systems. *Brain, behavior and evolution* **50**, 244–252.
- Norris, H. W. (1929). The distribution and innervation of the ampullae of Lorenzini of the dogfish, *Squalus acanthias*. Some comparisons with conditions in other plagiostomes and corrections of prevalent errors. *Journal of Comparative Neurology* **47**, 449–465.
- Northcutt, R. G. (1985). The brain and sense organs of the earliest vertebrates: reconstruction of a morphotype. In *Evolutionary Biology of Primitive Fishes* (ed. R. E. Foreman, A. Gorbman, J. M. Dodd and R. Olsson), pp. 81–112. Plenum, New York.
- Northcutt, R. G. (1986a). Electroreception in nonteleost bony fishes. In *Electroreception* (ed. Bullock T H and H. Wahnschaffe), pp. 257–285. John Wiley & Sons, New York.
- Northcutt, R. G. (1986b). Lungfish neural characters and their bearing on sarcopterygian phylogeny. *Journal of Morphology* **190**, 277–297.
- Northcutt, R. G., Brändle, K. and Fritsch, B. (1995). Electroreceptors and mechanosensory lateral line organs arise from single placodes in axolotls. *Developmental Biology* **168**, 358–373.
- Northcutt, R. G. and Gans, C. (1983). The genesis of neural crest and epidermal placodes: a reinterpretation of vertebrate origins. *Quarterly Review of Biology* **58**, 1–28.

- Obara, S. (1976). Mechanism of electroreception in ampullae of Lorenzini of the marine catfish *Plotosus*. In *Electrobiology of Nerve, Synapse and Muscle* (ed. J. P. Reuben, D. P. Purpura, M. L. V. Bennett and E. R. Kandel), pp. 128–147. Raven Press, New York.
- Ørvig, T. (1960). New finds of acanthodians, arthrodires, crossopterygians, ganoids and dipnoans in the upper Middle Devonian calcareous flags (oberer Plattenkalk) of the Bergisch Gladbach-Paffrath Trough. *Paläontologische Zeitschrift* **34**, 295–335.
- Ørvig, T. (1961). New finds of acanthodians, arthrodires, crossopterygians, ganoids and dipnoans in the upper Middle Devonian calcareous flags (Oberer Plattenkalk) of the Bergisch Gladbach-Paffrath trough. *Paläontologische Zeitschrift* **35**, 10–27.
- Ørvig, T. (1969). Cosmine and cosmine growth. *Lethaia* **2**, 241–260.
- Ørvig, T. (1971). Comments on the lateral line system of some brachythoracid and ptyctodontid arthrodires. *Zoologica Scripta* **1**, 5–35.
- Ørvig, T. (1975). Description, with special reference to the dermal skeleton, of a new radotinid arthrodire from the Gedinian of Arctic Canada. *Colloques Internationaux du Centre National de la Recherche Scientifique* **218**, 43–71.
- Ørvig, T. (1989). Histologic studies of ostracoderms, placoderms and fossil elasmobranchs. 6. Hard tissues of Ordovician vertebrates. *Zoologica Scripta* **18**, 427–446.
- Proske, U., Gregory, J. E. and Iggo, A. (1998). Sensory receptors in monotremes. *Philosophical Transactions of the Royal Society of London B* **353**, 1187–1198.

- Qu, Q., Blom, H., Sanchez, S. and Ahlberg, P. (2015). Three - dimensional virtual histology of silurian osteostracan scales revealed by synchrotron radiation microtomography. *Journal of Morphology* **276**, 873–888.
- Raschi, W. (1978). Notes on the gross functional morphology of the ampullary system in two similar species of skates, *Raja erinacea* and *R. ocellata*. *Copeia* **1978**, 48–53.
- Raschi, W. (1986). A morphological analysis of the ampullae of Lorenzini in selected skates (Pisces, Rajoidei). *Journal of Morphology* **189**, 225–247.
- Raschi, W., Keithan, E. D. and Rhee, W. C. H. (1997). Anatomy of the ampullary electroreceptor in the freshwater stingray, *Himantura signifer*. *Copeia* **1997**, 101–107.
- Ritchie, A. (1973). *Wuttagoonaspis* gen. nov., an unusual arthrodire from the Devonian of Western New South Wales, Australia. *Palaeontographica Abteilung A Palaeozoologie-Stratigraphie* **143**, 58–72.
- Ronan, M. (1988). Anatomical and physiological evidence for electroreception in larval lampreys. *Brain Research* **448**, 173–177.
- Ronan, M. C. and Bodznick, D. (1986). End buds: non-ampullary electroreceptors in adult lampreys. *Journal of Comparative Physiology A* **158**, 9–15.
- Roth, A. (1973). Electroreceptors in Brachiopterygii and Dipnoi. *Naturwissenschaften* **60**, 106–106.
- Roth, A. and Tschardtke, H. (1976). Ultrastructure of the ampullary electroreceptors in lungfish and Brachiopterygii. *Cell and tissue research* **173**, 95–108.

- Ruta, M., Coates, M. I. and Quicke, D. L. J. (2003). Early tetrapod relationships revisited. *Biological Reviews* **78**, 251–345.
- Sakellariou, A., Sawkins, T., Senden, T. and Limaye, A. (2004). X-ray tomography for mesoscale physics applications. *Physica A: Statistical Mechanics and its Applications* **339**, 152–158.
- Sand, A. (1938). The function of the ampullae of Lorenzini, with some observations on the effect of temperature on sensory rhythms. *Proceedings of the Royal Society of London B* **125**, 524–553.
- Sansom, R. S., Freedman, K., Gabbott, S. E., Aldridge, R. J. and Purnell, M. A. (2010). Taphonomy and affinity of an enigmatic Silurian vertebrate, *Jamoytius kerwoodi* White. *Palaeontology* **53**, 1393–1409.
- Schultze, H.-P. (2016). Scales, enamel, cosmine, ganoine, and early osteichthyans. *Comptes Rendus Palevol* **15**, 83–102.
- Schultze, H.-P. and Cumbaa, S. L. (2017). A new Early Devonian (Emsian) arthrodire from the Northwest Territories, Canada, and its significance for paleogeographic reconstruction. *Canadian Journal of Earth Sciences* **54**, 461–476.
- Shu, D.-G., Morris, S. C., Han, J., Zhang, Z.-F., Yasui, K., Janvier, P., Chen, L., Zhang, X.-L., Liu, J.-N. and Li, Y. (2003). Head and backbone of the Early Cambrian vertebrate *Haikouichthys*. *Nature* **421**, 526–529.
- Sire, J. Y., Donoghue, P. C. J. and Vickaryous, M. K. (2009). Origin and evolution of the integumentary skeleton in non - tetrapod vertebrates. *Journal of Anatomy* **214**, 409–440.

- Stensiö, E. A. (1927). The Downtonian and Devonian vertebrates of Spitsbergen. I, Family Cephalaspidae. *Skrifter om Svalbard og Ishavet* **12**, 1–391.
- Stensiö, E. A. (1963). *Anatomical studies on the arthrodiran head*. Almqvist & Wiksell, Stockholm.
- Szabo, T., Kalmijn, A. J., Enger, P. S. and Bullock, T. H. (1972). Microampullary organs and a submandibular sense organ in the fresh water ray, *Potamotrygon*. *Journal of Comparative Physiology A* **79**, 15–27.
- Teeter, J. H., Szamier, R. B. and Bennett, M. V. L. (1980). Ampullary electroreceptors in the sturgeon *Scaphirhynchus platyrhynchus* (Rafinesque). *Journal of Comparative Physiology* **138**, 213–223.
- Theiss, S. M., Collin, S. P. and Hart, N. S. (2011). Morphology and distribution of the ampullary electroreceptors in wobbegong sharks: implications for feeding behaviour. *Marine Biology* **158**, 723–735.
- Thomson, K. S. (1975). On the biology of cosmine. *Bulletin of the Peabody Museum of Natural History* **40**, 1–59.
- Thomson, K. S. (1977). On the individual history of cosmine and a possible electroreceptive function of the pore-canal system in fossil fishes. In *Problems in vertebrate evolution. Linnean Society Symposium Series* (ed. S. M. Andrews, R. S. Miles and A. D. Walker), pp. 247–271. Academic Press, London.
- Thomson, K. S. and Campbell, K. S. W. (1971). The structure and relationships of the primitive Devonian lungfish—*Dipnorhynchus sussmilchi* (Etheridge). *Bulletin of the Peabody Museum of Natural History* **38**, 1–109.

- Tricas, T. C. (2001). The neuroecology of the elasmobranch electrosensory world: why peripheral morphology shapes behavior. *Environmental Biology of Fishes* **60**, 77–92.
- Tricas, T. C. and Sisneros, J. A. (2004). Ecological functions and adaptations of the elasmobranch electrosense. In *The Senses of Fish: Adaptations for the Reception of Natural Stimuli* (ed. G. Von der Emde, J. Mogdans and B. G. Kapoor), pp. 308–329. Kluwer Academic Publishers, Boston.
- Trinajstić, K., Long, J. A., Johanson, Z., Young, G. and Senden, T. (2012). New morphological information on the ptyctodontid fishes (Placodermi, Ptyctodontida) from Western Australia. *Journal of Vertebrate Paleontology* **32**, 757–780.
- Wängsjö, G. (1952). The Downtonian and Devonian vertebrates of Spitsbergen. IX, Morphologic and systematic studies of the Spitsbergen cephalaspids. *Norsk Polarinstitutts Skrifter* **97**, 1–611.
- Watson, D. M. S. (1954). A consideration of ostracoderms. *Philosophical Transactions of the Royal Society B* **238**, 1–25.
- Watt, M., Evans, C. S. and Joss, J. M. P. (1999). Use of electroreception during foraging by the Australian lungfish. *Animal Behaviour* **58**, 1039–1045.
- Weisel, G. F. (1978). The integument and caudal filament of the shovelnose sturgeon, *Scaphirhynchus platorynchus*. *American Midland Naturalist*, 179–189.
- Westoll, T. S. (1936). On the structures of the dermal ethmoid shield of *Osteolepis*. *Geological Magazine* **73**, 157–171.

- White, E. I. (1978). The larger arthrodiran fishes from the area of the Burrinjuck Dam, NSW. *The Transactions of the Zoological Society of London* **34**, 149–262.
- White, E. I. and Toombs, H. A. (1972). The bichanosteid arthrodiras of Australia. *Bulletin of the British Museum (Natural History) Geology* **22**, 379–419.
- Whitear, M. and Lane, E. B. (1983). Multivillous cells: epidermal sensory cells of unknown function in lamprey skin. *Journal of Zoology* **201**, 259–272.
- Whitehead, D. L., Tibbetts, I. R. and Daddow, L. Y. M. (1999). Distribution and morphology of the ampullary organs of the salmontail catfish, *Arius graeffei*. *Journal of Morphology* **239**, 97–105.
- Whitehead, D. L., Tibbetts, I. R. and Daddow, L. Y. M. (2000). Ampullary organ morphology of freshwater salmontail catfish, *Arius graeffei*. *Journal of Morphology* **246**, 142–149.
- Whitehead, D. L., Tibbetts, I. R. and Daddow, L. Y. M. (2003). Microampullary organs of a freshwater eel - tailed catfish, *Plotosus (tandanus) tandanus*. *Journal of Morphology* **255**, 253–260.
- Wilkins, L. A., Russell, D. F., Pei, X. and Gurgens, C. (1997). The paddlefish rostrum functions as an electrosensory antenna in plankton feeding. *Proceedings of the Royal Society of London B: Biological Sciences* **264**, 1723–1729.
- Winther-Janson, M., Wueringer, B. E. and Seymour, J. E. (2012). Electroreceptive and mechanoreceptive anatomical specialisations in the epaulette shark (*Hemiscyllium ocellatum*). *PLoS one* **7**, e49857.
- Witmer, L. M. (1995). The extant phylogenetic bracket and the importance of reconstructing soft tissues in fossils. In *Functional morphology in vertebrate*

- paleontology* (ed. J. J. Thomason), pp. 19–33. Cambridge University Press, New York.
- Wueringer, B. E. and Tibbetts, I. R. (2008). Comparison of the lateral line and ampullary systems of two species of shovelnose ray. *Reviews in Fish Biology and Fisheries* **18**, 47–64.
- Young, G. C. (1979). New information on the structure and relationships of *Buchanosteus* (Placodermi: Euarthrodira) from the Early Devonian of New South Wales. *Zoological Journal of the Linnean Society* **66**, 309–352.
- Young, G. C. (1980). A new Early Devonian placoderm from New South Wales, Australia, with a discussion of placoderm phylogeny. *Palaeontographica Abteilung A Palaeozoologie-Stratigraphie* **167**, 10–76.
- Young, G. C. (1986). The relationships of placoderm fishes. *Zoological Journal of the Linnean Society* **88**, 1–57.
- Young, G. C. (2003). A new species of *Atlantidosteus* Lelièvre, 1984 (Placodermi, Arthrodira, Brachythoraci) from the Middle Devonian of the Broken River area (Queensland, Australia). *Geodiversitas* **25**, 681–694.
- Young, G. C. (2011). Wee Jasper-Lake Burrinjuck fossil fish sites: scientific background to national heritage nomination. *Proceedings of the Linnean Society of New South Wales* **132**, 83–107.
- Young, G. C. and Goujet, D. (2003). Devonian fish remains from the Dulcie Sandstone and Cravens Peak Beds, Georgina Basin, central Australia. *Records of the Western Australian Museum Supplement* **65**, 1–80.

- Young, G. C., Lelièvre, H. and Goujet, D. (2001). Primitive jaw structure in an articulated brachythoracid arthrodire (placoderm fish; Early Devonian) from Southeastern Australia. *Journal of Vertebrate Paleontology* **21**, 670–678.
- Young, G. C., Long, J. A. and Ritchie, A. (1992). Crossopterygian fishes from the Devonian of Antarctica. *Records of the Australian Museum Supplement* **14**, 1–77.
- Young, G. C. and Zhang, G. (1996). New information on the morphology of yunnanolepid antiarchs (placoderm fishes) from the Early Devonian of South China. *Journal of Vertebrate Paleontology* **16**, 623–641.
- Zhang, M.-M. and Yu, X.-B. (1981). A new crossopterygian, *Youngolepis praecursor*, gen. et sp. nov., from lower Devonian of East Yunnan, China. *Scientia Sinica* **24**, 89–99.
- Zhu, M. (1996). The phylogeny of the Antiarcha (Placodermi, Pisces), with the description of early Devonian antiarchs from Qujing, Yunnan, China. *Bulletin du Muséum national d'histoire naturelle. Section C, Sciences de la terre, paléontologie, géologie, minéralogie* **18**, 233–347.
- Zhu, M., Yu, X., Lu, J., Qiao, T., Zhao, W. and Jia, L. (2012). Earliest known coelacanth skull extends the range of anatomically modern coelacanths to the Early Devonian. *Nature Communications* **3**, 772.
- Zhu, Y. A. and Zhu, M. (2013). A redescription of *Kiangyousteus yohii* (Arthrodira: Eubrachythoraci) from the Middle Devonian of China, with remarks on the systematics of the Eubrachythoraci. *Zoological Journal of the Linnean Society* **169**, 798–819.

Zhu, Y. A., Zhu, M. and Wang, J. Q. (2015). Redescription of *Yinostius major* (Arthrodira: Heterostiidae) from the Lower Devonian of China, and the interrelationships of Brachythoraci. *Zoological Journal of the Linnean Society* **176**, 806–834.

Chapter 3

Bayesian morphological clock methods resurrect placoderm monophyly and reveal rapid early evolution in jawed vertebrates

Benedict King¹, Tuo Qiao², Michael S.Y. Lee^{1,3}, Min Zhu², John A. Long¹

¹School of Biological Sciences, Flinders University, PO Box 2100, Adelaide, South Australia 5001, Australia. ²Key Laboratory of Vertebrate Evolution and Human Origins of Chinese Academy of Sciences, Institute of Vertebrate Paleontology and Paleoanthropology, Chinese Academy of Sciences, PO Box 643, Beijing 100044, China. ³Earth Sciences Section, South Australian Museum, North Terrace, Adelaide 5000, Australia

Context

In this chapter I examine the relationships of early gnathostomes from a new angle, by using tip-dated Bayesian methods. This chapter also includes a new data matrix, designed specifically for use in a tip-dating approach, and revisions to important characters. I also examine differences between tip-dating and parsimony phylogenetic methods through a simulation study.

Statement of authorship

BK collected data, analysed the data, performed simulation study, wrote the manuscript and prepared figures. QT assembled initial compilation of early gnathostome characters, and contributed some codings. JAL, MSYL and MZ commented on the manuscript.

Abstract

The phylogeny of early gnathostomes provides an important framework for understanding one of the most significant evolutionary events within vertebrates, the origin and diversification of jawed vertebrates. A series of recent cladistic analyses have suggested that the placoderms, an extinct group of armoured fish, form a paraphyletic group basal to all other jawed vertebrates. We revised and expanded this morphological dataset, most notably by sampling autapomorphies in a similar way to parsimony-informative traits, thus ensuring this data (unlike most existing morphological datasets) satisfied an important assumption of Bayesian tip-dated morphological clock approaches. We also found problems with characters supporting placoderm paraphyly, including logical character correlation and incorrect codings. Analysis of this dataset reveals that paraphyly and monophyly of placoderms (excluding maxillate forms) are essentially equally parsimonious. The two alternative topologies have different root positions for the jawed vertebrates but are otherwise similar. However, analysis using tip-dated clock methods reveals strong support for placoderm monophyly (excluding maxillate forms), due to this analysis favouring trees with more balanced rates of evolution. Furthermore, enforcing placoderm paraphyly results in higher levels and unusual patterns of rate heterogeneity among branches, similar to that generated from simulated trees reconstructed with incorrect root positions. These simulations also show that Bayesian tip-dated clock methods outperform parsimony when the outgroup is largely uninformative (e.g. due to inapplicable characters), as might be the case here. The analysis also reveals that gnathostomes underwent a

rapid burst of evolution during the Silurian period which declined during the Early Devonian. This rapid evolution during a period with few articulated fossils might partly explain the difficulty in ascertaining the root position of jawed vertebrates.

Introduction

The phylogeny of early vertebrates is vital for understanding the acquisition of key characters at the origin of gnathostomes. Jawed vertebrates, today comprising the bony fish (osteichthyans) and the cartilaginous sharks and rays (chondrichthyans), contain over 99% of living vertebrate diversity, and share derived features including jaws, teeth, paired fins, paired nasal capsules and three semicircular canals that are absent in living jawless vertebrates. Key to the early evolution of jawed vertebrates are the placoderms, a group of armoured fishes which dominated vertebrate faunas until their extinction at the end of the Devonian period (c. 359Ma). Early treatments of placoderm relationships considered them to be a paraphyletic group, giving rise independently various groups of elasmobranchs (Ørvig 1962; Stensiö 1963; Stensiö 1969). This hypothesis was later rejected and placoderm monophyly was advocated (Goujet 1982; Goujet 1984b; Goujet 2001). Placoderm monophyly was challenged by a study on the vascularisation of the pectoral fin of antiarchs (Johanson 2002), but this was disputed (Young 2008). Placoderms have been hypothesised to be the sister group to chondrichthyans (Miles and Young 1977; Janvier 1996), or osteichthyans (Forey 1980; Gardiner 1984a), but are more often considered sister to other gnathostomes (Schaeffer 1975; Young 1986; Goujet 2001; Goujet and Young 2004). The first cladistic studies that explicitly tested placoderm monophyly rejected it in favour of a phylogenetic hypothesis in which placoderms were a paraphyletic assemblage of stem gnathostomes (Friedman 2007; Brazeau 2009). Although placoderms share many features not found in other gnathostome groups (Young 2010), these characters are contentious as, amongst other problems, many cannot be polarised by outgroup comparison (Brazeau 2009; Brazeau and Friedman 2014).

The current view of placoderm paraphyly implies that features common to placoderms are primitive for all gnathostomes. This has important implications for the study of key morphological features including teeth (Smith and Johanson 2003; Rücklin et al. 2012), braincase morphology (Dupret et al. 2014), the skull and jawbones (Zhu et al. 2013) and internal fertilisation (Long et al. 2015). However, support for placoderm paraphyly is acknowledged to be weak (Brazeau and Friedman 2015). The discovery that dermal claspers and therefore internal fertilisation is apparently widespread across placoderm groups (Miles and Young 1977; Long et al. 2015; Trinajstić et al. 2015) also weakens support for placoderm paraphyly as it requires a reversal to external fertilisation at the crown gnathostome node (Brazeau and Friedman 2015). There is little or no evidence of a reversal from internal to external fertilisation, or from viviparity to oviparity, occurring in any recent group of fishes (Blackburn 2015), despite multiple origins, and it is possible that internal fertilisation is an irreversible or nearly irreversible character. The uncertainty in phylogenetic relationships at the base of the gnathostomes is potentially driven by outgroups with morphologies that are difficult to compare with gnathostomes, or lack detailed neurocranial preservation.

The recent application of relaxed clock Bayesian methods to morphological palaeontological data (Lee et al. 2014; Close et al. 2015; Gavryushkina et al. 2017), provides the opportunity to gain a more complete picture of the evolution of extinct groups. Here this method is applied to an expanded early gnathostome dataset, with the aim of testing evolutionary relationships and investigating rates of evolution. Although character support for either placoderm monophyly or paraphyly is essentially equivocal, the tip-dated, morphological clock method finds strong support for placoderm monophyly, suggesting that this approach can have effects on tree topology as well as analysing rates of evolution. Observed and simulated patterns of rate heterogeneity provide tentative evidence that the result from the tip-dated clock analysis may be the correct one. The possibility of a very different topology in early gnathostome phylogeny - in which placoderms are monophyletic and thus not necessarily representative of the plesiomorphic gnathostome condition - must be considered when studying early vertebrate evolution. Throughout this paper, we use the term placoderms to refer to

the core group, excluding the maxillate placoderms such as *Entelognathus*. It is monophyly of this core group that is strongly supported by Bayesian tip-dated clock methods.

Materials and Methods

Data matrix

Characters were drawn from previous analyses on early gnathostomes (Brazeau 2009; Davis et al. 2012; Zhu et al. 2013; Dupret et al. 2014; Brazeau and de Winter 2015; Giles et al. 2015; Long et al. 2015), from a number of matrices of particular subgroups (Coates and Sequeira 2001; Friedman 2007; Zhu and Gai 2007; Dupret et al. 2009; Sansom 2009; Swartz 2009; Trinajstic and Long 2009; Carr and Hlavin 2010; Jia et al. 2010; Pradel et al. 2011; Lu et al. 2012; Pan et al. 2015; Zhu et al. 2015), as well as newly formulated characters.

To ensure the dataset satisfied the assumptions of tip-dated, morphological clock analysis, we attempted to sample characters with equal intensity across the whole phylogeny including terminal branches (undersampled in the vast majority of published morphological data matrices). We therefore included autapomorphies (character states found in only 1 sampled taxon), and characters applicable only to small subsets of taxa. 75 of 497 characters were therefore parsimony uninformative. We imported some autapomorphies from matrices of subclades in which they were phylogenetically informative due to denser taxon sampling. Others were new and selected if they constituted morphological variation qualitatively similar to the phylogenetically informative characters. We recoded terminal taxa at the species level, and reformulated the outgroup as constituent species rather than superspecific taxa. Galeaspid histological characters are best known from isolated fragments (Wang et al. 2005). We included these as a separate taxon, and constrained a group consisting of this purely histological taxon (polybranchiaspid sp. histological samples) and two polybranchiaspid species to be monophyletic in all analyses.

The matrix had a total of 117 taxa and 497 characters. The full list of characters, characters sources, taxa and taxon sources are in the supplementary information. New and revised characters are in bold. The matrix was assembled in Mesquite 3.04 (Maddison and Maddison 2015) and the nexus file is included in the Dryad repository (<http://dx.doi.org/10.5061/dryad.v30f1>).

Parsimony analysis

We performed parsimony analysis in TNT (Goloboff et al. 2008), using a traditional search strategy with 5000 random addition sequence replicates, saving 10 trees in each replicate. Due to the extremely large number of shortest trees we did not perform a fully exhaustive tree search. 6490 shortest trees of length 1175 were collected. We ran an additional analysis with a negative (=reverse) constraint on placoderm monophyly (i.e. to find the shortest tree in which placoderms were not monophyletic), resulting in 5950 trees of length 1176. One of the shortest trees from each analysis was loaded into PAUP* 4.0b10 (Swofford 2002) to extract lists of characters that differed in length between the two topologies.

Tip-Dated Morphological clock analysis

We used BEAST2.3.2 (Bouckaert et al. 2014) for tip-dated morphological clock analyses via Bayesian MCMC. We assembled Xml files manually, using output from both BEAUti2.3.2 and BEASTmaster (Matzke 2015).

We used a sampled-ancestor fossilised birth death tree prior (Gavryushkina et al. 2014). Due to the absence of extant taxa, we did not implement a rho parameter (proportion of extant species). We fixed removal probability at 0 as this describes an epidemiological process not applicable to fossils.

Recently there has been a trend towards partitioning morphological analyses by the number of states (Close et al. 2015; Gavryushkina et al. 2017), as opposed to using a single partition with the number of states equal to the maximum number observed in the matrix (Lee et al. 2014). The partitioned model typically has a far superior marginal likelihood (~1000 log likelihood units in this

case). The partitioned model, however, has the unintended side-effect of upweighting changes in multistate characters. This is due to the lower stationary frequencies in partitions with higher numbers of states. There is no clear biological justification for the effective upweighting of changes in characters with high number of states. Splitting characters into more states already artificially upweights them by increasing the number of changes, so it could be argued that each change in such characters should be, if anything, downweighted. Compounding this problem by using a typical existing partitioned model is undesirable. The solution employed here is to partition the dataset by number of states (one partition for 2 state characters and one for 3 state characters), but to increase the exchangeability values (mutationRate in the xml files) in the partition with 3 state characters. Increasing the exchangeability values to 1.5 for 3 state characters, 2 for 4 states etc. exactly counteracts effect of the lower stationary frequencies. This model will be referred to as the partitioned reweighted model. Two partitions were used as the data matrix only had characters with 2 or 3 states.

We tested different partitioning schemes and clock models using path sampling (Baele et al. 2012). After a burn-in of 30,000,000 generations, we ran path sampling analyses for 30 steps, each of 10,000,000 generations. Alpha was 0.3 and each step had an additional burn-in period of 10%. We tested three different partitioning schemes: unpartitioned, partitioned and partitioned reweighted (see above). We tested a strict clock against the lognormal uncorrelated relaxed clock (Drummond et al. 2006). Finally, we tested models with and without a gamma parameter with four discrete rate categories to account for rate variation across sites. The prior distributions for each parameter are detailed in the supplementary information.

We performed a number of sensitivity analyses to test the robustness of conclusions to various model assumption violations. One analysis excluded all taxa occurring after the Frasnian. This eliminates the large number of stratigraphically late chondrichthyans which were originally included to compensate for a depauperate Devonian record. However, the lack of sampling of non-

chondrichthyan taxa in this time period may bias the tree prior model which assumes equal sampling across the phylogeny. A second sensitivity analysis tested the effect of the stratigraphic uncertainty, i.e. the specified tip dates. We ran an analysis where 28 taxa with relatively large dating uncertainty (>c.5Myr) were given uniform age range priors over the period of uncertainty (see supplementary information for the age ranges used). Because the sampling process in this analysis can allocate separate ages to fossils found in the same site (and thus with the same age ranges), we used this analysis simply to test sensitivity to the tip date uncertainty.

We ran analyses for four independent runs of 200,000,000 generations each. Some analyses were run on the CIPRES Science Gateway (Miller et al. 2010). Convergence was assessed by superimposition of parameter traces of all four runs in Tracer (Rambaut et al. 2014) and ESS > 200 for all parameters. Post burn-in samples from the four runs were combined for further analysis and figures. The maximum clade consensus tree was calculated. Because of the significant phylogenetic uncertainty at the root of the ingroup (gnathostomes) found in the Bayesian clock analysis, we wrote an R function that returns the posterior probability of multiple clades being monophyletic (simultaneously) in the posterior sample of trees. This function was dependent on packages ape (Paradis et al. 2004) and caper (Orme et al. 2013). The function included the option to prune rogue taxa from all trees prior to analysis. For the credible set of topologies shown in Figure 4b, the unstable taxon *Ramirosuarezia* (Pradel et al. 2009) was dropped from all trees, and all probabilities assume that osteichthyans, placoderms and acanthodians/chondrichthyans are monophyletic. R code for this function (monophy.multi.R) is in the Dryad repository.

To examine how rates of evolution vary through time, the dataset was analysed in BEAST1.8.3 (Drummond et al. 2012), which implements an epoch clock (Bielejec et al. 2014), that assigns a separate evolutionary rate to specified time slices. As for the BEAST2 analysis, a partitioned model with reweighted 3-state characters was implemented. The tree prior was a birth-death serial sampled model (Stadler 2010). Seven time slices were specified. The first was pre-Silurian with no

upper bound, followed by the Silurian, Lochkovian/Pragian, Emsian, Middle Devonian, Late Devonian and Carboniferous. The epoch clock analysis was run for 100,000,000 generations (four independent runs) and convergence checked as above.

Because the epoch clock applies strict clock rates to each time slice, it may not be a realistic model when there is rate variation within time slices (e.g. across lineages). To see if the same patterns found in the epoch clock analysis held in the relaxed clock analysis (which allowed rates to vary across lineages), a function in R was written to extract weighted mean rates in each time slice across the posterior sample of trees and plot them against the geological timescale. The packages `OutbreakTools` (Jombart et al. 2014), `picante` (Kembel et al. 2010) and `geoscale` (Bell 2015) were required. The R code for these functions (`get.epoch.rates` and `geoplot.epoch.rates`) is in the Dryad repository.

Simulations: testing the performance of different methods in rooting phylogenetic trees in the absence of informative outgroups

Since very different root positions for the ingroup gnathostome clade were retrieved from the parsimony and Bayesian clock methods, simulations were performed to investigate the performance of these methods. Simulations were performed in BEAST2.3.2, using models and parameters based on the results from BEAST. Simulations were based on two trees taken from preliminary runs of the gnathostomes dataset in BEAST. The first was an unconstrained tree representing a relatively balanced phylogeny (i.e., with placoderms monophyletic). The second was from a constrained run with placoderms paraphyletic, representing a relatively unbalanced phylogeny. 500 two-state characters were simulated using values similar to empirical values: a lognormal relaxed clock with mean rate 0.08 and a gamma parameter with alpha 2 to represent among-character rate variation; the standard deviation of the clock lognormal distribution was 0.9 for the balanced tree and 1.0 for the unbalanced tree. 12 simulation replicates on each tree were performed. 73% of the simulated data was removed from the outgroup (reflecting the empirical situation here where only 27% of

characters are scorable to both the outgroup and the ingroup, a likely cause for instability in the root position). The simulated data was reanalysed in TNT using 1000 random addition sequence replicates saving 10 trees in each replicate, and strict and 50% majority rule consensus trees were calculated. Reanalysis in BEAST used the same model parameters and priors as the analysis on the empirical dataset, with the exception of a wide uniform prior on mean clock rate (0-1000). The correct clock model and tip ages were assumed. Analyses were run for 200,000,000 generations and convergence checked as for other BEAST analyses.

Revisions to characters supporting placoderm paraphyly

Position of the hyoid arch and orientation of the hyomandibular nerve

Evidence for placoderm paraphyly in previous analyses may have been inflated due to inclusion of multiple characters associated with the same morphological feature: the anterior position of the jaws in some placoderms, and the anterior position of the gill arches in osteostracans (an agnathan outgroup). The following characters have supported paraphyly with state 1 uniting a subset of placoderms (especially arthrodirens) and crown gnathostomes:

1. Position of hyomandibula articulation on the neurocranium: 0) below or anterior to orbit, on ventrolateral angle of braincase; 1) on otic capsule, posterior to orbit. Brazeau (2009) character 89; Davis et al., (2012) character 95; Zhu et al., (2013) character 95; Dupret et al., (2014) character 95; Long et al., (2015) character 95; Giles et al., (2015) character 163.
2. The main trunk of facial nerve (N.VII): elongate and passes anterolaterally through orbital floor; 1) stout, divides within otic capsule at the level of the transverse otic wall. Brazeau (2009) character 71; Davis et al., (2012) character 69; Zhu et al., (2013) character 69; Dupret et al., (2014) character 69; Long et al., (2015) character 69; Giles et al., (2015) character 137.

3. Position of upper mandibular arch cartilage (and associated cheek plate where present): 0) entirely suborbital; 1) with a postorbital extension. Giles et al., (2015) character 95.
4. Orbit dorsal or facing dorsolaterally, surrounded laterally by endocranium: 0) present; 1) absent. Brazeau (2009) character 68; Davis et al., (2012) character 66; Zhu et al., (2013) character 66; Dupret et al., (2014) character 66; Long et al., (2015) character 66; Giles et al., (2015) character 130.

The hyomandibular articulation and the hyomandibular nerve (Fig1). The hyomandibular nerve character is problematic for two reasons. Firstly, it is not clear that characters involving the division of the hyomandibular nerve can be applied to agnathans. The hyomandibular nerve of lampreys does not appear to have any pretrematic or palatine branches (Johnston 1905; Kuratani et al. 1997), and this appears to also be the case in osteostracans (Stensiö 1927). Therefore the division of the hyomandibular nerve mentioned by Brazeau and Friedman (2014) may not be equivalent to a palatine ramus. However, a character concerning only the orientation of the nerve may still be useful, but this is not independent from the position of the hyomandibular articulation. The hyomandibular nerve will necessarily go through the orbit when the hyoid arch is positioned anteriorly. The character concerning the nerve is therefore redundant and can be deleted in favour of the character concerning the attachment of the hyoid arch, which can be scored in more taxa. In addition, this character is variable within the outgroup. The hyoid arch in galeaspids is posterior to the orbits (Fig. 1E), and if it is scored as such then both placoderm monophyly and paraphyly are equally parsimonious for this character.

The upper mandibular arch. This character was only included by Giles et al. (2015). It refers to the suborbital position of the “upper mandibular arch cartilage” which was scored as “entirely suborbital” in the outgroups and some placoderms. However it is questionable whether or not this character should be scored in the outgroups. Mandibular arch derivatives occupy an extensive domain in living agnathans, as opposed to gnathostomes in which they are confined to a distinct domain between

the premandibular and hyoid regions (Miyashita 2015). The mandibular arch cartilages of living agnathans (the velar and lingual cartilages) are not exclusively suborbital, and it is not clear that one or the other can be homologised with the palatoquadrate in a straightforward manner. As far as can be assessed, conditions in the osteostracans and galeaspids are more similar to extant agnathans than gnathostomes (Janvier 1996; Miyashita 2015). This character should be inapplicable in outgroups. Within gnathostomes, this character is not independent from the character concerning the position of the hyomandibula articulation, as the mandibular and hyoid arches are expected to move forwards in tandem given the supporting role of the latter for the former. This character is deleted here due to redundancy, but it should not affect placoderm paraphyly/monophyly if correctly scored.

Orbit surrounded by endocranium. The orbit being surrounded by endocranium may also be linked to the anterior migration of the hyomandibular attachment. In most placoderms the hyomandibula attaches to the anterior postorbital process, but when the hyomandibula attaches in an anterior position this part of the braincase must also extend forward to provide a surface for attachment. In *Romundina*, *Macropetalichthys* and *Brindabellaspis* successively further anterior hyomandibular attachments lead to a greater proportion of the orbit being surrounded by neurocranium. However, because the condition in *Doliodus* demonstrates that this character is at least partly independent from the position of the hyomandibular attachment, this character has been retained in all analyses.

When this character complex is reduced to a simple character involving the position of the hyoid arch relative to the orbits, it can be seen to be effectively continuous (Fig. 1A-D), with the posterior of the orbit used to split the character into two states. Jawless vertebrates show similar variation in the positions of the gill arches relative to the orbits (Fig. 1E-G), with an extreme anterior position being a feature of osteostracans. Independent acquisition of an anterior hyoid arch in some placoderms and osteostracans (consistent with placoderm monophyly) is therefore equally parsimonious with a single acquisition and secondary loss (consistent with placoderm paraphyly).

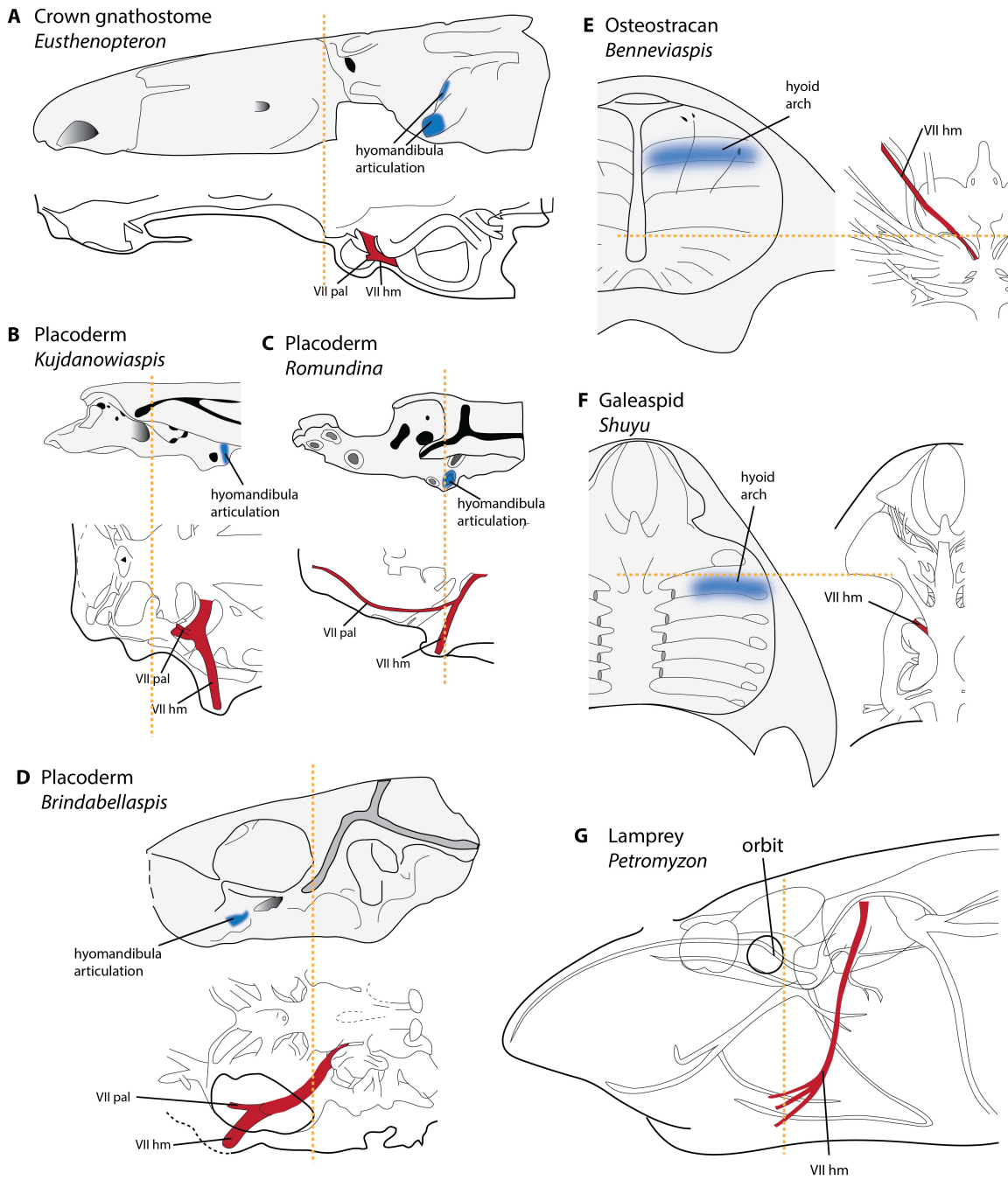


Figure 1. Characters that supported placoderm paraphyly, concerning the position of the hyoid arch and the orientation of the facial nerve, are correlated - and variable in the jawless outgroups. A-D) gnathostomes, external view of braincase in left lateral view and dorsal view of braincase showing outline of the cranial cavity and nerves (B is in ventral view). Dotted lines mark posterior of the orbits. The hyoid arch articulation character is effectively continuous, ranging from an articulation posterior to the orbits (A-B), to suborbital (D) or intermediate (C). The orientation of the hyomandibular nerve and the position of the division of the palatine nerve are correlated with the hyomandibular articulation position. E-F) agnathans, braincase in ventral view and ventral view showing outline of cranial cavity and nerves. G) lamprey in left lateral view showing outline of cranial nerves. The anterior position of the hyoid arch and facial

nerve in osteostracans (E) is not found in other agnathan groups (F-G). Characters based on the division of facial nerve are inapplicable in agnathans (G) as they do not have a palatine nerve. Sources: A) Jarvik (1980); B) Dupret (2010) and Goujet (1984a); C) Dupret et al. (2014); D) Young (1980); E) Janvier (1985); F) Gai et al. (2011); G) Johnston (1905) .

Trigemino-facial recess

Presence of a trigemino-facial recess, as scored in Giles et al. (2015) is an important character as it unites rhenanid placoderms with crown gnathostomes, thus supporting placoderm paraphyly. The character was introduced by Davis et al. (2012), citing Goodrich (1930), Schaeffer (1971), Gardiner (1984b) and Maisey (2005) as sources. These references give differing definitions however, and none would support a shared condition in rhenanids and crown gnathostomes.

Goodrich (1930), following Allis, described the trigemino-facial chamber as consisting of two parts. The first is the pars ganglionaris, a 'recess' of the cranial cavity (i.e. an outpocket) containing the trigeminal and facial ganglia. The second is the pars jugularis, a space between the lateral commissure and the lateral cranial wall through which the jugular vein passes. These form a divided chamber when the lateral endocranial wall is complete (prefacial commissure), and an undivided chamber when this is broken down such that the pars ganglionaris and pars jugularis are confluent. Goodrich defined the trigeminofacial recess as only the divided condition.

Schaeffer (1971) on the other hand, argued against the definition of using a single term for a divided chamber, when the division was such a fundamental feature as the endocranial wall. Schaeffer's definition restricted the term trigemino-facial recess to the space between the lateral cranial wall and the lateral commissure. Under this definition the actual position of the trigeminal and facial ganglion becomes irrelevant (Schaeffer 1971). Gardiner (1984) followed this definition and noted that it could also apply to chondrichthyans. This definition of the trigemino-facial recess is also not useful here, as the lateral commissure and jugular canal are already dealt with in other characters.

Also, in sarcopterygians such as *Eusthenopteron*, the lateral commissure is offset posteriorly from the trigeminal and facial nerves.

The rhenanid *Jagorina* is depicted as having a large trigemino-facial-acoustico recess in Stensiö (1969). This is an intramural recess of the cranial cavity, which might correspond to the pars ganglionaris of Goodrich (1930). It is not a trigemino-facial chamber under the definition formed by Schaeffer (1971) for the trigemino-facial chamber. Schaeffer in fact apparently had different definitions for the trigemino-facial chamber and the trigemino-facial recess, the latter referring to the intramural recess.

Thus, the condition in rhenanids corresponds to the trigemino-facial recess of Schaeffer, but not the trigemino-facial chamber. Davis et al. (2012) however refer to their trigemino-facial recess as extra-mural, and therefore appear to be referring to the chamber rather than the recess of Schaeffer. This cannot match the condition in rhenanids.

Maisey (2005) discussed the acoustico-trigemino-facial recess, an internal space containing the roots of the trigeminal, facial and acoustic nerves. Also discussed is the trigeminal pituitary fossa, which contains the pituitary vein, abducens nerve, external rectus muscle and the ganglia for the trigeminal and facial nerves in neoselachians. This fossa does not house the trigeminal or facial ganglia in *Cladodoides* and on this basis, a trigemino-facial recess was determined to be absent in *Cladodoides* (Maisey 2005). In the placoderm *Brindabellaspis* the trigeminal and facial nerves open into the myodome for the external rectus muscle, and so a trigemino-facial recess could be said to be present (Gardiner 1984, Maisey 2005).

If an expanded definition of a trigemino-facial recess is used, based on one of these references is used, possibilities for how they would be scored are as follows:

1. Goodrich (1930). A continuous space between the lateral commissure and the cranial cavity formed by the breakdown of the wall between the pars ganglionaris and the pars jugularis. Originally described in *Amia* and other basal actinopterygians; could be said to be present in *Acanthodes*.
2. Schaeffer (1971). The space between the lateral commissure and the lateral cranial wall. This character would not be independent of other characters concerning endocranial processes and the jugular vein, and the position of the trigeminal and facial nerves would be irrelevant.
3. Maisey (2005). A fossa containing the abducens nerve, external rectus muscle, pituitary vein and the trigeminal nerve. This would be present in some chondrichthyans and *Brindabellaspis*.

While the trigeminal and facial nerves and their respective ganglia are no doubt a source of useful characters, no condition clearly links rhenanids and crown gnathostomes. In the current matrix this character is deleted, but reinstatement in modified form at a later date is likely.

Results

Parsimony

Parsimony analysis showed that placoderm paraphyly and monophyly are essentially equally parsimonious. The strict consensus tree has placoderms monophyletic, but placoderm paraphyly is a single step longer (Fig. 2). The two topologies are essentially identical apart from the root position within the ingroup clade (gnathostomes). The first topology places the gnathostome root between placoderms and all other gnathostomes, resulting in reciprocal monophyly; the second topology places the root within placoderms, thus rendering placoderms paraphyletic with respect to crown gnathostomes. Characters that differ in length between the two topologies are shown in table 1.

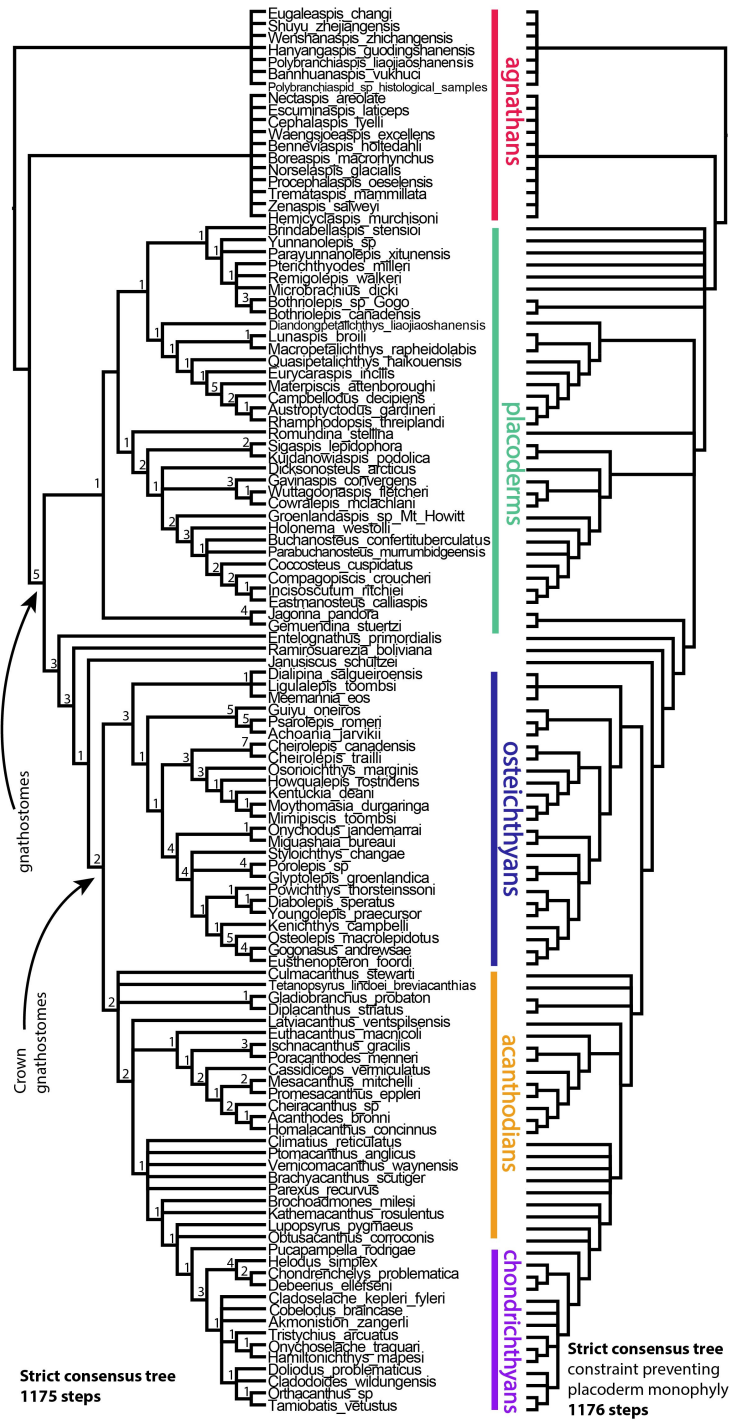


Figure 2. Results of parsimony analysis of the revised gnathostomes dataset show placoderm monophyly and paraphyly are essentially equally parsimonious. Left: Strict consensus tree of unconstrained analysis. Right: Strict consensus tree of an analysis with negative constraint on placoderm monophyly. Numbers on the left tree refer to Bremer support values. The grey box indicates placoderms.

Character	Number of steps when placoderms are paraphyletic	Number of steps when placoderms are monophyletic
20. Nasal openings: 0) dorsal, placed between orbits, 1) ventral and anterior to orbits	2	3
30. Orbit dorsal or facing dorsolaterally, surrounded laterally by endocranium: 0) absent; 1) present	3	4
73. Optic fissure: 0) present; 1) absent	2	1
76. Jugular canal: 0) long; 1) short; 2) absent	3	4
87. Paired occipital facets	2	1
208. Dermal plate associated with pineal eminence or foramen: 0) contributes to orbital margin; 1) separated from orbital margin	1	2
395. Intromittent organ not associated with pelvic fins	2	1
465. Synarcual	3	2
468. Longitudinal scale alignment in fin webs	4	3

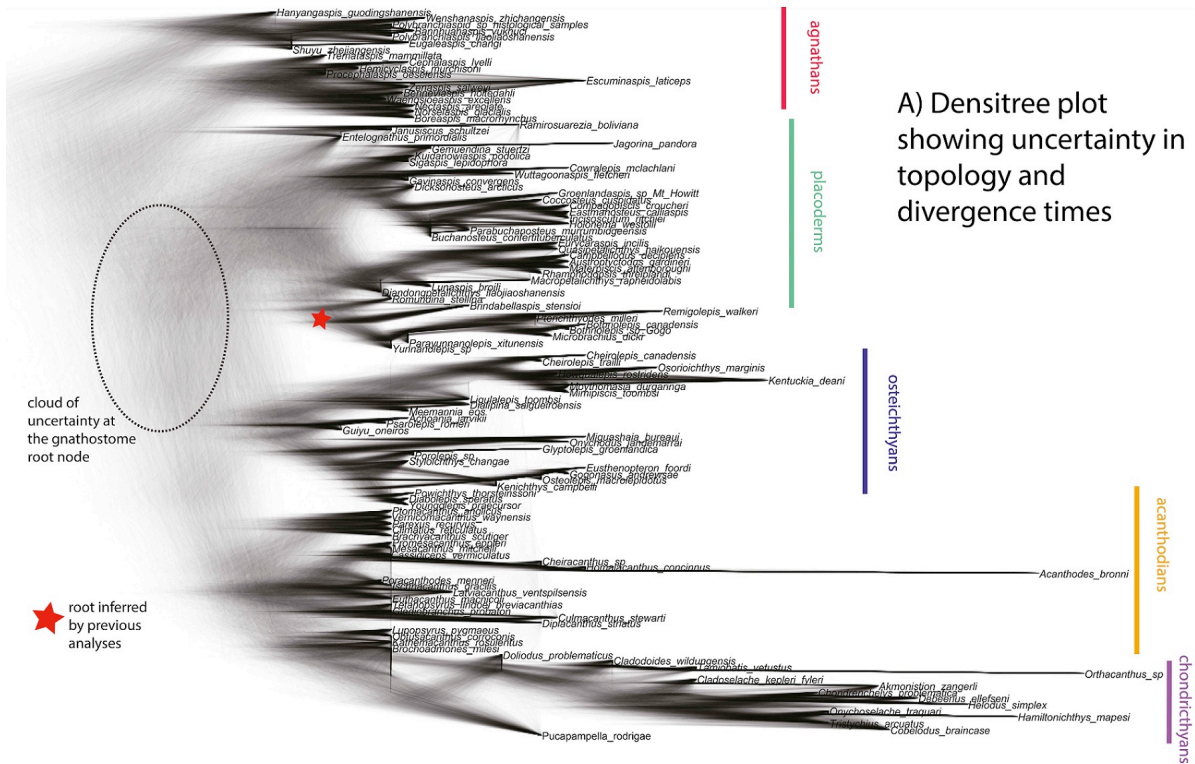
Table 1. Characters that differ in length between trees in which placoderms are paraphyletic and monophyletic. Bold denotes which topology is favoured (fewer character changes).

Bayesian morphological clock analysis

Stepping stone analysis supported partitioning of characters by the number of observed character states (marginal log likelihood -5601.52) over an unpartitioned model (-6601.78). There was a further increase in support for the model in which the substitution rates in the three-state partition were increased (to 1.5) to compensate for the lower stationary frequencies (marginal log likelihood -5589.64). The uncorrelated lognormal relaxed clock was supported over the strict clock (marginal log likelihood -5671.86) and use of a gamma parameter to describe among-character rate variation was preferred over a model with no such rate variation (marginal log likelihood -5646.95), with the latter two tests implemented under the partitioned reweighted model.

The tip-dated morphological clock analysis in BEAST strongly supports placoderm monophyly (Fig. 3), with a posterior probability of 0.997. Only 6 of the 7204 sampled trees correspond to a phylogeny consistent with placoderm paraphyly, in which antiarchs and acanthothoracids are sister group to other gnathostomes (pp=0.0008).

Many of the basal nodes in the phylogeny are however very weakly supported (Figs 3, 4). While the monophyly of placoderms, osteichthyans and the acanthodian-chondrichthyan clade receives strong posterior probabilities, their relationships to each other and to *Entelognathus* and *Janusiscus* are unresolved. This topological uncertainty is graphically demonstrated in the program DensiTree (Bouckaert 2010), which plots all trees in the posterior sample on top of each other. The DensiTree plot (Fig. 4A), shows complex webs at the base of the gnathostomes, among the placoderm orders, and among acanthodians. Relationships among osteichthyans generally appear more robust, with the exception of *Guiyu*, *Achoania* and *Psarolepis*, which appear to be flipping between various positions at the base of the osteichthyans. The instability at the gnathostome root means that the consensus tree (Fig. 3) does not represent a complete picture of the results. Ten different topologies representing different relationships among placoderms, osteichthyans, acanthodians/chondrichthyans, *Entelognathus* and *Janusiscus* account for 85% of the posterior density (*Ramirosuarezia* was pruned from all trees prior to calculation of posterior probabilities). Almost every possible topology concerning these five taxa is sampled at appreciable frequency. This is despite many of these topologies contradicting a large amount of cladistic morphological evidence, i.e. they are up to 16 steps longer under parsimony (Fig. 4B). Apparently, the morphological clock analysis can accommodate a substantial amount of homoplasy on temporally long basal branches without significant penalty. It is perhaps notable that despite this exaggerated uncertainty near the root, placoderm paraphyly is virtually never sampled.



A) Densitree plot showing uncertainty in topology and divergence times

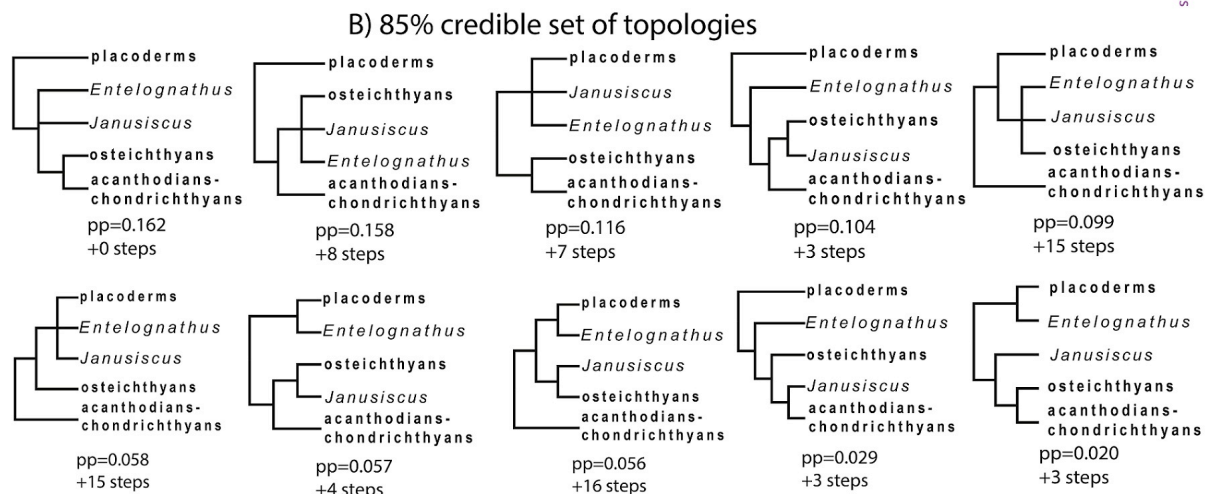


Figure 4. Topological uncertainty in the BEAST analysis. A) Densitree plot of the posterior sample of trees. B) posterior probabilities of various topologies involving the three major gnathostome groups (placoderms, osteichthyans and acanthodians-chondrichthyans) along with *Janusiscus* and *Entelognathus*. Posterior probabilities are conditional on placoderms, osteichthyans and acanthodians-chondrichthyans being monophyletic, and the unstable *Ramirosuarezia* was pruned from all trees prior to calculation. Many of these topologies are contradictory to much morphological evidence, as shown by their parsimony scores.

It is possible that the uncertainty near the root is being driven by the exceptionally fast rates on the branches leading to osteichthyans and acanthodians/chondrichthyans. A branch with outlier rate

may not fit the clock model well. Placing the gnathostome root on this branch effectively divides it into two branches, potentially with reduced rates. An analysis with artificially lowered rates on these branches (through character deletion) was used to test this, but a similar degree of uncertainty at the root was still found (not shown). Thus, sampling of unparsimonious topologies near the gnathostome root does not appear to be an artefact of fast-evolving branches.

Effect of character revisions on the outcome of analyses

To test the effect of the character revisions in the previous section on the outcome of the analyses we analysed a dataset with these characters (division of facial nerve, position of upper mandibular arch cartilage, trigemino-facial recess) reinstated. This included (what we regard as) incorrect codings that would lead these characters to support placoderm paraphyly (see above). The tip-dated morphological clock analysis still strongly supports placoderm monophyly (pp=0.962). This shows that consideration of stratigraphic ages and as well as rates of evolution can override weak cladistic signals regarding tree topology.

Rates of evolution in early vertebrates

The epoch clock analysis in BEAST1.8.3 shows a broad picture of declining rates following an initial burst during the early period of gnathostome evolution (Fig. 5A). The earliest time bin (prior to the Silurian) has a very wide posterior distribution, as expected due to the small number of branches. The last two time bins (Late Devonian and Carboniferous) are unlikely to be meaningful due to poor sampling of non-chondrichthyan taxa. The other four time bins (Silurian, Lochkovian-Pragian, Emsian, Middle Devonian) should therefore form the basis of comparison. The posterior distributions of the rate estimates do not overlap between the Silurian and the Emsian and Middle Devonian, whereas the Lochkovian-Pragian rates are intermediate. The mean posterior estimates for the evolutionary rate during these time slices are 0.00670, 0.00496, 0.00204, and 0.00272, suggesting that rates of evolution were approximately three times greater during the Silurian than the latter part of the Devonian.

The weighted mean rate estimates over the same time slices from the posterior sample of trees constructed using the uncorrelated lognormal relaxed clock in BEAST2.3.2 shows a similar pattern of declining rates (Fig. 5b), although the overall differences between epochs are slightly less substantial. The mean posterior estimates for weighted mean rate in the Silurian, Lochkovian-Pragian, Emsian and Middle Devonian are 0.00558, 0.00487, 0.00360 and 0.00358. Therefore during the Silurian, rates were only about 50% higher than during the latter part of the Devonian according to the relaxed clock. The higher rate estimates in the Silurian are inferred despite a total absence of any internal node or root age constraints. When a maximum age of 440Ma is applied to the gnathostome node, rates in these time slices become 0.00917, 0.00608, 0.00390 and 0.00407, more in line with the results from the epoch clock although the increase in rates across all time slices is intriguing. The pattern of declining rates appears to be robust, and also present in the sensitivity analyses (Figs. S1-S3). Analyses with constrained placoderm paraphyly, no post-Frasnian taxa or variable tip dates show the same pattern.

In terms of rates on individual branches, the relaxed clock analysis shows exceptionally high rates of evolution at the base of the osteichthyans and the acanthodian-chondrichthyan clade (Fig. 3). No such burst is present at the origin of placoderms.

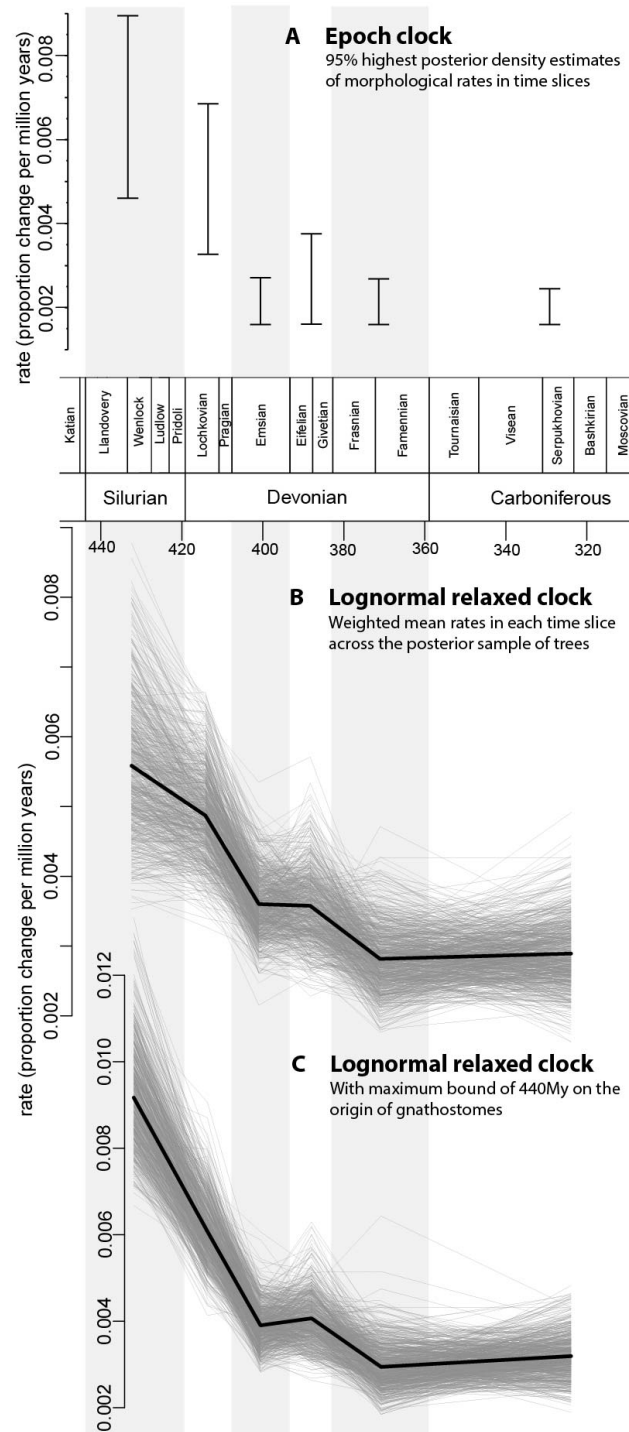


Figure 5. Rates of evolution during the Silurian and Devonian. A) Epoch clock analysis in Beast 1. 95% HPD intervals for evolutionary rate in each time slice, which correspond to the indicated geological intervals. B) Weighted mean rates in each time slice estimated for each tree in the posterior sample from a relaxed clock analysis, with no node age constraints. C) Same as B, but with an informative prior on the maximum age of gnathostome divergence at 440Ma, accentuating the early burst of evolution. The tree samples for B and C were thinned by a factor of 10 before plotting.

Performance of different methods in simulations

To test the performance of parsimony and the tip-dated morphological clock analysis in rooting the ingroup, simulations of 500-character datasets (using the mkv model), with 73% of data removed from the outgroup (discussed above) were performed. Simulations (12 replicates on each tree) were performed on two trees, the first was a relatively balanced tree taken from a preliminary BEAST analysis, corresponding to the situation in which placoderms are monophyletic. The second was a relatively unbalanced tree, corresponding to placoderm paraphyly. Results of the simulations are shown in table 1. Numbers indicate the number of nodes separating the correct (simulated) root from the inferred root (as found on the consensus tree); 0 means the correct root was found.

Both methods are found to perform significantly better on the balanced tree than the unbalanced tree (likely due to the shorter branch lengths around the root in the unbalanced tree). Parsimony performs badly (root incorrect by 4 or more nodes) in 1 out of 12 of the balanced trees and 8 out of 12 unbalanced trees. The consensus tree from the tip-dated morphological clock analyses performs better, with corresponding frequencies for badly-estimated roots being 0 out of 12, and 2 out of 12. As in the analysis of the empirical dataset, this analysis shows much uncertainty regarding the root position. Only 2 out of the 24 simulations show strong support for the correct root. However, only a single simulation analysis failed to sample the correct root at appreciable probability, and in this case parsimony found the identical, incorrect tree.

This limited simulation study suggests that when the outgroup is inapplicable (or unknown) for many characters, phylogenetic analysis struggles to root the tree correctly. However, it is notable that when the results from parsimony and the tip-dated clock analysis are very different, the tip-dated clock analysis is always more accurate. At least for datasets similar to this one, this simulation study shows that tip-dated clock methods outperform parsimony in inferring the root position of the tree when traits in the outgroup are not very informative, but neither method performs particularly well. The major caveat of this approach, as for all such simulations, is that the simulation used the same

models as BEAST, and therefore the results are only useful if the model realistic at least to some extent. It is notable that the parsimony results appear affected by a high level of long branch attraction in the reanalysis of the simulated data. The tip-dated clock analysis was not affected by this problem, but it complicated the results as parsimony tree was often highly inaccurate in other ways apart from being incorrectly rooted.

Tree 1			simulation number	Tree 2		
parsimony	BEAST	posterior probability		parsimony	BEAST	posterior probability
9	0	0.708	1	6	6	0.000
0	0	0.989	2	2*	1	0.241
polytomy	0	0.419	3	5	1	0.184
2	1	0.527	4	1	2	0.103
0	0	0.499	5	9	1	0.151
1	0	0.869	6	5	2	0.013
0	1	0.409	7	4	4	0.061
1	1	0.227	8	8*	2	0.042
0	0	0.998	9	4*	2	0.058
0*	1	0.191	10	0	1	0.385
2	1	0.516	11	1*	2	0.082
0	0	0.398	12	4	3	0.442

Table 2. Results from simulations. Two trees were used for the simulations, tree one similar to the consensus tree from BEAST (a balanced tree with corresponding to placoderm monophyly) and tree two an unbalanced tree corresponding to placoderm paraphyly. 73% of data in the outgroup was removed prior to reanalysis in BEAST and parsimony. Numbers refer to the number of nodes between the root found in the consensus tree and the correct root (i.e. lower is better and 0 means the correct root was found). For parsimony a strict consensus tree was used, but where this resulted in an uninformative polytomy a 50% majority rule tree was used, marked by an asterisk. In one case this still resulted in a polytomy. Bold denotes when there are significant differences between the results of the two methods, and in these instances BEAST is always more accurate.

Predictable patterns of rate variability in trees with the wrong root

Simulation 1 on the balanced tree has parsimony rooting the ingroup in the wrong position, producing an unbalanced tree similar in shape to an empirical parsimony tree in which placoderms are paraphyletic. This provides potential for comparison of patterns of rate variation between

simulated trees known to be incorrectly rooted, and the empirical trees that are suspected to be so (Fig. 6). A tree that is incorrectly rooted on a derived nested taxon artificially temporally compresses the "backbone" of branches between this taxon and the true root (grey branches, Fig. 6AB). The side branches coming off this backbone would conversely be temporally stretched (black branches, Fig. 6AB). Rates of evolution along the backbone should therefore be artificially increased, whereas rates on side lineages should be artificially decreased, when the tree has been rooted incorrectly. It is thus possible to characterise a clock "signature" of incorrect rooting, by comparing incorrectly and correctly rooted trees. A Bayesian clock analysis of the data from simulation 1 was run, but this time with the tree constrained to match the (incorrect) results from parsimony (Fig. 6B). Rates along the branches from the root inferred by parsimony were compared with rates along the lineages branching off this backbone. These were compared to rates on the equivalent branches in the correctly rooted trees. In the correctly rooted trees, rates on the (true) backbone and the (true) side lineages showed broadly overlapping distributions around the mean rates inferred for the whole tree. As predicted, in the incorrectly rooted tree, the (incorrectly inferred) backbone branch rates were greatly accelerated, whereas the (incorrectly inferred) side branch rates were decreased (Fig. 6c).

The empirical data from the gnathostome phylogeny shows remarkably similar patterns (Fig. 6d). The pattern from the placoderm monophyly tree (Fig. 3) matches the pattern from the correctly rooted tree from the simulations. However, repeating the analysis but constraining the data to one of the shortest parsimony trees implying placoderm paraphyly results in patterns of rate heterogeneity that closely match the simulated incorrectly rooted tree. In fact, the empirical data show an even stronger pattern: under placoderm paraphyly, there is no overlap at all between the rates on the backbone branches and the side branches, and no overlap of either with the mean rate for the tree.

It is important to note that the tip-dated consensus tree (with placoderm monophyly, Fig. 3) differs from the parsimony tree (with placoderm paraphyly) not just in the position of the gnathostome root, but also in other weakly supported topological details. Therefore it is possible that the rate heterogeneity seen in the analysis of the second tree is a product of topological constraints other than a different gnathostome root. To test this, another analysis was run such that the topologies of the consensus trees were identical aside from the root position, with the precise reverse constraints of the constrained paraphyly analysis (i.e. the placoderm paraphyly tree was rerooted to produce placoderm monophyly). Patterns of rate heterogeneity for this constrained monophyly tree (Fig. S4) were essentially identical to those on the unconstrained placoderm monophyly tree (Fig. 6). This shows that the patterns of rate heterogeneity for the placoderm paraphyly tree are a consequence of paraphyly itself rather than an artefact of constraining topology.

The incorrectly rooted simulated trees, and the empirical trees re-rooted with paraphyletic placoderms, show extreme amounts and distinct distributions of rate variation on basal branches, leading to increased among-lineage variability in evolutionary rates. The standard deviation of the lognormal rate distribution in the placoderm paraphyly tree is 1.108, while it is 0.973 in the monophyly tree, although the posterior distributions are overlapping (the 95% HPD intervals are 0.9233-1.2954 for the paraphyly tree and 0.7918-1.1628 for the monophyly tree). The estimated standard deviation in the incorrectly rooted simulation tree is 1.038 (HPD 0.8967-1.1731), compared to 0.942 (HPD 0.8191-1.0818) in the correctly rooted tree.

Although it is possible that the paraphyletic rooting in the empirical tree is correct, and the attendant rate patterns are "simply what happened", the striking resemblance of these patterns to those in known misrooted trees of simulated data suggest that placoderm paraphyly also represents an incorrect rooting.

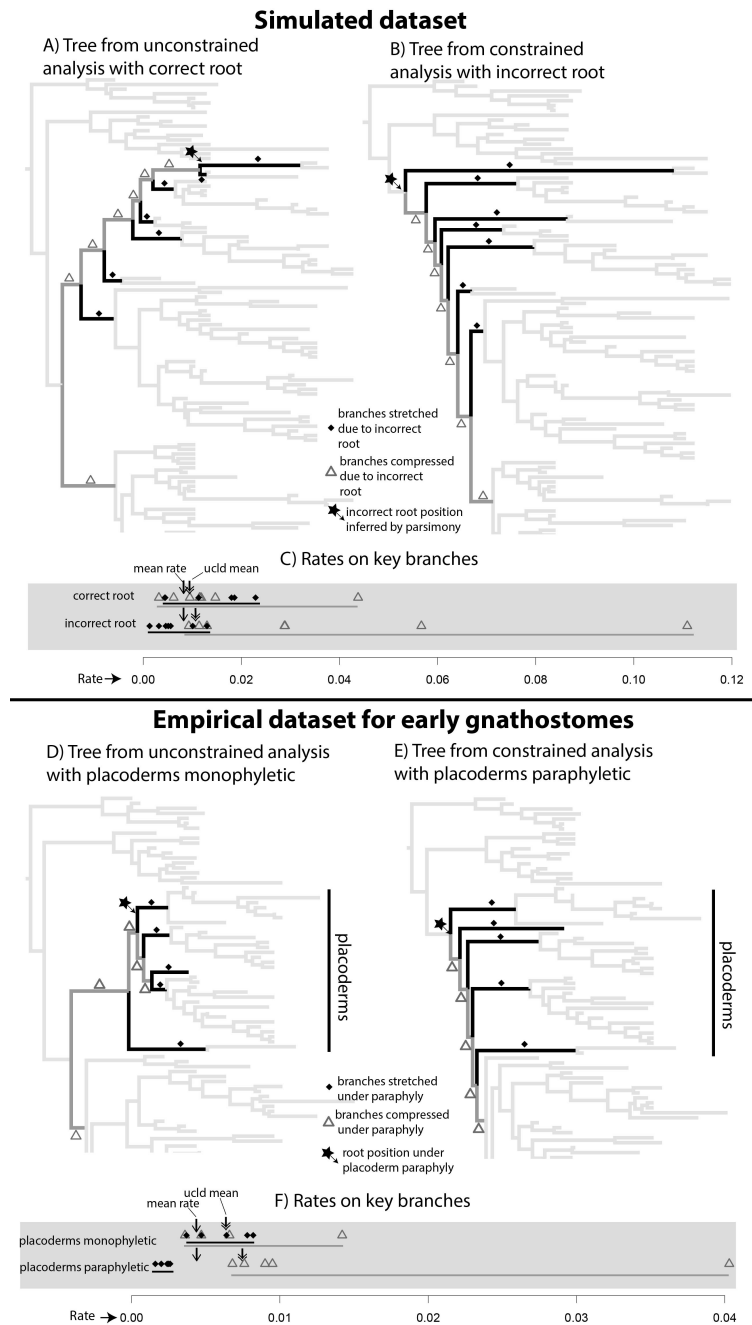


Figure 6. Trees known to be incorrectly rooted exhibit distinct patterns of evolutionary rates, similar to those in the empirical trees with placoderm paraphyly. A-C) Results for a simulated dataset (simulation 1 on tree 1 table 2). A) Tree from unconstrained tip dating analysis, which retrieved the correct root position. B) Tree from constrained tip dating analysis with incorrect root position (the root position found in parsimony analysis of the same dataset). Star indicates the incorrect root. Dark grey branches (triangles) are temporally compressed in the incorrectly rooted tree and black branches (diamonds) temporally lengthened, thus increasing and decreasing evolutionary rates respectively. C) Branch rates on the trees with the correct root (Figure A) and the incorrect root (Figure B). Branch rates on the lineage between the correct and the incorrect root (Fig. A-B, dark grey) are inflated when analysed with the incorrect root, and side branches (Fig. A-B, black) have reduced rates. The ranges of

rates on these two sets of branches overlap around the (weighted) mean rate for the whole tree (arrow) in the correctly-rooted tree, but are sharply divergent in the incorrectly-rooted tree. Similar patterns are found in the empirical gnathostomes dataset (D-F). D) Unconstrained tree, with placoderm monophyly tree, E) Constrained tree, enforcing placoderm paraphyly. Star indicates the root under placoderm paraphyly. Dark grey branches (triangles) would be temporally compressed in the paraphyly tree and black branches (diamonds) temporally lengthened. When placoderms are retrieved as monophyletic, rates for these 2 sets of branches broadly overlap each other and with weighted mean rate (arrow) for the rest of the tree, but when placoderms are constrained to be paraphyletic, rates for these 2 sets of branches are sharply divergent.

Discussion

Topological effects of using tip-dated clock methods

Although placoderm paraphyly and monophyly are almost equally parsimonious, the tip-dated morphological clock analysis strongly supports placoderm monophyly over paraphyly. Even after reinstating revised characters so that parsimony supported paraphyly, the tip-dated clock analysis still retrieved strong support for monophyly. Tip-dated clock analysis utilises a broader range of evolutionary data than other methods, incorporating stratigraphic ages of terminal taxa and estimates of rates of character change. Even if there is little cladistic character information available to choose between alternative topologies, these alternative topologies might still be expected to produce contrasting patterns of rates of evolution, when tip-age data is taken into account. Only a morphological clock analysis would be able to make use of this information directly during topology search. In the early gnathostomes dataset, the outgroup taxa are highly derived, and their body plans are so fundamentally different to gnathostomes that they are not particularly useful for polarising characters. Only about a quarter of characters are scoreable to both the outgroup and the ingroup, and some of these are invariant in the ingroup. Thus, the outgroups provide limited power to distinguish between alternative rootings where placoderms are either monophyletic or paraphyletic.

However, placoderm paraphyly apparently requires extremely unbalanced rates of evolution, with the branches leading to each placoderm subgroup exhibiting greatly decreased rates relative to the gnathostome stem lineage (Fig. 6). Simulations suggest that such patterns might be symptomatic of an incorrect rooting, and also suggest that Bayesian tip-dated morphological clock methods outperform parsimony in rooting trees when the outgroup and ingroup shared few applicable characters. The tip-dated clock method is likely to also select trees that are more consistent with stratigraphy: any model which assumes morphological change is (even very roughly) proportional to time will favour a basal position for ancient, plesiomorphic forms, and a nested position for recent, apomorphic forms. The resultant tree with placoderm monophyly indeed suggests a more basal position for very ancient forms such as *Entelognathus* and other Silurian taxa.

It is easy to imagine convergent evolution resulting in parsimony grouping together distantly-related taxa that might also be of very different ages. However, morphological clock analyses might reveal that this artefactual topology implies unusual patterns of evolutionary rates and implied stratigraphic ranges. It is notable that major topological differences obtained from using a tip-dated clock analysis have not been previously reported (to our knowledge). Major topological differences appear in this gnathostomes dataset, where the derived nature of the outgroup would be expected to cause issues with rooting the tree, and where the typical parsimony result (Brazeau 2009) is known to be controversial (Brazeau and Friedman 2015; Long et al. 2015).

There are however caveats associated with Bayesian tip-dated clock methods. The simulation study necessarily uses the same model as the analysis, so whether or not the superior performance of the Bayesian method is meaningful depends on the ability of the model to replicate the actual process underlying real morphological data. In addition, the tip-dated clock analysis appears to inflate uncertainty near the root of the tree, where topologies can be sampled which are contradictory to a large amount of character evidence. For example, placoderms as sister group to osteichthyans is at least 15 steps longer under parsimony. On the basal branches of the tree where large amounts of

character change occurs due to fast evolutionary rates, the Bayesian analysis can accommodate a large amount of homoplasy. Whether these allowed amounts of homoplasy are realistic or not needs to be more fully investigated.

Rates of evolution, divergence time and topological uncertainty

The elevated rates of evolution during the Silurian period retrieved in this analysis suggests that there was a rapid adaptive radiation following the origin of jaws. Our results mirror the findings from measures of lower jaw disparity (Anderson et al. 2011), which showed an increase in disparity into the Early Devonian, and relative stability thereafter.

There is strong information in the ages and morphologies of the fossil terminal taxa (tips) about divergence dates and rates of evolution across the tree. The divergence time for gnathostomes is given as 459Ma (95% HPD 446.09-473.83) in the focal analysis. This is retrieved without any informative priors (constraints) on the root age of the tree or any internal nodes. This ancient age implies a ghost range of ~35Myr for gnathostomes. However, fragmentary remains of the putative gnathostome *Skiichthys* (Smith and Sansom 1997) occur at c.450Ma. *Skiichthys* was suggested to have acanthodian or placoderm affinity, i.e. nested within gnathostomes. This would imply that the dates retrieved from the Bayesian analysis are not old enough. Mongolepids are a group of putative chondrichthyans that appear in the early Silurian (Karatujute-Talimaa et al. 1990). *Tantalepis* (Sansom et al. 2012) and *Areyonga* (Young 1997) are putative chondrichthyan taxa known only from scales from the Darriwilian (c. 458-467 Ma) of Australia. A chondrichthyan affinity for these taxa would similarly require the tree to be stretched further back. Nevertheless, these putative crown group gnathostomes are fragmentary and their stratigraphic age stands in great contrast to the younger ranges of articulated remains.

Similarly, even without any informative root or node age priors, the analysis shows elevated rates of evolution prior to the Devonian. Forcing a younger age for the origin of gnathostomes (bringing age estimates more in line with the ranges of undisputed articulated gnathostome fossils) would

compress branches at the base of the tree and thus accentuate this pattern further, as shown in the analysis with a maximum age of 440My on the gnathostome node. Such “ancient dates or accelerated rates” have been shown for mammals (Beck and Lee 2014). Regardless, gnathostomes were already quite disparate by the late Silurian, and this may be a major cause of the difficulty in determining the tree topology during this period. The inability of morphological data alone to resolve relationships among even well-known living vertebrates is well known (e.g. Reeder et al. 2015), and similar problems should be expected in early gnathostomes.

Convergent evolution in morphological datasets, and basal benthic placoderms

Convergent evolution is well known to be a major cause of problems in morphological datasets, and it is common for groups with similar ecologies to be incorrectly grouped together, as exemplified by legless lizards and snakes (Lee 1998; Reeder et al. 2015). It is notable therefore that both outgroups and the most basal placoderm taxa (under the paraphyly hypothesis) are presumably benthic species. Adaptation to a benthic niche might be expected to lead to convergent adaptations that could be (mis)interpreted as homologous plesiomorphies shared by the outgroup and certain placoderms. Such traits include a dorsal migration of the orbits and nares and a concomitant anterior migration of the jaws. Three of the four characters supporting paraphyly can be linked to these changes, most obviously the characters involving the dorsal position of the orbits and nares. The contact of the pineal plate with the orbits is also likely to be linked with migration of the orbits towards the midline. Since the nasal capsules are part of an independent endocranial unit in adult placoderms (one of the characters supporting placoderm monophyly), this likely had a profound effect on the development of placoderm braincases, possibly increasing the degree to which the nasal capsules could move relative to other sense organs. The possibility that morphological clock methods, through consideration of additional sources of information such as stratigraphy and inferred evolutionary rates, can better identify and accommodate morphological convergence may be a productive area for future study.

Implications of placoderm monophyly versus paraphyly

The hypotheses of placoderm monophyly and paraphyly offer starkly contrasting frameworks with important ramifications for the understanding key events in early vertebrate evolution. Under placoderm paraphyly, shared features of placoderms are presumed to be primitive and thus ancestral for all gnathostomes, whereas under placoderm monophyly, these features become unique specialisations of placoderms alone. The evolution of jaw bones was previously assumed to start with the simple jaws of placoderms, with a single dermal lower jaw bone and no upper jaw (maxilla). Dermal jaw bones were then added near the crown gnathostome node with the appearance of a maxilla, dentary, infradentaries and gulars. Under placoderm monophyly, this scenario can no longer be assumed to be correct. The position of *Entelognathus* is key, and it is retrieved as sister group to placoderms fairly often in the Bayesian analysis. If this is correct then it would mean that osteichthyan-like jaw bones could be the ancestral condition for jawed vertebrates. Jaws may have first evolved with a complex covering of dermal bones which was later reduced to a single lower jawbone and palatal toothplates in placoderms.

Placoderms might therefore be viewed as highly specialised dead end, rather than the ground plan for all other gnathostomes. In particular, the presence of a unique set of claspers and internal fertilisation are potential placoderm synapomorphies likely profoundly affecting their biology. Another consequence of placoderm monophyly would be a significant decrease in the number of known nodes in the phylogeny between the origin of jaws and the common ancestor of crown gnathostomes. Placoderm paraphyly results in a highly asymmetrical tree where basal gnathostomes are all placoderms, but placoderm monophyly has a more balanced tree where placoderms, *Entelognathus*, osteichthyans and chondrichthyans could be considered almost equally "basal" (Fig. 4B). Thus, the ancestral condition for gnathostomes becomes much more uncertain, with the major groups of placoderms, acanthodians and osteichthyans already diversified by the late

Silurian. The rates analysis is consistent with this scenario, with fast morphological rates and long ghost lineages being found at the base of the tree.

Acknowledgements

Mike Coates, Vincent Dupret, Per Ahlberg, Jing Lu, You'an Zhu, Brian Choo, Zerina Johanson and Alice Clement are thanked for discussions on early vertebrate morphology, and Nick Matzke for discussions about tip-dating. Alexandra Gavryushkina and Guy Baele answered questions via the BEAST google group. Martin Brazeau provided helpful comments on the manuscript, and we thank Thomas Near as editor. This work was supported by the Australian Research Council (To John Long).

References

- Anderson, P. S., Friedman, M., Brazeau, M. D. and Rayfield, E. J. (2011). Initial radiation of jaws demonstrated stability despite faunal and environmental change. *Nature* **476**, 206–209.
- Baele, G., Lemey, P., Bedford, T., Rambaut, A., Suchard, M. A. and Alekseyenko, A. V. (2012). Improving the accuracy of demographic and molecular clock model comparison while accommodating phylogenetic uncertainty. *Molecular Biology and Evolution* **29**, 2157–2167.
- Beck, R. M. D. and Lee, M. S. Y. (2014). Ancient dates or accelerated rates? Morphological clocks and the antiquity of placental mammals. *Proceedings of the Royal Society B* **281**, 20141278.
- Bell, M. (2015). geoscale: geological time scale plotting. In *R package version 2.0*. <https://CRAN.R-project.org/package=geoscale>.
- Bielejec, F., Lemey, P., Baele, G., Rambaut, A. and Suchard, M. A. (2014). Inferring heterogeneous evolutionary processes through time: from sequence substitution to phylogeography. *Systematic Biology* **63**, 493–504.

- Blackburn, D. G. (2015). Evolution of vertebrate viviparity and specializations for fetal nutrition: a quantitative and qualitative analysis. *Journal of Morphology* **276**, 961–990.
- Bouckaert, R., Heled, J., Kühnert, D., Vaughan, T., Wu, C.-H., Xie, D., Suchard, M. A., Rambaut, A. and Drummond, A. J. (2014). BEAST 2: a software platform for Bayesian evolutionary analysis. *PLoS Computational Biology* **10**, e1003537.
- Bouckaert, R. R. (2010). DensiTree: making sense of sets of phylogenetic trees. *Bioinformatics* **26**, 1372–1373.
- Brazeau, M. D. (2009). The braincase and jaws of a Devonian ‘acanthodian’ and modern gnathostome origins. *Nature* **457**, 305–308.
- Brazeau, M. D. and de Winter, V. (2015). The hyoid arch and braincase anatomy of *Acanthodes* support chondrichthyan affinity of ‘acanthodians’. *Proceedings of the Royal Society B* **282**, 20152210.
- Brazeau, M. D. and Friedman, M. (2014). The characters of Palaeozoic jawed vertebrates. *Zoological Journal of the Linnean Society* **170**, 779–821.
- Brazeau, M. D. and Friedman, M. (2015). The origin and early phylogenetic history of jawed vertebrates. *Nature* **520**, 490–497.
- Carr, R. K. and Hlavin, W. J. (2010). Two new species of *Dunkleosteus* Lehman, 1956, from the Ohio Shale Formation (USA, Famennian) and the Kettle Point Formation (Canada, Upper Devonian), and a cladistic analysis of the Eubrachythoraci (Placodermi, Arthrodira). *Zoological Journal of the Linnean Society* **159**, 195–222.
- Close, R. A., Friedman, M., Lloyd, G. T. and Benson, R. B. (2015). Evidence for a mid-Jurassic adaptive radiation in mammals. *Current Biology* **25**, 2137–2142.
- Coates, M. and Sequeira, S. (2001). A new stethacanthid chondrichthyan from the Lower Carboniferous of Bearsden, Scotland. *Journal of Vertebrate Paleontology* **21**, 438–459.
- Davis, S. P., Finarelli, J. A. and Coates, M. I. (2012). *Acanthodes* and shark-like conditions in the last common ancestor of modern gnathostomes. *Nature* **486**, 247–250.

- Drummond, A. J., Ho, S. Y., Phillips, M. J. and Rambaut, A. (2006). Relaxed phylogenetics and dating with confidence. *PLoS Biology* **4**, e88.
- Drummond, A. J., Suchard, M. A., Xie, D. and Rambaut, A. (2012). Bayesian phylogenetics with BEAUti and the BEAST 1.7. *Molecular Biology and Evolution* **29**, 1969–1973.
- Dupret, V. (2010). Revision of the genus *Kujdanowiaspis* Stensiö, 1942 (Placodermi, Arthrodira, “Actinolepida”) from the Lower Devonian of Podolia (Ukraine). *Geodiversitas* **32**, 5–63.
- Dupret, V., Sanchez, S., Goujet, D., Tafforeau, P. and Ahlberg, P. E. (2014). A primitive placoderm sheds light on the origin of the jawed vertebrate face. *Nature* **507**, 500–503.
- Dupret, V., Zhu, M. and Wang, J. Q. (2009). The morphology of *Yujiangolepis liujingensis* (Placodermi, Arthrodira) from the Pragian of Guangxi (South China) and its phylogenetic significance. *Zoological Journal of the Linnean Society* **157**, 70–82.
- Forey, P. (1980). *Latimeria*: a paradoxical fish. *Proceedings of the Royal Society B* **208**, 369–384.
- Friedman, M. (2007). *Styloichthys* as the oldest coelacanth: implications for early osteichthyan interrelationships. *Journal of Systematic Palaeontology* **5**, 289–343.
- Gai, Z., Donoghue, P. C., Zhu, M., Janvier, P. and Stampanoni, M. (2011). Fossil jawless fish from China foreshadows early jawed vertebrate anatomy. *Nature* **476**, 324–327.
- Gardiner, B. G. (1984a). The relationship of placoderms. *Journal of Vertebrate Paleontology* **4**, 379–395.
- Gardiner, B. G. (1984b). The relationships of the paleoniscid fishes. a review based on new specimens of *Mimia* and *Moythomasia* from the upper Devonian of Western Australia. *Bulletin of the British Museum (Natural History) Geology* **37**, 173–248.
- Gavryushkina, A., Heath, T. A., Ksepka, D. T., Stadler, T., Welch, D. and Drummond, A. J. (2017). Bayesian total evidence dating reveals the recent crown radiation of penguins. *Systematic Biology* **66**, 57–73.

- Gavryushkina, A., Welch, D., Stadler, T. and Drummond, A. J. (2014). Bayesian inference of sampled ancestor trees for epidemiology and fossil calibration. *PLoS Computational Biology* **10**, e1003919.
- Giles, S., Friedman, M. and Brazeau, M. D. (2015). Osteichthyan-like cranial conditions in an Early Devonian stem gnathostome. *Nature* **520**, 82–85.
- Goloboff, P. A., Farris, J. S. and Nixon, K. C. (2008). TNT, a free program for phylogenetic analysis. *Cladistics* **24**, 774–786.
- Goodrich, E. S. (1930). *Studies on the Structure and Development of Vertebrates*. Macmillan, London.
- Goujet, D. (1982). Les affinités des placodermes, une revue des hypothèses actuelles. *Geobios* **15**, 27–38.
- Goujet, D. (1984a). *Les poissons placodermes du Spitzberg: Arthrodires Dolichothoraci de la Formation de Wood Bay (Dévonien inférieur)*. Cahiers de Paléontologie, Section Vertébrés. CNRS, Paris.
- Goujet, D. (1984b). Placoderm interrelationships: a new interpretation, with a short review of placoderm classifications. In *Proceedings of the Linnean Society of New South Wales*, vol. 107, pp. 211–243.
- Goujet, D. (2001). Placoderms and basal gnathostome apomorphies. In *Major Events in Early Vertebrate Evolution* (ed. P. E. Ahlberg), pp. 209–222. Taylor and Francis, London and New York.
- Goujet, D. and Young, G. C. (2004). Placoderm anatomy and phylogeny: new insights. In *Recent advances in the origin and early radiation of vertebrates* (ed. G. Arratia, M. V. H. Wilson and R. Cloutier), pp. 109–126. Verlag Dr. Friedrich Pfeil, München.
- Janvier, P. (1985). *Les Céphalaspides du Spitzberg. Anatomie, phylogénie et systématique des Ostéostracés siluro-dévonien*. Révision des Ostéostracés de la formation de Wood Bay (Dévonien inférieur du Spitzberg). Cahiers de Paléontologie, Section Vertébrés. CNRS, Paris.
- Janvier, P. (1996). *Early vertebrates*. Clarendon Press, Oxford.

- Jarvik, E. (1980). *Basic structure and evolution of vertebrates*. Academic Press, London.
- Jia, L.-T., Zhu, M. and Zhao, W.-J. (2010). A new antiarch fish from the Upper Devonian Zhongning Formation of Ningxia, China. *Palaeoworld* **19**, 136–145.
- Johanson, Z. (2002). Vascularization of the osteostracan and antiarch (Placodermi) pectoral fin: similarities, and implications for placoderm relationships. *Lethaia* **35**, 169–186.
- Johnston, J. B. (1905). The cranial nerve components of *Petromyzon*. *Gegenbaurs Morphologisches Jahrbuch* **34**, 149–203.
- Jombart, T., Aanensen, D. M., Baguelin, M., Birrell, P., Cauchemez, S., Camacho, A., Colijn, C., Collins, C., Cori, A. and Didelot, X. (2014). OutbreakTools: A new platform for disease outbreak analysis using the R software. *Epidemics* **7**, 28–34.
- Karatujute-Talimaa, V., Novitskaya, L. I., Rozman, K. S. and Sodov, Z. (1990). *Mongolepis*—a new lower Silurian genus of elasmobranchs from Mongolia. *Paleontologicheskii Zhurnal* **1990**, 76–86.
- Kembel, S. W., Cowan, P. D., Helmus, M. R., Cornwell, W. K., Morlon, H., Ackerly, D. D., Blomberg, S. P. and Webb, C. O. (2010). Picante: R tools for integrating phylogenies and ecology. *Bioinformatics* **26**, 1463–1464.
- Kuratani, S., Ueki, T., Aizawa, S. and Hirano, S. (1997). Peripheral development of cranial nerves in a cyclostome, *Lampetra japonica*: morphological distribution of nerve branches and the vertebrate body plan. *Journal of Comparative Neurology* **384**, 483–500.
- Lee, M. S. Y. (1998). Convergent evolution and character correlation in burrowing reptiles: towards a resolution of squamate relationships. *Biological Journal of the Linnean Society* **65**, 369–453.
- Lee, M. S. Y., Cau, A., Naish, D. and Dyke, G. J. (2014). Morphological clocks in paleontology, and a mid-Cretaceous origin of crown Aves. *Systematic Biology* **63**, 442–449.
- Long, J. A., Mark-Kurik, E., Johanson, Z., Lee, M. S., Young, G. C., Min, Z., Ahlberg, P. E., Newman, M., Jones, R. and Den Blaauwen, J. (2015). Copulation in antiarch placoderms and the origin of gnathostome internal fertilization. *Nature* **517**, 196–199.

- Lu, J., Zhu, M., Long, J. A., Zhao, W., Senden, T. J., Jia, L. and Qiao, T. (2012). The earliest known stem-tetrapod from the Lower Devonian of China. *Nature Communications* **3**, 1160.
- Maddison, W. P. and Maddison, D. R. (2015). Mesquite: a modular system for evolutionary analysis. Version 3.04 <http://mesquiteproject.org>.
- Maisey, J. G. (2005). Braincase of the Upper Devonian shark *Cladodoides wildungensis* (Chondrichthyes, Elasmobranchii), with observations on the braincase in early chondrichthyans. *Bulletin of the American Museum of Natural History* **288**, 1–103.
- Matzke, N. J. (2015). BEASTmaster: R tools for automated conversion of NEXUS data to BEAST2 XML format, for fossil tip-dating and other uses. Instructions at PhyloWiki, <http://phylo.wikidot.com/beastmaster>.
- Miles, R. S. and Young, G. C. (1977). Placoderm interrelationships reconsidered in the light of new ptyctodontids from Gogo, Western Australia. *Linnean Society Symposium Series* **4**, 123–198.
- Miller, M. A., Pfeiffer, W. and Schwartz, T. (2010). Creating the CIPRES Science Gateway for inference of large phylogenetic trees. In *Gateway Computing Environments Workshop (GCE), 2010*, pp. 1–8. IEEE.
- Miyashita, T. (2015). Fishing for jaws in early vertebrate evolution: a new hypothesis of mandibular confinement. *Biological Reviews* **91**, 611–657.
- Orme, D., Freckleton, R., Thomas, G., Petzoldt, T., Fritz, S., Isaac, N. and Pearse, W. (2013). caper : comparative analysis of phylogenetics and evolution in R. In *R package version 0.5.2*. <https://CRAN.R-project.org/package=caper>.
- Ørving, T. (1962). Y at-il une relation directe entre les arthrodires ptyctodontides et les holocephales. *Colloques Internationaux du Centre National de la Recherche Scientifique* **104**, 49–61.
- Pan, Z., Zhu, M., Zhu, Y. A. and Jia, L. (2015). A new petalichthyid placoderm from the Early Devonian of Yunnan, China. *Comptes Rendus Palevol* **14**, 125–137.
- Paradis, E., Claude, J. and Strimmer, K. (2004). APE: analyses of phylogenetics and evolution in R language. *Bioinformatics* **20**, 289–290.

- Pradel, A., Maisey, J. G., Tafforeau, P. and Janvier, P. (2009). An enigmatic gnathostome vertebrate skull from the Middle Devonian of Bolivia. *Acta Zoologica* **90**, 123–133.
- Pradel, A., Tafforeau, P., Maisey, J. G. and Janvier, P. (2011). A new Paleozoic Symmoriiformes (chondrichthyes) from the Late Carboniferous of Kansas (USA) and cladistic analysis of early chondrichthyans. *PloS one* **6**, e24938.
- Rambaut, A., Suchard, M. A., Xie, D. and Drummond, A. J. (2014). Tracer v1.6, Available from <http://beast.bio.ed.ac.uk/Tracer>.
- Reeder, T. W., Townsend, T. M., Mulcahy, D. G., Noonan, B. P., Wood Jr, P. L., Sites Jr, J. W. and Wiens, J. J. (2015). Integrated analyses resolve conflicts over squamate reptile phylogeny and reveal unexpected placements for fossil taxa. *PloS one* **10**, e0118199.
- Rücklin, M., Donoghue, P. C., Johanson, Z., Trinajstić, K., Marone, F. and Stampanoni, M. (2012). Development of teeth and jaws in the earliest jawed vertebrates. *Nature* **491**, 748–751.
- Sansom, I. J., Davies, N. S., Coates, M. I., Nicoll, R. S. and Ritchie, A. (2012). Chondrichthyan - like scales from the Middle Ordovician of Australia. *Palaeontology* **55**, 243 – 247.
- Sansom, R. S. (2009). Phylogeny, classification and character polarity of the Osteostraci (Vertebrata). *Journal of Systematic Palaeontology* **7**, 95–115.
- Schaeffer, B. (1971). *The braincase of the holostean fish Macrepistius, with comments on neurocranial ossification in the Actinopterygii*. American Museum of Natural History.
- Schaeffer, B. (1975). Comments on the origin and basic radiation of the gnathostome fishes with particular reference to the feeding mechanism. *Colloques Internationaux du Centre National de la Recherche Scientifique* **218**, 101–109.
- Smith, M. M. and Johanson, Z. (2003). Separate evolutionary origins of teeth from evidence in fossil jawed vertebrates. *Science* **299**, 1235–1236.
- Smith, M. M. and Sansom, I. J. (1997). Exoskeletal micro-remains of an Ordovician fish from the Harding Sandstone of Colorado. *Palaeontology* **40**, 645–658.

- Stadler, T. (2010). Sampling-through-time in birth–death trees. *Journal of Theoretical Biology* **267**, 396–404.
- Stensiö, E. A. (1927). The Downtonian and Devonian vertebrates of Spitsbergen. I, Family Cephalaspidae. *Skrifter om Svalbard og Ishavet* **12**, 1–391.
- Stensiö, E. A. (1963). *Anatomical studies on the arthrodiran head*. Almqvist & Wiksell, Stockholm.
- Stensiö, E. A. (1969). Elasmobranchiomorphi Placodermata Arthrodires. In *Traité de paléontologie*, vol. 4 (ed. J. Piveteau), pp. 71–692. Masson, Paris.
- Swartz, B. A. (2009). Devonian actinopterygian phylogeny and evolution based on a redescription of *Stegotrachelus finlayi*. *Zoological Journal of the Linnean Society* **156**, 750–784.
- Swofford, D. (2002). PAUP 4.0 b10: Phylogenetic analysis using parsimony. Sinauer Associates, Sunderland, MA, USA.
- Trinajstić, K., Boisvert, C., Long, J., Maksimenko, A. and Johanson, Z. (2015). Pelvic and reproductive structures in placoderms (stem gnathostomes). *Biological Reviews of the Cambridge Philosophical Society* **90**, 467–501.
- Trinajstić, K. and Long, J. A. (2009). A new genus and species of Ptyctodont (Placodermi) from the Late Devonian Gneudna Formation, Western Australia, and an analysis of Ptyctodont phylogeny. *Geological Magazine* **146**, 743–760.
- Wang, N.-Z., Donoghue, P. C., Smith, M. M. and Sansom, I. J. (2005). Histology of the galeaspid dermoskeleton and endoskeleton, and the origin and early evolution of the vertebrate cranial endoskeleton. *Journal of Vertebrate Paleontology* **25**, 745–756.
- Young, G. C. (1980). A new Early Devonian placoderm from New South Wales, Australia, with a discussion of placoderm phylogeny. *Palaeontographica Abteilung A Palaeozoologie-Stratigraphie* **167**, 10–76.
- Young, G. C. (1986). The relationships of placoderm fishes. *Zoological Journal of the Linnean Society* **88**, 1–57.

- Young, G. C. (1997). Ordovician microvertebrate remains from the Amadeus Basin, central Australia. *Journal of Vertebrate Paleontology* **17**, 1–25.
- Young, G. C. (2008). The relationships of antiarchs (Devonian placoderm fishes)—evidence supporting placoderm monophyly. *Journal of Vertebrate Paleontology* **28**, 626–636.
- Young, G. C. (2010). Placoderms (armored fish): dominant vertebrates of the Devonian period. *Annual Review of Earth and Planetary Sciences* **38**, 523–550.
- Zhu, M. and Gai, Z. (2007). Phylogenetic relationships of galeaspids (Agnatha). *Frontiers of Biology in China* **2**, 151–169.
- Zhu, M., Yu, X., Ahlberg, P. E., Choo, B., Lu, J., Qiao, T., Qu, Q., Zhao, W., Jia, L., Blom, H. and Zhu, Y.-A. (2013). A Silurian placoderm with osteichthyan-like marginal jaw bones. *Nature* **502**, 188–193.
- Zhu, Y. A., Zhu, M. and Wang, J. Q. (2015). Redescription of *Yinostius major* (Arthrodira: Heterostiidae) from the Lower Devonian of China, and the interrelationships of Brachythoraci. *Zoological Journal of the Linnean Society* **176**, 806–834.

Chapter 4

New information on *Brindabellaspis stensioi* Young, 1980, highlights morphological disparity in Early Devonian placoderms

Benedict King¹, Gavin C. Young^{2,3}, John A. Long¹

¹College of Science and Engineering, Flinders University, PO Box 2100, Adelaide, South Australia 5001, Australia. ²Research School of Physics and Engineering (RSPE), Australian National University, Canberra 0200, Australian Capital Territory, Australia. ³Australian Museum Research Institute, 1 Williams Street, Sydney New South Wales 2010, Australia

Context

In this chapter I describe new specimens of the placoderm *Brindabellaspis*, which has been one the key taxa used in discussions of placoderm relationships. This chapter also describes a unique specialization of the lateral line sensory system in *Brindabellaspis*.

Statement of authorship

BK produced CT restorations, illustrations (Fig. 1) and initial descriptions and draft manuscript. GCY added significantly to the manuscript and produced illustrations (Fig. 5). JAL commented on the manuscript.

Abstract

When acid prepared specimens of the placoderm *Brindabellaspis stensioi* from the Early Devonian (Emsian) Taemas-Wee Jasper limestones of New South Wales, Australia were first described, they revealed placoderm endocranial anatomy in unprecedented detail. More recently, *Brindabellaspis* has become a key taxon in discussions of early gnathostome phylogeny. Here we present new specimens of *Brindabellaspis*, revealing the previously unknown anterior region of the skull. Strikingly, these specimens reveal that *Brindabellaspis* had an exceptionally long premedian plate, forming a paddlefish-like rostrum that extended far anterior to the orbits. Overlap surfaces on either side of the premedian plate were presumably for the suborbital plate, in an anterior position. The premedian plate has a unique midline sensory canal that forks at the anterior end. Digital rendering of a synchrotron radiation CT scan of this canal reveals that it is likely be the ethmoid commissure, which has doubled back and fused into a midline canal. The visceral surface of the premedian plate has a plexus of anastomosing perichondral bone canals, also known in the ‘acanthothoracid’ placoderm *Romundina*. The premedian plate appears to have been supported by a thin anterior extension of the postethmo-occipital unit of the braincase. The new specimens of *Brindabellaspis* also provide an updated skull roof reconstruction. The unusual morphology of *Brindabellaspis*, suggesting a benthic foraging role, shows that the early reef fish fauna from Taemas-Wee Jasper was home to a diverse range of fishes with specialised ecological roles.

Introduction

The Pragian-Emsian Wee Jasper-Lake Burrinjuck limestones preserve an ancient tropical reef gnathostome assemblage, which includes over 70 species of fossil fishes (Young 2011). The placoderms were the dominant vertebrate group in this fauna, with at least 45 species, including arthrodires, acanthothoracids, petalichthyids, ptyctodontids, and a ‘rhenanid’ (the status of acanthothoracids and rhenanids is discussed below). One of the most significant

discoveries from the fauna was the ‘acanthothoracid’ placoderm *Brindabellaspis stensioi* Young, 1980, which revealed endocranial anatomy in unprecedented detail. Recently the endocranial anatomy of another acanthothoracid, *Romundina stellina*, was described in great detail by (Dupret et al. 2017), based on synchrotron radiation CT scans.

Acanthothoracids are a poorly defined placoderm group, sharing characters including dorsal nasal capsules, a premedian plate and a short trunk armour, but none of these features is unique to acanthothoracids (Goujet and Young 2004). Acanthothoracids are of special interest in the question of gnathostome phylogenetics, namely whether placoderms form a paraphyletic grade (Brazeau 2009; Brazeau and Friedman 2014) or a clade (Young 2010; King et al. 2017). Phylogenetic analyses that have retrieved placoderm paraphyly invariably show *Brindabellaspis* in an unnested position (e.g. Brazeau 2009; Davis et al. 2012), and the dorsal nasal capsules and elongate trabecular region of *Romundina* have been suggested to be an intermediate between the cranial anatomies of jawless and jawed vertebrates (Dupret et al. 2014).

Brindabellaspis has an unusual morphology when compared with other placoderms, with the nasal capsules situated within the anterior cavity of the orbits and external openings indistinguishable from the orbits, and the braincase unusually deep (Young 1980). Of particular note is the extreme anterior position of the hyoid arch attachment, an interpretation disputed, for example by (Gardiner 1984) who argued that the posterior articulation (the opercular cartilage articulation of Young 1980) was in fact for the hyomandibula. The anterior hyoid arch attachment indicated that the jaws of *Brindabellaspis* (unknown) were situated largely anterior to the orbits. However, the anterior region was missing in the two skull specimens originally described by Young (1980).

Here we present descriptions of new specimens of *Brindabellaspis* showing an elongate premedian plate forming a prolonged rostral extension to the skull, supported by a thin expansion of the postethmo-occipital unit of the endocranium. The premedian plate bears an unusual dorsal midline sensory canal, a feature not seen in any other placoderm. CT scans reveal that this is likely to be the ethmoid commissure, folded back and fused in the midline.

The new specimens help to clarify the pattern of dermal bones on the anterior part of the skull roof. The highly specialised morphology of *Brindabellaspis* expands the known morphological disparity of early placoderms.

SYSTEMATIC PALEONTOLOGY

Class PLACODERMI McCoy, 1848

Order BRINDABELLASPIDA Gardiner 1993

Family BRINDABELLASPIDAE Gardiner 1993

Remarks— Based on general resemblances, in particular the relatively dorsal position of the nasal capsules, *Brindabellaspis* has been compared with, assigned to, or listed as a member of the order Acanthothoraci by various authors (e.g. Gardiner 1984; Long 1984; Janvier 1996; Goujet and Young 2004; Young 2011). However Gardiner (1993) recognised its distinctive morphology by erecting a new order and family for this genus. Phylogenetic analyses of early gnathostomes that have included two ‘acanthothoracids’ (*Brindabellaspis* and *Romundina*) have never recovered ‘acanthothoracids’ as a monophyletic group (Dupret et al. 2014; Giles et al. 2015; Long et al. 2015; Qiao et al. 2016; King et al. 2017). Thus, the relationships of *Brindabellaspis* to other placoderms remain very uncertain and they lack features that can’t be considered general gnathostome features.

Young (1980) originally placed *Brindabellaspis* within a ‘rhenanid’ grouping defined by dorsal nasal openings. Included were ‘gemuendinids’ plus the ‘palaeacanthaspids’ *Kolymaspis*, *Romundina*, *Kimaspis*, *Radotina*, *Kosoraspis* and *Palaeacanthaspis*. These were all united by having nares in a mid-dorsal position, compared to the more lateral position in *Brindabellaspis*. Embryological evidence from living groups was cited to support a ventral position for nasal openings being the primitive condition. Denison (1978) grouped the above ‘palaeacanthaspids’ in the order Acanthothoraci Stensiö, 1944, with the above six genera plus *Dobrowlania* all within a single family Palaeacanthaspidae Stensiö, 1944. Most

subsequent authors have followed this usage, the informal 'acanthothoracid' replacing 'palaeacanthaspid'. Denison (1978) considered the dorsal nares of 'gemuendinids' to be independently acquired, and comprising a separate order Rhenanida (genera *Asterosteus*, *Gemuendina*, *Jagorina*, and the scale taxon *Ohioaspis*). In the same year White (1978) described another genus of 'palaeacanthaspid', *Weejasperaspis* from the Burrinjuck fish assemblage, which he placed in its own family within the order Acanthothoraci. Young (1980) suggested that *Brindabellaspis* might be closely related to *Weejasperaspis* on the evidence of trunk-shield morphology. Long (1984) erected a third Australian 'acanthothoracid' genus, *Murrindalaspis*, also placed in the family Weejasperaspidae White, 1978 on the evidence of two similarities: the ornament, and a crest on the median dorsal plate. Since the skull of *Murrindalaspis* and the median dorsal plate of *Brindabellaspis* were both unknown, whether one or the other might be closer to *Weejasperaspis* could not be determined on available evidence (Long 1984).

Other genera that have been assigned to 'Acanthothoraci' include *Breizosteus* Goujet 1980, *Hagiangella* Dupret et al. 2011, and *Arabosteus* Olive et al. 2011. Of these, only *Arabosteus* is represented by skull and braincase material that can be compared with *Brindabellaspis*. Olive et al. (2011) assigned *Arabosteus* to the family Palaeacanthaspidae on the basis that this was the only family (but Weejasperaspidae of White 1978 was overlooked). Similarly, Early Devonian forms from the Prague Basin have been assigned to the order Acanthothoraci and family Palaeacanthaspidae without definition (Vařkaninová and Ahlberg 2017), although other authors (e.g. White 1978) had expressed reservations that *Radotina* and associated forms belonged with 'typical' acanthothoracids, as represented by *Romundina* Orvig 1975. *Romundina* is the best known Northern Hemisphere acanthothoracid (Ørvig 1975; Goujet and Young 2004; Dupret et al. 2010; Dupret et al. 2014; Dupret et al. 2017).

Burrow (2006,p.61-62) modified Denison's (1978) diagnosis of the order Acanthothoraci using characters from Goujet and Young (1995). Burrow and Turner (1998) described scales of *Brindabellaspis* sp. from the Wee Jasper area (type locality), and 'proto-brindabellaspid' scales with similar histology to *Brindabellaspis* from the late Lochkovian of eastern Australia,

the same strata yielding skull remains of *Romundina* sp. (illustrated by Burrow et al. 2010). Of various recent publications that describe or analyse ‘acanthothoracids’, the only one to provide an updated diagnosis is Olive et al. (2011). Apart from three features (deep posterior skull embayment bounded by strongly projecting paranuchals; some skull bones separated or overlain by tesserae; ornamental tubercles commonly stellate) *Brindabellaspis* conforms to that diagnosis. Olive *et al.* (2011) noted that the ornament of *Arabosteus* differed from typical acanthothoracids, and resembled *Brindabellaspis*, in lacking stellate tuberculation, but they considered its other morphological features to indicate provisional assignment to the family Palaeacanthaspidae, rather than Brindabellaspidae.

Genus *BRINDABELLASPIS* Young, 1980

BRINDABELLASPIS STENSIOI Young, 1980

Type skull material—Two specimens were described by Young (1980): the Holotype (**ANU V1677**), and another eroded skull revealing much of the endocranial cavity (**ANU V1678**).

New skull material—Five new specimens of *Brindabellaspis* provide additional evidence on skull morphology: **AMF 81911** (partial skull and braincase, partly acid-etched from limestone, the basis for the skull reconstruction of Young, 2010); **ANU 49493** (partial skull and braincase, completely acid-etched; left lateral view figured by Goujet and Young, 2004); **ANU V1224** (flattened premedian plate with abraded dorsal surface); **ANU V2584** (incomplete distorted skull with complete posterior margin); **ANU V3247** (distorted premedian plate and underlying perichondral ossifications, broken off at the anterior edge of the orbit and nasal cavity).

Revised diagnosis—Jawed vertebrate with nasal cavities placed in the anterodorsal corner of the orbital cavity; orbits large, enclosed laterally by dermal bone, and occupying almost half of total skull length. Skull-roof more or less parallel-sided; includes a large nuchal plate, probably rostrineal and premedian plates, and a postorbital or possibly a paraorbital plate enclosing the orbit laterally; a large postmarginal may be present; premedian plate forms elongate broad rostrum with lateral overlap surfaces. Endolymphatic duct openings placed

at ossification centre of nuchal plate; elongate section of lateral line sensory groove between occipital commissure and posterior pitline; postmarginal canal and postorbital part of infraorbital canal reduced; central sensory canal and middle pitline absent; ethmoid commissure on premedian plate doubled back and fused into midline canal. Endocranium formed by fusion of rhinocapsular and postethmo-occipital bones into a single ossification, unusually deep with prominent laterobasal angles and extensive subocular shelves enclosing orbits ventrally and laterally, and incorporating anterior postorbital processes; well developed preorbital space bounded dorsally by endocranial antorbital process; Eyestalk attachment area large and L-shaped; posterior postorbital process represented by post-glossopharyngeal ridge; paravagal fossa well developed and extensively enclosed ventrally by a shelf-like expansion of the supravagal process; prominent craniospinal process carrying a lateral articular facet for the neck-joint; two articular facets on anterior postorbital process in front of and behind hyomandibular nerve foramen, and another on the lateral endocranial wall behind the posterior jugular foramen. Hyomandibular and palatine branches of facial nerve passing through the orbit; separate canal for profundus nerve; pharyngeal branch of glossopharyngeal nerve emanating anteriorly through subocular shelf.; vagus canal short and wide with smaller anterior branch; first spino-occipital nerve canal lacking a dorsal branch, and fifth passing out through foramen magnum. Jugular canal continuous through endocranial wall; anterior and posterior divisions of lateral dorsal aorta enclosed in endocranial walls and floor; occipital artery well developed; internal carotid reduced or absent; efferent hyoidean artery reduced; orbital and efferent pseudobranchial arteries well-developed. Palatoquadrate unknown, but probably anteriorly placed; submarginal plate large, ovate and probably anteriorly placed, and attached to an opercular cartilage. Trunk-shield short and high, with extensive postbranchial lamina; ventral wall fairly flat with elongate anterior ventrolaterals and deeply embayed posterior margin; spinal plate reduced, lacking spine; pectoral fin stenobasal and ventrally placed; scapulocoracoid with prominent scapular and coracoid processes. Dermal ornament of closely spaced tubercles, with flat upper surface of enameloid and steep undercut walls.

Materials and methods

The type material of Young (1980), and the new specimens listed above, have been partly (AMF 81911, ANU V1224) or completely (ANU 49493, V2584, V3247) removed from the

limestone matrix by etching in dilute acetic or formic acid, the bone strengthened with mowital or paraloid during extraction.

ANU V3247 was scanned at the imaging and medical beam of the Australian Synchrotron facility in Melbourne. A total of 26 overlapping 3mm slices were imaged, covering an oblique longitudinal strip from the right anterior to the left posterior of the specimen. It was scanned with a monochromatic beam at 30keV. Sample to detector distance was 325mm. Pixel size was 6.122 microns and an nRuby detector was used. A total of 1800 projections over 180 degrees were taken. The raw data was processed using the X-TRACT software. The images from the overlapping 3mm slices were concatenated for segmentation. 3-D segmenting of the bone and internal canals was performed using MIMICS 17.0.

Institutional abbreviations—**AM**, Australian Museum, Sydney, Australia; **ANU**, Australian National University, Canberra, Australia; **NHMUK**, Natural History Museum, London, U.K.

Anatomical abbreviations—**ao**, antorbital plate; **APNu**, anterior paranuchal plate; **C**, central plate; **c.prod**, dorsomesial branch of preorbital canal; **c.prov**, ventral branch of preorbital canal; **dep.hyp**, hypophysial depression; **epsb**, efferent pseudobranchial artery; **eth.com**, ethmoid commissure; **fo.hyp**, hypophysial fossa; **ifc**, infraorbital sensory canal; **lam.sn**, subnasal lamina; **M**, marginal plate; **nc**, nasal capsule; **Nu**, nuchal plate; **PM**, postmarginal plate; **PN**, postnasal plate; **PPNu**, posterior paranuchal plate; **PrM**, premedian plate; **PrO**, preorbital plate; **PtO**, postorbital plate; **R**, rostral plate; **rec.pro**, preorbital recess; **sn.vas**, subnasal vascular plexus; **SO**, suborbital plate; **so.os**, overlap surface for suborbital plate; **sor.a**, anterior suborbital ridge; **vioid**, median ventral interorbital depression;

Results

The premedian plate and overlapping bones

AMF 81911, ANU 49493, V1224 and V3247 (Fig. 1) provide new data to reconstruct the pattern of dermal bones anterior to the orbits. The original skull reconstruction (Young 1980,

fig. 1) was based on two specimens with the preorbital part broken away at the same level, so the highly unusual rostral elongation was completely unknown.

ANU V3247 shows the most complete premedian plate (Fig. 1C-F); the anterior end is broken off in all other specimens. This example shows the premedian was greatly elongated, with prominent overlap surfaces (Fig. 1E, so.os) complete on both sides (although they are asymmetrical due to distortion). These overlap surfaces have a patchy distribution of tubercles, suggesting the overlapping bone had a somewhat loose connection. It is assumed *Brindabellaspis* had the palatoquadrate fused inside a dermal suborbital plate, by comparison with *Romundina* and other placoderms, so these large overlaps were most likely for that bone, despite its unusual anterior position. In *Romundina*, palatoquadrate attachments are present on the endocranium to the anterior margin of the premedian plate (Ørvig 1975; Dupret et al. 2014). An 'ectethmoid process' carrying this articulation was restored for *Brindabellaspis* by Young (1986, fig. 15a). Such an attachment (not preserved in available material) may have been situated far anteriorly, given that the overlap surface for the suborbital plate stretched for the entire length of the premedian plate.

The anterior end of the premedian plate is complete on the right side of V3247 (Fig. 1C-F); the left side has a small broken portion (due to distortion the left side is stretched slightly forward). The anterior margin has a small median embayment. The lack of tubercles on the anterior margin, and numerous small foramina opening into the median embayment, suggests that the anterior end of the rostrum was continued as soft tissue.

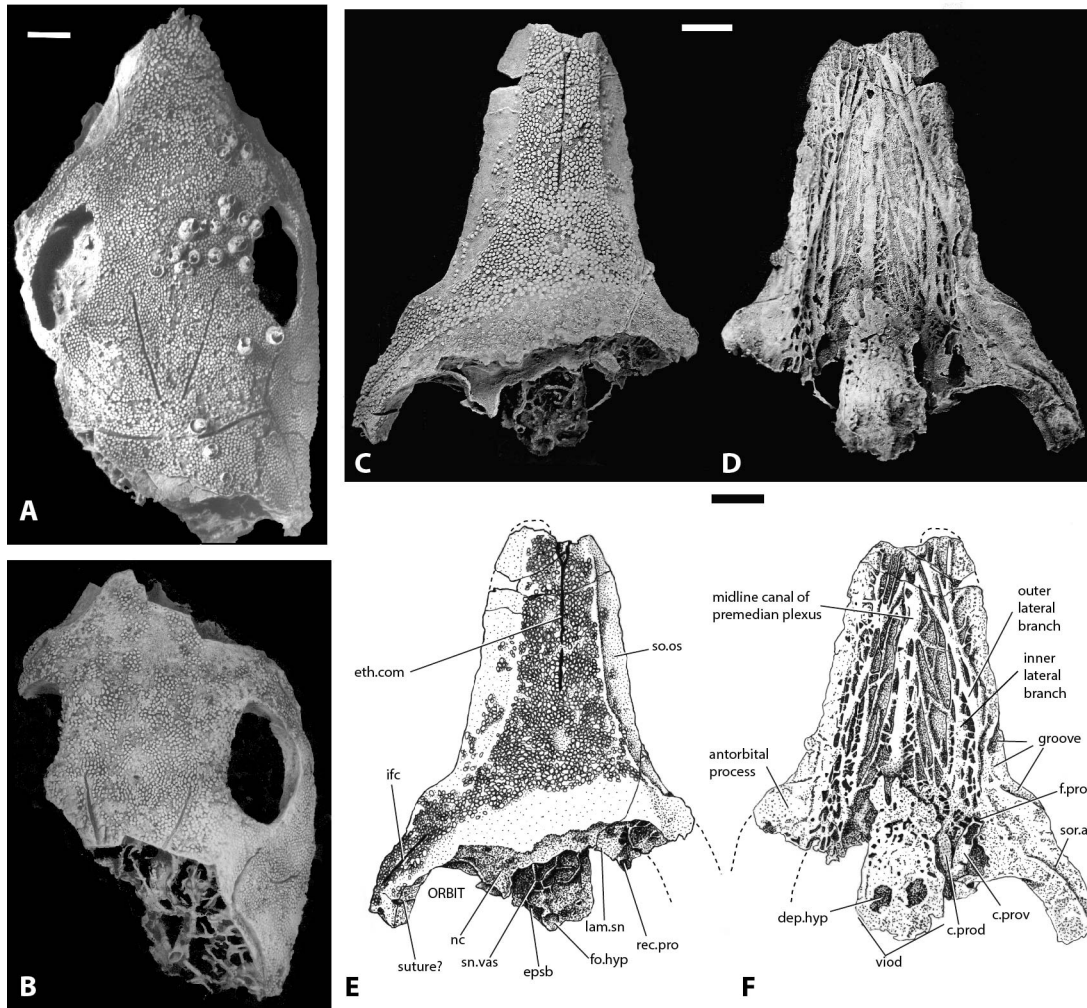


Figure 1. New specimens of *Brindabellaspis stensioi*. A) AMF 81911, dorsal view. B) ANU 49493, dorsal view. C,D) ANU V3247 in dorsal (C) and ventral (D) views. E,F) interpretative drawings of C and D. Scale bars represent 10mm.

Visceral surface of the premedian plate

Best exposed in ANU V3247, this shows a plexus of perichondrally ossified canals in the basal dermal bone layer (Fig. 1D, F), representing the boundary between the dermal premedian plate above, and the cartilage of the endocranium below. An anastomosing network at the same level below the premedian plate was described for *Romundina* by Dupret et al. (2010). In ANU V3247 an enlarged central canal runs forward in the midline (Fig. 1F), and two large anastomosing lateral branches on each side converge near the anterior end of the central canal. Although the premedian plate of *Romundina* is quite different in shape, its

neurovascular network in the preorostral region also comprises larger canals running forward in the midline, and converging anteromesially from both sides (Dupret et al. 2010, fig. 2B2). The median canal within the plexus likely carried, via the dorsal preorbital canals, the profundus and superficial ophthalmic branches of the trigeminal nerve to supply the skin on the dorsal surface of the snout.

On the left-hand side of ANU V3247 the dorsal and ventral branches of the preorbital canal are preserved (c.prov, c.prod, Fig. 1F). These were first described by Young (1980, fig. 12), but the continuation of the dorsal branch was previously unknown. In ANU V3247 the dorsal branch of each side meets in an anastomosing plexus just beneath the overlying dermal bone, from which the median perichondral canal arises, to run forward to the anterior end of the premedian plate. The dorsal preorbital canal also gives off one large lateral branch (and many smaller anastomosing branches), the main one connecting to the inner lateral branch running forward. Distinct foramina in front of and behind the 'preorbital foramen' of Young (1980), where the ventral preorbital canal opens into the lateral preorbital space (preserved on the left side of V3247; Fig. 1F: f.pro), also lead into larger canals joining the lateral anastomosing network. It is presumed these were branches from the structure contained within the ventral preorbital canal. The outer lateral branch arises from a foramen farther forward, just inside the dermal groove beneath the posterior end of the SO overlap area (Fig. 1D,F). In *Romundina*, Dupret et al. (2010) suggested that the larger lateral branches of the transverse neurovascular web (single, not double as in *Brindabellaspis*) may have transmitted left and right rami of the buccalis lateralis nerve to the ethmoid commissure. A similar interpretation may be applied to *Brindabellaspis*. Young (1980) suggested that the dorsomesial branch of the preorbital canal may be equivalent to the ophthalmicus lateralis canal of *Macropetalichthys*, restored by Stensiö (1963) to have carried superficialis and lateralis fibres to the rostrum.

In *Brindabellaspis* the endocranium is preserved as a single ossification, although a double perichondral lamina within the endocranium was interpreted as the line of fusion between the rhino-capsular and postethmo-occipital units (lam.sn, Young 1980 fig. 4). This lamina is

present at the posterior end of ANU V3247 (Fig. 1D, lam.sn) but its anterior termination is incomplete. In AMF 81911 two perichondral laminae extend forward beneath the dermal rostrum (Fig. 2). The upper one may represent the anterior continuation of the subnasal lamina, or the upper surface of the subnasal shelf (unclear because central and posterior parts of this specimen are obscured by remaining limestone matrix). The left side of AMF 81911 shows the upper perichondral lamina attaching to the inner dermal bone surface just anterior to the suture crossing the overlap area on the external surface.

Anterior to this, the premedian plate in *Brindabellaspis* is supported only by an anterior expansion of the postethmo-occipital unit of the endocranium, its floor preserved as a single perichondral lamina, and the overlying cartilage supporting the premedian plate evidently reduced to about 3 mm thick anteriorly. Similarly, in *Romundina* (Dupret et al., 2014), although the rhinocapsular unit is smaller and posteriorly placed between the orbits, the postethmo-occipital unit (specifically the trabecular region) extends anteriorly and underlies the premedian plate. In *Brindabellaspis* this trabecular region extended even further than in *Romundina*. AMF 81911 also shows that the curvature of the ventral surface of the endocranium continued forward beneath the premedian plate, mirroring the curvature of the overlying dermal bone.

The ventral surface of ANU V3247 shows a smooth platform on either side just anterior to the orbits (fig1D), representing the undersurface of the antorbital process of the braincase, as previously described (Young 1980). Poorly defined grooves on the adjacent dermal bone surface could be related to attachment of the levator palatoquadrati muscles.

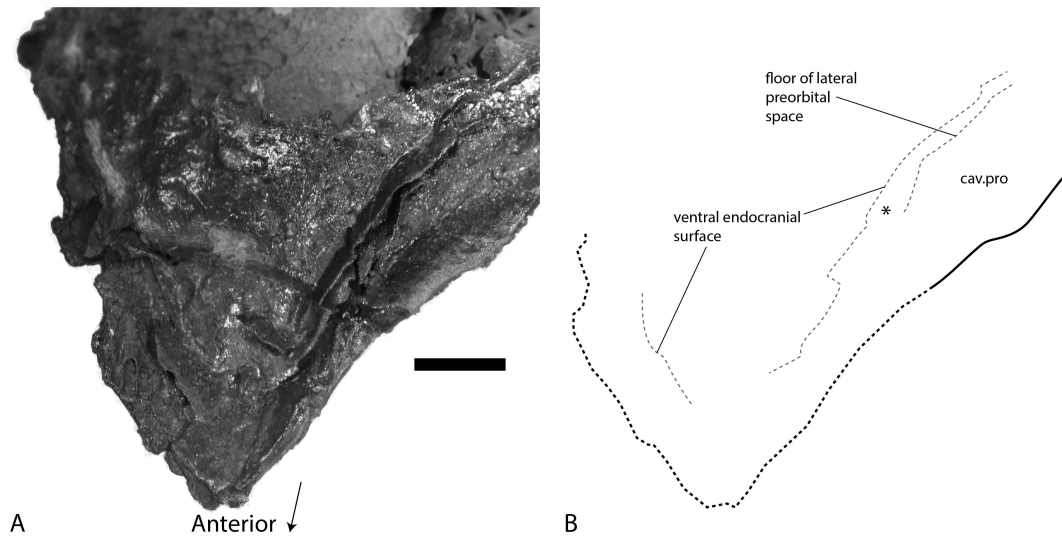


Figure 2. A thin layer of cartilage underlay the premedian plate in *Brindabellaspis*. Oblique ventral view of AMF 81911, which preserves some of the ventral endocranial surface beneath the premedian plate, showing that the cartilage in this area was very thin. Scale bar represents 10mm.

Ethmoid commissure

The premedian plate bears a median sensory line canal (preserved in AMF 81911, ANU V1224, V3247), the last specimen the only one showing its forked anterior end (Fig. 1E, eth.com). Paired foramina, clearly visible in anterior view on the anterior margin, may indicate continuation of these sensory canals into the soft tissue of the rostrum.

A midline sensory canal in this position is, to our knowledge, unknown in any other vertebrate. A transverse ethmoid commissure is present on the premedian plate of some other placoderms, including *Romundina* and antiarchs. The fork at the anterior end of the midline canal in *Brindabellaspis* suggests that this midline canal is the ethmoid commissure which has folded back on itself and fused in the midline. The CT scans support this interpretation, showing a “double canal” morphology anteriorly, fusing into a “single canal” morphology posteriorly (Fig. 3A).

The median sensory canal on the premedian plate in ANU V3247 is connected to the perichondral plexus on the ventral surface of the plate via two pairs of canals (Fig. 3B), presumed to carry nerves. They run in a posterodorsal direction from the large midline canal in the perichondral plexus below the premedian plate, and connect to the sensory line at a

slight constriction (Fig. 3B). At this same point the cross-section of the sensory line changes from being obviously double anteriorly, to a single fused sensory line posteriorly. Individual CT slices at three points (Fig. 3C) show the transition from a double canal anteriorly to a fused single canal posteriorly. Cross-sectional area of the ethmoid-commissure mask in *Mimics*, plotted along the anterior-posterior axis (Fig. 3D) shows that the anterior section (with the double canal morphology) has a much larger cross-sectional area than the posterior section (with the single canal morphology), and also clearly shows a constriction at the transition between the “double” and “single” sections.

The point of entry of the nerve canals likely represents the position of a neuromast organ. In some cases, neuromast organs in living species can occur at constrictions in the sensory canal (Montgomery and Saunders 1985), which may increase sensitivity by amplifying particle motions within the canal (Montgomery 1989). Since the nerve canals consist of two pairs in ANU V3247, it is possible that the ethmoid commissure has fused at the point of two neuromasts that previously lay either side of the midline in a transverse ethmoid commissure. The posterodorsal orientation of the nerve canals suggest that they carried fibres that entered the plexus anteriorly. The ethmoid commissure in *Amia* is innervated by the buccal nerve (Jarvik 1980). The buccal nerve is associated with the maxillary branch of the trigeminal, which in *Brindabellaspis* runs through the preorbital space. It may enter the perichondral plexus from the anterior to innervate the ethmoid commissure, effectively following the path of the ethmoid commissure itself.

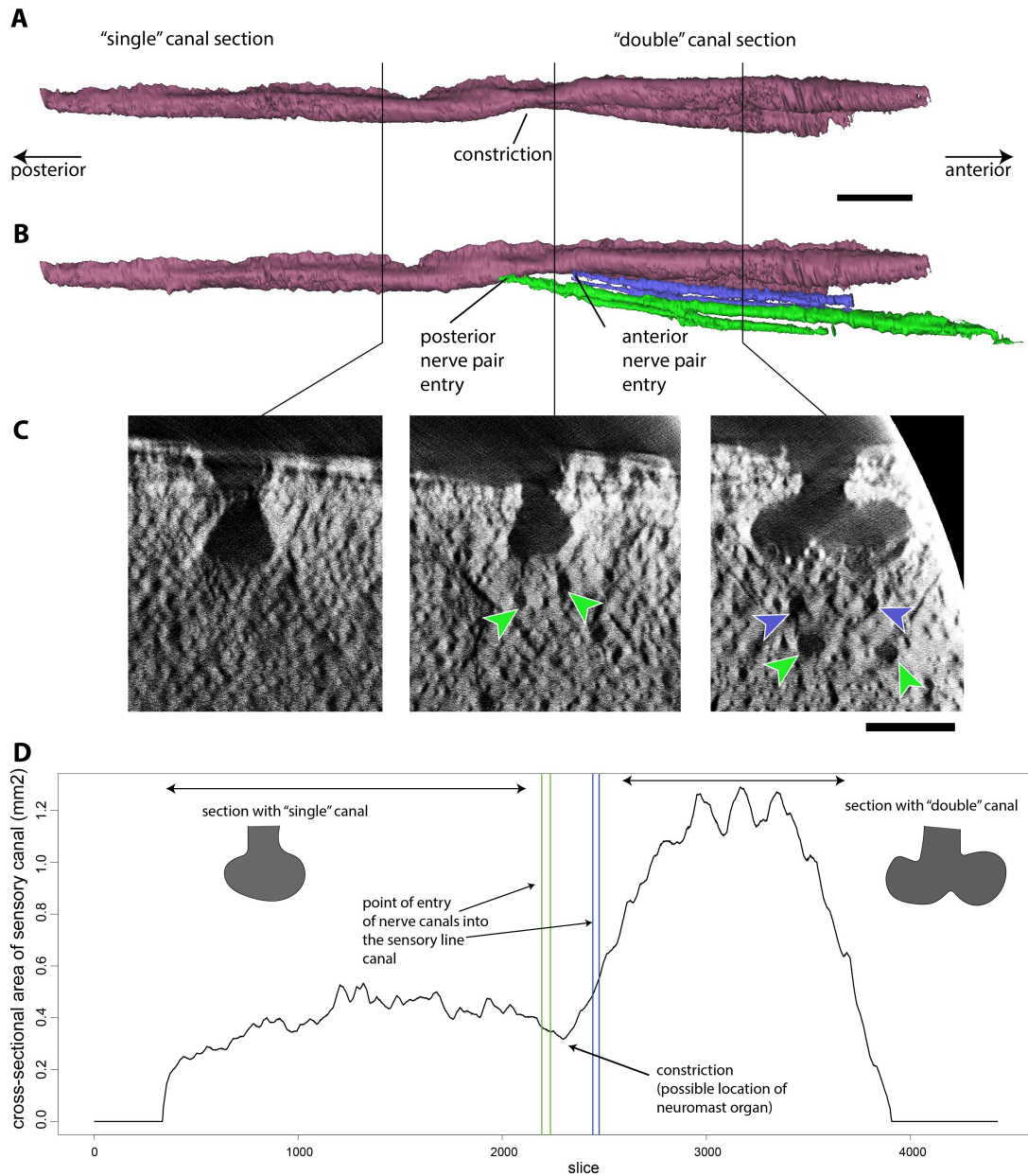


Figure 3. Ethmoid commissure of *Brindabellaspis*. A) 3-dimensional rendering of the canal in Mimics, right ventrolateral view. B) Right lateral view of the ethmoid commissure and associated nerve canals. C) CT slices from three different points along the ethmoid commissure, showing transition from "double" morphology anteriorly to "single" morphology posteriorly. D) Cross-sectional area of ethmoid commissure along the anteroposterior axis, showing constriction at the point of nerve canal entry. Scale bars represent 2mm (A, B) and 1mm (C).

Dermal skull roof reconstruction

Bone sutures are generally not readily distinguishable in any skull specimen of *Brindabellaspis*, so our new interpretation remains provisional. The preorbital area is of key interest, being completely unpreserved in the original material. The long rostrum, with extensive overlap areas for the suborbital plate, is based mainly on ANU V3247; in ANU V1224 (only the right side preserved) the overlap has an irregular expansion towards the front, which is added to our restoration (Fig. 4C). For the post-pineal part of the skull (used by Zhu et al. 2013, suppl fig. 4C, to compare with osteichthyans), our new reconstruction (Fig. 4C) generally follows that of Young (1980). This was based on radiographs, radiating striations on the inner surface of the holotype, and assumptions about sensory grooves passing through ossification centres of skull bones (right side, Fig. 4A). However, ornament alignment in AMF 81911 and ANU 49493 (Fig. 1A-B) suggests that the suture behind the pineal opening may be more V-shaped than first reconstructed. This region was previously only known from one abraded specimen (the holotype). The interpretation of bone sutures lateral and posterolateral to the orbits remains very uncertain, and alternatives as discussed by Young (1980) are shown on left and right sides of Figure 4C.

No specimen shows clear evidence of an anterior suture separating the pineal from the rostral plate, so we interpret a composite rostopineal in this position. Small bones (ao, Fig. 4B), were interpreted by Young (2010) to lie anterior to each orbit in AMF 81911, because of a slightly raised area delimited by notches in the orbital margin. These bones do not have an obvious equivalent in other placoderms, and if present would be apomorphic for *Brindabellaspis*. However, both sides of ANU 49493 lack this elevated area of ornament, so this is a variable feature in *Brindabellaspis*. The right side of ANU V1224 does show an elevated area and notch similar to AMF 81911, but the notch in the orbital margin is more pronounced, its morphology suggesting it could represent an opening from the nasal cavity rather than a bone suture.

The left side of ANU 49493 shows traces of a suture crossing the overlap area in front of the orbit, and in AMF 81911 the same suture is clearly visible on both sides (Fig. 1A-B). In the

anterior wall of the left orbit in this specimen is a vertical partition that suggests the posterior end of this suture (anterior continuation obscured by rock matrix). The new evidence of these specimens now suggests that the raised ornamented area in AMF 81911, variably developed or absent in other examples of *Brindabellaspis*, does not delimit a separate bone, but is more likely equivalent to elevations anterior to the orbits seen in some other placoderms, for example the petalichthyid *Shearsbyaspis* (Young 1985).

Previously, Young (1980) interpreted a 'postnasal' element around the anterior margin of the orbit, but this would be actually anterior to the nasal openings in *Brindabellaspis*. However, there is good evidence from a posterior suture lateral to the orbit for a separate bone in this position, namely the clear overlap area preserved on the right side of ANU V1678 (Young 1980, fig. 4). In AMF 81911 the infraorbital sensory groove passes onto the suborbital overlap area on both sides, but in ANU V3247 the groove terminates well behind the overlap. This variation is shown on left and right sides of the reconstruction (Fig. 2C). The 'postnasal' element shows a notch in its orbital margin in some specimens (well developed on the right side of ANU V1224), which could possibly be related to a nasal opening, and thus comparable to the notched postnasal of brachythoracid arthrodires (e.g. Miles and Westoll 1968). In *Radotina* a postnasal element has been restored lateral to the nasal opening (Westoll 1967), but mesial to the orbit, whereas in *Brindabellaspis* the equivalent element is lateral and anterolateral to the orbit. The postnasal element can be assumed to connect mesially with the unpaired rostromeatal plate, which would include the slight nasal notches in the anterodorsal corner of the orbital opening shown in the previous skull roof reconstruction of Young (2010), based on AMF 81911. The left side of this specimen suggests a connecting groove to the nasal cavity, which may have carried a nasal tube. This part of the orbital margin was completely unknown in the original material (badly abraded in the holotype; missing in ANU V1678). A distinct process in the left orbit of AMF 81911 (less developed on the right side) delineates a separate anterior notch, now considered to be the end of the bone suture discussed above. The anterodorsal margin of the orbit is otherwise preserved only in ANU 49493 (both sides) and ANU V1224 (right side), where these slight notches are less distinct, and variably developed. Possibly the nasal opening was bounded

laterally by a dermal process of the sclerotic capsule (unknown for *Brindabellaspis*), as in the isolated weejasperaspid example described by Long and Young (1988), and also in early brachythoracids (Hu et al. 2017) and other more distantly related placoderm taxa such as antiarchs (Young and Zhang 1996) and *Entelognathus* (Zhu et al. 2013).

The anterior suture to a rostromedial element, separating it from an unpaired premedian plate, may be inferred by comparison with other 'acanthothoracids', as was indicated by a dashed line in Young (1980; see Fig. 4A). However, no indication of this suture can be discerned on the skull roof in any of the new specimens, so the posterior extent of the premedian plate remains very uncertain. It can be assumed the suture was anterior to the nasal notches, and posterior to the median sensory groove (ethmoid commissure), that we assume is confined to the premedian plate, as in other placoderms where present.

As interpreted (Fig. 4C), the skull roof pattern of *Brindabellaspis* is unique, with a large rostromedial plate sutured firmly to the rest of the skull roof, which shows unique preorbital elongation resulting from its long premedian plate. This places the centre of the orbits in the posterior half of skull roof length (about 42% of skull length from the posterior margin). Other placoderms with orbits enclosed in the skull roof have orbits in a more anterior position, even when a pronounced rostrum is developed. Thus, in *Wuttagoonaspis* (which lacks a premedian plate) the orbits are 33-45% of skull length from the anterior margin (Young and Goujet 2003), and in petalichthyids (e.g. *Macropetalichthys*) this is about 30% (accentuated by the nuchal region being more elongate in petalichthyids compared to *Wuttagoonaspis* or *Brindabellaspis*). Also unique is the position of the nasal capsules entirely within the orbits with no separate openings, in contrast to other acanthothoracids (as represented by *Romundina*) where the nasal openings occupy the space between the rostral capsule and the premedian plate (Dupret et al. 2010; Dupret et al. 2014; Dupret et al. 2017). *Brindabellaspis* adds further evidence that dermal skull roof patterns in acanthothoracids, which can vary within individual taxa (Westoll 1967; Olive et al. 2011), are more variable than other placoderm groups.

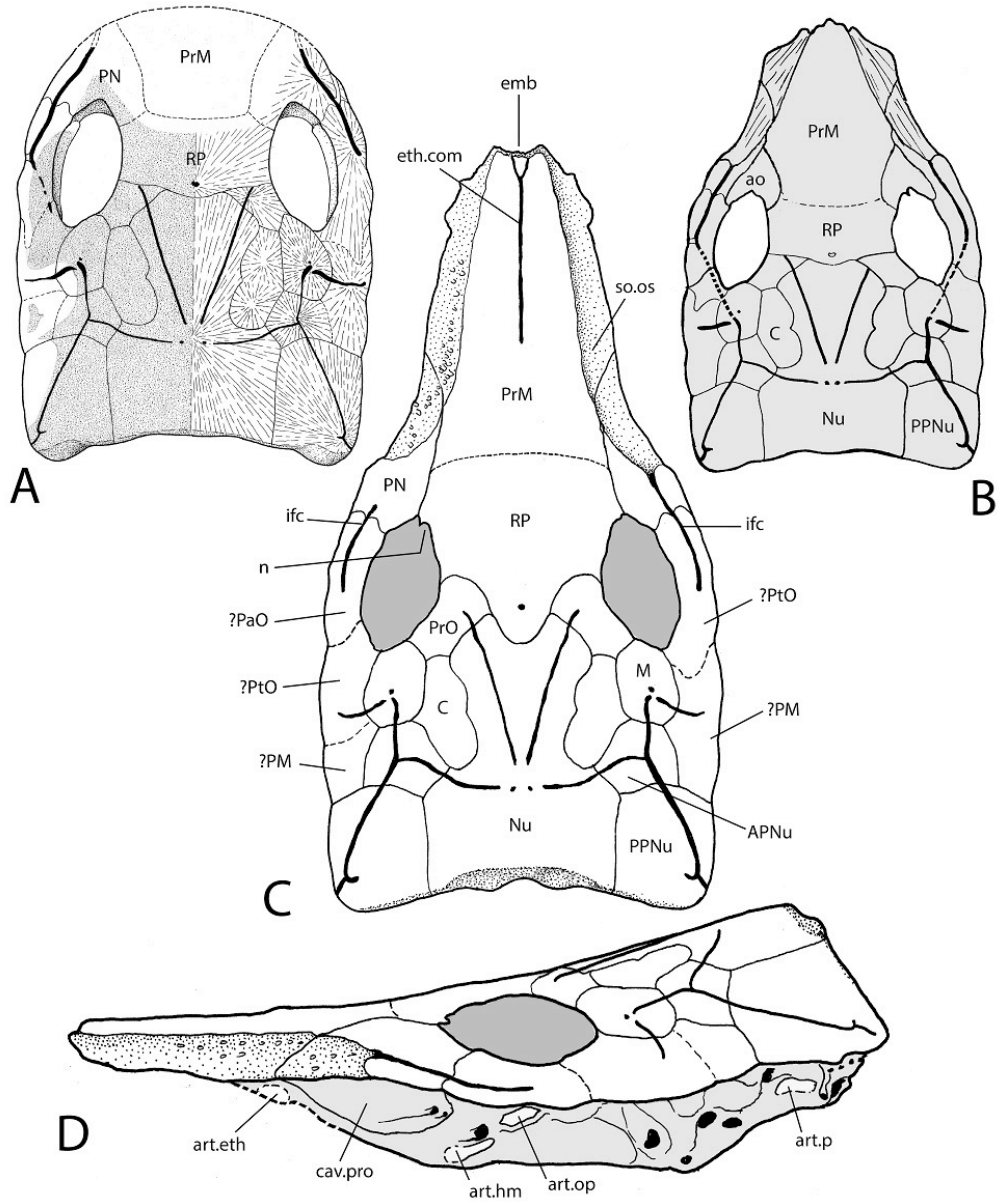


Figure 4. Reconstructions of the pattern of dermal skull roof bones in *Brindabellaspis*. A) based on Young (1980, fig. 1A). B) after Young (2010, fig. 4h), based on AMF 81911. C) provisional new interpretation in dorsal view; D) in lateral view. Relative proportions of preorbital region based on ANU V3247; posterior margin after ANU V2584; nasal notches in left and right orbit are as developed in AMF 81911. Scale bar represents 10mm.

Discussion

As interpreted (Fig. 5C), the skull roof pattern of *Brindabellaspis* is unique. The large rostromedial plate is sutured firmly to the rest of the skull roof, which shows unique rostral elongation resulting from its long premedian plate. This places the centre of the orbits in the posterior half of skull roof length (about 42% of skull length from the posterior margin). Other placoderms with orbits enclosed in the skull roof have orbits in a more anterior position, even when a pronounced rostrum is developed. Thus, in *Wuttagoonaspis* (which lacks a premedian plate) the orbits are 33-45% of skull length from the anterior margin (Young and Goujet 2003), and in petalichthyids (e.g. *Macropetalichthys*) this is about 30% (accentuated by the nuchal region being more elongate in petalichthyids compared to *Wuttagoonaspis* or *Brindabellaspis*). Also unique is the position of the nasal capsules within the orbits, in contrast to other acanthothoracids (as represented by *Romundina*) where the nasal openings occupy the space between the rostral capsule and the premedian plate (Dupret et al. 2010; Dupret et al. 2014; Dupret et al. 2017).

The unusual skull roof pattern is also shown in the position of the postnasal element, around the anterior margin of the orbit. This would be anterior to the nasal openings of *Brindabellaspis*, presumably located within the orbits as previously interpreted (Young 1980). In *Radotina* a postnasal element has been restored lateral to the nasal opening (Westoll 1967), but mesial to the orbit, whereas in *Brindabellaspis* the equivalent element is lateral and anterolateral to the orbit. The postnasal element shows notches in its orbital margin in some specimens. If representing nasal openings, this would be comparable to the notched postnasal of brachythoracid arthrodires (e.g. Miles and Westoll 1968). Possibly the nasal opening was bounded laterally by a dermal process of the sclerotic capsule (unknown for *Brindabellaspis*), as in the isolated weejasperaspid sclerotic capsule previously described (Long and Young 1988). This structure is also seen in early brachythoracids (Hu et al. 2017) and other more distantly related placoderm taxa such as antiarchs (Young and Zhang 1996) and *Entelognathus* (Zhu et al. 2013). Given that sometimes two notches are preserved, possibly both incurrent and excurrent nasal openings were dorsal in position for

Brindabellaspis, because the floor of the orbit and preorbital space likely occluded any ventral passage.

The braincase of *Brindabellaspis* may be compared with that of *Romundina*, and the proportions differ greatly due to the rostral elongation in *Brindabellaspis*. As previously shown (Young 1980), the division of the braincase into separately ossified postethmo-occipital and rhinocapsular units is still evident in *Brindabellaspis*, with these units fused together and the division represented by a double perichondral lamina (the subnasal lamina, lam.sn Fig. 2A, C) within the braincase. The skull roof is also consolidated, showing no trace of division into a separate rostral capsule, and the nasal capsules are in a more lateral position within the orbits. In *Romundina*, the rhinocapsular unit is separately ossified, and posteriorly placed between the orbits. The postethmo-occipital unit (specifically the trabecular region) extends anteriorly and underlies the premedian plate (Dupret et al. 2014). In *Brindabellaspis* the subnasal lamina evidently terminated adjacent to the posterior end of the premedian plate, and the entire premedian plate is underlain by a thin extension of the postethmo-occipital part of the braincase. Thus the trabecular region in *Brindabellaspis* would have an even larger preorbital extension than in *Romundina*.

Clearly the morphology of *Brindabellaspis* is quite different from other 'acanthothoracids'. Dermal skull roof patterns were already recorded to be highly variable within that assemblage, sometimes including zones of tesserae between the larger bones (Westoll 1967). Dermal bone patterns have also been found to vary intraspecifically (Olive et al. 2011), although similar variation in '*Radotina*' has been explained by previously unknown species diversity (Vařkaninová and Ahlberg 2017). This variability in dermal bone pattern might be taken as additional evidence that 'acanthothoracids' may not be monophyletic, although dermal skull roof characters are often difficult to polarise.

Comparing the morphology of *Brindabellaspis* with *Romundina*, obvious differences can be explained by two, possibly related changes: great rostral elongation of the ethmoid region, and the consolidation of the rostral capsule with the rest of the skull. In *Romundina* the nasal capsules occupy the space between the rostral capsule and the premedian plate.

However, in *Brindabellaspis* the rostral is firmly fused to the premedian, which would be possible only with a more lateral position for the nasal capsules within the orbits. Similarly the comparatively long premedian plate, the extensive underlying trabecular region and the anterior position of the hyoid arch attachment are all likely to be related: these features have essentially the same relative positions as in *Romundina*, but the whole ethmoid region is stretched anteriorly in comparison.

Another similarity with *Romundina* is the plexus of perichondral canals underlying the premedian plate. Possibly such a plexus was a common feature of all placoderms with a premedian plate, with the lack of braincase ossification obscuring its presence in antiarchs. The base of the premedian plate in the antiarch *Bothriolepis* shows significant porosity (Young 1984, pl. 57), which could be related to a similar plexus. In both *Romundina* and *Brindabellaspis*, the plexus comprises larger canals running forward in the midline, and converging anteromesially from both sides (Dupret et al. 2010, fig. 2B2). However it is difficult to say on present evidence whether these similarities could be characters linking all acanthothoracids, due to the absence of an equivalent degree of preservation in most other placoderms.

Rostral tubules

The similarity of the plexus of canals associated with the premedian plate in *Brindabellaspis* and *Romundina* is potentially a character linking all acanthothoracids. Alternatively, this plexus may have been a common feature of all placoderms with a premedian plate, with the lack of braincase ossification obscuring its presence in antiarchs. The base of the premedian plate in *Bothriolepis* shows significant porosity (Young 1984, pl. 57), which may indicate the presence of a similar plexus. The functional significance of the plexus is unclear. Lungfishes also possess a system of perichondral tubes in the cartilage of the snout (Thomson and Campbell 1971; Miles 1977; Cheng 1989), although this forms an upwardly branching system rather than a horizontal plexus at the interface of the cartilage and dermal bone. The function of the lungfish tubuli has been a matter of debate (Campbell and Barwick 1986; Cheng 1989; Bemis and Northcutt 1992) although comparisons with extant lungfishes

suggest they might represent lymphatic vessels that function to protect the snout (Kemp 2014). In placoderms, such a plexus may be a common feature where endocranial cartilage meets dermal bone over an extended area. Extensive vascularisation is also found at the interface of dermal and perichondral bone in *Romundina* (Dupret et al. 2017).

Ecology of Brindabellaspis

The unusual morphology of *Brindabellaspis* indicates a specialised role, but inferences about the biology of *Brindabellaspis* are somewhat limited without preservation of the jaws.

Although many fishes in a variety of ecological roles have elongate rostrums (for example garfishes, needlefishes etc.), but the dorsally positioned eyes of *Brindabellaspis* suggest a benthic niche, and the rostrum formed by the premedian plate may have functioned in detection of bottom dwelling prey. One possible analogue is the paddlefishes *Polyodon* and *Psephurus*. The rostral paddle is used as an antenna to seek out plankton, aided by a dense array of electroreceptors on the underside (Wilkins et al. 1997). Similarly, the rostrum of shovelnose rays has dense electroreceptors on the ventral surface for prey detection (Wueringer and Tibbetts 2008). However, a precise modern analogue to *Brindabellaspis*, with the anteriorly positioned jaws, long broad rostrum and dorsal eyes, does not exist.

There is now good evidence that during the Devonian reef ecosystems were, as today, major centres for biodiversity (Long and Trinajstić 2010; Young 2011), and *Brindabellaspis* provides evidence for disparate body forms as well as diversity. In the Late Devonian Gogo Formation, another highly diverse reef assemblage, a long snouted lungfish *Griphognathus* (Miles 1977) may have filled a similar ecological niche to that of *Brindabellaspis* in the Early Devonian.

Acknowledgements

For acid preparation of specimens, and making them available for study, we thank A. Ritchie (AMF 81911), R. Dunstone (ANU V1224), C. Findlay (ANU V2584), B. Young (ANU V3247), and P. Pridmore, V. Elder and C. Findlay (ANU 49493). For initial photography from which images were scanned we thank B. Young (ANU V3247) and C. Findlay (ANU 49493). For assistance with synchrotron scanning we thank Anton Maksimenko, Kate Trinajstic and Vincent Dupret. For discussion and comments on the manuscript we thank Marco Castiello. This research was supported by Australian Research Council Discovery Grants DP 0772138 and 140104161.

References

- Bemis, W. E. and Northcutt, R. G. (1992). Skin and blood vessels of the snout of the Australian lungfish, *Neoceratodus forsteri*, and their significance for interpreting the cosmine of Devonian lungfishes. *Acta Zoologica* **73**, 115–139.
- Brazeau, M. D. (2009). The braincase and jaws of a Devonian ‘acanthodian’ and modern gnathostome origins. *Nature* **457**, 305–308.
- Brazeau, M. D. and Friedman, M. (2014). The characters of Palaeozoic jawed vertebrates. *Zoological Journal of the Linnean Society* **170**, 779–821.
- Burrow, C. and Turner, S. (1998). Devonian placoderm scales from Australia. *Journal of Vertebrate Paleontology* **18**, 677–695.
- Burrow, C. J. (2006). Placoderm fauna from the Connemarra Formation (? late Lochkovian, Early Devonian), central New South Wales. *Alcheringa: An Australasian Journal of Palaeontology* **30**, 59–88.

- Burrow, C. J., Turner, S. and Young, G. C. (2010). Middle Palaeozoic microvertebrate assemblages and biogeography of East Gondwana (Australasia, Antarctica). *Palaeoworld* **19**, 37–54.
- Campbell, K. S. W. and Barwick, R. E. (1986). Paleozoic lungfishes—a review. *Journal of Morphology Supplement* **1**, 93–131.
- Cheng, H. (1989). On the tubuli in Devonian lungfishes. *Alcheringa* **13**, 153–166.
- Davis, S. P., Finarelli, J. A. and Coates, M. I. (2012). *Acanthodes* and shark-like conditions in the last common ancestor of modern gnathostomes. *Nature* **486**, 247–250.
- Denison, R. H. (1978). *Placodermi*. Gustav Fischer Verlag, Stuttgart and New York.
- Dupret, V., Phuong, T. H., Thanh, T.-D., Phong, N. D., Janvier, P. and Clément, G. (2011). The skull of *Hagiangella goujeti* Janvier, 2005, a high-crested acanthothoracid (Vertebrata, Placodermi) from the Lower Devonian of northern Vietnam. *Journal of Vertebrate Paleontology* **31**, 531–538.
- Dupret, V., Sanchez, S., Goujet, D. and Ahlberg, P. (2017). The internal cranial anatomy of *Romundina stellina* Ørvig, 1975 (Vertebrata, Placodermi, Acanthothoraci) and the origin of jawed vertebrates—Anatomical atlas of a primitive gnathostome. *PloS one* **12**, e0171241.
- Dupret, V., Sanchez, S., Goujet, D., Tafforeau, P. and Ahlberg, P. E. (2010). Bone vascularization and growth in placoderms (Vertebrata): The example of the premedian plate of *Romundina stellina* Ørvig, 1975. *Comptes Rendus Palevol* **9**, 369–375.

- Dupret, V., Sanchez, S., Goujet, D., Tafforeau, P. and Ahlberg, P. E. (2014). A primitive placoderm sheds light on the origin of the jawed vertebrate face. *Nature* **507**, 500–503.
- Gardiner, B. G. (1984). The relationship of placoderms. *Journal of Vertebrate Paleontology* **4**, 379–395.
- Gardiner, B. G. (1993). Placodermi. *The fossil record* **2**, 583–588.
- Giles, S., Friedman, M. and Brazeau, M. D. (2015). Osteichthyan-like cranial conditions in an Early Devonian stem gnathostome. *Nature* **520**, 82–85.
- Goujet, D. (1980). Les Poissons. *Mémoires de la Société Géologique et Minéralogique de Bretagne* **23**, 305-308.
- Goujet, D. and Young, G. C. (1995). Interrelationships of placoderms revisited. *Geobios* **28**, 89-95.
- Goujet, D. and Young, G. C. (2004). Placoderm anatomy and phylogeny: new insights. In *Recent advances in the origin and early radiation of vertebrates* (ed. G. Arratia, M. V. H. Wilson and R. Cloutier), pp. 109–126. Verlag Dr. Friedrich Pfeil, München.
- Hu, Y., Lu, J. and Young, G. C. (2017). New findings in a 400 million-year-old Devonian placoderm shed light on jaw structure and function in basal gnathostomes. *Scientific reports* **7**, 7813.
- Janvier, P. (1996). *Early vertebrates*. Clarendon Press, Oxford.
- Jarvik, E. (1980). *Basic structure and evolution of vertebrates*. Academic Press, London.
- Kemp, A. (2014). Skin structure in the snout of the Australian lungfish, *Neoceratodus forsteri* (Osteichthyes: Dipnoi). *Tissue and Cell* **46**, 397–408.

- King, B., Qiao, T., Lee, M. S., Zhu, M. and Long, J. A. (2017). Bayesian Morphological Clock Methods Resurrect Placoderm Monophyly and Reveal Rapid Early Evolution in Jawed Vertebrates. *Systematic Biology* **66**, 499–516.
- Long, J. A. (1984). New placoderm fishes from the Early Devonian Buchan Group, eastern Victoria. *Proceedings of the Royal Society of Victoria* **96**, 173–186.
- Long, J. A., Mark-Kurik, E., Johanson, Z., Lee, M. S., Young, G. C., Min, Z., Ahlberg, P. E., Newman, M., Jones, R. and Den Blaauwen, J. (2015). Copulation in antiarch placoderms and the origin of gnathostome internal fertilization. *Nature* **517**, 196–199.
- Long, J. A. and Trinajstic, K. (2010). The Late Devonian Gogo Formation lagerstätte of Western Australia: exceptional early vertebrate preservation and diversity. *Annual Review of Earth and Planetary Sciences* **38**, 255–279.
- Long, J. A. and Young, G. C. (1988). Acanthothoracid remains from the Early Devonian of New South Wales, including a complete sclerotic capsule and pelvic girdle. *Memoirs of the Association of Australasian Palaeontologists* **7**, 65-80.
- Miles, R. S. (1977). Dipnoan (lungfish) skulls and the relationships of the group: a study based on new species from the Devonian of Australia. *Zoological Journal of the Linnean Society* **61**, 1–328.
- Miles, R. S. and Westoll, T. S. (1968). IX.—The Placoderm Fish *Coccosteus cuspidatus* Miller ex Agassiz from the Middle Old Red Sandstone of Scotland. Part I. Descriptive Morphology. *Transactions of the Royal Society of Edinburgh* **67**, 373–476.

- Montgomery, J. C. (1989). Lateral line detection of planktonic prey. In *The mechanosensory lateral line* (ed. S. Coombs, P. Görner and H. Münz), pp. 561–574. Springer, New York.
- Montgomery, J. C. and Saunders, A. J. (1985). Functional morphology of the piper *Hyporhamphus ihi* with reference to the role of the lateral line in feeding. *Proceedings of the Royal Society of London B: Biological Sciences* **224**, 197–208.
- Olive, S., Goujet, D., Lelièvre, H. and Janjou, D. (2011). A new Placoderm fish (Acanthothoraci) from the Early Devonian Jauf Formation (Saudi Arabia). *Geodiversitas* **33**, 393–409.
- Ørvig, T. (1975). Description, with special reference to the dermal skeleton, of a new radotinid arthrodire from the Gedinnian of Arctic Canada. *Colloques Internationaux du Centre National de la Recherche Scientifique* **218**, 43–71.
- Qiao, T., King, B., Long, J. A., Ahlberg, P. E. and Zhu, M. (2016). Early gnathostome phylogeny revisited: multiple method consensus. *PloS one* **11**, e0163157.
- Stensiö, E. A. (1944). Contributions to the knowledge of the vertebrate fauna of the Silurian and Devonian of western Podolia. 2, Notes on Two Arthrodires from the Downtonian of Podolia. *Arkiv für Zoologi* **35**, 1–83.
- Stensiö, E. A. (1963). *The Brain and the Cranial Nerves in Fossil, Lower Craniate Vertebrates*. Universitetsforlaget, Oslo.
- Thomson, K. S. and Campbell, K. S. W. (1971). The structure and relationships of the primitive Devonian lungfish—*Dipnorhynchus sussmilchi* (Etheridge). *Bulletin of the Peabody Museum of Natural History* **38**, 1–109.

- Vaškaninová, V. and Ahlberg, P. E. (2017). Unique diversity of acanthothoracid placoderms (basal jawed vertebrates) in the Early Devonian of the Prague Basin, Czech Republic: A new look at *Radotina* and *Holopetalichthys*. *PLoS one* **12**, e0174794.
- Westoll, T. S. (1967). *Radotina* and other tesserate fishes. *Zoological Journal of the Linnean Society* **47**, 83–98.
- White, E. I. (1978). The larger arthrodiran fishes from the area of the Burrinjuck Dam, NSW. *The Transactions of the Zoological Society of London* **34**, 149–262.
- Wilkins, L. A., Russell, D. F., Pei, X. and Gurgens, C. (1997). The paddlefish rostrum functions as an electrosensory antenna in plankton feeding. *Proceedings of the Royal Society of London B: Biological Sciences* **264**, 1723–1729.
- Wueringer, B. E. and Tibbetts, I. R. (2008). Comparison of the lateral line and ampullary systems of two species of shovelnose ray. *Reviews in Fish Biology and Fisheries* **18**, 47–64.
- Young, G. C. (1980). A new Early Devonian placoderm from New South Wales, Australia, with a discussion of placoderm phylogeny. *Palaeontographica Abteilung A Palaeozoologie-Stratigraphie* **167**, 10–76.
- Young, G. C. (1984). Reconstruction of the jaws and braincase in the Devonian placoderm fish *Bothriolepis*. *Palaeontology* **27**, 635–661.
- Young, G. C. (1985). Further petalichthyid remains (placoderm fishes, Early Devonian) from the Taemas-Wee Jasper region, New South Wales. *Bureau of Mineral Resources Journal of Australian Geology and Geophysics* **9**, 121-131.

- Young, G. C. (1986). The relationships of placoderm fishes. *Zoological Journal of the Linnean Society* **88**, 1–57.
- Young, G. C. (2010). Placoderms (armored fish): dominant vertebrates of the Devonian period. *Annual Review of Earth and Planetary Sciences* **38**, 523–550.
- Young, G. C. (2011). Wee Jasper-Lake Burrinjuck fossil fish sites: scientific background to national heritage nomination. *Proceedings of the Linnean Society of New South Wales* **132**, 83–107.
- Young, G. C. and Goujet, D. (2003). Devonian fish remains from the Dulcie Sandstone and Cravens Peak Beds, Georgina Basin, central Australia. *Records of the Western Australian Museum Supplement* **65**, 1–80.
- Young, G. C. and Zhang, G. (1996). New information on the morphology of yunnanolepid antiarchs (placoderm fishes) from the Early Devonian of South China. *Journal of Vertebrate Paleontology* **16**, 623–641.
- Zhu, M., Yu, X., Ahlberg, P. E., Choo, B., Lu, J., Qiao, T., Qu, Q., Zhao, W., Jia, L., Blom, H. and Zhu, Y.-A. (2013). A Silurian placoderm with osteichthyan-like marginal jaw bones. *Nature* **502**, 188–193.

Chapter 5

New information on the enigmatic early osteichthyan

'Ligulalepis'

Alice M. Clement^{1,2,3*}, **Benedict King**^{1*}, Sam Giles^{4*}, Brian Choo¹, Per E. Ahlberg², Gavin C. Young^{5,6},
John A. Long^{1,3}

¹ College of Science and Engineering, Flinders University, Adelaide, South Australia 5042, Australia. ²

Department of Organismal Biology, Evolutionary Biology Centre, Uppsala University, Uppsala 75236,
Sweden. ³ Department of Sciences, Museum Victoria, Melbourne, Victoria 3001, Australia. ⁴

Department of Earth Sciences, University of Oxford, South Parks Road, Oxford OX1 3AN, U.K. ⁵

Department of Applied Mathematics, Research School of Physics & Engineering, Australian National
University, Canberra ACT 2601, Australia. ⁶ Australian Museum Research Institute, 1 Williams Street,
Sydney New South Wales 2010, Australia

* These authors contributed equally to this work.

Context

In this chapter I present a detailed description of the early osteichthyan *Ligulalepis*. New information comes from two sources: a second specimen and CT scans. This study provides new insight into

characters used to reconstruct phylogenetic trees of early osteichthyans, and includes a phylogenetic analysis.

Statement of authorship

The project was conceived by AMC and JAL. AMC, SG, BK and JAL generated the CT renderings. AMC, SG, BK, JAL and BC produced figures. GCY and BK conducted fieldwork. SG and BK conducted the phylogenetic analyses. PEA, GCY and JAL all contributed materials to the project. All authors participated in the interpretation of the specimen and writing of the manuscript.

Abstract

The skull of 'Ligulalepis' from the Early Devonian of Australia (AM-F101607) has significantly expanded our knowledge of early osteichthyan anatomy, but its phylogenetic position has remained uncertain. We herein describe a second skull of 'Ligulalepis' and present micro-CT data on both specimens to reveal novel anatomical features, including cranial endocasts. Several features previously considered to link 'Ligulalepis' with actinopterygians are now considered generalized osteichthyan characters or of uncertain polarity. The presence of a lateral cranial canal is shown to be variable in its development between specimens. Other notable new features include the presence of a pineal foramen, the some detail of skull roof sutures, the shape of the nasal capsules, a placoderm-like hypophysial vein, and a chondrichthyan-like labyrinth system. New phylogenetic analyses place 'Ligulalepis' as a stem osteichthyan, specifically as the sister taxon to 'psarolepids' plus crown osteichthyans. The precise position of 'psarolepids' differs between parsimony and Bayesian analyses.

Introduction

Our knowledge of the assembly of the osteichthyan (bony fish) body plan is hampered by our lack of understanding of the phylogenetic relationships of the early members of this clade. In particular, stem osteichthyans have a poor fossil record. No indisputable stem osteichthyans are known.

Dialipina (Schultze 1968) was originally diagnosed as an actinopterygian, based on scale morphology.

More recent cladistic analyses have resolved *Dialipina* either as an early actinopterygian (Schultze and Cumbaa 2001; Giles et al. 2015a) or stem osteichthyan (Friedman and Brazeau 2010; Giles et al.

2015b; Lu et al. 2016a; Qiao et al. 2016; Choo et al. 2017). *Psarolepis* (Yu 1998) was first referred to the sarcopterygian crown group as a “porolepiform-like” fish, but later it was suggested to be either

the sister taxon to all osteichthyans or sarcopterygians (Zhu et al. 1999). It has been relatively

consistently resolved as a stem sarcopterygian in most subsequent analyses (Zhu et al. 2001;

Brazeau 2009; Zhu et al. 2009; Lu et al. 2016a; Qiao et al. 2016; Choo et al. 2017), and Long (2001)

noted similarities between *Psarolepis* and onychodont fishes. Recent genomic and palaeohistological

work supports the placement of *Psarolepis* as a stem osteichthyan (Qu et al. 2015). *Guiyu* (Zhu et al.

2009) was deemed a stem sarcopterygian in a clade with *Ligulalepis*, *Meemannia*, *Psarolepis* and

Achoania when described. It has been fairly consistently resolved as a stem sarcopterygian in

subsequent analyses (Lu et al. 2016a; Choo et al. 2017). A Bayesian tip-dating approach provides no

resolution regarding the phylogenetic position of *Guiyu*, *Achoania* and *Psarolepis* (King et al. 2017).

Difficulty in polarising osteichthyan characters may be the explanation for uncertainty regarding

early osteichthyan relationships. Indeed, it has been suggested, “stem-group osteichthyans might

not be recognized, even when their remains are discovered” (Friedman and Brazeau 2010: p. 38).

One specimen that may help to further elucidate osteichthyan stem group phylogeny belongs to

“*Ligulalepis*”. *Ligulalepis toombsi* was first described from isolated scales by Schultze (Schultze 1968)

based on a collection from the Taemas Limestones of the Burrinjuck area of New South Wales,

Australia. Schultze attributed the scales to the Actinopterygii due to the presence of ganoine ridges,

a narrow peg-and-socket articulation and a well-developed anterodorsal process. A second species based on isolated scales from the Silurian (Ludlow) Miaokao Formation of Yunnan, China was subsequently described as *Ligulalepis yunnanensis* (Wang & Dong 1989). Further to this, there have been a number of other occurrences of isolated scales attributed to the genus from Australia (Burrow 1997). Schultze (2016) has described acrodin, a typically actinopterygian tissue (Ørvig 1973), from a tooth of a specimen attributed to *Ligulalepis* from the Early Devonian trundle beds of New South Wales.

An incomplete ossified braincase and skull roof, AM F101607, known from the same Taemas limestones was tentatively assigned to *Ligulalepis* (Basden et al. 2000). Originally those authors suggested that AM F101607 might represent the “most primitive osteichthyan braincase” known, emphasizing its unusual combination of morphological characters. Phylogenetic analyses since the discovery of the *Ligulalepis* skull have differed in its recovered phylogenetic position.

This study presents a second skull of '*Ligulalepis*', including the previously unknown anterior part. Both skull have also been CT scanned to reveal new features of internal anatomy. The exceptional preservation of this material allows the reconstruction of braincase anatomy in an early osteichthyan with a level of detail not available in other early osteichthyans. This provides important data for comparison of other taxa, and provides new information for phylogenetic analysis.

Materials and methods

Material

This study involves the incomplete skull of “*Ligulalepis*” AM F101607, which was previously described (Basden et al. 2000; Basden and Young 2001), and a new specimen, ANU V3628, discovered in late 2015. Both specimens came from the limestone outcrops on private land (Cathles' 'Cooradigbee' property) at the southern end of Goodradigbee Inlet, Wee Jasper. ANU V3628 was found in the Bloomfield Limestone Member of the Taemas Formation near Rocky Flat, and AMF 101607 was probably from a similar horizon, possibly at Caravan Point about 300 m to the north, although precise locality and horizon were not recorded for this specimen. ANU V3628 was embedded in resin etched out using dilute acetic acid, and hardened with paraloid. This second specimen is ventrally incomplete where it was exposed prior to collection.

Due to the difficulty in definitively attributing the scales and teeth with the cranial material, we will herein examine specimens AM F101607 and ANU V3628 in isolation.

Micro-computed tomography scanning and visualisation

AM F101607 was scanned at the Australian National University (ANU) High Resolution Micro X-ray Computed Tomography facility (Sakellariou et al. 2004) with a resultant scan resolution of 30.4 microns. ANU V3628 was scanned at Adelaide Microscopy with resultant voxel size 8.5 microns. Three-dimensional modeling and segmentation was completed using the software *VGStudio Max*, version 2.2 (Volume Graphics Inc., Germany), and *Mimics* 18.0 (Materialise Medical Co, Belgium). *Drishti* version 2.6 (Limaye 2006) and *Blender* (blender.org; Stitching Blender Foundation, Amsterdam, the Netherlands) were also used for presentation purposes.

Anatomical abbreviations

0	canal for terminal nerve 0
I	canal for olfactory nerve I

II	canal for optic nerve II
III	canal for oculomotor nerve III
IV	canal for trochlear nerve IV
V	canal for trigeminal nerve V
VII	canal for facial nerve VII
acv	anterior cerebral vein
ant.amp	ampulla on anterior semicircular canal
ap.f	foramen in anterior pocket
asc	anterior semicircular canal
bpt	basipterygoid process
br.prof	canal for branches of the profundus nerve V
br.max	canals for branches of the maxillary nerve in the postnasal wall
bsp	basisphenoid
cc	crus commune
cer	space for cerebellar auricles
com.V.jug	communication between the trigeminal nerve and the jugular canal
It(Dsph)	intertemporal bone (equivalent to the dermosphenotic of actinopterygians)
die	space for the diencephalon
ehy	canal for the efferent hyoid artery
epsb	canal for the efferent pseudobranchial artery
esc	exterior semicircular canal
ext.amp	ampulla on exterior semicircular canal
ey	area for attachment of eyestalk
f.ica	foramen for entry of internal carotid artery
frla	foramina for ramus lateralis accessorius
g.dend	possible groove for endolymphatic duct
hmf	hyomandibular facet
hyp	space for hypophysis
hyp.v	hypophysial vein
ica	groove for internal carotid artery
ioc	infraorbital sensory line
io.lat.1/2	lateralis nerve branches for the dorsal part of the infraorbital canal
jug.c	canal for jugular vein
lcc?	possible lateral cranial canal
mcv	canal for middle cerebral vein
mpl	middle pit line
my.IV	myodome for superior oblique eye muscle/dorsal myodome
my.III	myodome for oculomotor-innervated eye muscle
myVI	myodome for abducens-innervated eye muscle
n.cap	nasal capsule
olf.b	space for olfactory bulb
opha	ophthalmic artery
opt.l	space for optic lobes
otc	otic section of main sensory line canal
ot.lat	otic lateralis nerve branches
"p"	extension of the main sensory canal beyond infraorbital canal
Par	parietal
pcv	posterior cerebral vein
pdf	posterodorsal fontanelle
pin	pineal canal
por	postorbital process

PP	postparietal
ppl	posterior pit line
prof	canal for profundus branch of nerve V
psc	posterior semicircular canal
pv	pituitary vein
s.su	sinus superior
sac	sacculus
soc	supraorbital sensory canal
soph	canal for the superficial ophthalmic nerve
sp.n	spiracular notch
St(It)	supratemporal bone (equivalent to the intertemporal of actinopterygians)
Tab(St)	tabular bone (equivalent to the supratemporal of actinopterygians)
tel	space for telencephalon
vam	ventral anterior myodome
VII.lat	canal for lateralis branch of the facial nerve VII
vm	ventral myodome
Vmd	canal for mandibular trunk of trigeminal nerve V
vom	area for attachment of vomer

Phylogenetic analyses

The character matrix used was based upon the dataset of Lu et al. for their recent work on *Ptyctolepis*, which contained 278 characters and 94 taxa (Lu et al., 2016a). '*Ligulalepis*' was coded from the two skulls only; scale characters were not included. Based on new information from the scans, the coding for character #31 (Sensory canals/grooves) was updated from state 0 (within thickness of skull bones) to state 1 (prominent ridges on visceral surface of skull bones). Seven other characters previously unknown in '*Ligulalepis*' were coded for the first time: #41, Pineal opening in dermal skull roof (present); #47, Number of bones of skull roof lateral to postparietals (two); #132, Canal for jugular in postorbital process (present); #152, External/ horizontal semicircular canal (joins the vestibular region dorsal to posterior ampulla); #259, Position of anterior nostril (facial); #261, Three large pores associated with each side of ethmoid (absent); #263, Size of profundus canal in postnasal wall (small). We clarified the definition of character #115 to refer only to presence or absence of dermal bone separating the nostril and orbit. Previously, the definition of this character simply referred to 'association' or 'confluence' of the nostril and the orbit, but this is not entirely satisfactory in the case of '*Ligulalepis*' where the nostril directly enters the orbit, but the dermal bones around the external opening are not completely known. A new character was introduced to reflect the different conditions of the endoskeleton around the posterior nostril. This was character #281 endoskeletal lamina (postnasal wall) separating posterior nostril and orbit: 0 (absent); 1 (present). Another new character was introduced concerning the pituitary vein, following Castiello

and Brazeau, 2018. This was character #282 pituitary vein canal: 0 (discontinuous, enters endocranial cavity); 1 (discontinuous, enters hypophysial chamber); 2 (continuous transverse canal). Other minor changes were #240 from one to inapplicable for *Cladoselache*, *Climatius* and *Cobelodus*. State 1 of character #267 (endoskeletal spiracular canal: partial enclosure or spiracular bar) was changed to (spiracular bar), to avoid grey areas as to what constitutes 'partial enclosure'. *Raynerius* was recoded as state 0 (open), and *Cheirolepis* as 0/1 (open/spiracular bar) due to uncertainty interpreting the crushed specimen (Giles et al., 2015a). One character (trigemino-facial recess present/absent) was deleted following King et al., 2017. One skull roof character (Lu et al., 2017) character 43: Series of paired median skull roofing bones that meet at the dorsal midline of the skull) was reformulated into four: #277, Postparietals/centrals (0 absent/1 present); #278, Condition of postparietals/centrals (0 meet in midline/1 do not meet in midline/2 single median bone); #279, Parietals (0 absent/1 present), and #280, Condition of parietals (0 meet in midline/1 do not meet in midline). The final matrix comprises 282 characters (see SI 3), scored for the same 94 taxa as Lu et al., 2017. Multistate characters were treated as unordered except for numbers 63, 125, 164, 260, 262 and 266. Parsimony analysis was performed in TNT v1.5 (Goloboff and Catalano, 2016). Analyses initially used new technology search for 1000 replications, using ratchet, tree fusing, sectorial search and drift search algorithms with default settings. TBR branch swapping was then performed on the resulting trees to explore the tree islands more thoroughly. A total of 1936 trees (using collapsing rule 1) of length 818 were found, and the strict consensus tree was saved. Gnathostomes (i.e. all taxa except Galeaspida and Osteostraci) were constrained to be monophyletic, and trees were rooted on Galeaspida. Bremer support values were calculated through a series of tree searches each with a negative constraint on a node in the strict consensus tree. Each of these constrained searches used the same new technology search settings as for the main analysis, for 200 replications. Bootstrap values were calculated using 1000 bootstrap replications. Within each bootstrap replication, the same new technology search settings as above were used, for 100 random addition sequence

Skull roof and braincase

Skull Roof

Scans of AM F101607 reveal for the first time some of the sutures between the skull roofing bones (Fig. 1) showing a pattern remarkably different from the original depiction, which was based on

patterns of ornament (Basden and Young 2001). Parallel bands, of higher density than the surrounding bone, are assumed to follow sutures. In this way, the outline of the postparietals and the posterior edges of the parietals can be followed (Fig. 1). No midline suture is visible on the postparietal but given that other presumed skull sutures are also not visible these cannot be assumed to be absent. A faint suture appears to be present between the parietals. The lateral margin of the postparietal is scalloped in such a way as to provide contact faces for a series of three bones. The most posterior of these most likely corresponds to the tabular (of sarcopterygians; referred to as the supratemporal in actinopterygians), and this is in turn preceded by the similarly-sized supratemporal (of sarcopterygians; referred to as the intertemporal in actinopterygians), and finally the broad and elongate intertemporal (of sarcopterygians; referred to as the dermosphenotic in actinopterygians). Unfortunately, sutures cannot be visualized in the same way in ANU V3628, despite the higher scan resolution, suggesting that presence of high density bands following sutures may vary between individuals or growth phases. However the presence of middle and posterior pitlines, and the supraorbital canals extending to the posterior edge of the postparietals, is confirmed in ANU V3628.

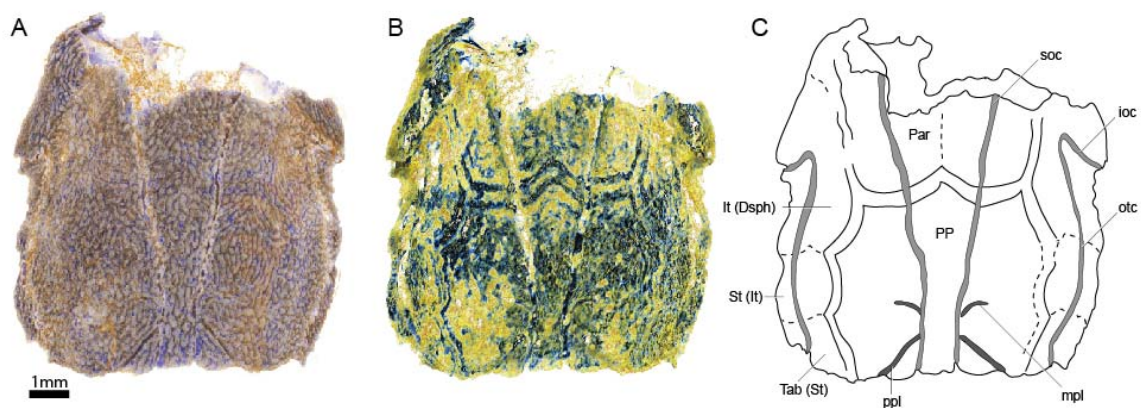


Figure 1. Skull roof of *Ligulalepis* in dorsal view. Artificial colouration added in Drishti to highlight A, sensory canals; and B, bone sutures. C, interpretive diagram showing skull roof pattern. It(Dsph), Intertemporal (dermosphenotic); ioc, infraorbital canal; mpl,

middle pit line; otc, otic sensory canal; Par, parietal; PP, postparietal; ppl, posterior pit line; St(It), supratemporal (intertemporal); soc, supraorbital sensory canal; Tab (St), tabular (supratemporal). Bone names use sarcopterygian conventions, with actinopterygian conventions in brackets.

Although Basden and Young (2001) described a notch for a preopercular sensory line, scans reveal that there is no sensory line branching from the otic canal posterior to the infraorbital canal in ANU V3628, although this canal is present in AMF 101607. There is a short extension of the otic canal anterior to the infraorbital canal, more developed in ANU V3628 than AM F101607. This is the “P” canal of Northcutt (1989). It is present in some acanthodians, e.g. *Acanthodes* (Watson 1937) and some actinopterygians, namely *Mimipiscis* and *Moythomasia* (Gardiner 1984). The condition in *Ligulalepis* is particularly similar to that in the Gogo actinopterygians, with the otic canal bending down to form the infraorbital canal, and the “P” extension appearing as an anterior branch. The “P” canal is apparently absent in *Howqualepis* and *Cheirolepis*, although it may be impossible to recognize without the use of CT scans or other tomographic techniques, as in *Ligulalepis*.

ANU V3628 preserves the previously unknown anterior portion of the skull roof (Fig. 2). A pineal foramen is present, but is unclear if a separate pineal plate was present: sutures in the anterior part of the skull are unclear.

The supraorbital sensory canals become grooves anterior to the level of the pineal foramen, then terminate. This is somewhat equivalent to the “nasal pitlines” described for *Mimipiscis* (Gardiner 1984, fig. 41, 102), although in *Mimipiscis* the supraorbital canals continue anterior to the pitline. ANU V3628 is ventrally incomplete, so it is not clear if an ethmoid commissure was present. If an ethmoid commissure was present, the supraorbital canals did not communicate with it.

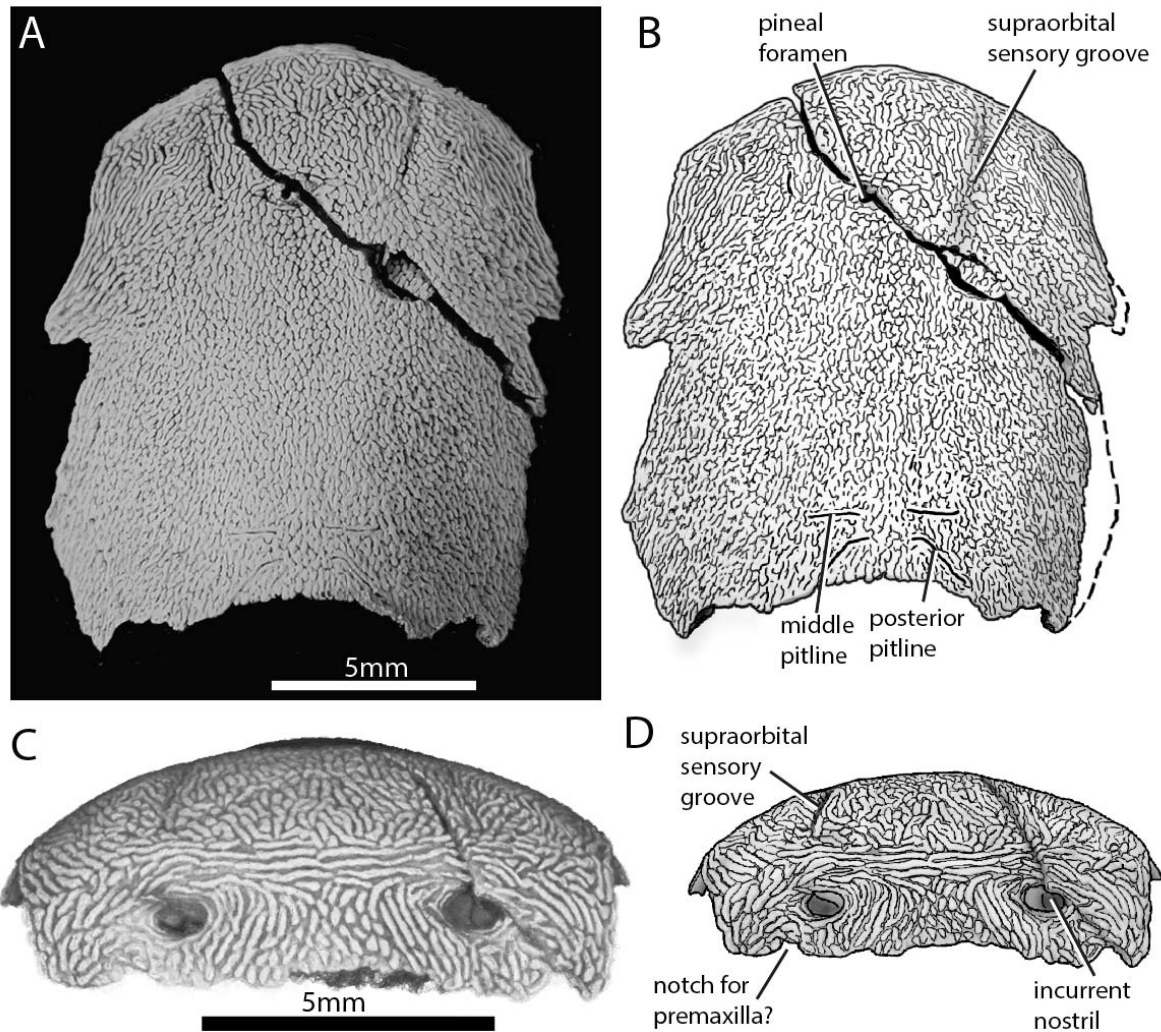


Figure 2. Skull of *Ligulalepis* ANU V3628. A) Dorsal view, photograph of specimen whitened with ammonium chloride. B) line drawing of A. C) Anterior view, imaged using drishti to reveal parts embedded in resin. D) line drawing of C.

There is an abrupt change in ornamentation on the snout, from short anteriorly directed ridges to elongate transverse ridges (Fig. 2C). A similar pattern is shown in *Dialipina* (Schultze and Cumbaa 2001).

The incurrent nostrils are large and widely separated from the excurrent nostrils, which appear to lie entirely within the orbits (Figure 3). Basden and Young (2001) also assumed communication of the posterior nostril with the orbit, including a notch for the nostril on the anterior margin of the orbital fenestra. Neither specimen of '*Ligulalepis*' show evidence for such a notch, although the ventral part of the nostril and orbital margin are unknown. A nostril confluent with the orbit is typically

considered an actinopterygian character, but without preservation of the premaxilla and cheek bones in '*Ligulalepis*' we cannot rule out the possibility that dermal bone separated the external opening of the nostril from the orbit – for example a postero-dorsal process of the premaxilla as in *Psarolepis* (Yu, 1998), and perhaps *Cheirolepis* (Gardiner, 1984, Fig. 49). However, in '*Ligulalepis*' the opening for the posterior nostril in the endocranium lies directly within the orbit (Figure 3A). This is in contrast to the situation in both actinopterygians and sarcopterygians, where an endoskeletal lamina (the postnasal wall) separates the nostril and the orbit (e.g. Gardiner, 1984, Fig. 13). '*Ligulalepis*' lacks such a lamina, and in this respect more closely resembles some placoderms such as *Parabuchanosteus* (Young, 1979) and *Dicksonosteus* (Goujet, 1984).

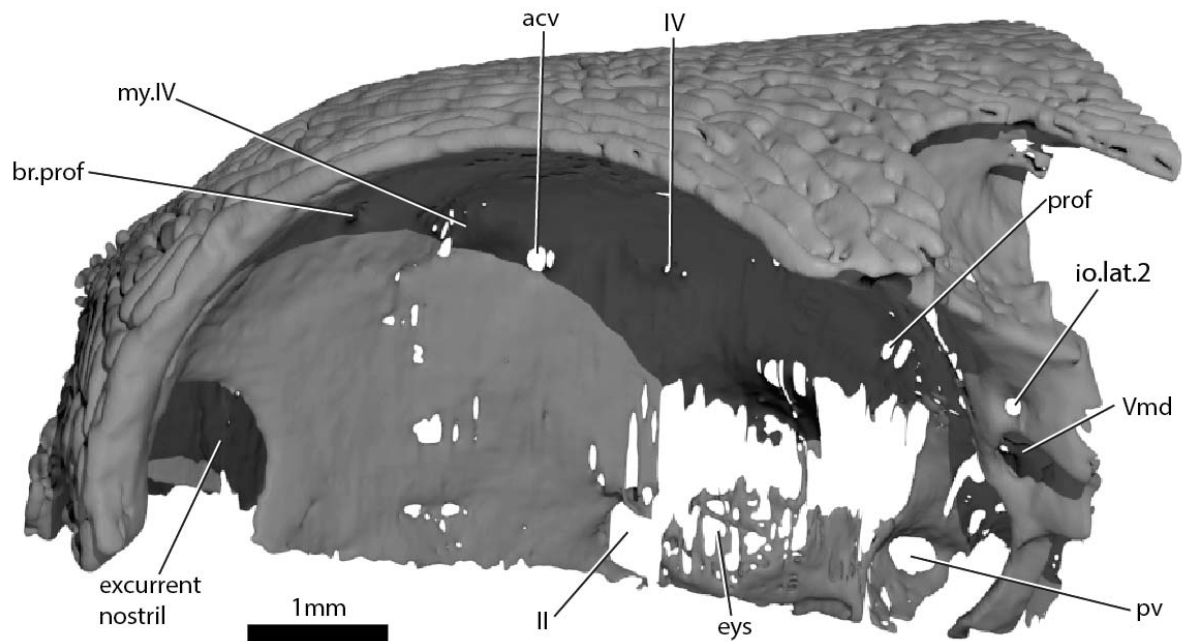


Figure 3. Skull of *Ligulalepis* ANU V3628 in left lateral view. Segmented model of dermal and perichondral bone of the left orbit, showing the posterior nostril within the orbit and endochondral bone in the eyestalk.

Ethmoid region

The ethmoid region is very short, and is moderately well ossified. It is separated from the orbitotemporal region by a poorly developed postnasal wall. A canal leaves the cranial cavity at the left lateral limit of the pineal opening and runs posterolaterally to open into the orbit (Fig. 4, 5, acv).

This canal was identified by Basden and Young (2001) as for the trochlear nerve (n.IV), but its anterior position suggests it may have housed the anterior cerebral vein. This canal is present on one side of the head only in some sarcopterygians such as *Latimeria* (Robineau 1975), and early actinopterygians including *Mimipiscis* (Giles and Friedman 2014) and *Kansasiella* (Poplin 1974). Anterior to this, a ramifying network of canals (identified previously as for the anterior cerebral vein; Basden & Young 2001: fig. 1) may have transmitted branches of the profundus nerve from the orbit to the skull roof, but their course is incomplete (Fig. 2a,c).

Basden and Young (2001) identified a number of foramina in the dorsal wall of the orbit as branches of the superficial ophthalmic nerve. However, the main trunk of the superficial ophthalmic nerve does not enter the orbit, and is shown to remain within the neurocranium, passing below the supraorbital sensory line (Fig. 5, 6). The foramina in the orbit likely carried branches of the profundus nerve to the skull roof. The internal course of the superficial ophthalmic nerve may be related to the relatively wide interorbital septum in *Ligulalepis*.

Below the large opening for the olfactory canal, the posterior face of the nasal capsule is pierced by six foramina in three groups (Fig. 2e). The two dorsal-most foramina enter the nasal capsule from the orbit, and most likely transmitted branches of the profundus (Vprof) nerve (Fig. 5, 6). The most ventral three foramina also extend from the orbit, and may have carried branches of the maxillary and buccal nerves. As noted by Basden and Young (2001), the remaining canal originates in the forebrain, but its purpose is unclear.

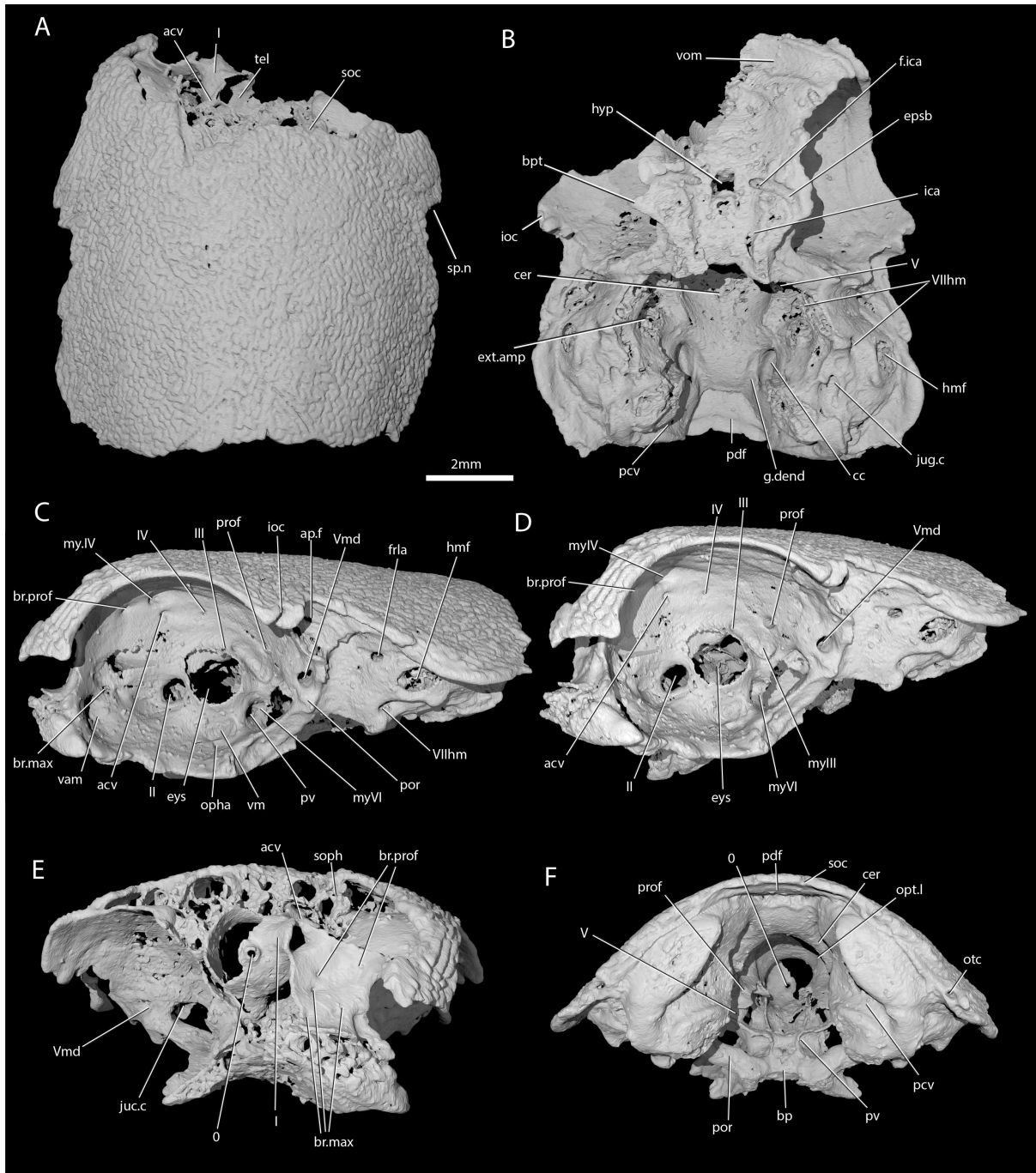


Figure 4. Cranium of *Ligulelepis* AM F101607. A, dorsal; B, ventral; C, left lateral; D, left sagittal slice showing details of orbit; E, anterior; and F, posterior view. For anatomical abbreviations, please see SI 1.

Orbitotemporal region

The eyestalk in AMF101607 is a large hole, and was recognized as an eyestalk due to its everted rims (Basden et al. 2000). In ANU V3628, the scan reveals delicate endochondral bone laminae fill the

eyestalk, forming a rough surface as seen on other articular surfaces in many osteichthyans. It is not clear whether this ossification was present in AMF101607 and lost during preparation (the area is protected by resin in ANU V3628), or if it reflects a more advanced stage of ossification in ANU V3628.

The oculomotor (III) and profundus (Vprof) nerves, as well as the jugular canal opening in the orbit, were correctly identified by Basden & Young (2001: fig. 2), although there is no communication between the profundus nerve and the canal described by Basden & Young (2001) as housing the orbital artery. The position of the pituitary vein and ophthalmic artery foramina can also be confirmed.

The pituitary vein is continuous between the orbits, and is connected to the hypophysial chamber by a median hypophysial vein (Fig. 5D). This condition is similar to the transverse pituitary vein in some placoderms, particularly *Brindabellaspis* (Young 1980), *Parabuchanosteus* (Young 1979), *Jagorina* (Stensiö 1969) and probably *Romundina* (Dupret et al. 2017). Some early arthrodire placoderms such as *Kujdanowiaspis* and *Dicksonosteus* have a pituitary vein that is continuous, but exits the braincase via the subpituitary fossa. However, there is no foramen in the hypophysial fossa that could have carried a median hypophysial vein in these taxa (Stensiö 1963a; Goujet 1984). The condition in *Ligulalepis* contrasts with other osteichthyans in which the pituitary vein enters the hypophysial chamber directly. A transverse pituitary vein is essentially due to relatively posterior position of the vein relative to the hypophysial chamber; this feature may be partly linked with the relative position of the forebrain and the angle of the hypophyseal chamber.

The trochlear (IV) nerve enters the orbit dorsal to the eyestalk attachment area, some way posterior to the dorsal myodome and anterior cerebral vein (Fig. 2C,D). This position is more in line with the exit of the trochlear nerve in most other early gnathostomes such as *Buchanosteus* (Young 1979),

Cladodooides (Maisey 2005), *Mimipiscis* (Gardiner 1984), *Youngolepis* (Chang 1982) and in hybodont sharks (Lane 2010).

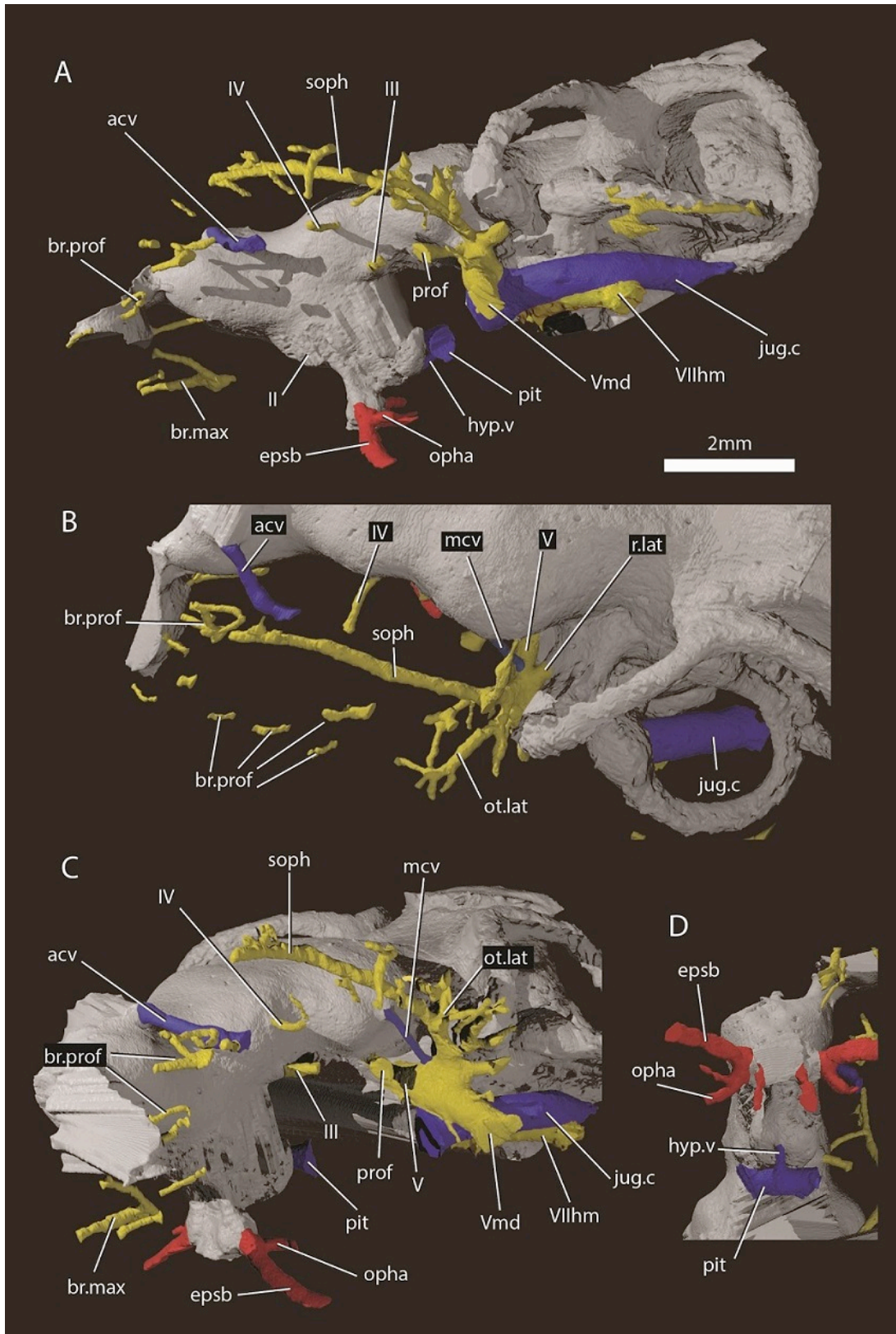


Figure 5. Cranial nerves and vessels of *Ligulelepis* AM F101607. A, left lateral; B, dorsal; C, left anterolateral and D, ventral view. Cranial endocast in grey, nerves in yellow, veins in blue and arteries in red. For anatomical abbreviations, please see SI 1.

A large opening on the postorbital process was identified by (Basden and Young 2001) as housing the orbital artery, in line with the position of this feature in placoderms. Segmentation of the internal course of this canal shows that it connects with a large opening beneath the cerebellar portion of the cranial cavity, most parsimoniously identified as the root of the trigeminal (V) nerve (Fig. 3b,c). As such, the large foramen in the orbit most likely transmitted the mandibular branch of the trigeminal nerve. This canal also aligns with a notch in the postorbital process, along which the mandibular nerve would have travelled. This morphology is similar to that seen in chondrichthyans for example *Cladodoides* (Maisey 2005) and "*Cobelodus*", (Maisey 2007). Small branches are given off the trigeminal nerve within the braincase. One of these (Fig. 6B-C: io.lat.1) enters the posterodorsal part of the orbit at a steep angle and likely carried lateralis fibres to small canals in the roof of the orbit that lead to the dorsal part of the infraorbital canal. A second branch (Fig. 6B-C: io.lat.2), previously suggested as carrying the posterior branch of the oculomotor (III) nerve (Basden and Young 2001), opens onto the postorbital process just dorsal to the opening for the mandibular branch. This may also have carried lateralis fibres to the infraorbital canal.

Posterior to the root of the trigeminal nerve, a canal (r.lat) leaves the anterior face of the utricular region and enters the "trigemino-facialis chamber" (Figure 5B). This is interpreted as the root of the anterior lateral line nerves, in a similar position as in other early osteichthyans (Jarvik, 1980; Chang, 1982; Giles and Friedman, 2014). An additional canal (mcv) exits the cranial cavity from the midpoint of the cerebellum and enters the "trigemino-facialis chamber" at a steep angle (Figure 5C). Due to its position and orientation, this is interpreted as the middle cerebral vein. The jugular canal communicates with the "trigemino-facialis chamber" via an opening in the roof of the canal (Figure 6B, com.V.jug), through which the middle cerebral vein and the maxillary branch of the trigeminal nerve may have been transmitted (Basden and Young, 2001).

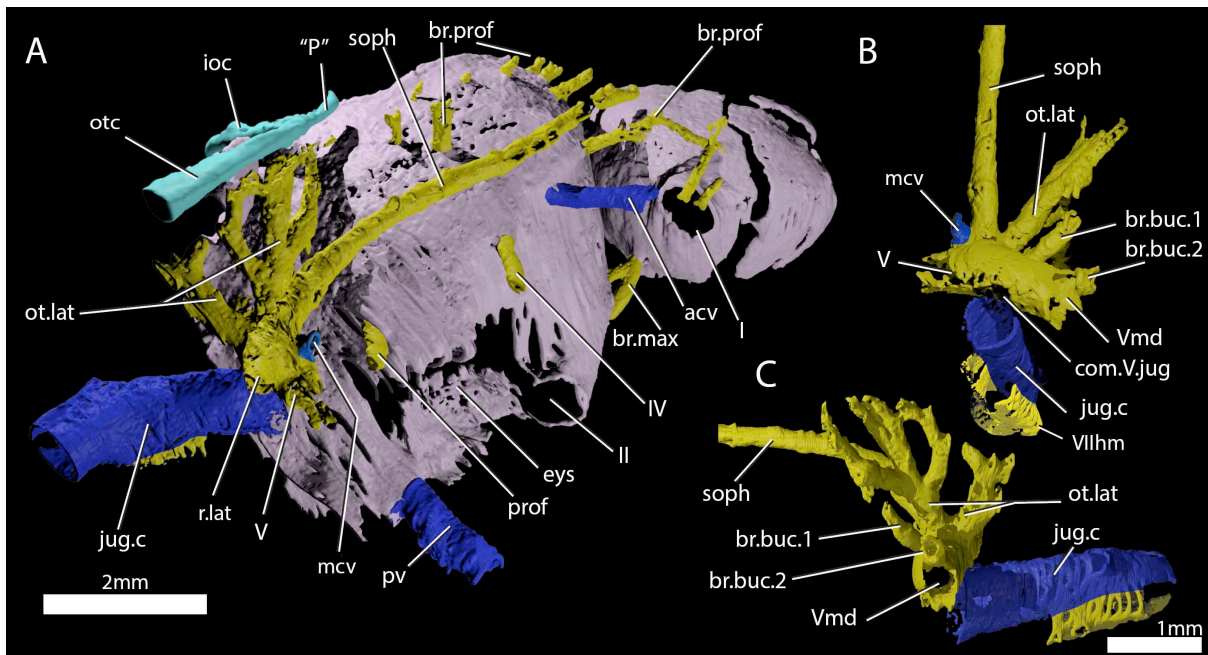


Figure 6. A) ANU V3628, segmentation of the interior of the left orbital region, viewed from a postero-dorsal-medial viewpoint. The cranial endocast is not shown. Perichondral bone lining the orbit and nasal capsules is in lilac. Nerves are yellow, veins blue and sensory canals are in turquoise. B-C) The trigeminal and facial nerves and their branches and the jugular vein, viewed from an anterior-ventral (B) and left lateral (C) viewpoints.

The identity of the large foramen in the dorsal portion of the anterior pocket (Fig. 4C, ap.f) is hard to discern. Segmentation reveals a cavity that is continuous ventrally and dorsally with the infraorbital canal, and may be related to the spiracle. The cavity is also connected with the otic nerve anteriorly. The openings identified by Basden and Young (2001: fig 2) ventral to this foramen do not continue within the bone.

Further clarifications can be made to the identity of the large foramina on the lateral and ventral face of the otic region (Fig. 4). The canal ventral to the hyomandibular facet intersects the ventral portion of the jugular canal and can be traced to the ventral otic fissure (the remainder of the path is presumably on the missing ventral portion of the braincase). It can be identified as the hyomandibular trunk of the facial nerve (VIIhm; Basden & Young 2001: figs 2,3).

The foramen identified by Basden & Young (2001: figs 2,3) as for the glossopharyngeal nerve is in fact the posterior exit of the jugular canal; the glossopharyngeal nerve presumably exited through the otic-occipital fissure. As no exit for the hyomandibular branch of the facial nerve can be identified, it likely exited the braincase via the jugular canal, as in *Janusiscus* (Giles et al. 2015b) and osteichthyans (Gardiner 1984).

Ventral Surface

As outlined by Basden & Young (2001), the internal carotids enter the braincase through two foramina flanking the median hypophysial opening before giving off the efferent pseudobranchial and ophthalmic artery (Fig 2b). As in chondrichthyans (Maisey 2005; Maisey 2007), but unlike in osteichthyans (Chang 1982; Gardiner 1984) and placoderms (Young 1980; Hu et al. 2017), there is no evidence of a parabasal canal carrying the palatine artery anterior to this point. Basden and Young (2001) identified grooves on the ventral surface of the basisphenoid as for the lateral dorsal aorta. However, since these grooves are likely anterior to the efferent hyoid artery we prefer to refer to them as the internal carotid arteries (ica, Fig. 4). Although Basden & Young (2001: fig. 3) identified foramina for the palatine branch of the facial nerve and the orbital artery in the roof of the canal for the internal carotid (their lateral dorsal aorta) the roof appears to be complete.

Cranial Endocast

The endocast is largely complete, although as the parachordal plate and occipital arch of the braincase are not preserved its ventral and posterior extent is uncertain. Overall, the endocast of '*Ligulalepis*' is short and broad, particularly the otic region (Fig. 7A,B). The proportions occupied by different regions are similar to early chondrichthyans, with the forebrain comprising less than 20% of the total length, the midbrain around 15%, and the hindbrain some 65%. As in many placoderms, for example *Kujdanowiaspis* (Stensiö 1963a), chondrichthyans such as *Orthacanthus* (Schaeffer 1981)

and sarcopterygians (Jarvik 1980), the endocast appears to have been a relatively poor fit for the brain, with little to demarcate different regions.

Description of the endocast allows the identity of features within the cranial cavity to be revised. A distinct depression in the roof of the cranial cavity, medial to the otic capsule, was considered by Zhu et al. (2010, fig. 4c) to be evidence of a lateral cranial canal. This embayment is in fact the crus commune of the anterior and posterior semicircular canal (Fig. 4b). The groove anterior to this is somewhat shallower in the braincase and indicates where the roof of the utricular region joins the rest of the cranial cavity (the groove for anterior and posterior semicircular canals of Basden & Young 2001: fig. 3).

Forebrain

The region of the endocast corresponding to the forebrain comprises space for the olfactory bulbs, telencephalon and diencephalon. This region in *Ligulalepis* is relatively wide (Fig. 7A,B), comparable to the forebrain in placoderms such as *Macropetalichthys* (Stensiö 1963b) and chondrichthyans such as *Orthacanthus* (Schaeffer 1981). However, it is still only half the width of the cerebellum. The short, wide olfactory tracts leave the anterolateral corners of the telencephalic region in separate tracts and connect to the bulbous nasal capsules, preserved in ANU V3628. The short olfactory tracts are similar to those of placoderms, for example *Buchanosteus* (Young 1979) and *Kujdanowiaspis* (Stensiö 1963a) as well as chondrichthyans such as *Cladodooides* (Maisey 2005) and *Orthacanthus*, Schaeffer, 1981), but also some sarcopterygians such as *Tungsenia* (Lu et al. 2012) and *Qingmenodus* (Lu et al. 2016b). A small canal for the terminal nerve (n.0) exits from the anterior face of the forebrain, between the olfactory tracts.

The telencephalon is the widest and highest portion of the forebrain. It is developed into a slight lobes dorsolaterally; these may represent olfactory bulbs (Fig. 7A). The dorsal roof of this region is preserved in ANU V3628, as is the canal to the pineal opening (Fig 7B,D). The oblique crack across

ANU V3628 intersects the pineal opening, so it is unclear whether or not a parapineal organ was present. The margin between the telencephalic and diencephalic regions is marked by a gentle constriction in the endocranial cavity.

The region corresponding to the diencephalon is short and narrow in dorsal view, but ventrally continues to the floor of the cranial cavity and is continuous with the hypophyseal fossa, as well as extending posteriorly under the mesencephalon (Fig. 7A,C). This region is unfinished posteriorly, and it is unclear whether a saccus vasculosus was present as in actinopterygians (Giles and Friedman 2014). Additionally, a large portion of the lateral wall of the diencephalon is unfinished for the eyestalk attachment area in AMF 101607. The optic nerves enter the orbit through a large foramen at the anterolateral limit of the diencephalon (Fig. 7C). Beneath this opening, a vertical ridge on the side of the hypophysial chamber likely shows the course of the internal carotid artery after it enters the braincase. The efferent pseudobranchial artery joins the internal carotid at the point of entry into the braincase (f.ica, Fig. 4B), and internally the ophthalmic artery branches from the same point and enters the orbit (opha, Fig. 5D). The hypophysis is oriented ventrally as in sarcopterygians such as *Youngolepis* (Chang 1982) and actinopterygians such as *Mimipiscis* (Giles and Friedman 2014), but unlike the posteroventrally-oriented hypophysis seen in *Cladodoides* (Maisey 2005).

Midbrain

Posterior to the diencephalic part of the forebrain, the endocast widens very slightly into a region corresponding to the midbrain (mesencephalon). The midbrain cavity is not differentiated into separate recesses for each optic lobe, which appears to be the general gnathostome condition.

There are similarly slight bulges in chondrichthyans (e.g. *Cladodoides*, *Xenacanthus*), whereas highly distinct optic lobes are seen in actinopterygians crownward of *Mimipiscis* (Coates 1999; Giles and Friedman 2014). A narrow, dorsally positioned canal leaves the cranial cavity and enters the orbit.

This foramen was illustrated, but not identified, by Basden & Young (2001: fig. 2b, the opening posterior to that labeled IV and dorsal to the eyestalk). The position of the canal strongly suggests it

housed the trochlear nerve (n.IV), given a similar placement in chondrichthyans (e.g. Maisey 2005), sarcopterygians (e.g. Chang 1982) and actinopterygians (e.g. Giles and Friedman 2014). More ventrally, the oculomotor (III) nerve leaves the midbrain and enters the orbit (Fig. 5C); there is no evidence that this nerve bifurcated along its course. The oculomotor nerve does not typically bifurcate in chondrichthyans (e.g. *Cladodoides*, Maisey 2005) or sarcopterygians (e.g. *Eusthenopteron*, Jarvik 1980; *Youngolepis*, Chang 1982), and is variably developed in actinopterygians such as *Mimipiscis* (Giles & Friedman 2014) and *Lawrenciella* (Hamel and Poplin 2008).

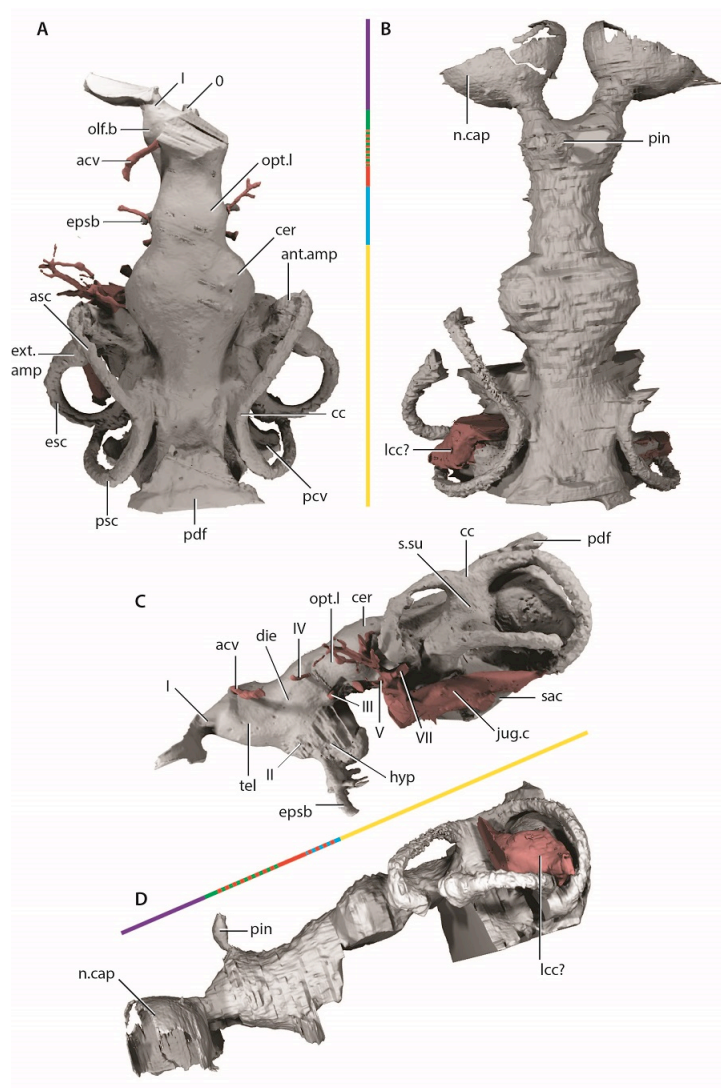


Figure 7. Endocast of “*Ligulalepis*”. A) AM F101607, dorsal view. B) ANU V3628, dorsal view. C) AM F101607 lateral view. D) ANU V3628 lateral view. Possible lateral cranial canal in red. Scale bars represent 2mm

Hindbrain

The hindbrain is composed of the metencephalic and myelencephalic regions and represents the widest portion of the endocast. The cerebellum extends anterior to the labyrinth (Fig. 7A), as in chondrichthyans (e.g. *Cladodoidea*, Maisey 2005) and, to a lesser extent, sarcopterygians (e.g. *Eusthenopteron*, Jarvik 1980). Although the dorsal surface bears a slight suggestion of two lobes, these can hardly be compared to the distinct cerebellar auricles of actinopterygians such as *Mimipiscis* (Giles and Friedman 2014). Similarly, there is no obvious protrusion housing the cerebellum corpus.

The profundus nerve leaves the cranial cavity separately from the trigeminal nerve and enters the orbit. Northcutt and Bemis (1993) made a case that the profundus should be considered a phylogenetically separate nerve rather than a branch of the trigeminal, based on developmental evidence and the separation of these nerves in chondrichthyans, basal actinopterygians and *Latimeria*. *Ligulalepis* adds to a growing body of evidence from fossil endocranial studies that the separation of the trigeminal and profundus nerves is indeed the plesiomorphic state for crown gnathostomes (Chang 1982; Maisey 2005; Giles and Friedman 2014).

Posterior to the cerebellum, the dorsal part of the hindbrain narrows and drops in height, before the endocast broadens again at the midpoint of the labyrinth. The entire dorsal surface of the hindbrain is smooth, and does not rise as high dorsally as the crus commune of the anterior and posterior semicircular canals (Fig. 7C,D). The anterior margin of the posterior dorsal fontanelle is trapezoidal in outline. A ridge on the dorsal surface at the lateral edge of the hindbrain may indicate the path of the endolymphatic ducts within the cranial cavity into the posterior dorsal fontanelle (Fig. 7A).

ANU V3628 appears to have a lateral cranial canal, as in actinopterygians (Giles et al. 2016). Basden

and Young (2001: Fig. 3) identified a groove for the posterior cerebral vein in AMF 101607, in a corresponding position to a similar groove in *Mimipiscis* and *Moythomasia* (Gardiner 1984). In ANU V3628, the dorsal part of this groove contains a large foramen (Fig. 8C-D), in the same position to the opening for the lateral cranial canal in *Moythomasia* (Gardiner 1984, fig. 27) and *Mimipiscis* (Gardiner 1984, fig. 11). Segmentation reveals that this foramen opens into a large unossified space (Fig. 7, 8E), as expected for a lateral cranial canal (Patterson 1975; Gardiner 1984).

However, the identification of a lateral cranial canal in AMF 101607 remains unclear. Basden and Young (2001) identified foramina in the posterior cerebral vein groove, and identified them as anterior tributaries of the posterior cerebral vein. Although the foramina on the left hand side are indeed small (Fig. 8B), on the right hand side there is a larger, more distinct formamen (Fig. 8A). The lateral cranial canal may have been variable in its development. It seems certain however, that the foramina in ANU V3628 are far too large to be identified as tributaries of the posterior cerebral vein.

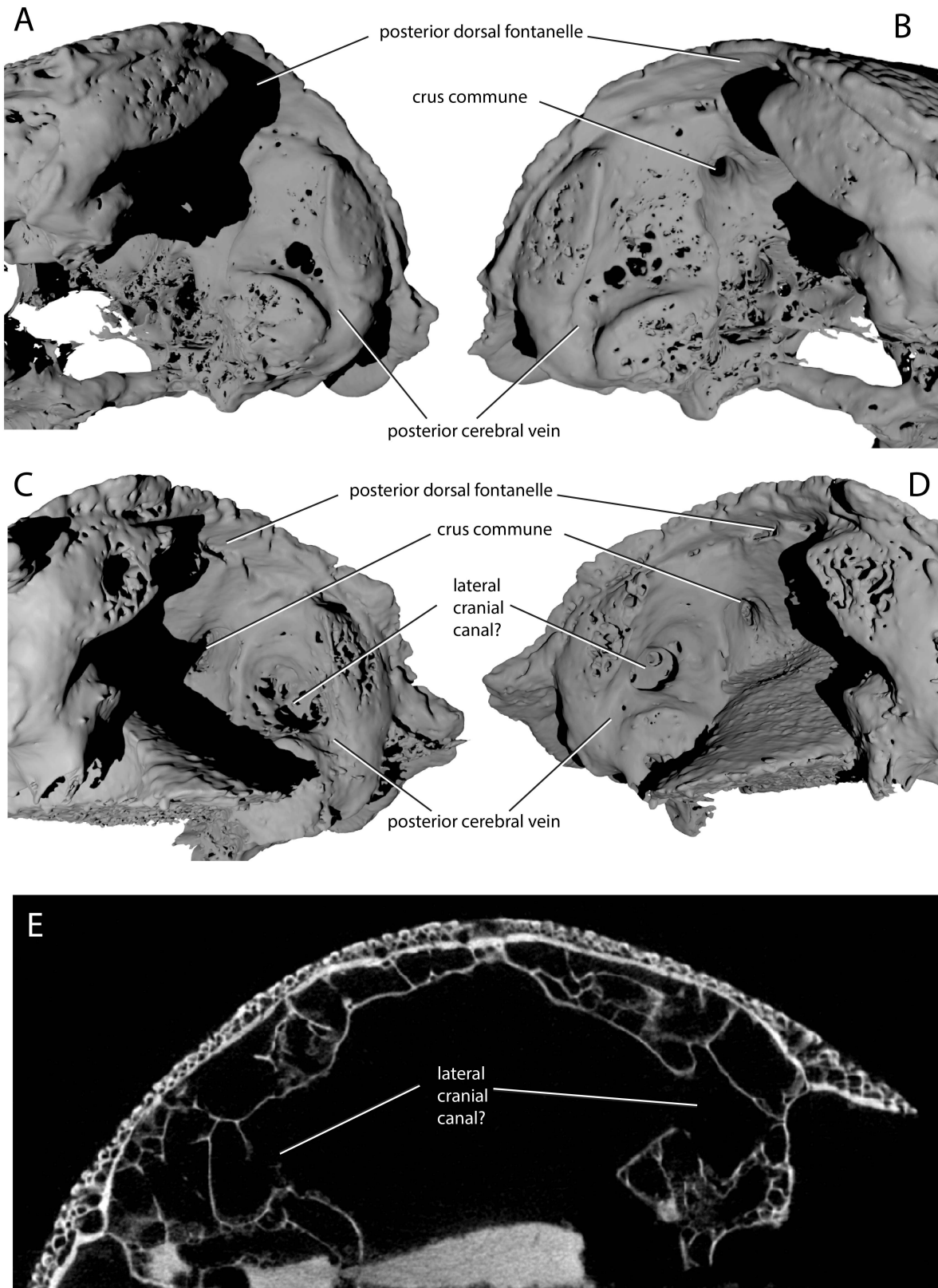


Figure 8. Variability in the development of a lateral cranial canal in *Ligulalepis*. A-B) Ventrolateral view of AM F101607, showing internal view of the otic region on the right hand side (A) and the left hand side (B). C-D) Ventrolateral view of ANU V3628, showing

internal view of the otic region on the right hand side (C) and the left hand side (D). E) CT scan cross-section of ANU V3628 showing diverticula that may represent a lateral cranial canal.

Labyrinth

The labyrinth region in *Ligulalepis* is well preserved (Fig. 7), with three complete, slender semicircular canals present, and all carrying small expansions for ampullae.

A short portion of preampullary canal separates the posterior ampulla from the cranial cavity. The posterior semicircular canal curves back underneath the horizontal semicircular canal to meet the cranial cavity far ventrally. This ventral position of the posterior canal is also seen in placoderms (e.g. *Dicksonosteus*; Goujet 1984), chondrichthyans (Schaeffer, 1981; Maisey, 2007), early sarcopterygians (e.g. *Youngolepis*; Chang, 1982) and, to a slightly lesser extent, in the early actinopterygian *Mimipiscis* (Giles & Friedman 2014).

Strikingly, the horizontal canal is positioned obliquely at an angle of about 30 degrees from the cranial cavity, and completes nearly a full circle before entering the cranial cavity. The entrance to the cranial cavity is swollen, almost giving the appearance of an ampulla like that at the anterior extent of the canal.

Other notable features of the vestibular system are the relatively shallow superior sinus situated below the crus commune, seen elsewhere in *Cladodoidea*, *Youngolepis* and *Kansasiella* (Poplin, 1974, Chang 1982, Maisey 2005), but not in *Mimipiscis* or *Acanthodes* (Davis et al. 2012). As well as the crus commune, a portion of the sinus superior, anterior and posterior semicircular canals project dorsally above the endocranial roof. The same condition is found in chondrichthyans and early actinopterygians (Giles and Friedman 2014).

Although incompletely known ventrally, the sacculus is not laterally extensive and appears to have been shallow. The general morphology of the labyrinth, including the dorsoventrally extensive posterior canal, which projects above the endocranial roof as well as below the cerebellar floor, and

the inclined horizontal canal, recalls that of an early chondrichthyan such as *Cladodoides* (Maisey 2005) or perhaps even *Acanthodes* (Davis et al. 2012). The labyrinth is far removed from that seen in *Mimipiscis* (Giles and Friedman 2014), or sarcopterygians such as *Eusthenopteron* and Devonian lungfishes (Jarvik 1980; Clement and Ahlberg 2014).

Sensory canals

The supraorbital canal (Fig. 9A) appears to be formed from two separate sections. The sections overlap approximately at the level of the postorbital process, the posterior section pinching out and sitting on top of the anterior section (Fig. 9A, arrow). Tubuli connecting the supraorbital canal to the surface are small and few in number. Tubuli from the infraorbital and otic canals are larger (Fig. 9B, arrows). The tubuli do not appear to be branched (although they may have branched in the skin above the bone), in contrast to the highly branched tubuli of some early sarcopterygians (Bjerring 1972; Clément and Ahlberg 2010). It is not clear whether not the pores for the sensory canals figured for *Mimipiscis* and *Moythomasia* originate from branched or individual tubuli (Gardiner 1984).

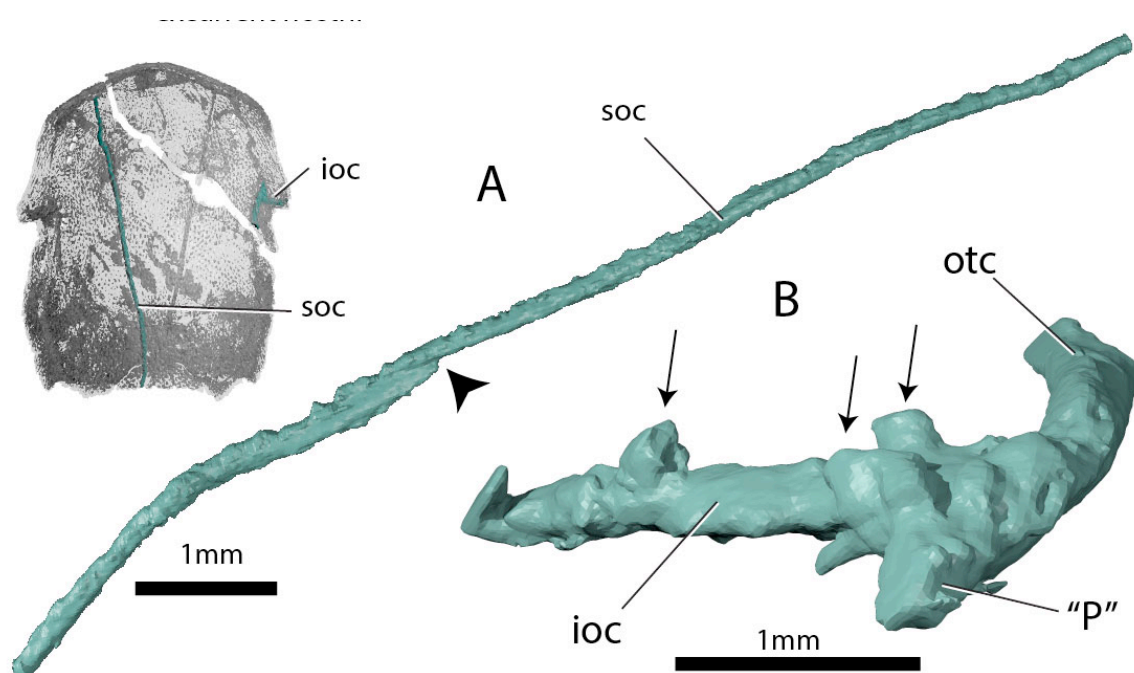


Figure 9. Sensory canal morphology in *Ligulalepis*, from ANU V3628. A) Left supraorbital canal in left lateral view. Arrow indicates point where an anterior and posterior canal section overlap. B) Right infraorbital and otic canal in anterior view. Arrows indicate tubules that connect the canal to the surface.

Phylogenetic analysis

AM-F101607 and ANU V3628 were coded into an updated phylogenetic analysis modified from Lu et al., 2017. As well as changes to anatomical scores for 'Ligulalepis', codes for several taxa were updated and some characters were deleted or reformulated to give a total of 282 characters coded for 94 taxa (for full details see the 'phylogenetic methods' section). This dataset was analysed using both parsimony and Bayesian inference. The parsimony analysis retrieves Dialipina, 'Ligulalepis', and 'psarolepids' as successively branching sister taxa to the osteichthyan crown node (Figure 10A). However, support for the clade that comprises crown osteichthyans (as retrieved from this analysis) is low, with Bremer support of 1 and a bootstrap of just 4. This is very weak support, although we note that bootstrap values obtained from TNT are likely to be much more conservative than those produced by PAUP*: bootstrap values in TNT are calculated from the strict consensus trees found in each replicate (Goloboff et al., 2008), whereas PAUP* uses all the shortest trees from each replicate, weighted by the reciprocal of the number of trees found in that replicate (Swofford, 2003).

There are six unambiguous character state changes on the branch leading to crown osteichthyans. These are #78 (enameloid on teeth gained), #110 (shape of parashenoid splint shaped), #116 (olfactory tracts long), #130 (eyestalk absent), #184 (median dorsal plate absent), #211 (dorsal fin spines absent). Of these, only the olfactory tracts and eyestalk are known in 'Ligulalepis'.

Alternative phylogenetic placements under parsimony were tested using two constrained searches, one with 'Ligulalepis' constrained within actinopterygians and another with 'psarolepids' constrained within sarcopterygians. A stem actinopterygian position for 'Ligulalepis' requires a single additional step, and the grouping of 'Ligulalepis' and actinopterygians was found in 18% of the

bootstrap replicates. Enforcing this topology also resulted in 'psarolepids' being resolved as stem sarcopterygians (Figure 10B). A single additional step is required to place 'psarolepids' on the sarcopterygian stem, and this grouping is found in 16% of bootstrap replicates. When this grouping is enforced it leads to 'Ligulalepis' falling into a polytomy with actinopterygians and sarcopterygians (Figure 10B).

The Bayesian analysis retrieves 'psarolepids' on the sarcopterygian stem with moderately strong support (pp = 0.94, Figure 11). 'Ligulalepis' is resolved as a stem osteichthyan in the 50% majority rule tree (Figure 11), although the crown osteichthyan clade has weak support (0.61). However, an actinopterygian position for 'Ligulalepis' has a posterior probability of 0.22.

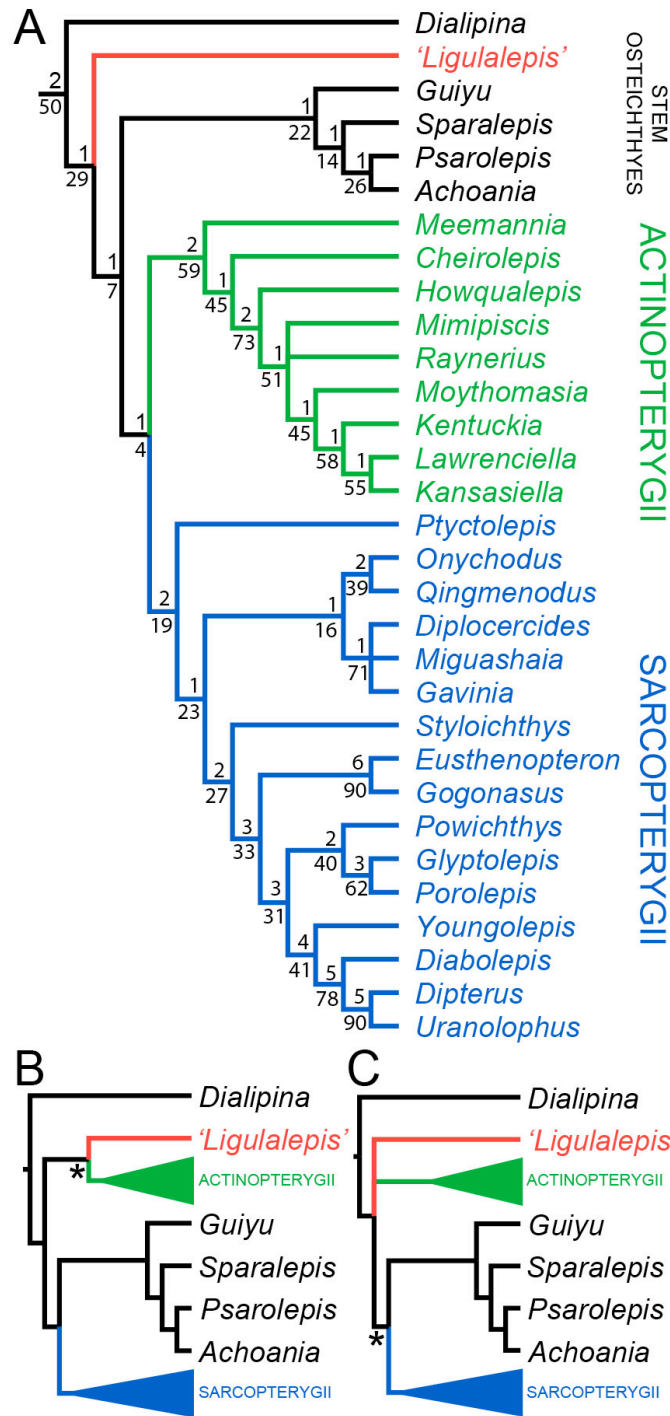


Figure 10. Results of parsimony phylogenetic analysis. A) Strict consensus tree. Numbers above nodes refer to bremer support, numbers below nodes represent bootstrap support. B) Strict consensus tree after enforcing *Ligulalepis* as sister group to actinopterygians. C) Strict consensus tree after constraining the *Guiyu* group to be sarcopterygians. Asterisks indicate constrained nodes.

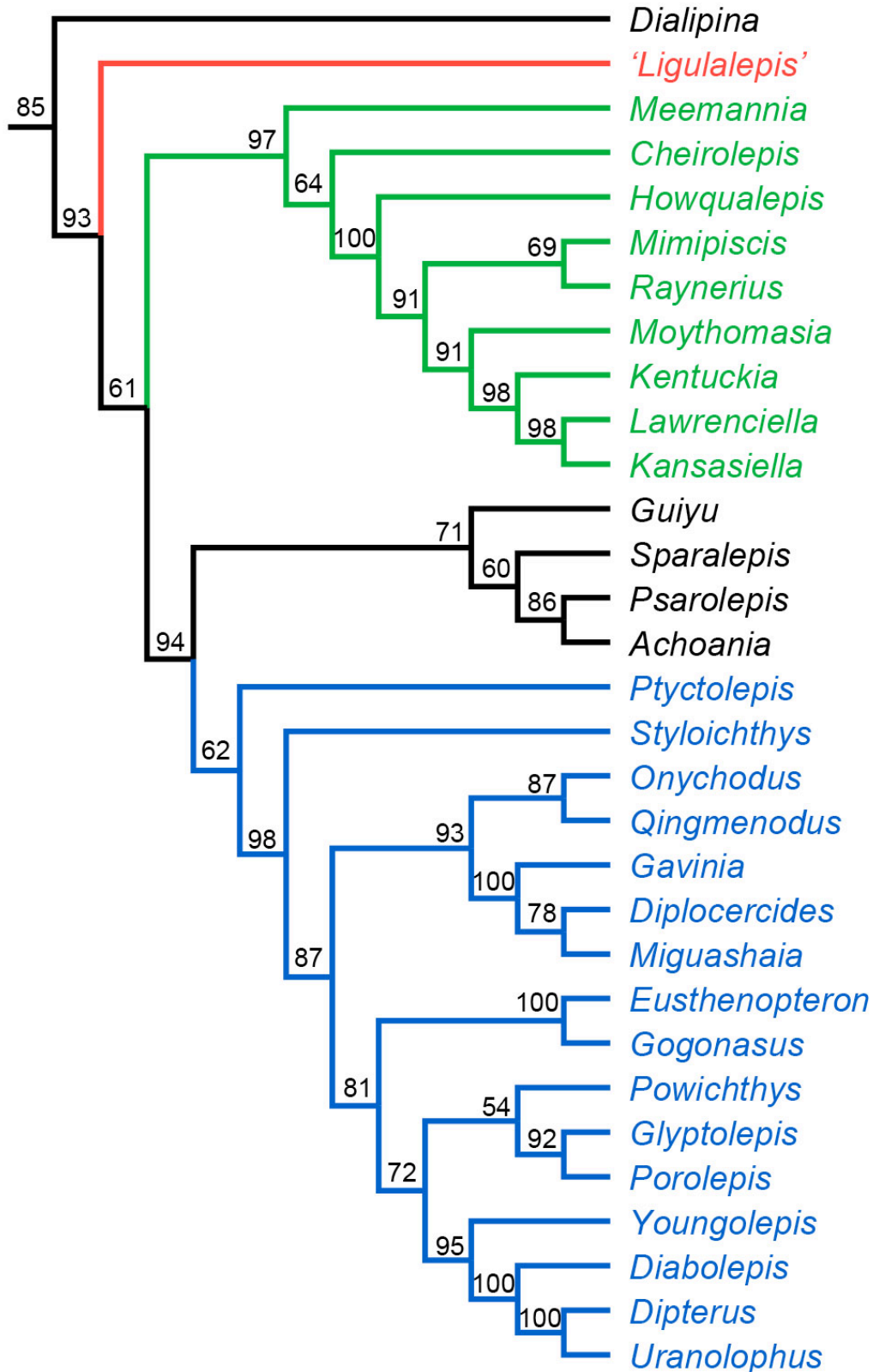


Figure 11. Bayesian phylogenetic analysis does not robustly resolve the position of *Ligulalepis*, but places the *Guiyu* clade on the sarcopterygian stem. Maximum clade credibility tree. Numbers represent posterior probabilities, displayed as percentages for presentation purposes.

Discussion

Ligulalepis and early osteichthyan phylogeny

Ligulalepis is recovered as a stem osteichthyan in the parsimony phylogenetic analysis, together with *Dialipina* and the “*Guiyu* group” (*Guiyu*, *Sparalepis*, *Psarolepis*, *Achoania*). However, the constraint experiments reveal that the relationships of these early osteichthyans are somewhat interdependent, as constraining *Ligulalepis* to be an actinopterygian also leads to the *Guiyu* group appearing on the sarcopterygian stem. This is because characters that support a stem osteichthyan position for *Ligulalepis* (the eyestalk and short olfactory tracts) are also found in *Psarolepis* and *Achoania* (Zhu et al. 2001; Zhu et al. 2013) and only support a stem osteichthyan position if all these taxa are recovered on the stem. Evidence for a stem osteichthyan position for the *Guiyu* group is now accumulating, with characters such as dorsal fin spines, a median dorsal plate and absence of tooth enamel supporting a stem osteichthyan position (Zhu et al. 2009; Qu et al. 2015). This in turn has implications for *Ligulalepis* as it increases support for a stem osteichthyan position.

An actinopterygian position for *Ligulalepis* is only a single step longer. The characters used to support an actinopterygian position for *Meemannia* (Lu et al. 2016a) are either absent or uncertain in *Ligulalepis*. *Meemannia* shares with actinopterygians a similar shape to the posterior skull roof, with the most posterior canal-bearing bones extending posterior to the postparietals. However the homology of the relevant bones in *Meemannia* and actinopterygians is uncertain: In *Meemannia* the most posterior canal-bearing bone was suggested to be equivalent to the actinopterygian intertemporal by Zhu et al. (2006), but later was compared to the actinopt supratemporal (Lu et al. 2016a).

Another important character is the lateral cranial canal. A lateral cranial canal is typically considered an actinopterygian character (Gardiner 1984; Coates 1999). Presence of a lateral cranial canal was a key character uniting *Meemannia* with actinopterygians (Lu et al. 2016a). The lateral cranial canal

may variously be an independent blind-ending canal, communicate with the fossa bridgei or communicate with the cranial cavity (Patterson 1975; Giles et al. 2015a). Furthermore, the shape and even the presence of this character can vary between individuals of the same species (Patterson 1975). Even in *Mimipiscis*, the lateral cranial canal in some specimens can occupy the whole area between the posterior and anterior semicircular canals, while in others be “little more than a pocket in front of the posterior semicircular canal” (Gardiner 1984). Gardiner (1984, p. 241) claimed that the lateral cranial canal can be expressed simply in terms of the degree of ossification of the dorsal otic region. The two specimens of *Ligulalepis* appear to confirm this idea, with the development of a lateral cranial canal variable between specimens. Notably *Meemannia* endocranial anatomy is only known from a single skull specimen, so variability in development of the lateral cranial canal cannot be studied in this taxon. It is also problematic to compare *Ligulalepis*, which has been acid prepared, with the mechanically prepared *Meemannia*, as fragile endochondral bone laminae are easily lost during mechanical preparation. This shows the importance of the well-preserved acid-prepared material of ‘*Ligulalepis*’ for comparisons with other early osteichthyans

‘*Ligulalepis*’ possesses a placoderm-like median hypophysial vein. This character was suggested to be a placoderm synapomorphy by Castiello and Brazeau (2018). Its presence in ‘*Ligulalepis*’ is the first time this is known outside placoderms, but does not necessarily disqualify it from being a placoderm synapomorphy.

Ligulalepis, histology and the problem of associated material

The original scales described for *Ligulalepis* (Schultze 1968) are not disqualified from belonging to the same animal as the braincase investigated herein. The scale material itself was described as possessing typically ‘actinopterygian’ characters; an anterodorsal process on the scale, multilayered

ganoine and a peg-and-socket articulation (Schultze 1968; Schultze 2016). However, these characters have uncertain polarity (Friedman and Brazeau 2010), and the utility of ganoine as a phylogenetic character is debated (Richter and Smith 1995; Friedman and Brazeau 2010).

However, the tooth and jaw fragment attributed to *Ligulalepis* recently figured by Schultze (2016, Fig. 13) presents a different problem. A vertical thin section through the tooth clearly shows an acrodin tip. Acrodin is a highly mineralized form of dentine restricted to actinopterygians crownward of *Cheirolepis* (Friedman and Brazeau 2010). However, this tooth comes from a different fossil site, of an earlier age (Trundle Group, Pragian), than the skulls described in this study. It is unclear which characters were used to identify this specimen as *Ligulalepis*, but it most likely does not belong to the same species as the braincase and/or scale material.

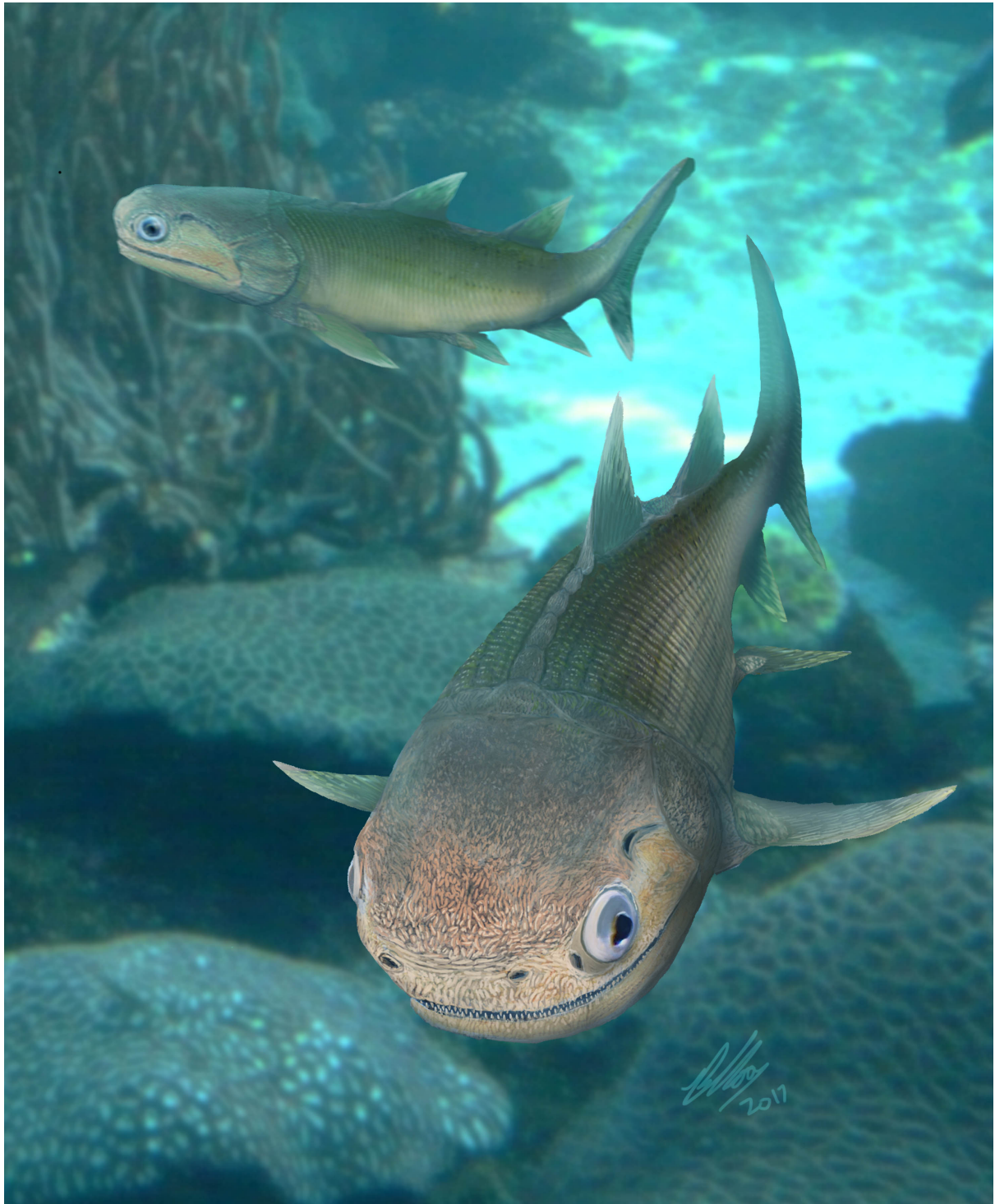


Figure 12. Life reconstruction of *Ligulalepis*.

Acknowledgements

Thanks to Helen and Ian Cathles for access to the fossil site, Ben Young and Vincent Dupret for assistance in the field, Carey Burke for assistance with acid preparation and Ruth Williams for CT scanning.

References

- Basden, A. M. and Young, G. C. (2001). A primitive actinopterygian neurocranium from the Early Devonian of southeastern Australia. *Journal of Vertebrate Paleontology* **21**, 754–766.
- Basden, A. M., Young, G. C., Coates, M. I. and Ritchie, A. (2000). The most primitive osteichthyan braincase? *Nature* **403**, 185–188.
- Bjerring, H. C. (1972). Morphological observations on the exoskeletal skull roof of an osteolepiform from the Carboniferous of Scotland. *Acta Zoologica* **53**, 73–92.
- Brazeau, M. D. (2009). The braincase and jaws of a Devonian ‘acanthodian’ and modern gnathostome origins. *Nature* **457**, 305–308.
- Burrow, C. J. (1997). Microvertebrate assemblages from the Lower Devonian (pesavis/sulcatus zones) of central New South Wales, Australia. *Modern Geology* **21**, 43–77.
- Chang, M.-M. (1982). *The braincase of Youngolepis, a Lower Devonian crossopterygian from Yunnan, south-western China*. Swedish Museum of Natural History, Stockholm.
- Choo, B., Zhu, M., Qu, Q., Yu, X., Jia, L. and Zhao, W. (2017). A new osteichthyan from the late Silurian of Yunnan, China. *PloS one* **12**, e0170929.

- Clement, A. M. and Ahlberg, P. E. (2014). The first virtual cranial endocast of a lungfish (Sarcopterygii: Dipnoi). *PloS one* **9**, e113898.
- Clément, G. and Ahlberg, P. E. (2010). The endocranial anatomy of the early sarcopterygian *Powichthys* from Spitsbergen, based on CT scanning. In *Morphology, Phylogeny and Paleobiogeography of Fossil Fishes* (ed. D. K. Elliott, J. G. Maisey, X. Yu and D. Miao), pp. 363–378. Verlag Dr. Friedrich Pfeil, München.
- Coates, M. I. (1999). Endocranial preservation of a Carboniferous actinopterygian from Lancashire, UK, and the interrelationships of primitive actinopterygians. *Philosophical Transactions of the Royal Society B: Biological Sciences* **354**, 435–462.
- Davis, S. P., Finarelli, J. A. and Coates, M. I. (2012). *Acanthodes* and shark-like conditions in the last common ancestor of modern gnathostomes. *Nature* **486**, 247–250.
- Dupret, V., Sanchez, S., Goujet, D. and Ahlberg, P. (2017). The internal cranial anatomy of *Romundina stellina* Ørvig, 1975 (Vertebrata, Placodermi, Acanthothoraci) and the origin of jawed vertebrates—Anatomical atlas of a primitive gnathostome. *PloS one* **12**, e0171241.
- Friedman, M. and Brazeau, M. D. (2010). A reappraisal of the origin and basal radiation of the Osteichthyes. *Journal of Vertebrate Paleontology* **30**, 36–56.
- Gardiner, B. G. (1984). The relationships of the paleoniscid fishes. a review based on new specimens of *Mimia* and *Moythomasia* from the upper Devonian of Western Australia. *Bulletin of the British Museum (Natural History) Geology* **37**, 173–248.
- Giles, S., Darras, L., Clément, G., Blicek, A. and Friedman, M. (2015a). An exceptionally preserved Late Devonian actinopterygian provides a new model for primitive cranial anatomy in ray-finned fishes. *Proceedings of the Royal Society B* **282**, 20151485.

- Giles, S. and Friedman, M. (2014). Virtual reconstruction of endocast anatomy in early ray-finned fishes (Osteichthyes, Actinopterygii). *Journal of Paleontology* **88**, 636–651.
- Giles, S., Friedman, M. and Brazeau, M. D. (2015b). Osteichthyan-like cranial conditions in an Early Devonian stem gnathostome. *Nature* **520**, 82–85.
- Giles, S., Rogers, M. and Friedman, M. (2016). Bony labyrinth morphology in early neopterygian fishes (Actinopterygii: neopterygii). *Journal of Morphology*, 10.1002/jmor.20551.
- Goujet, D. (1984). *Les poissons placodermes du Spitzberg: Arthrodires Dolichothoraci de la Formation de Wood Bay (Dévonien inférieur)*. *Cahiers de Paléontologie, Section Vertébrés*. CNRS, Paris.
- Hamel, M.-H. and Poplin, C. (2008). The braincase anatomy of *Lawrenciella schaefferi*, actinopterygian from the Upper Carboniferous of Kansas (USA). *Journal of Vertebrate Paleontology* **28**, 989–1006.
- Hu, Y., Lu, J. and Young, G. C. (2017). New findings in a 400 million-year-old Devonian placoderm shed light on jaw structure and function in basal gnathostomes. *Scientific reports* **7**, 7813.
- Jarvik, E. (1980). *Basic structure and evolution of vertebrates*. Academic Press, London.
- King, B., Qiao, T., Lee, M. S., Zhu, M. and Long, J. A. (2017). Bayesian Morphological Clock Methods Resurrect Placoderm Monophyly and Reveal Rapid Early Evolution in Jawed Vertebrates. *Systematic Biology* **66**, 499–516.
- Lane, J. A. (2010). Morphology of the braincase in the Cretaceous hybodont shark *Tribodus limae* (Chondrichthyes: Elasmobranchii), based on CT scanning. *American Museum Novitates* **3681**, 1–70.
- Long, J. A. (2001). On the relationships of *Psarolepis* and the onychodontiform fishes. *Journal of Vertebrate Paleontology* **21**, 815–820.

- Lu, J., Giles, S., Friedman, M., den Blaauwen, J. L. and Zhu, M. (2016a). The oldest actinopterygian highlights the cryptic early history of the hyperdiverse ray-finned fishes. *Current Biology* **26**, 1602–1608.
- Lu, J., Zhu, M., Ahlberg, P. E., Qiao, T., Zhu, Y. a., Zhao, W. and Jia, L. (2016b). A Devonian predatory fish provides insights into the early evolution of modern sarcopterygians. *Science Advances* **2**, e1600154.
- Lu, J., Zhu, M., Long, J. A., Zhao, W., Senden, T. J., Jia, L. and Qiao, T. (2012). The earliest known stem-tetrapod from the Lower Devonian of China. *Nature Communications* **3**, 1160.
- Maisey, J. G. (2005). Braincase of the Upper Devonian shark *Cladodoides wildungensis* (Chondrichthyes, Elasmobranchii), with observations on the braincase in early chondrichthyans. *Bulletin of the American Museum of Natural History* **288**, 1–103.
- Maisey, J. G. (2007). The braincase in Paleozoic symmoriiform and cladoselachian sharks. *Bulletin of the American Museum of Natural History* **307**, 1–122.
- Northcutt, R. G. and Bemis, W. E. (1993). Cranial nerves of the coelacanth, *Latimeria chalumnae* [Osteichthyes: Sarcopterygii: Actinistia], and comparisons with other craniata. *Brain, behavior and evolution* **42**, 1–76.
- Ørvig, T. (1973). Fossila fisktänder i svepelektronmikroskopet: gamlafrågeställningar i ny belysning. *Fauna Flora* **68**, 166–173.
- Patterson, C. (1975). The braincase of pholidophorid and leptolepid fishes, with a review of the actinopterygian braincase. *Philosophical Transactions of the Royal Society of London B: Biological Sciences* **269**, 275–579.
- Poplin, C. M. (1974). *Etude de quelques paleoniscides pennsylvaniens du Kansas*. CNRS, Paris.

- Qiao, T., King, B., Long, J. A., Ahlberg, P. E. and Zhu, M. (2016). Early gnathostome phylogeny revisited: multiple method consensus. *PLoS one* **11**, e0163157.
- Qu, Q., Haitina, T., Zhu, M. and Ahlberg, P. E. (2015). New genomic and fossil data illuminate the origin of enamel. *Nature* **526**, 108–111.
- Richter, M. and Smith, M. (1995). A microstructural study of the ganoine tissue of selected lower vertebrates. *Zoological Journal of the Linnean Society* **114**, 173–212.
- Robineau, D. (1975). The jugular vein system and its homologies in *Latimeria chalmunae* (Pisces, Crossopterygii, Coelacanthidae). *Comptes rendus hebdomadaires des seances de l'Academie des sciences. Serie D: Sciences naturelles* **281**, 45–48.
- Sakellariou, A., Sawkins, T., Senden, T. and Limaye, A. (2004). X-ray tomography for mesoscale physics applications. *Physica A: Statistical Mechanics and its Applications* **339**, 152–158.
- Schaeffer, B. (1981). The xenacanth shark neurocranium, with comments on elasmobranch monophyly. *Bulletin of the American Museum of Natural History* **169**, 3–66.
- Schultze, H.-P. (1968). Palaeoniscoidea-Schuppen aus dem Unterdevon Australiens und Kanadas und aus dem Mitteldevon Spitzbergens. *Bulletin of the British Museum (Natural History) Geology* **16**, 341–368.
- Schultze, H.-P. (2016). Scales, enamel, cosmine, ganoine, and early osteichthyans. *Comptes Rendus Palevol* **15**, 83–102.
- Schultze, H.-P. and Cumbaa, S. L. (2001). *Dialipina* and the characters of basal actinopterygians. In *Major Events in Early Vertebrate Evolution* (ed. P. Ahlberg), pp. 315–332. Taylor and Francis, London and New York.
- Stensiö, E. A. (1963a). *Anatomical studies on the arthrodiran head*. Almqvist & Wiksell, Stockholm.

- Stensiö, E. A. (1963b). *The Brain and the Cranial Nerves in Fossil, Lower Craniate Vertebrates*. Universitetsforlaget, Oslo.
- Stensiö, E. A. (1969). Elasmobranchiomorphi Placodermata Arthrodires. In *Traité de paléontologie*, vol. 4 (ed. J. Piveteau), pp. 71–692. Masson, Paris.
- Watson, D. M. S. (1937). The acanthodian fishes. *Philosophical Transactions of the Royal Society of London. Series B, Biological Sciences*, 49–146.
- Young, G. C. (1979). New information on the structure and relationships of *Buchanosteus* (Placodermi: Euarthrodira) from the Early Devonian of New South Wales. *Zoological Journal of the Linnean Society* **66**, 309–352.
- Young, G. C. (1980). A new Early Devonian placoderm from New South Wales, Australia, with a discussion of placoderm phylogeny. *Palaeontographica Abteilung A Palaeozoologie-Stratigraphie* **167**, 10–76.
- Yu, X. (1998). A new porolepiform-like fish, *Psarolepis romeri*, gen. et sp. nov. (Sarcopterygii, Osteichthyes) from the Lower Devonian of Yunnan, China. *Journal of Vertebrate Paleontology* **18**, 261–274.
- Zhu, M., Wang, W. and Yu, X. (2010). *Meemannia eos*, a basal sarcopterygian fish from the Lower Devonian of China—expanded description and significance. In *Morphology, Phylogeny and Paleobiogeography of Fossil Fishes* (ed. D. Elliot, J. Maisey, X. Yu and D. Miao), pp. 199–214. Verlag Dr. Friedrich Pfeil, München.
- Zhu, M., Yu, X. and Ahlberg, P. E. (2001). A primitive sarcopterygian fish with an eyestalk. *Nature* **410**, 81–84.

Zhu, M., Yu, X., Ahlberg, P. E., Choo, B., Lu, J., Qiao, T., Qu, Q., Zhao, W., Jia, L., Blom, H. and Zhu, Y.-A. (2013). A Silurian placoderm with osteichthyan-like marginal jaw bones. *Nature* **502**, 188–193.

Zhu, M., Yu, X. and Janvier, P. (1999). A primitive fossil fish sheds light on the origin of bony fishes. *Nature* **397**, 607–610.

Zhu, M., Yu, X., Wang, W., Zhao, W. and Jia, L. (2006). A primitive fish provides key characters bearing on deep osteichthyan phylogeny. *Nature* **441**, 77–80.

Zhu, M., Zhao, W., Jia, L., Lu, J., Qiao, T. and Qu, Q. (2009). The oldest articulated osteichthyan reveals mosaic gnathostome characters. *Nature* **458**, 469–474.

Chapter 6

Bayesian tip-dating methodology: topological effects, stratigraphic fit and the relationships of early osteichthyans

Benedict King¹

¹ College of Science and Engineering, Flinders University, Adelaide, South Australia 5042, Australia.

Context

This chapter examines the implications of tip-dated Bayesian phylogenetics, also used in chapter 3, for the recovery of evolutionary relationships. In the first part of the chapter, I look at how the use of the stratigraphic ages of fossils as part of the analysis can affect the tree topology. The second part of the paper applies tip-dating and the concepts learnt in the first part to the phylogenetic problem introduced in the previous chapter: the relationships of *Ligulalepis* and early osteichthyans generally.

Abstract

Bayesian tip-dating (or morphological clock) phylogenetic methods are revolutionising studies of macroevolutionary patterns, but how these methods affect the recovery of evolutionary relationships has not been fully explored. Here I show, through analysis of several datasets of vertebrate and invertebrate fossils with multiple phylogenetic methods, that parsimony and non-clock Bayesian methods produce tree topologies that are broadly similar, while topologies produced by Bayesian tip-dating can be more different, based on Robinson-Foulds distances. As expected, trees recovered by tip-dating analysis have better fit to stratigraphy than trees recovered by other methods, due to trees with better stratigraphic fit being assigned a higher prior probability. Differences in stratigraphic fit and tree topology between tip-dating and other methods appear to be concentrated in parts of the tree with weaker character signal and a stronger influence of the prior, as shown by successive deletion of the most incomplete taxa from a sauropod dataset. Tip dating, when applied to early osteichthyan relationships, reveals strong support for an actinopterygian position for the enigmatic taxon "*Ligulalepis*" (possibly due to better stratigraphic fit), which is unresolved in parsimony analysis. Further investigation reveals that this strong support is due to a combination of the tree prior and the data. It is concluded that tip-dated Bayesian analyses are a promising approach for investigating both macro-evolutionary patterns and evolutionary relationships simultaneously.

Introduction

The question of whether or not the ages of fossils should be taken into account when estimating phylogeny is a major debate within palaeontology (Wagner 1995; Lockwood 1998; Smith 1998; Heyning and Thacker 1999; Geiger et al. 2001; Alroy 2002). This debate centred around stratocladistics (Fisher 2008), a parsimony method that considers stratigraphic parsimony debt alongside traditional morphological parsimony debt. Recently, the rise of Bayesian tip-dating

methods (Ronquist et al. 2012a), has introduced a new way of incorporating fossil ages into phylogenetic inference. However, the extent to which the use of stratigraphic ages during tip-dating influences tree topology has yet to be fully investigated.

At the heart of tip-dating methods is the tree prior, the prior probability distribution of divergence dates and branch lengths. Early attempts at tip-dating analysis used the uniform tree prior (Ronquist et al. 2012a), which is relatively uninformative regarding tree shape, and not very biologically realistic. The uniform tree prior has been superseded by serially sampled tree priors (Stadler 2010; Heath et al. 2014), which model diversification, extinction and sampling. Recently, these have been updated to allow sampled ancestors (Gavryushkina et al. 2014). Serially sampled tree priors, which include assumptions of constant rates of diversification, extinction and sampling, likely affect tree topology, and indeed assumptions of approximately constant sampling rates between lineages at specified time intervals is a key component of stratocladistics (Fisher 2008).

Tip-dating has been used on a number of datasets to examine the phylogeny of fossil forms, including Mesozoic birds (Lee et al. 2014b), Mesozoic mammals (Close et al. 2015), theropod dinosaurs (Lee et al. 2014a; Bapst et al. 2016), pufferfish (Close et al. 2016) and penguins (Gavryushkina et al. 2017). Most of these studies have concentrated on macro-evolutionary patterns and divergence dates. Bapst et al. (2016) reported topological differences between tip-dated Bayesian, non-clock Bayesian and parsimony analysis of the same dataset, as well as between different implementations of tip-dating. Turner et al. (2017) showed that violations to the assumptions of serial sampled tree priors can affect tree topology in an analysis of crocodylomorphs, and also that tip-dating analysis disfavors long unsampled branches. King et al. (2017) showed that tip dating can have major effects on tree topology by attempting to balance inferred rates of evolution.

Stratigraphic fit measures are explicit measures for assessing how well a phylogeny fits with the order of appearance (i.e. geological ages) of its taxa. Historically, they have been put to a number of

uses, including assessing the quality of the fossil record (Benton et al. 2000) and comparisons of the stratigraphic congruence between major groups (O'Connor and Wills 2016). These indices include the Stratigraphic Consistency Index (SCI), Manhattan Stratigraphic Measure (MSM) and the Gap Excess Ratio (GER). The SCI (Huelsenbeck 1994) calculates the number of consistent nodes, where a consistent node is one whose oldest descendant is the same age or younger than the oldest descendant of its sister node. The MSM (Siddall 1998) and GER (Wills 1999) both rely on measuring the Minimum Implied Gap (MIG), a measure of the smallest possible sum of ghost lineages implied by a particular tree topology.

This study aims to investigate topological differences between tip-dating methods and other phylogenetic methods. First, topology differences between methods and stratigraphic congruence measures are calculated across several datasets. Second, I test whether or not these topology differences are concentrated in parts of the phylogeny with weak character data. Finally, tip dating is used to investigate the phylogeny of early osteichthyan fossils, which remain in a state of flux (Friedman and Brazeau 2010; Lu et al. 2016b; Qiao et al. 2016), with a particular focus on the enigmatic "*Ligulalepis*", the subject of the previous chapter. The prior probability distribution on the tree topology of early osteichthyans is also investigated, to gain insights into why results from tip-dating differ from other methods.

Materials and methods

Comparing tree topology and stratigraphic fit across methods

I selected a number of recent datasets for testing the topological differences between parsimony, undated Bayesian (hereafter referred to as non-clock) and tip-dated Bayesian methods. These were datasets of ichthyosaurs (Ji et al. 2016), eurypterids (Lamsdell and Selden 2017), horseshoe crabs (Lamsdell 2016), baleen whales (Marx and Fordyce 2015), turtles (Perea et al. 2014), sauropods (Poropat et al. 2016) and Mesozoic birds (Wang et al. 2015). Stratigraphic range data were taken

from these publications where available, otherwise from the Fossilworks (<http://fossilworks.org/>). Stratigraphic ranges were converted to age ranges using the international chronostratigraphy chart version 2016/12 (<http://www.stratigraphy.org/index.php/ics-chart-timescale>) and the geowhen database (<http://www.stratigraphy.org/upload/bak/geowhen/index.html>).

To avoid issues with violations of relatively equal sampling across time and space, some taxa were pruned from the following datasets prior to analysis: ichthyosaurs (all outgroup taxa except *Hupesuchus*), horseshoe crabs (all non-xiphosuran taxa except some synziphosurines), turtles (all outgroup taxa, tree rooted on *Odontochelys*), Mesozoic birds (modern taxa deleted). Characters that became invariant following taxon pruning were deleted from the datasets.

Parsimony analyses in TNT (Goloboff et al. 2008) employed new technology search, using sectorial search and tree fusing with default settings for 1000 random addition sequences. Due to the large total number of most-parsimonious trees for some datasets, and the computational burden of downstream analyses, I saved only the set of trees output from the new technology search, without running a traditional search to find all possible most-parsimonious trees.

Non-clock Bayesian analyses were performed in MrBayes (Ronquist et al. 2012b). The Mkv model (Lewis 2001) was used, with a gamma parameter to account for rate variation across sites. 4 independent runs of each analysis, each with four chains, were run for 10 million generations, saving 2000 trees. Convergence of the four runs was confirmed in Tracer (Rambaut et al. 2014).

Tip-dated Bayesian analyses were performed in BEAST2 (Bouckaert et al. 2014). The Mkv model (Lewis 2001) was used, with a gamma parameter to account for rate variation across sites.

Characters were partitioned according to the number of character states, with the substitution rate reweighted following King et al. (2017). The clock model was an uncorrelated lognormal clock (Drummond et al. 2006) except for the horseshoe crabs dataset, where a random local clock (Drummond and Suchard 2010) was used due to the low number of characters. The tree prior was a

sampled-ancestor fossilised birth-death model (Gavryushkina et al. 2014). A rho parameter was used for those datasets containing modern taxa (horseshoe crabs, whales, turtles). For the four datasets without modern taxa, sampled ancestors was turned off (by setting removal probability to 1), due to identifiability issues when all taxa have a different age (Gavryushkina et al. 2014). A standard set of uninformative priors was used for all analyses, details of which are in the xml files. Analyses were run for 200 million generations with sampling every 100 000 (i.e. 2000 trees saved). Convergence of four independent runs was checked in Tracer. Each dataset was also analysed using the prior only, without character data.

To assess the extent of topological differences between the three phylogenetic methods, I calculated Robinson-Foulds distances (Robinson and Foulds 1981) in R using the package phangorn (Schliep 2010). Every tree produced by one method was compared to every tree produced by both of the other methods. Robinson-Foulds distances were rescaled to a percentage difference following Wright and Hillis (2014). In addition to comparisons between methods, trees from each set were compared to each other as a measure of resolution within each method.

Stratigraphic fit, using the Gap Excess Ratio (Wills 1999), was calculated using the R package strap (Bell and Lloyd 2015). The Stratigraphic Completeness Index (Huelsenbeck 1994) was also calculated, with very similar results. To avoid problems with the different treatment of outgroups between methods, outgroups were removed from all trees prior to calculation. P-values were calculated for each stratigraphic fit. These P-values are calculated based on a null distribution of the mean and standard deviation of stratigraphic fit measures of a set of random trees, using the same taxa and age values (Bell and Lloyd 2014). P-values for all stratigraphic fit calculations were highly significant, showing that all methods produce trees with better fit to stratigraphy than expected by chance.

Because the results (see below) showed that Bayesian tip-dated methods place a higher prior probability on trees with better stratigraphic fit, I hypothesised that this prior would be particularly influential on tree topology when the character data were weak. I therefore tested the effect of

incomplete taxa on the stratigraphic fit of tip-dated and non-clock Bayesian phylogenetic trees. This was achieved through sequential removal of incomplete taxa. The sauropod dataset was chosen due to the wide range of data completeness across taxa and the large number of taxa. For each deletion iteration (total of 5), I removed the 6 remaining most incomplete taxa and reanalysed the data reanalysed and calculated stratigraphic fit as above. As a control, to test whether or not the act of removing taxa changes stratigraphic fit regardless of the completeness of those taxa, I repeated the process but deleted 6 random taxa in each iteration.

Analysis of early osteichthyan phylogeny

The data matrix was based on King et al. (2017), with a small number of changes (sources for codings as in King et al. 2017 supplementary information). Character 38 (ascending basisphenoid pillar pierced by internal carotid) was coded as inapplicable for taxa without a basisphenoid pillar (i.e. those coded as state 0 in character 37). Character 125 (internal carotid meets efferent pseudobranchial in orbit) was deleted due to redundancy with character 38. Character 24 (position of myodome for superior oblique eye muscles) was coded as unknown for *Lunaspis*, *Diandongpetalichthys* and *Wuttagoonaspis*. Character 283 (sensory line network) was scored as “open grooves” in *Culmacanthus*. Character 492 (peg on rhomboid scale) was scored as narrow in *Dialipina* and broad in *Guiyu* and *Psarolepis*. Character 188 (complete enclosure of spiracle by skull roof bones) was coded as unknown in *Osorioichthys* and absent in *Compagopiscis* and *Materpiscis*. Character 365 (enamel(oid) on teeth) was coded as unknown in *Achoania*. Character 289 (position of middle and posterior pit lines) was coded as unknown in *Dialipina*. Character 189 (paranuchal number) had its definition changed to “number of bones bearing otic sensory canal between the dermosphenotic and the lateral extrascapular”. All antiarchs were recoded as unknown, while *Meemannia* and *Dialipina* were coded as state 0 (1 bone) and *Cheirolepis canadensis* as 0/1. Character 113 (bar across spiracular groove) was changed to “endocranial spiracular enclosure: 0, absent; 1, present and 2, spiracular canal” (Lu et al. 2016a; chapter 5) and recoded accordingly. Eight

new characters (new to this particular matrix) were added as follows. Crus commune: 0, dorsal to endocranial roof; 1, ventral to endocranial roof (chapter 5). Interlocking lepidotrichial segments: 0, absent; 1, present (Friedman 2007). Optic lobes: 0, narrower than cerebellum; 1, same width or wider than cerebellum (chapter 5). Hypophysial chamber: 0, projects posteroventrally; 1, projects anteriorly or anteroventrally (chapter 5). Horizontal semicircular canal: 0, horizontally orientated; 1, obliquely orientated (chapter 5). Canal for palatine nerve: 0 absent; 1, present (new). Most posterior bones flanking postparietals: 0, level with posterior margin of postparietals; 1, extend posterior to posterior margin of postparietals (Lu et al. 2016a). Size of profundus canal in postnasal wall: 0, small; 1, large (Lu et al. 2016a and references therein).

Parsimony analysis was performed in TNT, using new technology search with ratchet, tree fusing, drift and sectorial searches in default settings for 1000 random addition sequence replicates. TBR swapping was then used on the trees in memory to more thoroughly explore the tree islands. The strict consensus tree was calculated (Fig. 5A).

Bayesian analysis was performed using the same models and tip-dates as King et al. (2017). Tip-dates for a number of taxa were given uniform priors over the period of uncertainty (King et al. 2017, supplementary information). In the tree prior, removal probability was set to one, so that sampled ancestors were not used, thus allowing use of variable tip-dates (see above). Four independent replicates of the analysis were run for 200 million generations, and convergence assessed in Tracer. Posterior samples of the four runs were combined for summary and further analysis.

To gain understanding about how the tree prior affects the recovered topology of early osteichthyans, a separate analysis was run from the prior only. The tree topology was largely fixed to the topology found in the maximum clade credibility tree of the main analysis. Only six osteichthyan taxa were unconstrained: *Guiyu*, *Psarolepis*, *Achoania*, *Dialipina*, *Meemannia* and *Ligulalepis*. These were free to move between stem osteichthyan, stem sarcopterygian and stem actinopterygian positions. This analysis effectively imitates the situation faced by most analyses of early

osteichthyans: the core groups of sarcopterygians and actinopterygians are strongly supported, but these six taxa are unresolved.

Because there are a several taxa under investigation, node support values do not necessarily give an informative idea about the probability that an individual taxon is an actinopterygian, sarcopterygian or stem osteichthyan. This was calculated separately from the posterior and prior tree samples in R, making use of the ape and phytools packages (Paradis et al. 2004; Revell 2012). The proportion of the sample for which each taxon shared a more recent common ancestor with *Howqualepis* (actinopterygian), *Eusthenopteron* (sarcopterygian) or neither (i.e. equally related to both) was calculated, thus giving probabilities of an actinopt, sarcopt or stem position respectively (Table 1).

Results

Tree topology

Tree topology of non-clock Bayesian and parsimony trees were more similar to each other than either was to tip-dated Bayesian trees (Fig. 1). This is further shown by plotting the number of parsimony steps for the trees produced by Bayesian methods with and without the tip-dating (Fig. 2). The output from parsimony is more resolved than the output from the Bayesian methods (fig. 1), as previously reported (O'Reilly et al. 2016). Topological differences between non-clock Bayesian and parsimony trees are in general not greater than the differences within the posterior sample of non-clock trees. These results suggest that it is the use of tip-dating and associated tree models, rather than a model of morphological evolution, that has the most significant effect on tree topology.

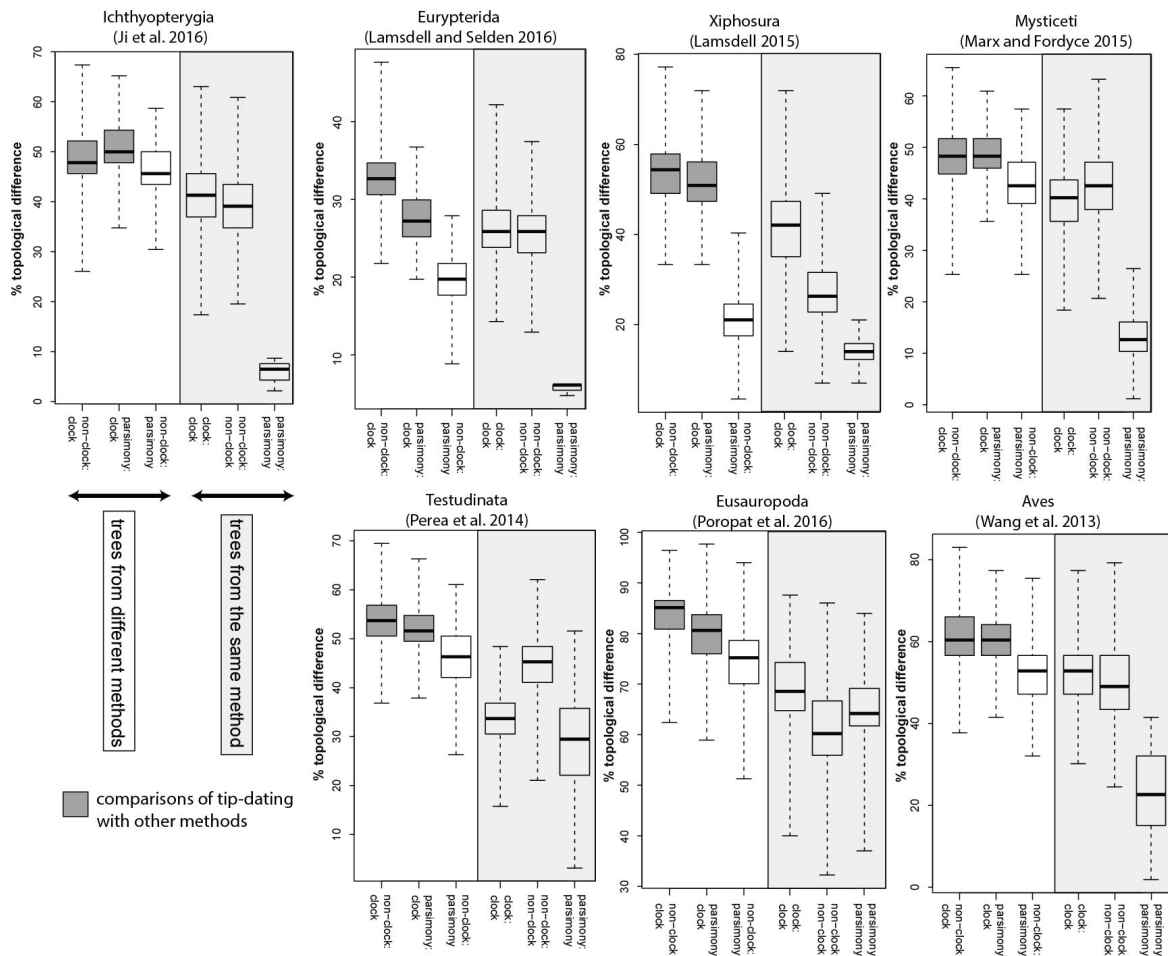


Figure 1. Bayesian tip-dating methods produce trees that are more different from trees produced by parsimony and non-clock Bayesian analyses, which are similar to each other. % topological difference (Robinson-Foulds distance) is plotted for each comparison, across seven datasets. Bayesian tip-dated (clock) methods vs. other methods (Bayesian non-clock and parsimony) are shaded in dark grey. Every tree from the posterior sample or set of shortest trees is compared to the sample from an alternative method, and the resulting range of values shown as a boxplot (whiskers span full range). Tree samples from each method are also compared to themselves as a measure of resolution.

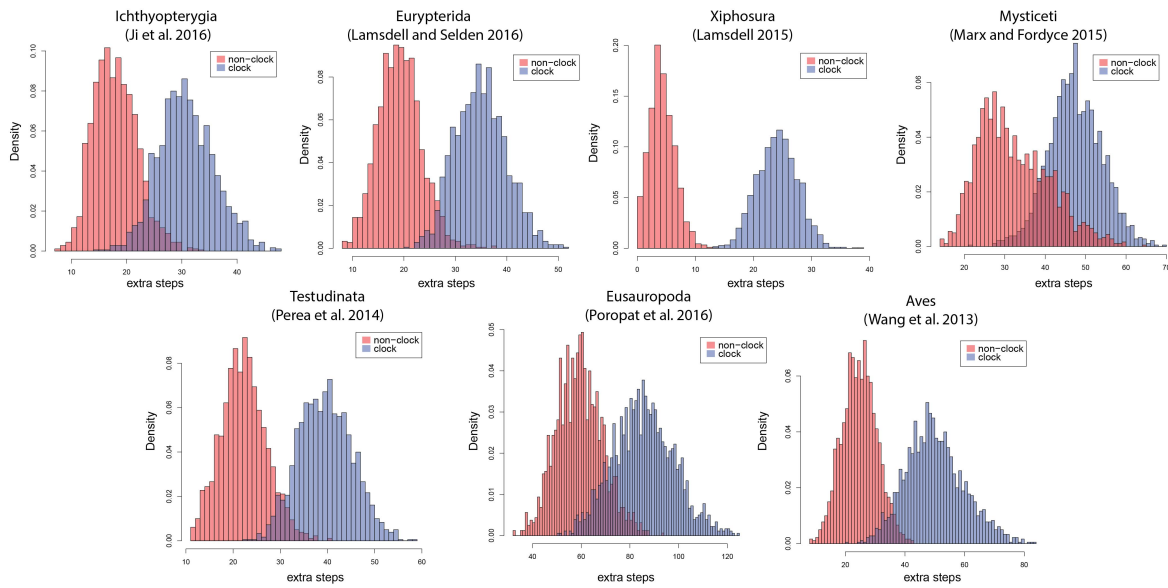


Figure 2. Bayesian tip-dating produces trees that are less parsimonious than non-clock Bayesian analysis. Histograms of the number of additional steps required by trees produced by tip-dating and non-clock Bayesian analysis, compared to the tree length of the most parsimonious trees. For the smallest dataset (Xiphosura), some of the trees produced by non-clock analysis are identical to parsimony trees.

Stratigraphic fit

As expected, tip-dating approaches produce trees with a better stratigraphic fit than non-clock Bayesian or parsimony (Fig. 3). Trees produced when the analysis samples solely from the prior have a particularly high stratigraphic fit, as expected. Plots showing the prior probability of trees against stratigraphic fit for each dataset show positive and highly significant correlations across all methods (Fig. 3). Stratigraphic fit is lower for the posterior sample of trees from the tip-dating analysis compared to the prior, but still higher than trees for the other two methods. Neither non-clock Bayesian nor parsimony outperforms the other in terms of stratigraphic fit. These results suggest that tip-dating methods assign a higher prior probability to trees with a better stratigraphic fit. This leads to a better stratigraphic fit for the tree topologies in the posterior sample, compared to trees produced by other methods. This is likely to be the cause of the topology differences between tip-dating and the other methods shown in the previous section.

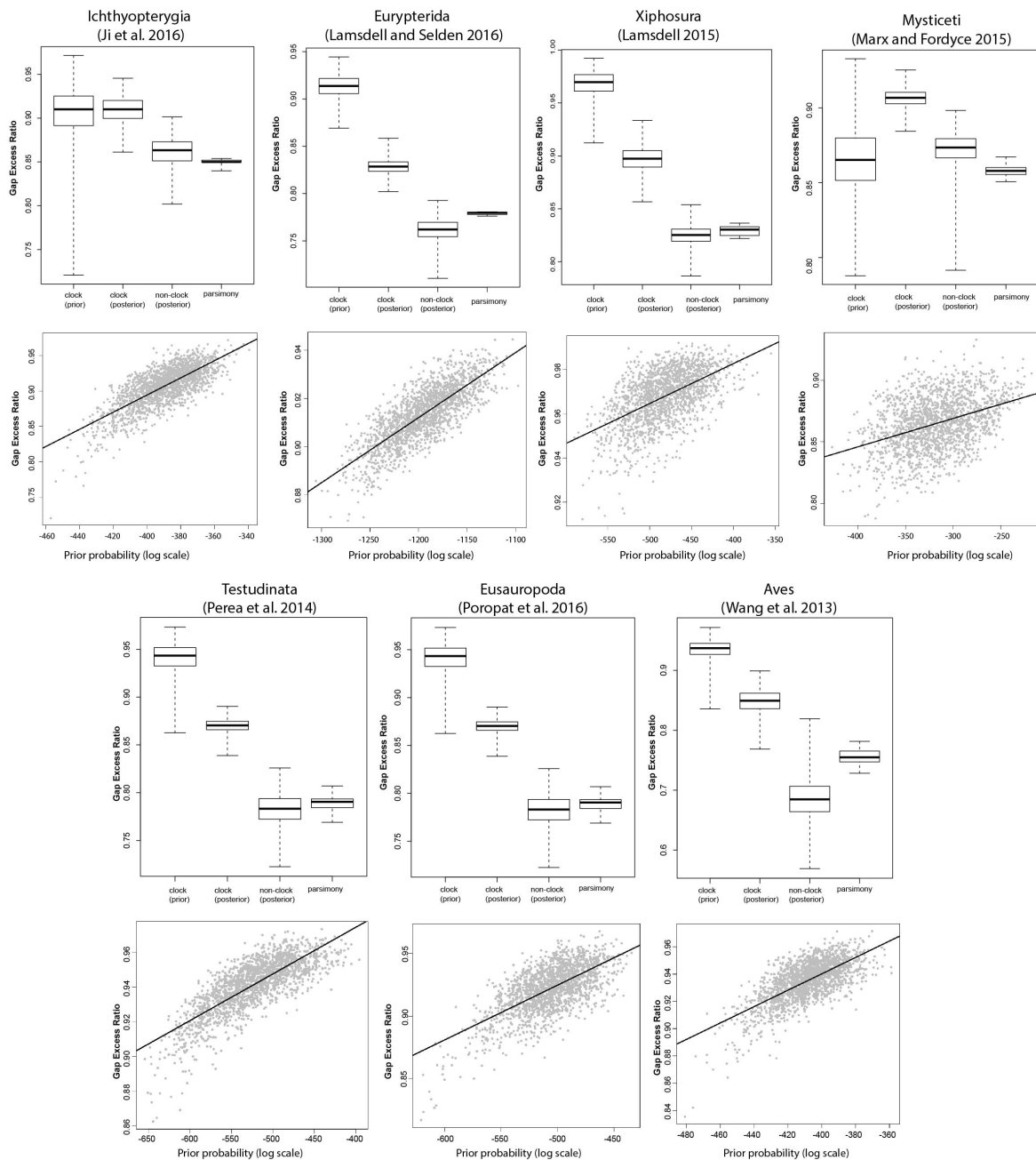


Figure 3. Bayesian tip-dating methods recover trees with better fit to stratigraphy than other methods. Upper panels: Gap Excess Ratio for every tree in each sample is shown as a box plot (whiskers span full range). Lower panels: A positive correlation exists between fit to stratigraphy and prior probability for every dataset (each data point represents a tree from the prior sample for tip-dating).

Effect of incomplete taxa

A feature of Bayesian analyses is that the prior is most important when data are weak, while strong data overwhelm the prior. Since tip-dating places a higher prior probability on trees with better fit to stratigraphy, it is reasonable to expect that this becomes most important in poorly resolved parts of

the phylogeny. Iterative deletion of incomplete taxa from the sauropods dataset supports the hypothesis that much of the difference in tree topology and stratigraphic fit between tip-dated and non-clock Bayesian methods are in parts of the phylogeny which cannot be resolved by the morphological data. With each successive deletion of incomplete taxa, the stratigraphic fit of trees from the non-clock Bayesian analyses increases, whereas the stratigraphic fit of the tree from tip-dating is essentially unchanged (Fig. 4A). Topological differences between the methods generally decline with each deletion (Fig. 4B). Random deletion of taxa does not lead to changes in stratigraphic fit for either method (Fig. 4C), and topological differences do not change (Fig. 4D). This shows that the observed patterns are due to the deletion of incomplete taxa, not merely a result of deletion of taxa in general. This suggests that tip-dated analyses constrain the phylogenetic position of incomplete taxa based on their stratigraphic age, leading to topological differences when compared to other methods.

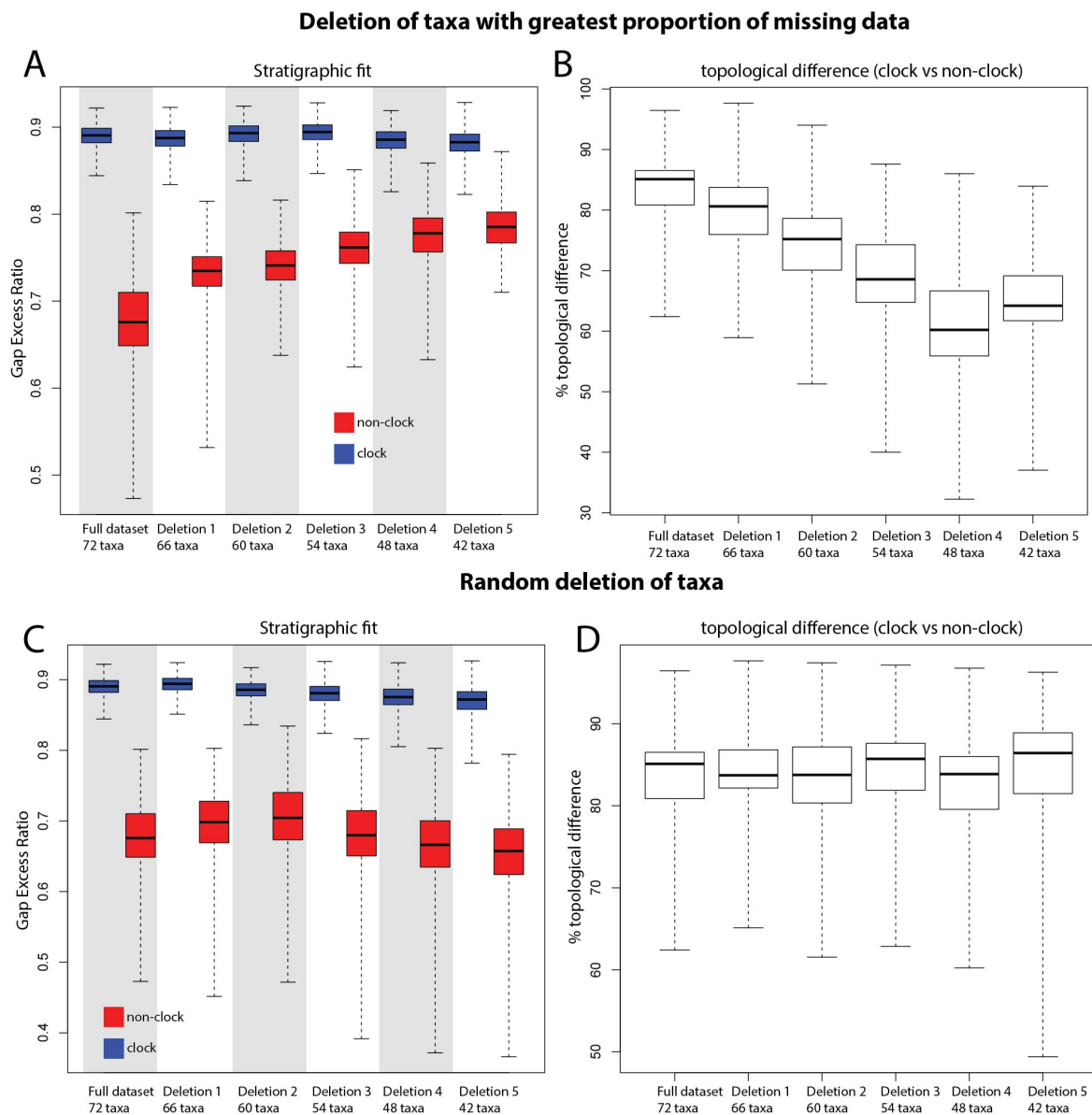


Figure 4. Differences between tip-dating and non-clock Bayesian methods in terms of topology and stratigraphic fit are concentrated in uncertain parts of the phylogeny.

This study utilises the sauropod dataset of Poropat et al. (2016). Successive deletion of the most incomplete taxa (top) leads to an increase in stratigraphic fit for non-clock analysis, but not tip-dating. Topological differences between these methods also successively decrease. Random deletion of taxa (bottom) shows that these patterns are not purely an artefact of fewer taxa.

Early osteichthyan phylogeny

The strict consensus tree from the parsimony analysis shows *Dialipina*, *Ligulalepis*, *Meemannia* and the *Guiyu* clade (*Guiyu*, *Psarolepis*, *Achoania*) in a polytomy with actinopterygians and

clade including *Ligulalepis*, *Meemannia*, *Dialipina* and actinopterygians is weak, but support for *Ligulalepis* as an actinopt disregarding the position of *Meemannia* and *Dialipina* is strong (see table 1). C) MCC tree from analysis without data, with tree topology constrained apart from 6 early osteichthyans (*Guiyu*, *Psarolepis*, *Achoania*, *Meemannia*, *Dialipina* and *Ligulalepis*). This reveals that a weak prior favouring an actinopterygian placement for most of these taxa.

taxon	posterior probability			prior probability		
	actinopt	sarcopt	stem	actinopt	sarcopt	stem
<i>Ligulalepis toombsi</i>	0.95	0.02	0.03	0.77	0.11	0.12
<i>Meemannia eos</i>	0.93	0.03	0.04	0.64	0.17	0.18
<i>Dialipina salgueiroensis</i>	0.81	0.05	0.14	0.76	0.12	0.12
<i>Achoania jarvikii</i>	0.11	0.72	0.17	0.64	0.18	0.19
<i>Psarolepis romeri</i>	0.11	0.72	0.17	0.58	0.21	0.21
<i>Guiyu oneiros</i>	0.11	0.72	0.17	0.32	0.25	0.44

Table 1. Probability of each of six taxa falling into one of three positions at the base of osteichthyans: either stem actinopterygian, stem sarcopterygian or stem osteichthyan. Left: The unconstrained tip-dating analysis. Right: analysis run without data, with topology constrained except the 6 taxa under investigation. Most taxa (apart from *Guiyu*) have a weak prior favouring an actinopt position. *Ligulalepis* is strongly supported as an actinopterygian in the posterior.

Discussion

The results show that parsimony and non-clock Bayesian analysis produce trees with similar topologies, as previously reported (Turner et al. 2017). Bayesian tip-dating approaches produce tree topologies that are more different from parsimony and non-clock Bayesian methods than either is to the other (Figs. 1-2). This suggests that the use of tip-dating and a serial-sampled tree prior has a greater effect on tree topology than the use of a model of morphological evolution, the latter also being used in non-clock Bayesian approaches that return trees very similar to parsimony .

The difference in tree topology appears to be driven by the effective prior probabilities placed on tree topologies in the tip-dating analysis. Tree topologies with a better stratigraphic fit are given a higher prior probability (Fig. 3). The stratigraphic fit of the posterior distribution of tree topologies is intermediate between the prior and the values from non-clock Bayesian and parsimony approaches (Fig. 3), reflecting the interplay of the prior and the evidence from the data.

In Bayesian analysis, the prior becomes more important when fewer data is available, so it might be predicted that the prior probabilities favouring trees with good fit to stratigraphy are most influential in weakly resolved parts of the tree. This was tested by successive deletion of the most incomplete taxa from the sauropods dataset (Fig. 4). As hypothesised, this led to successive increases in the stratigraphic fit of topologies estimated by non-clock Bayesian analyses, and a decrease in the topological differences between non-clock and tip-dating Bayesian approaches (over and above decreases observed when taxa were deleted randomly with respect to completeness). This suggests that much of the topological difference between tip-dating and other phylogenetic methods is driven by the placement of incomplete taxa. In other methods these incomplete taxa may fit into several positions on the tree even if these are incongruent with their stratigraphic age, but such unusual positions require stronger morphological evidence in the tip-dating approach. These results suggest that as morphological data improve, topologies recovered from non-clock Bayesian or parsimony approaches might become more similar to those produced by tip-dating. This is echoed in the results of Benton and Storrs (1994), which showed an increase in stratigraphic fit between phylogenies produced in 1967 and 1993.

Amongst the datasets investigated, stratigraphic fit measures are lowest in the eurypterid dataset, aligning with findings that stratigraphic fit for arthropod phylogenies are lower than for other groups (O'Connor and Wills 2016). The oldest eurypterid, *Pentecopterus*, is found in a deeply nested position in parsimony analysis (Lamsdell and Selden 2017), and this is retained in the tip-dating approach, showing that even highly stratigraphically incongruent topologies can still be recovered if

there is sufficient morphological evidence. Notably, the tip-dating analysis for eurypterids also estimated an ancient divergence date for eurypterids, more than 30 million years before the appearance of *Pentecopterus*. A younger divergence date would require extremely rapid divergences at the base of tree, violating the assumptions of constant diversification rates in the tree prior. It is probable that extreme heterogeneity in sampling or divergence dates contribute towards producing phylogenies incongruent with stratigraphy, rather than a poorly sampled fossil record *per se*, but further investigation is required to test this hypothesis.

Tip-dating methods provide moderate to strong support for *Ligulalepis* and *Meemannia* being actinopterygians, despite the parsimony analysis being unresolved (Fig. 5; Table 1). Running the analysis without data shows that there is a weak prior probability favouring an actinopterygian position. This is likely due to the presence of several taxa during the Early Devonian for which morphology supports sarcopterygian or stem osteichthyan position (e.g. *Styloichthys*, *Diabolepis*, *Youngolepis*, *Porolepis*, *Powichthys*, *Achoania*, *Psarolepis*). Not until *Cheirolepis trailli* in the Middle Devonian do well supported actinopterygians appear. There is therefore a long ghost lineage for actinopterygians, unless some of the uncertain taxa such as *Ligulalepis* and *Meemannia* are placed within actinopterygians. The prior therefore favours breaking up the long actinopterygian stem by placing these taxa as actinopterygians. It should be noted that this prior is only appropriate if assumptions of continuous sampling are met. Future work will need to address these questions, such the undersampling of sarcopterygians vs actinopterygians in this analysis.

However the prior probability that *Ligulalepis* is an actinopterygian is not strong, and cannot fully account for the strong support of *Ligulalepis* as an actinopterygian in the posterior. This might be explained by interaction with other taxa, particularly *Guiyu*, *Psarolepis* and *Achoania*. Scrutiny of the set of trees from the parsimony analysis shows that in the trees where *Ligulalepis* is found as a stem osteichthyan or sarcopterygian, it occurs below the *Guiyu* group. Since *Guiyu* is Silurian and *Ligulalepis* Emsian (approx. 24 Million years younger), this leads to stratigraphic incongruence.

Although the overall prior probability that *Ligulalepis* is an actinopterygian is not strong, only a subset of tree topologies is supported by the data: the subset of topologies supported by the data in which *Ligulalepis* is a stem osteichthyan is rejected by the prior but other possibilities for which *Ligulalepis* is a stem osteichthyan have a higher prior probability but are rejected by the data. Interaction of the tree prior and the data leads to fairly strong support for *Ligulalepis* as an actinopterygian in this instance.

These results support the view that inclusion of stratigraphic age data in tip-dated Bayesian phylogenetic analysis directly affects tree topology. Highly incomplete taxa are more constrained to positions congruent with stratigraphy in tip-dated analysis, even if the (limited) character data are also consistent with other, less stratigraphically congruent positions. Conversely, taxa for which abundant data are available can be placed in stratigraphically incongruent positions if there is sufficient character support. This is intuitive, and in some respect already resembles the approach informally taken by most palaeontologists: extraordinary claims require extraordinary evidence. Tip-dating is therefore a promising approach to elucidating not just macro-evolutionary patterns, but also evolutionary relationships.

References

- Alroy, J. (2002). Stratigraphy in phylogeny reconstruction—reply to Smith (2000). *Journal of Paleontology* **76**, 587–589.
- Bapst, D. W., Wright, A. M., Matzke, N. J. and Lloyd, G. T. (2016). Topology, divergence dates, and macroevolutionary inferences vary between different tip-dating approaches applied to fossil theropods (Dinosauria). *Biology Letters* **12**, 20160237.
- Bell, M. A. and Lloyd, G. T. (2015). strap: an R package for plotting phylogenies against stratigraphy and assessing their stratigraphic congruence. *Palaeontology* **58**, 379–389.
- Benton, M. J. and Storrs, G. W. (1994). Testing the quality of the fossil record: paleontological knowledge is improving. *Geology* **22**, 111–114.

- Benton, M. J., Wills, M. and Hitchin, R. (2000). Quality of the fossil record through time. *Nature* **403**, 534–537.
- Bouckaert, R., Heled, J., Kühnert, D., Vaughan, T., Wu, C.-H., Xie, D., Suchard, M. A., Rambaut, A. and Drummond, A. J. (2014). BEAST 2: a software platform for Bayesian evolutionary analysis. *PLoS Computational Biology* **10**, e1003537.
- Close, R. A., Friedman, M., Lloyd, G. T. and Benson, R. B. (2015). Evidence for a mid-Jurassic adaptive radiation in mammals. *Current Biology* **25**, 2137–2142.
- Close, R. A., Johanson, Z., Tyler, J. C., Harrington, R. C. and Friedman, M. (2016). Mosaicism in a new Eocene pufferfish highlights rapid morphological innovation near the origin of crown tetraodontiforms. *Palaeontology* **59**, 499–514.
- Drummond, A. J., Ho, S. Y., Phillips, M. J. and Rambaut, A. (2006). Relaxed phylogenetics and dating with confidence. *PLoS Biology* **4**, e88.
- Drummond, A. J. and Suchard, M. A. (2010). Bayesian random local clocks, or one rate to rule them all. *BMC biology* **8**, 114.
- Fisher, D. C. (2008). Stratocladistics: integrating temporal data and character data in phylogenetic inference. *Annual Review of Ecology, Evolution, and Systematics* **39**, 365–385.
- Friedman, M. (2007). *Styloichthys* as the oldest coelacanth: implications for early osteichthyan interrelationships. *Journal of Systematic Palaeontology* **5**, 289–343.
- Friedman, M. and Brazeau, M. D. (2010). A reappraisal of the origin and basal radiation of the Osteichthyes. *Journal of Vertebrate Paleontology* **30**, 36–56.
- Gavryushkina, A., Heath, T. A., Ksepka, D. T., Stadler, T., Welch, D. and Drummond, A. J. (2017). Bayesian total evidence dating reveals the recent crown radiation of penguins. *Systematic Biology* **66**, 57–73.
- Gavryushkina, A., Welch, D., Stadler, T. and Drummond, A. J. (2014). Bayesian inference of sampled ancestor trees for epidemiology and fossil calibration. *PLoS Computational Biology* **10**, e1003919.

- Geiger, D. L., Fitzhugh, K. and Thacker, C. E. (2001). Timeless characters: a response to Vermeij (1999). *Paleobiology* **27**, 177–178.
- Goloboff, P. A., Farris, J. S. and Nixon, K. C. (2008). TNT, a free program for phylogenetic analysis. *Cladistics* **24**, 774–786.
- Heath, T. A., Huelsenbeck, J. P. and Stadler, T. (2014). The fossilized birth–death process for coherent calibration of divergence-time estimates. *Proceedings of the National Academy of Sciences* **111**, E2957–E2966.
- Heyning, J. E. and Thacker, C. (1999). Phylogenies, temporal data, and negative evidence. *Science* **285**, 1179–1179.
- Huelsenbeck, J. P. (1994). Comparing the stratigraphic record to estimates of phylogeny. *Paleobiology* **20**, 470–483.
- Ji, C., Jiang, D.-Y., Motani, R., Rieppel, O., Hao, W.-C. and Sun, Z.-Y. (2016). Phylogeny of the Ichthyopterygia incorporating recent discoveries from South China. *Journal of Vertebrate Paleontology* **36**, e1025956.
- King, B., Qiao, T., Lee, M. S., Zhu, M. and Long, J. A. (2017). Bayesian Morphological Clock Methods Resurrect Placoderm Monophyly and Reveal Rapid Early Evolution in Jawed Vertebrates. *Systematic Biology* **66**, 499–516.
- Lamsdell, J. C. (2016). Horseshoe crab phylogeny and independent colonizations of fresh water: ecological invasion as a driver for morphological innovation. *Palaeontology* **59**, 181–194.
- Lamsdell, J. C. and Selden, P. A. (2017). From success to persistence: Identifying an evolutionary regime shift in the diverse Paleozoic aquatic arthropod group Eurypterida, driven by the Devonian biotic crisis. *Evolution* **71**, 95–110.
- Lee, M. S., Cau, A., Naish, D. and Dyke, G. J. (2014a). Dinosaur evolution. Sustained miniaturization and anatomical innovation in the dinosaurian ancestors of birds. *Science* **345**, 562–6.
- Lee, M. S. Y., Cau, A., Naish, D. and Dyke, G. J. (2014b). Morphological clocks in paleontology, and a mid-Cretaceous origin of crown Aves. *Systematic Biology* **63**, 442–449.

- Lewis, P. O. (2001). A likelihood approach to estimating phylogeny from discrete morphological character data. *Systematic Biology* **50**, 913–925.
- Lockwood, C. (1998). Stratigraphy and phylogeny. *Evolutionary Anthropology: Issues, News, and Reviews* **6**, 153–154.
- Lu, J., Giles, S., Friedman, M., den Blaauwen, J. L. and Zhu, M. (2016a). The oldest actinopterygian highlights the cryptic early history of the hyperdiverse ray-finned fishes. *Current Biology* **26**, 1602–1608.
- Lu, J., Zhu, M., Ahlberg, P. E., Qiao, T., Zhu, Y. a., Zhao, W. and Jia, L. (2016b). A Devonian predatory fish provides insights into the early evolution of modern sarcopterygians. *Science Advances* **2**, e1600154.
- Marx, F. G. and Fordyce, R. E. (2015). Baleen boom and bust: a synthesis of mysticete phylogeny, diversity and disparity. *Open Science* **2**, 140434.
- O'Connor, A. and Wills, M. A. (2016). Measuring Stratigraphic Congruence Across Trees, Higher Taxa, and Time. *Systematic Biology* **65**, 792–811.
- O'Reilly, J. E., Puttick, M. N., Parry, L., Tanner, A. R., Tarver, J. E., Fleming, J., Pisani, D. and Donoghue, P. C. (2016). Bayesian methods outperform parsimony but at the expense of precision in the estimation of phylogeny from discrete morphological data. *Biology Letters* **12**, 20160081.
- Paradis, E., Claude, J. and Strimmer, K. (2004). APE: analyses of phylogenetics and evolution in R language. *Bioinformatics* **20**, 289–290.
- Perea, D., Soto, M., Sterli, J., Mesa, V., Toriño, P., Roland, G. and Da Silva, J. (2014). *Tacuarembemys kusteriae*, gen. et sp. nov., a new late Jurassic—? earliest Cretaceous continental turtle from western Gondwana. *Journal of Vertebrate Paleontology* **34**, 1329–1341.
- Poropat, S. F., Mannion, P. D., Upchurch, P., Hocknull, S. A., Kear, B. P., Kundrát, M., Tischler, T. R., Sloan, T., Sinapius, G. H. and Elliott, J. A. (2016). New Australian sauropods shed light on Cretaceous dinosaur palaeobiogeography. *Scientific reports* **6**.

- Qiao, T., King, B., Long, J. A., Ahlberg, P. E. and Zhu, M. (2016). Early gnathostome phylogeny revisited: multiple method consensus. *PloS one* **11**, e0163157.
- Rambaut, A., Suchard, M. A., Xie, D. and Drummond, A. J. (2014). Tracer v1.6, Available from <http://beast.bio.ed.ac.uk/Tracer>.
- Revell, L. J. (2012). phytools: an R package for phylogenetic comparative biology (and other things). *Methods in Ecology and Evolution* **3**, 217–223.
- Robinson, D. F. and Foulds, L. R. (1981). Comparison of phylogenetic trees. *Mathematical Biosciences* **53**, 131–147.
- Ronquist, F., Klopfstein, S., Vilhelmsen, L., Schulmeister, S., Murray, D. L. and Rasnitsyn, A. P. (2012a). A total-evidence approach to dating with fossils, applied to the early radiation of the Hymenoptera. *Systematic Biology* **61**, 973–999.
- Ronquist, F., Teslenko, M., van der Mark, P., Ayres, D. L., Darling, A., Höhna, S., Larget, B., Liu, L., Suchard, M. A. and Huelsenbeck, J. P. (2012b). MrBayes 3.2: efficient Bayesian phylogenetic inference and model choice across a large model space. *Systematic Biology* **61**, 539–542.
- Schliep, K. P. (2010). phangorn: phylogenetic analysis in R. *Bioinformatics*, btq706.
- Siddall, M. E. (1998). Forum. stratigraphic fit to phylogenies: a proposed solution. *Cladistics* **14**, 201–208.
- Smith, A. (1998). Is the fossil record adequate. *Nature online debates* (ed. AB Smith).
- Stadler, T. (2010). Sampling-through-time in birth–death trees. *Journal of Theoretical Biology* **267**, 396–404.
- Turner, A. H., Pritchard, A. C. and Matzke, N. J. (2017). Empirical and Bayesian approaches to fossil-only divergence times: A study across three reptile clades. *PloS one* **12**, e0169885.
- Wagner, P. J. (1995). Stratigraphic tests of cladistic hypotheses. *Paleobiology* **21**, 153–178.
- Wang, M., Zheng, X., O'Connor, J. K., Lloyd, G. T., Wang, X., Wang, Y., Zhang, X. and Zhou, Z. (2015). The oldest record of Ornithuomorpha from the early cretaceous of China. *Nature Communications* **6**, 6987.

Wills, M. A. (1999). Congruence between phylogeny and stratigraphy: randomization tests and the gap excess ratio. *Systematic Biology* **48**, 559–580.

Wright, A. M. and Hillis, D. M. (2014). Bayesian analysis using a simple likelihood model outperforms parsimony for estimation of phylogeny from discrete morphological data. *PloS one* **9**, e109210.

Chapter 7

General Discussion

This discussion draws together the major themes of this thesis, which seeks to gain a better understanding of the early evolution of jawed vertebrates. The phylogeny of early vertebrates forms a vital backbone on which inferences of character evolution are based. Two key phylogenetic problems are discussed: the relationships of the placoderms and the relationships of the early osteichthyans. These problems are in some ways similar; difficulties stem from a lack of character polarity and uncertainty regarding outgroups. In this thesis I have attempted to gain insight into these problems through the application of tip-dated Bayesian phylogenetic analysis. This work has implications for the use of competing phylogenetic methods more generally. Finally, the CT scan studies in this thesis have revealed interesting features of the electroreceptor and mechanoreceptor systems of early gnathostome fossils. The potential for further such studies to provide insights into the ecology and behaviour of the earliest gnathostomes is discussed here.

Are placoderms monophyletic or paraphyletic?

Chapter 3 “resurrects” the hypothesis that placoderms form a monophyletic group. This was previously advocated (Goujet 1982; Goujet 1984; Goujet 2001), but placoderms have been considered paraphyletic following the first cladistic analyses that explicitly tested placoderm monophyly (Friedman 2007; Brazeau 2009; Davis et al. 2012; Zhu et al. 2013; Brazeau and Friedman 2014; Dupret et al. 2014; Brazeau and de Winter 2015; Giles et al. 2015b; Long et al. 2015; Zhu et al.

2016). Chapter 3 does not resurrect previous morphological arguments for placoderm monophyly; instead placoderm monophyly is supported by alternative methodology (tip-dating). None of the expanded list of placoderm synapomorphies listed by Young (2010), are found to support placoderm monophyly in chapter 3, although most are not included in the matrix in the same form due to problems with character formulation (Brazeau and Friedman 2014). Of the characters listed in chapter 3 as supporting monophyly, only “paired occipital facets” was previously used in this regard, forming half of the second character listed by Goujet (1982).

Chapter 3 does not represent the final word regarding placoderm relationships, and caution is particularly advised given that tip-dating is a relatively new and unexplored methodology. Chapter 3 includes errors, including coding mistakes, some of which have been corrected in chapter 6. Presence of a synarcual is erroneously listed as a potential synapomorphy of placoderms despite being coded as unknown in all the outgroups in the final version of the matrix (but the reported tree lengths are correct). In addition, some codings from *Wuttagoonaspis* were erroneously scored from incorrect specimens (although the characters are also present in the correct specimens). The justification for the sampling rate prior in the Bayesian analysis is incorrect. None of these errors appear to affect the main result however, that placoderm monophyly is strongly supported under a tip-dating approach.

Whilst chapter 3 discusses problems with the characters supporting placoderm paraphyly, the characters listed as potential placoderm synapomorphies are not without problems of their own. The presence of claspers is perhaps the strongest evidence for placoderm monophyly, but they are unknown in two placoderm groups, the petalichthyids and the acanthothoracids. Claspers are also a difficult character to score as absent. Although present in the antiarch *Microbrachius* (Long et al. 2015), they are unknown in other antiarchs such as *Bothriolepis* despite the availability of thousands of specimens. Internal fertilisation was inferred in *Bothriolepis* based on the presence of pelvic plates in presumed females, and it was suggested that their claspers were entirely cartilaginous (Long et al.

2015), based partly on the absence of vertebral ossifications in antiarchs. However, the same argument about cartilaginous claspers could potentially apply to all other gnathostome fossils. Claspers are also unknown in the petalichthyid *Lunaspis* despite the presence of articulated specimens.

A second character supporting monophyly that may be problematic is the optic fissure. This is unknown in *Macropetalichthys* (Stensiö 1969) and arguably should be coded as absent. Evidence for an optic fissure in the rhenanid placoderm *Jagorina* and the antiarch *Bothriolepis* is not definitive (Young 1984; Young 1986).

There remain some arguments from morphology that placoderms are paraphyletic. Brazeau and Friedman (2014) argued that the presence of a utricular recess unites a subset of placoderms with crown gnathostomes. A utricular recess is absent in osteostracans, galeaspids and the placoderm *Brindabellaspis* (Young 1980; Janvier 1985; Gai et al. 2011). A utricular recess appears to be absent or indistinct in *Romundina* (Dupret et al. 2017), despite their puzzling identification of a “common recess for the anterior and external utriculi”. The utricular recess character has yet to be included in any phylogenetic analysis of early gnathostomes, but whether or not it should is a matter for debate. In the living jawless fishes there is a single “macula communis” and no differentiation into a separate saccule, lagena and utricle (Sienknecht 2013). The absence of a utricular recess is therefore not strictly comparable between living agnathans and gnathostomes. However, in fossils it is difficult to ascertain whether or not differentiated maculae are present when a utricular recess is absent. For example, a differentiated utriculus, saccule and lagena occur in the living coelacanth, which lacks a utricular recess (Duncan and Fritzsche 2012).

Another argument for placoderm paraphyly is that some placoderms possess an upper lip analogous to the upper lip of living lampreys and hagfishes (Dupret et al. 2014; Dupret et al. 2017). In gnathostomes, trabeculae cranii are a pair of cartilaginous rods that develop into the base of the anterior part of the braincase. Acanthothoracid placoderms such as *Romundina* have an extended

trabecular region of the braincase that extends far anterior to the orbits and nasal capsules (Dupret et al. 2014). The trabeculae of gnathostomes and the cartilages of the upper lip in lampreys derive from premandibular ectomesenchyme (Kuratani 2012). The dimensions of the trabecular region in *Romundina* were compared to the dimensions of the upper lip in agnathans (Dupret et al. 2014) and a hypothesis about the development of the gnathostome face was formed, specifically that the degree of proliferation of premandibular ectomesenchyme was unchanged through the origin of jaws.

This hypothesis cannot provide independent evidence for placoderm paraphyly however, as it cannot be converted into robust phylogenetic characters. One possible way of including it in a phylogenetic data matrix would be to code the extent of the trabecular region. However, the only known jawless vertebrate with a possible trabecula is the galeaspid *Shuyu*, where it takes the form of a small ethmoid rod between the nasal sacs (Gai et al. 2011). An alternative would be to introduce a character along the lines of “extent of region that develops from premandibular ectomesenchyme”, but this is necessarily vague and would not be possible to quantify (it also assumes that expansion of the trabecular region must occur in tandem with a reduction of the upper lip). Finally, new information on *Brindabellaspis* (chapter 4) shows a trabecular region that is even more extensive than *Romundina*, disrupting the elegant pattern presented by Dupret et al. (2014).

Dorsal nasal capsules is another character that supports placoderm paraphyly (Brazeau and Friedman 2014; Dupret et al. 2014). However, impressions on the internal headshield of heterostracans reveal paired nasal sacs anterior to the orbits (Janvier 1996). Heterostracans are not included as outgroups in phylogenetic analyses of early gnathostomes; the lack of preservation of the neurocranium precludes scoring of most characters. Heterostracans might however be informative about the plesiomorphic condition of the nasal capsules in gnathostomes.

Untangling early osteichthyan phylogeny

Chapter 5 presents abundant new information on *Ligulalepis*, a taxon first described from scales (Schultze 1968) and then a skull informally assigned to the same taxon (Basden et al. 2000; Basden and Young 2001). However, chapter 5 still fails to fully resolve its phylogenetic position, which has been controversial (Basden et al. 2000; Basden and Young 2001; Zhu et al. 2009; Friedman and Brazeau 2010). Further information on “*Ligulalepis*” may be difficult to produce, due to the disarticulated nature of the fossils from Taemas-Wee Jasper. Tip-dating analysis however places “*Ligulalepis*” as an actinopterygian with fairly strong support (see Chapter 6). Further progress on the phylogenetic position of *Ligulalepis*, and the problem of early osteichthyan evolution in general, might have to come from studies of taxa other than *Ligulalepis*. How then can further progress be made in studies of osteichthyan origins?

“*Ligulalepis*” is now unique amongst early osteichthyan fossils in that two skulls (one of which is newly discovered and described in this thesis) have been CT scanned and segmented. This has revealed intraspecific variation, notably in the lateral cranial canal, but also in details of the sensory canals. Scanning of multiple specimens of other early osteichthyan taxa may reveal which features are most reliable for phylogenetic analysis.

Chapter 5 also revealed that the phylogenetic positions of the various early osteichthyan taxa are somewhat interdependent. For example, “*Ligulalepis*” and the *Guiyu* clade tend to oscillate between the stem and crown of osteichthyans together. Further investigations of new and existing specimens of other early osteichthyan species will also be informative regarding “*Ligulalepis*”.

Dialipina salgueiroensis (Schultze 1968; Schultze and Cumbaa 2001) is recovered as the sister group to other osteichthyans in the phylogenetic analysis presented in chapter 5. However, *D. salgueiroensis* has yet to be fully described and additional material exists (pers. comm., Hans-Peter Schultze). Redescription of another “*Dialipina*” species, *Dialipina markae* (now renamed as

Janusiscus schultzei) revealed unexpected features that led to it being placed on the gnathostome stem, outside osteichthyans (Giles et al. 2015b). Redescription of *Dialipina salgueiroensis* may reveal similar surprises.

The current position of *Dialipina* at the base of osteichthyans affects the polarity of some characters, and therefore redescription of *Dialipina* may have implications for all early osteichthyans. For example, *Dialipina* affects the polarity of scale characters: its actinopt-like scales tend to push the *Guiyu* group (with their sarcopt-like scales) towards sarcopterygians, although this is in conflict with other characters. However, the plesiomorphic state for osteichthyan scales is still very much unknown. Several Silurian taxa are known from isolated scales, including *Ligulalepis yunnanensis* (Wang and Dong 1989) which has actinopt-like characters (a narrow scale peg and an antero-dorsal process). Other fragmentary Silurian taxa (e.g. *Lophosteus*, *Andreolepis*, *Naxilepis*) were hypothesised to be stem osteichthyans, based on their lack of a peg-and-socket articulation (Friedman and Brazeau 2010). However, some scales attributed to *Andreolepis* are now known to have a scale peg (Chen et al. 2012). Scales from articulated crown osteichthyans can have hugely variable morphology depending which part of the body they come from (Trinajstić 1999), with those from the caudal fin lacking a peg-and-socket articulation. It is therefore difficult to study isolated scales, and it is possible, for example, that scales attributed to *Ligulalepis yunnanensis* and *Naxilepis* are from the same or similar species. Detailed studies of scale characters, incorporating variability in scale morphology within taxa, is another way in which progress could be made regarding the resolution of osteichthyan phylogeny.

Further progress in studying osteichthyan origins can also be made by more detailed examinations of endocranial characters through the use of CT scanning. Incorporating this information into phylogenetic datasets would be significantly aided by the release of raw scan data when descriptions of individual taxa are published. There is a movement in palaeontology towards the free sharing of CT scan data (Davies et al. 2017), but scan data has not been released alongside most of the key

publications featuring CT scan investigations of early osteichthyan braincases (Giles and Friedman 2014; Giles et al. 2015a; Lu et al. 2016a; Lu et al. 2016b).

Tip-dating methods: assumptions and problems

Tip-dating, or Bayesian morphological clock methods, are explored in chapters 3 and 6 of this thesis. These chapters revealed how tip-dating methods can affect the recovery of evolutionary relationships, by balancing the pattern of evolutionary rates (chapter 3), and by producing trees with superior stratigraphic fit compared to other methods (chapter 6). This raises the obvious question, should tip-dating methods be more widely used by palaeontologists?

Tip-dating is an extension of Bayesian and likelihood methods of phylogenetic inference, which are parametric methods, in contrast to parsimony methods which are non-parametric (Sanderson and Kim 2000). As with all parametric methods, tip-dating methods make assumptions, and use of these methods may lead to incorrect results if these assumptions are violated. For example, Bayesian and likelihood methods have been shown to converge on an incorrect solution in simulation studies when evolutionary rates are strongly heterogeneous (Kolaczkowski and Thornton 2004). In addition, large differences in length between adjacent branches can distort the results of maximum likelihood analysis (Kück et al. 2012).

Parameters that allow rate heterogeneity to be estimated during phylogenetic analysis have gradually been incorporated into parametric methods, for example by including a gamma parameter to account for among-character rate variation (Yang 1996), or relaxed molecular clocks to account for among-lineage rate variation (Drummond et al. 2006). Parsimony on the other hand is equivalent to a highly parameterised model with a separate rate parameter for every character for every branch (Tuffley and Steel 1997). Introduction of new parameters to account for rate variation, such as the use of multiple morphological clocks (Lee 2016), in some sense moves parametric methods back towards parsimony (Goloboff et al. 2017). However, this does not necessarily mean that

parametric methods should be abandoned in favour of parsimony. For example King and Lee (2015) showed, in an analysis of viviparity in squamates, that likelihood models of ancestral state reconstruction which did not incorporate rate heterogeneity were misled. Although parsimony produced more sensible results, model-based methods with a degree of rate heterogeneity included still produced results that were different from parsimony in some respects; the main difference occurred in a clade (skinks) with high rates of parity mode evolution. Therefore, adding enough additional parameters to gain a greater degree of “biological realism”, justified by model testing, does not necessarily amount to a return to parsimony.

The advent of tip-dating methods (Ronquist et al. 2012) has introduced more tree parameters that are assumed to be approximately constant (Stadler 2010). Specifically, these parameters are speciation, extinction and sampling. Results of tip-dating analysis might be misled when these assumptions are violated. However, it is often difficult to determine to what extent these assumptions have been violated. For example, if a clade has a long ghost lineage (relative to its sister group), this could be because of lower speciation or sampling rates, but could also be because it actually nests *within* the proposed sister group (i.e. rates of speciation and sampling might in fact be approximately constant and the inferred extended ghost lineage symptomatic of an incorrect topology). However, it is clear from looking at modern taxa that rates of either speciation or extinction can be strongly heterogeneous, as seen by the many cases in which a small number of species form the sister group to a large clade. Clear cases of sampling rate heterogeneity are more difficult to pinpoint, but such heterogeneity can be expected to occur following major shifts in habitat or geographical range, or Lagerstätten (see below).

A common criticism of the use of stratigraphic ages in phylogenetic analysis is that the fossil record is too incomplete. However, a poorly but homogeneously sampled fossil record (which is likely to be common) is itself not necessarily an issue for tip-dated analysis. Sampling rate is estimated as part of the model (Stadler 2010), and low sampling rates should be manifested as a decrease in the

precision (but not necessarily the accuracy) of estimates of topology and divergence dates. Rather, it is heterogeneous sampling (including user-imposed sampling) that will cause problems for tip-dating.

Another problem for tip-dating methods is that sampling is not independent. In most phylogenetic analyses involving fossils, some fossil sites will provide multiple specimens. This Lagerstätten effect is particularly obvious in early vertebrates. For example, the dataset in chapter 3 has many Early Devonian acanthodians, but these mainly come from two fossil sites: Man On The Hill (MOTH) in Canada and Tillywhandland in Scotland. Furthermore, these sites are unusual in preserving almost exclusively acanthodians (Brazeau and Friedman 2015). The bias is inflated by the quality of preservation, as these sites preserve some of the most informative specimens of acanthodians, so they are more likely to be incorporated into data matrices than fossils from other sites. This concentration of Early Devonian acanthodians might bias results, for example by artificially pushing divergence dates back in time. Indeed, even when tip-dating was in its infancy, it was suggested that a model of random sampling of existing lineages at time-points representing fossil sites would be superior to serial sampling (Ronquist et al. 2012).

As mentioned before, chapter 3 proposes that placoderms in fact formed a monophyletic group. This is strongly supported in the Bayesian tip-dated analysis, despite the list of potential synapomorphies supporting placoderm monophyly and placoderm paraphyly being essentially of similar length. The different topology essentially amounts to a “clock rooting” of the tree (Huelsenbeck et al. 2002), balancing the inferred rates of evolution. Clock-rooting is in some sense analogous to phenetics. Indeed, Hennig (1966) noted that variations in evolutionary rates is a major reason for the superiority of cladistics over other methods. If evolution occurred according to a strict clock, phenetic clustering would essentially be accurate (as long as all taxa are the same age). However this does not mean that tip-dating is the same as phenetic clustering. First, a relaxed clock is almost always used, allowing some rate heterogeneity. Second, the balancing of evolutionary rates at the base of the tree chooses between two phylogenetic hypotheses (placoderm paraphyly and

monophyly) that have essentially an equal number of characters supporting them; the unrooted tree topology is still a cladistic, not a phenetic, topology.

Comparisons of different phylogenetic methods applied to morphology

The recent literature has seen a number of high profile papers advocating the use of parametric methods over parsimony following simulation studies (Wright and Hillis 2014; O'Reilly et al. 2016; Puttick et al. 2017), although none of these look at tip-dating methods. Two of these (O'Reilly et al. 2016; Puttick et al. 2017) advocate the use of Bayesian methods as they produce consensus trees that are less resolved than trees from other methods, thus recovering fewer incorrect nodes.

However, this approach has been criticised because the degree of resolution largely concerns tree summary methods (Brown et al. 2017; Goloboff et al. 2017). Exploring the accuracy of every sampled tree in a posterior sample would provide a better picture of the innate accuracy of methods, especially since a limited amount of topology difference amongst trees in a sample can lead to large polytomies in a consensus tree. In addition, there are ways of reducing the resolution of trees from competing methods, for example a parsimony bootstrap consensus tree could be used instead of a strict consensus. On the other hand, simulation studies which do not make the assumption that branch lengths are shared across all characters suggest that weighted parsimony outperforms all other methods (Goloboff et al. 2017). The latter study may not have implemented a gamma parameter during the Bayesian analysis (it is not discussed in the paper). The gamma parameter in model-based methods performs a similar function to implied weighting in parsimony analysis, accounting for rate variation across characters.

O'Reilly et al. (2016) and Puttick et al. (2017) find that trees resulting from Bayesian analysis are typically less resolved than other methods, and this is also found in chapter 5. However, there exist cases in which Bayesian analysis (without tip-dating) strongly support resolved topologies that are either not found in parsimony analysis, or are equally parsimonious. For the dataset presented in

chapter 3, tip-dating supports placoderm monophyly, while placoderm paraphyly is one step longer under parsimony. However, non-clock Bayesian analysis strongly supports placoderm paraphyly; this result was not included in chapter 3 as a satisfactory explanation for the difference could not be found. Another example is the Bayesian analysis in chapter 5, in which the *Guiyu* group are strongly supported as sarcopterygians, despite this topology being less parsimonious than a stem position for the *Guiyu* group. These differences cannot be explained merely as differences in resolution.

The occasional strongly supported node notwithstanding, the results of chapter 6 show that there is often not a lot of difference in topology between Bayesian (non-clock) and parsimony methods. In addition, there is no clear difference between these methods in terms of stratigraphic fit, which perhaps the most easily quantifiable independent indication of the accuracy of phylogenetic trees of fossil taxa. However, these results are from a limited number of datasets, and further exploration is required.

On the other hand, chapters 3 and 6 show that tip-dating can have significant (and explainable) effects on tree topology. Although use of stratigraphic ages in phylogenetic inference has been controversial, tip-dating, through the use of priors, establishes good stratigraphic fit and balanced evolutionary rates as a default position, requiring hard evidence from morphology to be overturned. This is a sensible and intuitive approach, as it precludes retrieving outrageous hypotheses when only a small amount of evidence exists. I conclude that tip-dating is a methodology that will be useful for many palaeontologists attempting to reconstruct the tree of life.

Vertebrate laterosensory systems, an underutilised source of information?

This thesis has revealed interesting features of the lateral line system in early vertebrate fossils.

Chapter 4 shows that the placoderm *Brindabellaspis* had a unique specialisation of the lateral line system: the ethmoid commissure has doubled back on itself and fused into a midline canal. Chapter 5 also examined the lateral line system of *Ligulalepis*. The supraorbital canals of *Ligulalepis* have the

appearance of two separate canals that join together end to end. This is particularly interesting because *Ligulalepis* has no anterior pit-line, which is confluent with the supraorbital canal in some early actinopterygians (Gardiner 1984). CT scans of other early vertebrates will surely reveal other interesting features of lateral line systems. This may provide characters for phylogenetic analysis, as well as inform reconstructions of behaviour and ecology.

The cranial lateral line canals of living species show great variation in morphology (Coombs et al. 1988; Webb 1989; Webb 2013). Widened canals, for example, have evolved in a number of groups, and commonly occur in species living in deep water, low light, or relatively still water conditions (Marshall 1971). Widened canals often function in prey detection (Schwalbe et al. 2012; Webb 2013). They can have extremely wide pores, and the external part of the canal is often covered by soft tissue, with bony struts only in the vicinity of the neuromasts (Coombs et al. 1988). The soft tissue covering the rest of the canals functions as a tympanum, with resonance properties conferring acute sensitivity to vibrations of a particular frequency (Denton and Gray 1988). Another morphological variation is the degree of branching of the tubuli connecting the canals to the exterior, and the area which the external pores cover. Widely spaced pores are thought to be an adaptation to turbulent conditions, by increasing the signal to noise ratio (Klein et al. 2013; Klein and Bleckmann 2015).

Studying morphological variation in lateral line systems in early vertebrate fossils might therefore be a productive avenue for understanding the ecology of ancient ecosystems. For example, many early coelacanths had relatively large openings for the supraorbital sensory canal (Forey 1998). Some early lungfish, such as the lungfish *Dipterus* and the tetrapodomorph *Megalichthys* had highly branched tubuli leading to many widely spaced pores (Ørvig 1961; Bjerring 1972).

As shown in chapter 2, “pore-group” pits on the skulls of fossil sarcopterygians possess features consistent with their identification as electroreceptors. Together with lateral line morphology, this can inform hypotheses about the ecological function of fossil fish. For example, the high density of electroreceptors on the snouts of fossil lungfish suggests this sense was highly important for early

lungfish, possibly functioning in the capture of hidden prey. The wide lateral line canals of some early coelacanth suggest they may have lived in relatively deep-water environments. Combined with the presence of a rostral organ, this suggests the ecology of early coelacanth may not have been too dissimilar from the extant *Latimeria*.

Future research

It is hard to envisage the phylogeny of early gnathostomes being fully resolved based purely on the current set of known fossils. The gap between the nearest outgroup, osteostracans, and early gnathostomes is too wide, making inferences of the plesiomorphic state for gnathostomes problematic. Although tip-dating methods appear to provide some insight into the problem (Chapter 3), it cannot fully resolve the problem with a high degree of certainty. There is of course still great potential for new fossil finds to improve our understanding of early gnathostome evolution.

CT scanning is now becoming standard practice in studies of early vertebrate fossils. In the future, CT studies of a wide variety of early vertebrates will be available, producing new characters, and characters that are currently known only in a handful of taxa will be more widely known and informative. It will also be possible to study evolutionary trends for example in the lateral line system. New detailed data from synchrotron scanning can also be incorporated in phylogenetic analysis. For example, histological characters used in current character matrices of early vertebrates are few in number and highly simplified. New data (e.g. Qu et al. 2017) will allow more specific characters (with improved hypotheses of primary homology) to be added.

Developments to methods of phylogenetic inference will also be important. One useful advance would be the introduction of a dynamic homology approach, which would account for uncertainty in assigning homologies (Ramírez 2007). The body plans of early gnathostome groups are so different that establishing homology is a difficult task. For example, there is uncertainty about the homology of placoderm tooth plates (Zhu et al. 2016), and a computational approach has been used before to

analyse the homologies of porolepiform and osteolepiform skull roof bones (Jardine 1969). Other improvements to the models used in tip-dating analysis, such as accounting for rate heterogeneity in diversification or sampling rates, will also refine results.

References

- Basden, A. M. and Young, G. C. (2001). A primitive actinopterygian neurocranium from the Early Devonian of southeastern Australia. *Journal of Vertebrate Paleontology* **21**, 754–766.
- Basden, A. M., Young, G. C., Coates, M. I. and Ritchie, A. (2000). The most primitive osteichthyan braincase? *Nature* **403**, 185–188.
- Bjerring, H. C. (1972). Morphological observations on the exoskeletal skull roof of an osteolepiform from the Carboniferous of Scotland. *Acta Zoologica* **53**, 73–92.
- Brazeau, M. D. (2009). The braincase and jaws of a Devonian ‘acanthodian’ and modern gnathostome origins. *Nature* **457**, 305–308.
- Brazeau, M. D. and de Winter, V. (2015). The hyoid arch and braincase anatomy of *Acanthodes* support chondrichthyan affinity of ‘acanthodians’. *Proceedings of the Royal Society B* **282**, 20152210.
- Brazeau, M. D. and Friedman, M. (2014). The characters of Palaeozoic jawed vertebrates. *Zoological Journal of the Linnean Society* **170**, 779–821.
- Brazeau, M. D. and Friedman, M. (2015). The origin and early phylogenetic history of jawed vertebrates. *Nature* **520**, 490–497.
- Brown, J. W., Parins-Fukuchi, C., Stull, G. W., Vargas, O. M. and Smith, S. A. (2017). Bayesian and likelihood phylogenetic reconstructions of morphological traits are not discordant when taking uncertainty into consideration: a comment on Puttick et al. *Proceedings of the Royal Society B* **284**, 20170986.

- Chen, D., Janvier, P., Ahlberg, P. E. and Blom, H. (2012). Scale morphology and squamation of the Late Silurian osteichthyan *Andreolepis* from Gotland, Sweden. *Historical Biology* **24**, 411–423.
- Coombs, S., Janssen, J. and Webb, J. F. (1988). Diversity of lateral line systems: evolutionary and functional considerations. In *Sensory biology of aquatic animals* (ed. Atema, R. R. Fay, A. N. Popper and W. N. Tavolga), pp. 553–593. Springer, New York.
- Davies, T. G., Rahman, I. A., Lautenschlager, S., Cunningham, J. A., Asher, R. J., Barrett, P. M., Bates, K. T., Bengtson, S., Benson, R. B. and Boyer, D. M. (2017). Open data and digital morphology. In *Proceedings of the Royal Society B*, vol. 284, pp. 20170194. The Royal Society.
- Davis, S. P., Finarelli, J. A. and Coates, M. I. (2012). *Acanthodes* and shark-like conditions in the last common ancestor of modern gnathostomes. *Nature* **486**, 247–250.
- Denton, E. J. and Gray, J. A. B. (1988). Mechanical factors in the excitation of the lateral lines of fishes. In *Sensory biology of aquatic animals* (ed. J. Atema, R. R. Fay, A. N. Popper and W. N. Tavolga), pp. 595–617. Springer, New York.
- Drummond, A. J., Ho, S. Y., Phillips, M. J. and Rambaut, A. (2006). Relaxed phylogenetics and dating with confidence. *PLoS Biology* **4**, e88.
- Duncan, J. S. and Fritzsche, B. (2012). Transforming the vestibular system one molecule at a time: the molecular and developmental basis of vertebrate auditory evolution. In *Sensing in Nature* (ed. C. Köppl, G. A. Manley, A. N. Popper and R. R. Fay), pp. 173–186. Springer, New York.
- Dupret, V., Sanchez, S., Goujet, D. and Ahlberg, P. (2017). The internal cranial anatomy of *Romundina stellina* Ørvig, 1975 (Vertebrata, Placodermi, Acanthothoraci) and the origin of jawed vertebrates—Anatomical atlas of a primitive gnathostome. *PloS one* **12**, e0171241.
- Dupret, V., Sanchez, S., Goujet, D., Tafforeau, P. and Ahlberg, P. E. (2014). A primitive placoderm sheds light on the origin of the jawed vertebrate face. *Nature* **507**, 500–503.
- Forey, P. L. (1998). *History of the Coelacanth Fishes*. Chapman and Hall, London.
- Friedman, M. (2007). *Styloichthys* as the oldest coelacanth: implications for early osteichthyan interrelationships. *Journal of Systematic Palaeontology* **5**, 289–343.

- Friedman, M. and Brazeau, M. D. (2010). A reappraisal of the origin and basal radiation of the Osteichthyes. *Journal of Vertebrate Paleontology* **30**, 36–56.
- Gai, Z., Donoghue, P. C., Zhu, M., Janvier, P. and Stampanoni, M. (2011). Fossil jawless fish from China foreshadows early jawed vertebrate anatomy. *Nature* **476**, 324–327.
- Gardiner, B. G. (1984). The relationships of the paleoniscid fishes. a review based on new specimens of *Mimia* and *Moythomasia* from the upper Devonian of Western Australia. *Bulletin of the British Museum (Natural History) Geology* **37**, 173–248.
- Giles, S., Coates, M. I., Garwood, R. J., Brazeau, M. D., Atwood, R., Johanson, Z. and Friedman, M. (2015a). Endoskeletal structure in *Cheirolepis* (Osteichthyes, Actinopterygii), An early ray-finned fish. *Palaeontology* **58**, 849–870.
- Giles, S. and Friedman, M. (2014). Virtual reconstruction of endocast anatomy in early ray-finned fishes (Osteichthyes, Actinopterygii). *Journal of Paleontology* **88**, 636–651.
- Giles, S., Friedman, M. and Brazeau, M. D. (2015b). Osteichthyan-like cranial conditions in an Early Devonian stem gnathostome. *Nature* **520**, 82–85.
- Goloboff, P. A., Torres, A. and Arias, J. S. (2017). Weighted parsimony outperforms other methods of phylogenetic inference under models appropriate for morphology. *Cladistics*.
- Goujet, D. (1982). Les affinités des placodermes, une revue des hypothèses actuelles. *Geobios* **15**, 27–38.
- Goujet, D. (1984). Placoderm interrelationships: a new interpretation, with a short review of placoderm classifications. In *Proceedings of the Linnean Society of New South Wales*, vol. 107, pp. 211–243.
- Goujet, D. (2001). Placoderms and basal gnathostome apomorphies. In *Major Events in Early Vertebrate Evolution* (ed. P. E. Ahlberg), pp. 209–222. Taylor and Francis, London and New York.
- Hennig, W. (1966). *Phylogenetic systematics*. University of Illinois Press.

- Huelsenbeck, J. P., Bollback, J. P. and Levine, A. M. (2002). Inferring the root of a phylogenetic tree. *Systematic Biology* **51**, 32–43.
- Janvier, P. (1985). *Les Céphalaspides du Spitsberg. Anatomie, phylogénie et systématique des Ostéostracés siluro-dévonien. Révision des Ostéostracés de la formation de Wood Bay (Dévonien inférieur du Spitsberg). Cahiers de Paléontologie, Section Vertébrés.* CNRS, Paris.
- Janvier, P. (1996). *Early vertebrates.* Clarendon Press, Oxford.
- Jardine, N. (1969). The observational and theoretical components of homology: a study based on the morphology of the dermal skull-roofs of rhipidistian fishes. *Biological Journal of the Linnean Society* **1**, 327–361.
- King, B. and Lee, M. S. Y. (2015). Ancestral state reconstruction, rate heterogeneity, and the evolution of reptile viviparity. *Systematic Biology* **64**, 532–544.
- Klein, A. and Bleckmann, H. (2015). Function of lateral line canal morphology. *Integrative zoology* **10**, 111–121.
- Klein, A., Münz, H. and Bleckmann, H. (2013). The functional significance of lateral line canal morphology on the trunk of the marine teleost *Xiphister atropurpureus* (Stichaeidae). *Journal of Comparative Physiology A* **199**, 735–749.
- Kolaczkowski, B. and Thornton, J. W. (2004). Performance of maximum parsimony and likelihood phylogenetics when evolution is heterogeneous. *Nature* **431**, 980–984.
- Kück, P., Mayer, C., Wägele, J.-W. and Misof, B. (2012). Long branch effects distort maximum likelihood phylogenies in simulations despite selection of the correct model. *PloS one* **7**, e36593.
- Kuratani, S. (2012). Evolution of the vertebrate jaw from developmental perspectives. *Evolution & development* **14**, 76–92.
- Lee, M. S. Y. (2016). Multiple morphological clocks and total-evidence tip-dating in mammals. *Biology Letters* **12**, 20160033.

- Long, J. A., Mark-Kurik, E., Johanson, Z., Lee, M. S., Young, G. C., Min, Z., Ahlberg, P. E., Newman, M., Jones, R. and Den Blaauwen, J. (2015). Copulation in antiarch placoderms and the origin of gnathostome internal fertilization. *Nature* **517**, 196–199.
- Lu, J., Giles, S., Friedman, M., den Blaauwen, J. L. and Zhu, M. (2016a). The oldest actinopterygian highlights the cryptic early history of the hyperdiverse ray-finned fishes. *Current Biology* **26**, 1602–1608.
- Lu, J., Zhu, M., Ahlberg, P. E., Qiao, T., Zhu, Y. a., Zhao, W. and Jia, L. (2016b). A Devonian predatory fish provides insights into the early evolution of modern sarcopterygians. *Science Advances* **2**, e1600154.
- Marshall, N. B. (1971). *Explorations in the life of fishes*. Harvard University Press.
- O'Reilly, J. E., Puttick, M. N., Parry, L., Tanner, A. R., Tarver, J. E., Fleming, J., Pisani, D. and Donoghue, P. C. (2016). Bayesian methods outperform parsimony but at the expense of precision in the estimation of phylogeny from discrete morphological data. *Biology Letters* **12**, 20160081.
- Ørvig, T. (1961). New finds of acanthodians, arthrodiros, crossopterygians, ganoids and dipnoans in the upper Middle Devonian calcareous flags (Oberer Plattenkalk) of the Bergisch Gladbach-Paffrath trough. *Paläontologische Zeitschrift* **35**, 10–27.
- Puttick, M. N., O'Reilly, J. E., Tanner, A. R., Fleming, J. F., Clark, J., Holloway, L., Lozano-Fernandez, J., Parry, L. A., Tarver, J. E. and Pisani, D. (2017). Uncertain-tree: discriminating among competing approaches to the phylogenetic analysis of phenotype data. *Proceedings of the Royal Society B* **284**, 20162290.
- Qu, Q., Sanchez, S., Zhu, M., Blom, H. and Ahlberg, P. E. (2017). The origin of novel features by changes in developmental mechanisms: ontogeny and three - dimensional microanatomy of polyodontode scales of two early osteichthyans. *Biological Reviews* **92**, 1189 – 1212.
- Ramírez, M. J. (2007). Homology as a parsimony problem: a dynamic homology approach for morphological data. *Cladistics* **23**, 588–612.

- Ronquist, F., Klopfstein, S., Vilhelmsen, L., Schulmeister, S., Murray, D. L. and Rasnitsyn, A. P. (2012). A total-evidence approach to dating with fossils, applied to the early radiation of the Hymenoptera. *Systematic Biology* **61**, 973–999.
- Sanderson, M. J. and Kim, J. (2000). Parametric phylogenetics? *Systematic Biology* **49**, 817–829.
- Schultze, H.-P. (1968). Palaeoniscoidea-Schuppen aus dem Unterdevon Australiens und Kanadas und aus dem Mitteldevon Spitzbergens. *Bulletin of the British Museum (Natural History) Geology* **16**, 341–368.
- Schultze, H.-P. and Cumbaa, S. L. (2001). *Dialipina* and the characters of basal actinopterygians. In *Major Events in Early Vertebrate Evolution* (ed. P. Ahlberg), pp. 315–332. Taylor and Francis, London and New York.
- Schwalbe, M. A., Bassett, D. K. and Webb, J. F. (2012). Feeding in the dark: lateral-line-mediated prey detection in the peacock cichlid *Aulonocara stuartgranti*. *Journal of Experimental Biology* **215**, 2060–2071.
- Sienknecht, U. J. (2013). Origin and development of hair cell orientation in the inner ear. In *Insights from comparative hearing research* (ed. C. Köppl, G. A. Manley, A. N. Popper and R. R. Fay), pp. 69–109. Springer, New York.
- Stadler, T. (2010). Sampling-through-time in birth–death trees. *Journal of Theoretical Biology* **267**, 396–404.
- Stensiö, E. A. (1969). Elasmobranchiomorphi Placodermata Arthrodiros. In *Traité de paléontologie*, vol. 4 (ed. J. Piveteau), pp. 71–692. Masson, Paris.
- Trinajstić, K. (1999). Scale morphology of the Late Devonian palaeoniscoid *Moythomasia durgaringa* Gardiner and Bartram, 1977. *Alcheringa* **23**, 9–19.
- Tuffley, C. and Steel, M. (1997). Links between maximum likelihood and maximum parsimony under a simple model of site substitution. *Bulletin of Mathematical Biology* **59**, 581–607.
- Wang, N. and Dong, Z. (1989). Discovery of Late Silurian microfossils of Agnatha and fishes from Yunnan, China. *Acta Palaeontologica Sinica* **28**, 192–206.

- Webb, J. F. (1989). Gross morphology and evolution of the mechanoreceptive lateral-line system in teleost fishes. *Brain Behavior and Evolution* **33**, 34–43.
- Webb, J. F. (2013). Morphological diversity, development, and evolution of the mechanosensory lateral line system. In *The Lateral Line System* (ed. S. Coombs, H. Bleckmann, R. R. Fay and A. N. Popper), pp. 17–72. Springer, New York.
- Wright, A. M. and Hillis, D. M. (2014). Bayesian analysis using a simple likelihood model outperforms parsimony for estimation of phylogeny from discrete morphological data. *PloS one* **9**, e109210.
- Yang, Z. (1996). Among-site rate variation and its impact on phylogenetic analyses. *Trends in Ecology & Evolution* **11**, 367–372.
- Young, G. C. (1980). A new Early Devonian placoderm from New South Wales, Australia, with a discussion of placoderm phylogeny. *Palaeontographica Abteilung A Palaeozoologie-Stratigraphie* **167**, 10–76.
- Young, G. C. (1984). Reconstruction of the jaws and braincase in the Devonian placoderm fish *Bothriolepis*. *Palaeontology* **27**, 635–661.
- Young, G. C. (1986). The relationships of placoderm fishes. *Zoological Journal of the Linnean Society* **88**, 1–57.
- Young, G. C. (2010). Placoderms (armored fish): dominant vertebrates of the Devonian period. *Annual Review of Earth and Planetary Sciences* **38**, 523–550.
- Zhu, M., Ahlberg, P. E., Pan, Z., Zhu, Y., Qiao, T., Zhao, W., Jia, L. and Lu, J. (2016). A Silurian maxillate placoderm illuminates jaw evolution. *Science* **354**, 334–336.
- Zhu, M., Yu, X., Ahlberg, P. E., Choo, B., Lu, J., Qiao, T., Qu, Q., Zhao, W., Jia, L., Blom, H. and Zhu, Y.-A. (2013). A Silurian placoderm with osteichthyan-like marginal jaw bones. *Nature* **502**, 188–193.
- Zhu, M., Zhao, W., Jia, L., Lu, J., Qiao, T. and Qu, Q. (2009). The oldest articulated osteichthyan reveals mosaic gnathostome characters. *Nature* **458**, 469–474.

Bibliography

- Afanassieva, O. B. (2004). Microrelief on the exoskeleton of some early osteostracans (Agnatha): preliminary analysis of its significance. *The Gross Symposium, Vol. 2*, 14–21.
- Ahlberg, P. E., Trinajstić, K., Johanson, Z. and Long, J. A. (2009). Pelvic claspers confirm chondrichthyan-like internal fertilization in arthrodires. *Nature* **460**, 888.
- Alroy, J. (2002). Stratigraphy in phylogeny reconstruction—reply to Smith (2000). *Journal of Paleontology* **76**, 587–589.
- Alves-Gomes, J. A. (2001). The evolution of electroreception and bioelectrogenesis in teleost fish: a phylogenetic perspective. *Journal of Fish Biology* **58**, 1489–1511.
- Anderson, P. S., Friedman, M., Brazeau, M. D. and Rayfield, E. J. (2011). Initial radiation of jaws demonstrated stability despite faunal and environmental change. *Nature* **476**, 206–209.
- Andreev, P., Coates, M. I., Karatajūtė-Talimaa, V., Shelton, R. M., Cooper, P. R., Wang, N.-Z. and Sansom, I. J. (2016). The systematics of the Mongolepidida (Chondrichthyes) and the Ordovician origins of the clade. *PeerJ* **4**, e1850.
- Andres, K. H. and Von Düring, M. (1988). Comparative anatomy of vertebrate electroreceptors. *Progress in Brain Research* **74**, 113–131.
- Baele, G., Lemey, P., Bedford, T., Rambaut, A., Suchard, M. A. and Alekseyenko, A. V. (2012). Improving the accuracy of demographic and molecular clock

- model comparison while accommodating phylogenetic uncertainty. *Molecular Biology and Evolution* **29**, 2157–2167.
- Baker, C. V. H., Modrell, M. S. and Gillis, J. A. (2013). The evolution and development of vertebrate lateral line electroreceptors. *Journal of Experimental Biology* **216**, 2515–2522.
- Bapst, D. W., Wright, A. M., Matzke, N. J. and Lloyd, G. T. (2016). Topology, divergence dates, and macroevolutionary inferences vary between different tip-dating approaches applied to fossil theropods (Dinosauria). *Biology Letters* **12**, 20160237.
- Bardack, D. and Zangerl, R. (1968). First fossil lamprey: a record from the Pennsylvanian of Illinois. *Science* **162**, 1265–1267.
- Baron, V. D. (2009). Electric discharges of two species of stargazers from the South China Sea (Uranoscopidae, Perciformes). *Journal of Ichthyology* **49**, 1065–1072.
- Barry, M. A. and Bennett, M. V. L. (1989). Specialized lateral line receptor systems in elasmobranchs: the spiracular organs and vesicles of Savi. In *The Mechanosensory Lateral Line* (ed. S. Coombs, P. Görner and H. Münz), pp. 591–606. Springer.
- Bartsch, P. (1993). Development of the snout of the Australian lungfish *Neoceratodus forsteri* (Krefft, 1870), with special reference to cranial nerves. *Acta Zoologica* **74**, 15–29.
- Basden, A. M. and Young, G. C. (2001). A primitive actinopterygian neurocranium from the Early Devonian of southeastern Australia. *Journal of Vertebrate Paleontology* **21**, 754–766.

- Basden, A. M., Young, G. C., Coates, M. I. and Ritchie, A. (2000). The most primitive osteichthyan braincase? *Nature* **403**, 185–188.
- Beck, R. M. D. and Lee, M. S. Y. (2014). Ancient dates or accelerated rates? Morphological clocks and the antiquity of placental mammals. *Proceedings of the Royal Society B* **281**, 20141278.
- Bedore, C. N. and Kajiura, S. M. (2013). Bioelectric fields of marine organisms: voltage and frequency contributions to detectability by electroreceptive predators. *Physiological and Biochemical Zoology* **86**, 298–311.
- Bell, M. (2015). geoscale: geological time scale plotting. In *R package version 2.0*. <https://CRAN.R-project.org/package=geoscale>.
- Bell, M. A. and Lloyd, G. T. (2015). strap: an R package for plotting phylogenies against stratigraphy and assessing their stratigraphic congruence. *Palaeontology* **58**, 379–389.
- Bellono, N. W., Leitch, D. B. and Julius, D. (2017). Molecular basis of ancestral vertebrate electroreception. *Nature* **543**, 391–396.
- Bemis, W. E. and Hetherington, T. E. (1982). The rostral organ of *Latimeria chalumnae*: Morphological evidence of an electroreceptive function. *Copeia* **1982**, 467–471.
- Bemis, W. E. and Northcutt, R. G. (1992). Skin and blood vessels of the snout of the Australian lungfish, *Neoceratodus forsteri*, and their significance for interpreting the cosmine of Devonian lungfishes. *Acta Zoologica* **73**, 115–139.
- Bennett, M. V. L. (1971). Electroreception. *Fish Physiology* **5**, 493–574.
- Benton, M. J. and Storrs, G. W. (1994). Testing the quality of the fossil record: paleontological knowledge is improving. *Geology* **22**, 111–114.

- Benton, M. J., Wills, M. and Hitchin, R. (2000). Quality of the fossil record through time. *Nature* **403**, 534–537.
- Berquist, R. M., Galinsky, V. L., Kajiura, S. M. and Frank, L. R. (2015). The coelacanth rostral organ is a unique low-resolution electro-detector that facilitates the feeding strike. *Scientific reports* **5**, 8962.
- Bielejec, F., Lemey, P., Baele, G., Rambaut, A. and Suchard, M. A. (2014). Inferring heterogeneous evolutionary processes through time: from sequence substitution to phylogeography. *Systematic Biology* **63**, 493–504.
- Bjerring, H. C. (1972). Morphological observations on the exoskeletal skull roof of an osteolepiform from the Carboniferous of Scotland. *Acta Zoologica* **53**, 73–92.
- Blackburn, D. G. (2015). Evolution of vertebrate viviparity and specializations for fetal nutrition: a quantitative and qualitative analysis. *Journal of Morphology* **276**, 961–990.
- Bodznick, D. and Boord, R. (1986). Electroreception in Chondrichthyes. Central anatomy and physiology. In *Electroreception* (ed. T. H. Bullock and W. Heiligenberg), pp. 225–257. John Wiley & Sons, New York.
- Bodznick, D. and Montgomery, J. C. (2005). The physiology of low-frequency electrosensory systems. In *Electroreception* (ed. T. H. Bullock, C. D. Hopkins, A. N. Popper and R. R. Fay), pp. 132–153. Springer, New York.
- Bodznick, D. and Northcutt, R. G. (1980). Segregation of electro- and mechanoreceptive inputs to the elasmobranch medulla. *Brain Research* **195**, 313–321.
- Bodznick, D. and Northcutt, R. G. (1981). Electroreception in lampreys: evidence that the earliest vertebrates were electroreceptive. *Science* **212**, 465–467.

- Bodznick, D. and Preston, D. G. (1983). Physiological characterization of electroreceptors in the lampreys *Ichthyomyzon unicuspis* and *Petromyzon marinus*. *Journal of Comparative Physiology* **152**, 209–217.
- Bohlin, B. (1941). The dorsal and lateral cephalic fields in the Osteostraci. *Zoologiska bidrag från Uppsala* **20**, 543–554.
- Bohlin, B. (1956). The dorsal and lateral sensory fields in the Osteostraci parts of the internal ear? *Zoologiska bidrag från Uppsala* **31**, 205–209.
- Borgen, U. (1989). Cosmine resorption structures on three osteolepid jaws and their biological significance. *Lethaia* **22**, 413–424.
- Borgen, U. (1992). The function of the pore canal system. In *Fossil Fishes as Living Animals* (ed. E. Mark-Kurik), pp. 141–151. Academy of Sciences of Estonia, Tallinn.
- Botella, H., Blom, H., Dorka, M., Ahlberg, P. E. and Janvier, P. (2007). Jaws and teeth of the earliest bony fishes. *Nature* **448**, 583.
- Bouckaert, R., Heled, J., Kühnert, D., Vaughan, T., Wu, C.-H., Xie, D., Suchard, M. A., Rambaut, A. and Drummond, A. J. (2014). BEAST 2: a software platform for Bayesian evolutionary analysis. *PLoS Computational Biology* **10**, e1003537.
- Bouckaert, R. R. (2010). DensiTree: making sense of sets of phylogenetic trees. *Bioinformatics* **26**, 1372–1373.
- Brazeau, M. D. (2009). The braincase and jaws of a Devonian ‘acanthodian’ and modern gnathostome origins. *Nature* **457**, 305–308.
- Brazeau, M. D. and de Winter, V. (2015). The hyoid arch and braincase anatomy of *Acanthodes* support chondrichthyan affinity of ‘acanthodians’. *Proceedings of the Royal Society B* **282**, 20152210.

- Brazeau, M. D. and Friedman, M. (2014). The characters of Palaeozoic jawed vertebrates. *Zoological Journal of the Linnean Society* **170**, 779–821.
- Brazeau, M. D. and Friedman, M. (2015). The origin and early phylogenetic history of jawed vertebrates. *Nature* **520**, 490–497.
- Brazeau, M. D., Friedman, M., Jerve, A. and Atwood, R. C. (2017). A three-dimensional placoderm (stem-group gnathostome) pharyngeal skeleton and its implications for primitive gnathostome pharyngeal architecture. *Journal of Morphology* **278**, 1120–1128.
- Brown, J. W., Parins-Fukuchi, C., Stull, G. W., Vargas, O. M. and Smith, S. A. (2017). Bayesian and likelihood phylogenetic reconstructions of morphological traits are not discordant when taking uncertainty into consideration: a comment on Puttick et al. *Proceedings of the Royal Society B* **284**, 20170986.
- Brundin, L. (1966). *Transantarctic relationships and their significance, as evidenced by chironomid midges*. Almqvist & Wiksell, Stockholm.
- Bullock, T. H., Bodznick, D. A. and Northcutt, R. G. (1983). The phylogenetic distribution of electroreception: evidence for convergent evolution of a primitive vertebrate sense modality. *Brain Research Reviews* **6**, 25–46.
- Burrow, C. and Turner, S. (1998). Devonian placoderm scales from Australia. *Journal of Vertebrate Paleontology* **18**, 677–695.
- Burrow, C. J. (1997). Microvertebrate assemblages from the Lower Devonian (pesavis/sulcatus zones) of central New South Wales, Australia. *Modern Geology* **21**, 43–77.

- Burrow, C. J. (2006). Placoderm fauna from the Connemarra Formation (? late Lochkovian, Early Devonian), central New South Wales. *Alcheringa: An Australasian Journal of Palaeontology* **30**, 59-88.
- Burrow, C. J. (2011). A partial articulated acanthodian from the Silurian of New Brunswick, Canada. *Canadian Journal of Earth Sciences* **48**, 1329–1341.
- Burrow, C. J., Newman, M. J., Davidson, R. G. and den Blaauwen, J. L. (2013). Redescription of *Parexus recurvus*, an Early Devonian acanthodian from the Midland Valley of Scotland. *Alcheringa: An Australasian Journal of Palaeontology* **37**, 392–414.
- Burrow, C. J., Turner, S. and Young, G. C. (2010). Middle Palaeozoic microvertebrate assemblages and biogeography of East Gondwana (Australasia, Antarctica). *Palaeoworld* **19**, 37–54.
- Burrow, C. J. and Young, G. C. (1999). An articulated teleostome fish from the Late Silurian (Ludlow) of Victoria, Australia. *Records of the Western Australian Museum Supplement* **57**, 1–14.
- Campbell, K. S. W. and Barwick, R. E. (1986). Paleozoic lungfishes—a review. *Journal of Morphology Supplement* **1**, 93–131.
- Campbell, K. S. W. and Barwick, R. E. (2000). The braincase, mandible and dental structures of the Early Devonian lungfish *Dipnorhynchus kurikae* from Wee Jasper, New South Wales. *Records of the Australian Museum* **52**, 103–128.
- Campbell, K. S. W., Barwick, R. E. and Senden, T. (2010). Perforations and tubules in the snout region of Devonian dipnoans. In *Morphology, Phylogeny and Paleobiogeography of Fossil Fishes* (ed. D. K. Elliott, J. G. Maisey, X. Yu and D. Miao), pp. 325–361. Verlag Dr. Friedrich Pfeil, München.

- Carr, R. K. and Hlavin, W. J. (2010). Two new species of *Dunkleosteus* Lehman, 1956, from the Ohio Shale Formation (USA, Famennian) and the Kettle Point Formation (Canada, Upper Devonian), and a cladistic analysis of the Eubrachythoraci (Placodermi, Arthrodira). *Zoological Journal of the Linnean Society* **159**, 195–222.
- Carr, R. K. and Jackson, G. L. (2010). The vertebrate fauna of the Cleveland Member (Famennian) of the Ohio Shale. In *Guide to the Geology and Paleontology of the Cleveland Member of the Ohio Shale. Ohio Geological Survey Guidebook 22* (ed. J. T. Hannibal).
- Challands, T. J. (2015). The cranial endocast of the Middle Devonian dipnoan *Dipterus valenciennesi* and a fossilized dipnoan otoconial mass. *Papers in Palaeontology* **1**, 289–317.
- Chang, M.-M. (1982). *The braincase of Youngolepis, a Lower Devonian crossopterygian from Yunnan, south-western China*. Swedish Museum of Natural History, Stockholm.
- Chang, M.-M. (1995). *Diabolepis* and its bearing on the relationships between porolepiforms and dipnoans. *Bulletin du Muséum national d'histoire naturelle. Section C, Sciences de la terre, paléontologie, géologie, minéralogie* **17**, 235–268.
- Chang, M.-m., Zhang, J. and Miao, D. (2006). A lamprey from the Cretaceous Jehol biota of China. *Nature* **441**, 972–974.
- Chang, M.-M. and Zhu, M. (1993). A new Middle Devonian osteolepidid from Qujing, Yunnan. *Memoirs of the Association of Australasian Palaeontologists* **15**, 183–198.

- Chasiotis, H., Kolosov, D., Bui, P. and Kelly, S. P. (2012). Tight junctions, tight junction proteins and paracellular permeability across the gill epithelium of fishes: a review. *Respiratory Physiology & Neurobiology* **184**, 269–281.
- Chen, D., Janvier, P., Ahlberg, P. E. and Blom, H. (2012). Scale morphology and squamation of the Late Silurian osteichthyan *Andreolepis* from Gotland, Sweden. *Historical Biology* **24**, 411–423.
- Cheng, H. (1989). On the tubuli in Devonian lungfishes. *Alcheringa* **13**, 153–166.
- Choo, B., Zhu, M., Qu, Q., Yu, X., Jia, L. and Zhao, W. (2017). A new osteichthyan from the late Silurian of Yunnan, China. *PloS one* **12**, e0170929.
- Clement, A. M. and Ahlberg, P. E. (2014). The first virtual cranial endocast of a lungfish (Sarcopterygii: Dipnoi). *PloS one* **9**, e113898.
- Clement, A. M., Nysjö, J., Strand, R. and Ahlberg, P. E. (2015). Brain–Endocast Relationship in the Australian Lungfish, *Neoceratodus forsteri*, Elucidated from Tomographic Data (Sarcopterygii: Dipnoi). *PloS one* **10**, e0141277.
- Clément, G. and Ahlberg, P. E. (2010). The endocranial anatomy of the early sarcopterygian *Powichthys* from Spitsbergen, based on CT scanning. In *Morphology, Phylogeny and Paleobiogeography of Fossil Fishes* (ed. D. K. Elliott, J. G. Maisey, X. Yu and D. Miao), pp. 363–378. Verlag Dr. Friedrich Pfeil, München.
- Close, R. A., Friedman, M., Lloyd, G. T. and Benson, R. B. (2015). Evidence for a mid-Jurassic adaptive radiation in mammals. *Current Biology* **25**, 2137–2142.
- Close, R. A., Johanson, Z., Tyler, J. C., Harrington, R. C. and Friedman, M. (2016). Mosaicism in a new Eocene pufferfish highlights rapid morphological

- innovation near the origin of crown tetraodontiforms. *Palaeontology* **59**, 499–514.
- Cloutier, R. (1996). The primitive actinistian *Miguashaia bureaui* Schultze (Sarcopterygii). In *Devonian Fishes and Plants of Miguasha, Quebec, Canada* (ed. H.-P. Schultze and R. Cloutier), pp. 227–247. Verlag Dr. Friedrich Pfeil, München.
- Coates, M. and Sequeira, S. (2001). A new stethacanthid chondrichthyan from the Lower Carboniferous of Bearsden, Scotland. *Journal of Vertebrate Paleontology* **21**, 438–459.
- Coates, M. I. (1999). Endocranial preservation of a Carboniferous actinopterygian from Lancashire, UK, and the interrelationships of primitive actinopterygians. *Philosophical Transactions of the Royal Society B: Biological Sciences* **354**, 435–462.
- Coombs, S., Janssen, J. and Webb, J. F. (1988). Diversity of lateral line systems: evolutionary and functional considerations. In *Sensory biology of aquatic animals* (ed. Atema, R. R. Fay, A. N. Popper and W. N. Tavolga), pp. 553–593. Springer, New York.
- Czech-Damal, N. U., Liebschner, A., Miersch, L., Klauer, G., Hanke, F. D., Marshall, C., Dehnhardt, G. and Hanke, W. (2012). Electroreception in the Guiana dolphin (*Sotalia guianensis*). *Proceedings of the Royal Society of London B* **279**, 663–668.
- Davies, T. G., Rahman, I. A., Lautenschlager, S., Cunningham, J. A., Asher, R. J., Barrett, P. M., Bates, K. T., Bengtson, S., Benson, R. B. and Boyer, D. M. (2017). Open data and digital morphology. In *Proceedings of the Royal Society B*, vol. 284, pp. 20170194. The Royal Society.

- Davis, S. P., Finarelli, J. A. and Coates, M. I. (2012). *Acanthodes* and shark-like conditions in the last common ancestor of modern gnathostomes. *Nature* **486**, 247–250.
- de Boef, M. and Larsson, H. C. E. (2007). Bone microstructure: quantifying bone vascular orientation. *Canadian Journal of Zoology* **85**, 63–70.
- Denison, R. H. (1947). The exoskeleton of *Tremataspis*. *American Journal of Science* **245**, 337–365.
- Denison, R. H. (1964). The Cyathaspididae: a family of Silurian and Devonian jawless vertebrates. *Fieldiana, Geology* **13**, 309–473.
- Denison, R. H. (1966). The origin of the lateral-line sensory system. *American Zoologist* **6**, 368–370.
- Denison, R. H. (1978). *Placodermi*. Gustav Fischer Verlag, Stuttgart and New York.
- Dennis, K. and Miles, R. S. (1979a). Eubrachythoracid arthrodires with tubular rostral plates from Gogo, Western Australia. *Zoological Journal of the Linnean Society* **67**, 297–328.
- Dennis, K. and Miles, R. S. (1979b). A second eubrachythoracid arthrodire from Gogo, Western Australia. *Zoological Journal of the Linnean Society* **67**, 1–29.
- Dennis, K. and Miles, R. S. (1982). A eubrachythoracid arthrodire with a snubnose from Gogo, Western Australia. *Zoological Journal of the Linnean Society* **75**, 153–166.
- Dennis-Bryan, K. (1987). A new species of eastmanosteid arthrodire (Pisces: Placodermi) from Gogo, Western Australia. *Zoological Journal of the Linnean Society* **90**, 1–64.

- Dennis-Bryan, K. and Miles, R. S. (1983). Further eubrachythoracid arthrodires from Gogo, Western Australia. *Zoological Journal of the Linnean Society* **77**, 145–173.
- Denton, E. J. and Gray, J. A. B. (1988). Mechanical factors in the excitation of the lateral lines of fishes. In *Sensory biology of aquatic animals* (ed. J. Atema, R. R. Fay, A. N. Popper and W. N. Tavolga), pp. 595–617. Springer, New York.
- Dijkgraaf, S. and Kalmijn, A. J. (1963). Untersuchungen über die Funktion der Lorenzinischen Ampullen an Haifischen. *Journal of Comparative Physiology A* **47**, 438–456.
- Donoghue, P. C., Forey, P. L. and Aldridge, R. J. (2000). Conodont affinity and chordate phylogeny. *Biological Reviews* **75**, 191–251.
- Drummond, A. J., Ho, S. Y., Phillips, M. J. and Rambaut, A. (2006). Relaxed phylogenetics and dating with confidence. *PLoS Biology* **4**, e88.
- Drummond, A. J. and Suchard, M. A. (2010). Bayesian random local clocks, or one rate to rule them all. *BMC biology* **8**, 114.
- Drummond, A. J., Suchard, M. A., Xie, D. and Rambaut, A. (2012). Bayesian phylogenetics with BEAUti and the BEAST 1.7. *Molecular Biology and Evolution* **29**, 1969–1973.
- Duncan, J. S. and Fritsch, B. (2012). Transforming the vestibular system one molecule at a time: the molecular and developmental basis of vertebrate auditory evolution. In *Sensing in Nature* (ed. C. Köppl, G. A. Manley, A. N. Popper and R. R. Fay), pp. 173–186. Springer, New York.
- Dunkle, D. H. and Schaeffer, B. (1973). *Tegeolepis clarki* (Newberry), a palaeonisciform from the Upper Devonian Ohio shale. *Palaeontographica Abteilung A* **143**, 151–158.

- Dupret, V. (2010). Revision of the genus *Kujdanowiaspis* Stensiö, 1942 (Placodermi, Arthrodira, “Actinolepida”) from the Lower Devonian of Podolia (Ukraine). *Geodiversitas* **32**, 5–63.
- Dupret, V., Phuong, T. H., Thanh, T.-D., Phong, N. D., Janvier, P. and Clément, G. (2011). The skull of *Hagiangella goujeti* Janvier, 2005, a high-crested acanthothoracid (Vertebrata, Placodermi) from the Lower Devonian of northern Vietnam. *Journal of Vertebrate Paleontology* **31**, 531–538.
- Dupret, V., Sanchez, S., Goujet, D. and Ahlberg, P. (2017a). The internal cranial anatomy of *Romundina stellina* Ørvig, 1975 (Vertebrata, Placodermi, Acanthothoraci) and the origin of jawed vertebrates—Anatomical atlas of a primitive gnathostome. *PloS one* **12**, e0171241.
- Dupret, V., Sanchez, S., Goujet, D., Tafforeau, P. and Ahlberg, P. E. (2010). Bone vascularization and growth in placoderms (Vertebrata): The example of the premedian plate of *Romundina stellina* Ørvig, 1975. *Comptes Rendus Palevol* **9**, 369–375.
- Dupret, V., Sanchez, S., Goujet, D., Tafforeau, P. and Ahlberg, P. E. (2014). A primitive placoderm sheds light on the origin of the jawed vertebrate face. *Nature* **507**, 500–503.
- Dupret, V., Zhu, M. and Wang, J.-Q. (2017b). Redescription of *Szelepis* Liu, 1981 (Placodermi, Arthrodira) from the Lower Devonian of China. *Journal of Vertebrate Paleontology*, e1312422.
- Dupret, V., Zhu, M. and Wang, J. Q. (2009). The morphology of *Yujiangolepis liujingensis* (Placodermi, Arthrodira) from the Pragian of Guangxi (South China) and its phylogenetic significance. *Zoological Journal of the Linnean Society* **157**, 70–82.

- Farris, J. (1983). The logical basis of phylogenetic analysis. In *Advances in Cladistics, Vol. 2* (ed. P. N. I and V. A. Funk), pp. 7–36. Columbia University Press, New York.
- Felsenstein, J. (1973). Maximum-likelihood estimation of evolutionary trees from continuous characters. *American Journal of Human Genetics* **25**, 471–492.
- Fettiplace, R. and Fuchs, P. A. (1999). Mechanisms of hair cell tuning. *Annual Review of Physiology* **61**, 809–834.
- Fields, R. D., Bullock, T. H. and Lange, G. D. (1993). Ampullary sense organs, peripheral, central and behavioral electroreception in chimeras (*Hydrolagus*, Holocephali, Chondrichthyes). *Brain, behavior and evolution* **41**, 269–289.
- Fields, R. D. and Lange, G. D. (1980). Electroreception in the ratfish (*Hydrolagus colliei*). *Science* **207**, 547–548.
- Fisher, D. C. (2008). Stratocladistics: integrating temporal data and character data in phylogenetic inference. *Annual Review of Ecology, Evolution, and Systematics* **39**, 365–385.
- Forey, P. (1980). *Latimeria*: a paradoxical fish. *Proceedings of the Royal Society B* **208**, 369–384.
- Forey, P. L. (1998). *History of the Coelacanth Fishes*. Chapman and Hall, London.
- Fox, D. L., Fisher, D. C. and Leighton, L. R. (1999). Reconstructing phylogeny with and without temporal data. *Science* **284**, 1816–1819.
- Fox, R. C., Campbell, K. S. W., Barwick, R. E. and Long, J. (1995). A new osteolepiform fish from the lower Carboniferous Raymond Formation, Drummond Basin, Queensland. *Memoirs of the Queensland Museum* **38**, 97–221.

- Friedman, M. (2007). *Styloichthys* as the oldest coelacanth: implications for early osteichthyan interrelationships. *Journal of Systematic Palaeontology* **5**, 289–343.
- Friedman, M. and Brazeau, M. D. (2010). A reappraisal of the origin and basal radiation of the Osteichthyes. *Journal of Vertebrate Paleontology* **30**, 36–56.
- Gagnier, P., Hanke, G. and Wilson, M. (1999). *Tetanopsyrus lindoei* gen. et sp. nov., an Early Devonian acanthodian from the Northwest Territories, Canada. *Acta Geologica Polonica* **49**, 81–96.
- Gai, Z., Donoghue, P. C., Zhu, M., Janvier, P. and Stampanoni, M. (2011). Fossil jawless fish from China foreshadows early jawed vertebrate anatomy. *Nature* **476**, 324–327.
- Gans, C. (1989). Stages in the origin of vertebrates: analysis by means of scenarios. *Biological Reviews* **64**, 221–268.
- Gans, C. and Northcutt, R. G. (1983). Neural crest and the origin of vertebrates: a new head. *Science* **220**, 268–273.
- Gardiner, B. G. (1984a). The relationship of placoderms. *Journal of Vertebrate Paleontology* **4**, 379–395.
- Gardiner, B. G. (1984b). The relationships of the paleoniscid fishes. a review based on new specimens of *Mimia* and *Moythomasia* from the upper Devonian of Western Australia. *Bulletin of the British Museum (Natural History) Geology* **37**, 173–248.
- Gardiner, B. G. (1993). Placodermi. *The fossil record* **2**, 583–588.

- Gardiner, B. G. and Miles, R. S. (1990). A new genus of eubrachythoracid arthrodire from Gogo, Western Australia. *Zoological Journal of the Linnean Society* **99**, 159–204.
- Gardiner, B. G. and Miles, R. S. (1994). Eubrachythoracid arthrodires from Gogo, Western Australia. *Zoological Journal of the Linnean Society* **112**, 443–477.
- Gauthier, J., Kluge, A. G. and Rowe, T. (1988). Amniote phylogeny and the importance of fossils. *Cladistics* **4**, 105–209.
- Gavryushkina, A., Heath, T. A., Ksepka, D. T., Stadler, T., Welch, D. and Drummond, A. J. (2017). Bayesian total evidence dating reveals the recent crown radiation of penguins. *Systematic Biology* **66**, 57–73.
- Gavryushkina, A., Welch, D., Stadler, T. and Drummond, A. J. (2014). Bayesian inference of sampled ancestor trees for epidemiology and fossil calibration. *PLoS Computational Biology* **10**, e1003919.
- Geiger, D. L., Fitzhugh, K. and Thacker, C. E. (2001). Timeless characters: a response to Vermeij (1999). *Paleobiology* **27**, 177–178.
- Georges, D. (1979). Gap and tight junctions in tunicates. Study in conventional and freeze-fracture techniques. *Tissue and Cell* **11**, 781–792.
- Gess, R. W., Coates, M. I. and Rubidge, B. S. (2006). A lamprey from the Devonian period of South Africa. *Nature* **443**, 981–984.
- Giles, S., Coates, M. I., Garwood, R. J., Brazeau, M. D., Atwood, R., Johanson, Z. and Friedman, M. (2015a). Endoskeletal structure in *Cheirolepis* (Osteichthyes, Actinopterygii), An early ray-finned fish. *Palaeontology* **58**, 849–870.

- Giles, S., Darras, L., Clément, G., Blicek, A. and Friedman, M. (2015b). An exceptionally preserved Late Devonian actinopterygian provides a new model for primitive cranial anatomy in ray-finned fishes. *Proceedings of the Royal Society B* **282**, 20151485.
- Giles, S. and Friedman, M. (2014). Virtual reconstruction of endocast anatomy in early ray-finned fishes (Osteichthyes, Actinopterygii). *Journal of Paleontology* **88**, 636–651.
- Giles, S., Friedman, M. and Brazeau, M. D. (2015c). Osteichthyan-like cranial conditions in an Early Devonian stem gnathostome. *Nature* **520**, 82–85.
- Giles, S., Rogers, M. and Friedman, M. (2016). Bony labyrinth morphology in early neopterygian fishes (Actinopterygii: neopterygii). *Journal of Morphology*, 10.1002/jmor.20551.
- Giles, S., Rücklin, M. and Donoghue, P. C. J. (2013). Histology of “placoderm” dermal skeletons: Implications for the nature of the ancestral gnathostome. *Journal of Morphology* **274**, 627–644.
- Gillis, J. A., Modrell, M. S., Northcutt, R. G., Catania, K. C., Luer, C. A. and Baker, C. V. H. (2012). Electrosensory ampullary organs are derived from lateral line placodes in cartilaginous fishes. *Development* **139**, 3142–3146.
- Gingerich, P. D. (1979). The stratophenetic approach to phylogeny reconstruction in vertebrate paleontology. *Phylogenetic Analysis and Paleontology*. Columbia University Press, New York, 41–77.
- Goloboff, P. A., Farris, J. S. and Nixon, K. C. (2008). TNT, a free program for phylogenetic analysis. *Cladistics* **24**, 774–786.

- Goloboff, P. A., Torres, A. and Arias, J. S. (2017). Weighted parsimony outperforms other methods of phylogenetic inference under models appropriate for morphology. *Cladistics*.
- Goodrich, E. S. (1930). *Studies on the Structure and Development of Vertebrates*. Macmillan, London.
- Goujet, D. (1975). *Dicksonosteus*, un nouvel arthrodire du Dévonien du Spitzberg—Remarques sur le squelette viscéral des Dolichothoraci. *Colloques Internationaux du Centre National de la Recherche Scientifique* **218**, 81–99.
- Goujet, D. (1980). Les Poissons. *Mémoires de la Société Géologique et Minéralogique de Bretagne* **23**, 305-308.
- Goujet, D. (1982). Les affinités des placodermes, une revue des hypothèses actuelles. *Geobios* **15**, 27–38.
- Goujet, D. (1984a). *Les poissons placodermes du Spitzberg: Arthrodirés Dolichothoraci de la Formation de Wood Bay (Dévonien inférieur)*. *Cahiers de Paléontologie, Section Vertébrés*. CNRS, Paris.
- Goujet, D. (1984b). Placoderm interrelationships: a new interpretation, with a short review of placoderm classifications. In *Proceedings of the Linnean Society of New South Wales*, vol. 107, pp. 211–243.
- Goujet, D. (2001). Placoderms and basal gnathostome apomorphies. In *Major Events in Early Vertebrate Evolution* (ed. P. E. Ahlberg), pp. 209–222. Taylor and Francis, London and New York.
- Goujet, D. and Young, G. C. (1995). Interrelationships of placoderms revisited. *Geobios* **28**, 89-95.

- Goujet, D. and Young, G. C. (2004). Placoderm anatomy and phylogeny: new insights. In *Recent advances in the origin and early radiation of vertebrates* (ed. G. Arratia, M. V. H. Wilson and R. Cloutier), pp. 109–126. Verlag Dr. Friedrich Pfeil, München.
- Gross, W. (1956). Über Crossopterygier und Dipnoer aus dem baltischen Oberdevon im Zusammenhang einer vergleichenden Untersuchung des Porenkanalsystems paläozoischer Agnathen und Fische. *Kungliga Svenska Vetenskapsakademiens Handlingar* **5**, 1–140.
- Gross, W. (1961). *Lunaspis broilii* und *Lunaspis heroldi* aus dem Hunsrückschiefer (Unterdevons, Rheinland). *Notizblatt Hessisches Landesamtes für Bodenforschung zu Wiesbaden* **89**, 17–43.
- Gross, W. (1963). *Gemuendina stuertzi* Traquair. Neuuntersuchung. *Sonderdruck aus dem Notizblatt des Hessischen Landesamtes für Bodenforschung zu Wiesbaden* **91**, 36–73.
- Gross, W. (1965). Über den Vorderschädel von *Ganorhynchus splendens* Gross (Dipnoi, Mitteldevon). *Paläontologische Zeitschrift* **39**, 113.
- Gross, W. (1968). Fragliche actinopterygier-schuppen aus dem silur gotlands. *Lethaia* **1**, 184–218.
- Gross, W. (1969). *Lophosteus superbus* Pander, ein Teleostome aus dem Silur Oesels. *Lethaia* **2**, 15–47.
- Hamel, M.-H. and Poplin, C. (2008). The braincase anatomy of *Lawrenciella schaefferi*, actinopterygian from the Upper Carboniferous of Kansas (USA). *Journal of Vertebrate Paleontology* **28**, 989–1006.

- Hamilton, R. F. M. and Trewin, N. H. (1988). Environmental controls on fish faunas of the Middle Devonian Orcadian Basin. *Memoir - Canadian Society of Petroleum Geologists* **14**, 589–600.
- Hanke, G. F. (2008). *Promesacanthus eppleri* n. gen., n. sp., a mesacanthid (Acanthodii, Acanthodiformes) from the Lower Devonian of northern Canada. *Geodiversitas* **30**, 287–302.
- Hanke, G. F. and Wilson, M. V. (2006). Anatomy of the Early Devonian acanthodian *Brochoadmones milesi* based on nearly complete body fossils, with comments on the evolution and development of paired fins. *Journal of Vertebrate Paleontology* **26**, 526–537.
- Hanke, G. F., Wilson, M. V. and Lindoe, L. A. (2001). New species of Silurian acanthodians from the Mackenzie Mountains, Canada. *Canadian Journal of Earth Sciences* **38**, 1517–1529.
- Hanke, G. F. and Wilson, M. V. H. (2010). The putative stem-group chondrichthyans *Kathemacanthus* and *Seretolepis* from the Lower Devonian MOTH locality, Mackenzie Mountains, Canada. In *Morphology, Phylogeny, and Paleobiogeography of Fossil Fishes, Honoring Meemann Chang* (ed. D. K. Elliott, J. G. Maisey, X. Yu and D. Miao), pp. 159–182. Verlag Dr. Friedrich Pfeil, München.
- Harris, J. E. (1938). The Dorsal Spine of Cladoselache. *Scientific Publications of the Cleveland Museum of Natural History* **8**, 1–6.
- Heath, T. A., Huelsenbeck, J. P. and Stadler, T. (2014). The fossilized birth–death process for coherent calibration of divergence-time estimates. *Proceedings of the National Academy of Sciences* **111**, E2957–E2966.

- Heimberg, A. M., Cowper-Sal, R., Sémon, M., Donoghue, P. C. and Peterson, K. J. (2010). microRNAs reveal the interrelationships of hagfish, lampreys, and gnathostomes and the nature of the ancestral vertebrate. *Proceedings of the National Academy of Sciences* **107**, 19379–19383.
- Hennig, W. (1966). *Phylogenetic systematics*. University of Illinois Press.
- Hetherington, T. E. and Wake, M. H. (1979). The lateral line system in larval *Ichthyophis* (Amphibia: Gymnophiona). *Zoomorphologie* **93**, 209–225.
- Heyning, J. E. and Thacker, C. (1999). Phylogenies, temporal data, and negative evidence. *Science* **285**, 1179–1179.
- Holland, T. (2014). The endocranial anatomy of *Gogonasmus andrewsae* Long, 1985 revealed through micro CT-scanning. *Earth and Environmental Science Transactions of the Royal Society of Edinburgh* **105**, 9–34.
- Hu, Y., Lu, J. and Young, G. C. (2017). New findings in a 400 million-year-old Devonian placoderm shed light on jaw structure and function in basal gnathostomes. *Scientific reports* **7**, 7813.
- Huelsenbeck, J. P. (1994). Comparing the stratigraphic record to estimates of phylogeny. *Paleobiology* **20**, 470–483.
- Huelsenbeck, J. P., Bollback, J. P. and Levine, A. M. (2002). Inferring the root of a phylogenetic tree. *Systematic Biology* **51**, 32–43.
- Huelsenbeck, J. P., Ronquist, F., Nielsen, R. and Bollback, J. P. (2001). Bayesian inference and its impact on evolutionary biology. *Science* **294**, 2310–2314.
- Istenič, L. and Bulog, B. (1984). Some evidence for the ampullary organs in the European cave salamander *Proteus anguinus* (Urodela, Amphibia). *Cell and tissue research* **235**, 393–402.

- Janvier, P. (1974). The sensory line system and its innervation in the Osteostraci (Agnatha, Cephalaspidomorphi). *Zoologica Scripta* **3**, 91–99.
- Janvier, P. (1981). The phylogeny of Craniata, with particular reference to the significance of fossil 'agnathans'. *Journal of Vertebrate Paleontology* **1**, 121–159.
- Janvier, P. (1985). *Les Céphalaspides du Spitsberg. Anatomie, phylogénie et systématique des Ostéostracés siluro-dévonien. Révision des Ostéostracés de la formation de Wood Bay (Dévonien inférieur du Spitsberg). Cahiers de Paléontologie, Section Vertébrés*. CNRS, Paris.
- Janvier, P. (1996a). The dawn of the vertebrates: characters versus common ascent in the rise of current vertebrate phylogenies. *Palaeontology* **39**, 259–287.
- Janvier, P. (1996b). *Early vertebrates*. Clarendon Press, Oxford.
- Janvier, P. (2015). Facts and fancies about early fossil chordates and vertebrates. *Nature* **520**, 483–489.
- Janvier, P., Arsenault, M. and Desbiens, S. (2004). Calcified cartilage in the paired fins of the osteostracan *Escuminaspis laticeps* (Traquair 1880), from the Late Devonian of Miguasha (Québec, Canada), with a consideration of the early evolution of the pectoral fin endoskeleton in vertebrates. *Journal of Vertebrate Paleontology* **24**, 773–779.
- Jardine, N. (1969). The observational and theoretical components of homology: a study based on the morphology of the dermal skull-roofs of rhipidistian fishes. *Biological Journal of the Linnean Society* **1**, 327–361.
- Jarvik, E. (1942). On the structure of the snout of crossopterygians and lower gnathostomes in general. *Zoologiska bidrag från Uppsala* **21**, 235–675.

- Jarvik, E. (1948). On the morphology and taxonomy of the Middle Devonian osteolepid fishes of Scotland. *Kungliga Svenska Vetenskapsakademiens Handlingar* **25**, 1–301.
- Jarvik, E. (1950). Middle Devonian vertebrates from Canning Land and Wegeners Halvö (East Greenland): Part II: Crossopterygii. *Meddelelser om Grønland* **96**, 1–132.
- Jarvik, E. (1965). Die Raspelzunge der Cyclostomen und die pentadactyle Extremität der Tetrapoden als Beweise für monophyletische Herkunft. *Zoologischer Anzeiger* **175**, 101–143.
- Jarvik, E. (1972). Middle and upper devonian porolepiformes from East Greenland with special reference to *Glyptolepis groenlandica* N. Sp.: and a discussion on the structure of the head in the porolepiformes. *Palaeontographica Abteilung A Palaeozoologie-Stratigraphie* **167**, 180–214.
- Jarvik, E. (1977). The systematic position of acanthodian fishes. In *Problems in vertebrate evolution* (ed. S. M. Andrews, R. S. Miles and A. D. Walker), pp. 199–224. Academic, London.
- Jarvik, E. (1980). *Basic structure and evolution of vertebrates*. Academic Press, London.
- Jessen, H. (1975). A new choanate fish, *Powichthys thorsteinssoni* n.g., n. sp., from the early Lower Devonian of the Canadian Arctic Archipelago. *Colloques Internationaux du Centre National de la Recherche Scientifique* **218**, 214–222.

- Ji, C., Jiang, D.-Y., Motani, R., Rieppel, O., Hao, W.-C. and Sun, Z.-Y. (2016). Phylogeny of the Ichthyopterygia incorporating recent discoveries from South China. *Journal of Vertebrate Paleontology* **36**, e1025956.
- Jia, L.-T., Zhu, M. and Zhao, W.-J. (2010). A new antiarch fish from the Upper Devonian Zhongning Formation of Ningxia, China. *Palaeoworld* **19**, 136–145.
- Johanson, Z. (2002). Vascularization of the osteostracan and antiarch (Placodermi) pectoral fin: similarities, and implications for placoderm relationships. *Lethaia* **35**, 169–186.
- Johnels, A. G. (1956). On the origin of the electric organ in *Malapterurus electricus*. *Journal of Cell Science* **3**, 455–463.
- Johnston, J. B. (1905). The cranial nerve components of *Petromyzon*. *Gegenbaurs Morphologisches Jahrbuch* **34**, 149–203.
- Jombart, T., Aanensen, D. M., Baguelin, M., Birrell, P., Cauchemez, S., Camacho, A., Colijn, C., Collins, C., Cori, A. and Didelot, X. (2014). OutbreakTools: A new platform for disease outbreak analysis using the R software. *Epidemics* **7**, 28–34.
- Jørgensen, J. M. (1980). The morphology of the Lorenzinian ampullae of the sturgeon *Acipenser ruthenus* (Pisces: Chondrostei). *Acta Zoologica* **61**, 87–92.
- Jørgensen, J. M. (1982). Fine structure of the ampullary organs of the bichir *Polypterus senegalus* Cuvier, 1829 (Pisces: Brachiopterygii) with some notes on the phylogenetic development of electroreceptors. *Acta Zoologica* **63**, 211–217.

- Jørgensen, J. M. (1989). Evolution of octavolateralis sensory cells. In *The Mechanosensory Lateral Line, Neurobiology and Evolution* (ed. S. Coombs, P. Görner and H. Münz), pp. 115–145. Springer, New York.
- Jørgensen, J. M. (2005). Morphology of electroreceptive sensory organs. In *Electroreception* (ed. T. H. Bullock, C. D. Hopkins, A. N. Popper and R. R. Fay), pp. 47–67. Springer, New York.
- Jørgensen, J. M. (2011). The lateral line system in lungfishes: mechanoreceptive neuromasts and electroreceptive ampullary organs. In *The Biology of Lungfishes* (ed. J. M. Jørgensen and J. Joss), pp. 477–492. CRC Press, Enfield.
- Jørgensen, J. M., Flock, Å. and Wersäll, J. (1972). The Lorenzinian ampullae of *Polyodon spathula*. *Zeitschrift für Zellforschung und Mikroskopische Anatomie* **130**, 362–377.
- Kajiura, S. M. (2001). Head morphology and electrosensory pore distribution of carcharhinid and sphyrnid sharks. *Environmental Biology of Fishes* **61**, 125–133.
- Kalmijn, A. J. (1971). The electric sense of sharks and rays. *Journal of Experimental Biology* **55**, 371–383.
- Kalmijn, A. J. (1974). The detection of electric fields from inanimate and animate sources other than electric organs. In *Electroreceptors and Other Specialized Receptors in Lower Vertebrates* (ed. A. Fessard), pp. 147–200. Springer, New York.
- Karatajute-Talimaa, V. and Predtechenskyj, N. (1995). The distribution of the vertebrates in the Late Ordovician and Early Silurian palaeobasins of the

- Siberian Platform. *Bulletin du Muséum national d'histoire naturelle. Section C, Sciences de la terre, paléontologie, géologie, minéralogie* **17**, 39–55.
- Karatujute-Talimaa, V., Novitskaya, L. I., Rozman, K. S. and Sodov, Z. (1990). *Mongolepis*—a new lower Silurian genus of elasmobranchs from Mongolia. *Paleontologicheskii Zhurnal* **1990**, 76–86.
- Kembel, S. W., Cowan, P. D., Helmus, M. R., Cornwell, W. K., Morlon, H., Ackerly, D. D., Blomberg, S. P. and Webb, C. O. (2010). Picante: R tools for integrating phylogenies and ecology. *Bioinformatics* **26**, 1463–1464.
- Kemp, A. (2014). Skin structure in the snout of the Australian lungfish, *Neoceratodus forsteri* (Osteichthyes: Dipnoi). *Tissue and Cell* **46**, 397–408.
- Kemp, A. (2017). Cranial nerves in the Australian lungfish, *Neoceratodus forsteri*, and in fossil relatives (Osteichthyes: Dipnoi). *Tissue and Cell* **49**, 45–55.
- Kemp, T. S. (1988). Haemothermia or Archosauria? The interrelationships of mammals, birds and crocodiles. *Zoological Journal of the Linnean Society* **92**, 67–104.
- King, B. and Lee, M. S. Y. (2015). Ancestral state reconstruction, rate heterogeneity, and the evolution of reptile viviparity. *Systematic Biology* **64**, 532–544.
- King, B., Qiao, T., Lee, M. S., Zhu, M. and Long, J. A. (2017). Bayesian Morphological Clock Methods Resurrect Placoderm Monophyly and Reveal Rapid Early Evolution in Jawed Vertebrates. *Systematic Biology* **66**, 499–516.
- Klein, A. and Bleckmann, H. (2015). Function of lateral line canal morphology. *Integrative zoology* **10**, 111–121.

- Klein, A., Münz, H. and Bleckmann, H. (2013). The functional significance of lateral line canal morphology on the trunk of the marine teleost *Xiphister atropurpureus* (Stichaeidae). *Journal of Comparative Physiology A* **199**, 735–749.
- Klembara, J. (1994). Electroreceptors in the Lower Permian tetrapod *Discosauriscus austriacus*. *Palaeontology* **37**, 609–626.
- Kolaczkowski, B. and Thornton, J. W. (2004). Performance of maximum parsimony and likelihood phylogenetics when evolution is heterogeneous. *Nature* **431**, 980–984.
- Kramer, B. (1996). *Electroreception and Communication in Fishes*. Gustav Fischer Verlag, Stuttgart.
- Kück, P., Mayer, C., Wägele, J.-W. and Misof, B. (2012). Long branch effects distort maximum likelihood phylogenies in simulations despite selection of the correct model. *PloS one* **7**, e36593.
- Kuratani, S. (2012). Evolution of the vertebrate jaw from developmental perspectives. *Evolution & development* **14**, 76–92.
- Kuratani, S., Ueki, T., Aizawa, S. and Hirano, S. (1997). Peripheral development of cranial nerves in a cyclostome, *Lampetra japonica*: morphological distribution of nerve branches and the vertebrate body plan. *Journal of Comparative Neurology* **384**, 483–500.
- Lamsdell, J. C. (2016). Horseshoe crab phylogeny and independent colonizations of fresh water: ecological invasion as a driver for morphological innovation. *Palaeontology* **59**, 181–194.
- Lamsdell, J. C. and Selden, P. A. (2017). From success to persistence: Identifying an evolutionary regime shift in the diverse Paleozoic aquatic arthropod

- group Eurypterida, driven by the Devonian biotic crisis. *Evolution* **71**, 95–110.
- Lane, J. A. (2010). Morphology of the braincase in the Cretaceous hybodont shark *Tribodus limae* (Chondrichthyes: Elasmobranchii), based on CT scanning. *American Museum Novitates* **3681**, 1–70.
- Lee, M. S., Cau, A., Naish, D. and Dyke, G. J. (2014a). Dinosaur evolution. Sustained miniaturization and anatomical innovation in the dinosaurian ancestors of birds. *Science* **345**, 562–6.
- Lee, M. S. Y. (1998). Convergent evolution and character correlation in burrowing reptiles: towards a resolution of squamate relationships. *Biological Journal of the Linnean Society* **65**, 369–453.
- Lee, M. S. Y. (2016). Multiple morphological clocks and total-evidence tip-dating in mammals. *Biology Letters* **12**, 20160033.
- Lee, M. S. Y., Cau, A., Naish, D. and Dyke, G. J. (2014b). Morphological clocks in paleontology, and a mid-Cretaceous origin of crown Aves. *Systematic Biology* **63**, 442–449.
- Lewis, P. O. (2001). A likelihood approach to estimating phylogeny from discrete morphological character data. *Systematic Biology* **50**, 913–925.
- Limaye, A. (2012). Drishti, a volume exploration and presentation tool. *SPIE Developments in X-Ray Tomography* **8506**, 85060X.
- Lisney, T. J. (2010). A review of the sensory biology of chimaeroid fishes (Chondrichthyes; Holocephali). *Reviews in Fish Biology and Fisheries* **20**, 571–590.
- Lissmann, H. W. (1951). Continuous Electrical Signals from the Tail of a Fish, *Gymnarchus niloticus* Cuv. *Nature* **167**, 201–202.

- Lissmann, H. W. and Machin, K. E. (1958). The mechanism of object location in *Gymnarchus niloticus* and similar fish. *Journal of Experimental Biology* **35**, 451–486.
- Liu, Y.-H. (1991). On a new petalichthyid, *Eurycaraspis incilis* gen. et sp. nov., from the middle Devonian of Zhanyi, Yunnan. In *Early Vertebrates and Related Problems of Evolutionary Biology* (ed. M.-M. Chang, Y.-H. Liu and G.-R. Zhang), pp. 139–177. Science Press, Beijing.
- Lockwood, C. (1998). Stratigraphy and phylogeny. *Evolutionary Anthropology: Issues, News, and Reviews* **6**, 153–154.
- Long, J. A. (1984a). New phyllolepid from Victoria and the relationships of the group. In *Proceedings of the Linnean Society of New South Wales*, vol. 107, pp. 263–308.
- Long, J. A. (1984b). New placoderm fishes from the Early Devonian Buchan Group, eastern Victoria. *Proceedings of the Royal Society of Victoria* **96**, 173–186.
- Long, J. A. (1988a). A new camuropiscid arthrodire (Pisces: Placodermi) from Gogo, Western Australia. *Zoological Journal of the Linnean Society* **94**, 233–258.
- Long, J. A. (1988b). New palaeoniscoid fishes from the Late Devonian and Early Carboniferous of Victoria. *Memoirs of the Association of Australasian Palaeontologists* **7**, 1–64.
- Long, J. A. (1992). Cranial anatomy of two new late Devonian lungfishes (Pisces: Dipnoi) from Mount Howitt, Victoria. *Records of the Australian Museum* **44**, 299–318.

- Long, J. A. (1995). A new plourdosteid arthrodire from the Upper Devonian Gogo Formation of Western Australia. *Palaeontology* **38**, 39–62.
- Long, J. A. (1997). Ptyctodontid fishes (Vertebrata, Placodermi) from the Late Devonian Gogo Formation, Western Australia, with a revision of the European genus *Ctenurella* Ørvig, 1960. *Geodiversitas* **19**, 515–555.
- Long, J. A. (1999). A new genus of fossil coelacanth (Osteichthyes: Coelacanthiformes) from the Middle Devonian of Southeastern Australia. *Records of the Western Australian Museum Supplement* **57**, 37–53.
- Long, J. A. (2001). On the relationships of *Psarolepis* and the onychodontiform fishes. *Journal of Vertebrate Paleontology* **21**, 815–820.
- Long, J. A., Barwick, R. E. and Campbell, K. S. W. (1997). Osteology and functional morphology of the osteolepiform fish *Gogonasus andrewsae* Long, 1985, from the Upper Devonian Gogo Formation, Western Australia. *Records of the Western Australian Museum Supplement* **53**, 1–89.
- Long, J. A., Mark-Kurik, E., Johanson, Z., Lee, M. S., Young, G. C., Min, Z., Ahlberg, P. E., Newman, M., Jones, R. and Den Blaauwen, J. (2015). Copulation in antiarch placoderms and the origin of gnathostome internal fertilization. *Nature* **517**, 196–199.
- Long, J. A., Mark-Kurik, E. and Young, G. C. (2014). Taxonomic revision of buchanosteoid placoderms (Arthrodira) from the Early Devonian of south-eastern Australia and Arctic Russia. *Australian Journal of Zoology* **62**, 26–43.
- Long, J. A. and Trinajstić, K. (2010). The Late Devonian Gogo Formation lagerstätte of Western Australia: exceptional early vertebrate

- preservation and diversity. *Annual Review of Earth and Planetary Sciences* **38**, 255–279.
- Long, J. A., Trinajstić, K. and Johanson, Z. (2009). Devonian arthrodire embryos and the origin of internal fertilization in vertebrates. *Nature* **457**, 1124.
- Long, J. A., Trinajstić, K., Young, G. C. and Senden, T. (2008). Live birth in the Devonian period. *Nature* **453**, 650–652.
- Long, J. A. and Young, G. C. (1988). Acanthothoracid remains from the Early Devonian of New South Wales, including a complete sclerotic capsule and pelvic girdle. *Memoirs of the Association of Australasian Palaeontologists* **7**, 65-80.
- Lorenzini, S. (1678). *Osservazioni intorno alle Torpedini. vol 1*, Florence.
- Løvtrup, S. (1976). *The phylogeny of Vertebrata*. Wiley, London.
- Lu, J., Giles, S., Friedman, M., den Blaauwen, J. L. and Zhu, M. (2016a). The oldest actinopterygian highlights the cryptic early history of the hyperdiverse ray-finned fishes. *Current Biology* **26**, 1602–1608.
- Lu, J., Zhu, M., Ahlberg, P. E., Qiao, T., Zhu, Y. a., Zhao, W. and Jia, L. (2016b). A Devonian predatory fish provides insights into the early evolution of modern sarcopterygians. *Science Advances* **2**, e1600154.
- Lu, J., Zhu, M., Long, J. A., Zhao, W., Senden, T. J., Jia, L. and Qiao, T. (2012). The earliest known stem-tetrapod from the Lower Devonian of China. *Nature Communications* **3**, 1160.
- Maddison, W. P. and Maddison, D. R. (2015). Mesquite: a modular system for evolutionary analysis. Version 3.04 <http://mesquiteproject.org>.

- Maisey, J., Miller, R. and Turner, S. (2009). The braincase of the chondrichthyan *Doliodus* from the Lower Devonian Campbellton formation of New Brunswick, Canada. *Acta Zoologica* **90**, 109–122.
- Maisey, J. G. (1986). Heads and tails: a chordate phylogeny. *Cladistics* **2**, 201–256.
- Maisey, J. G. (2001). A primitive chondrichthyan braincase from the Middle Devonian of Bolivia. In *Major events in early vertebrate evolution* (ed. P. Ahlberg), pp. 263–288. Taylor and Francis, London and New York.
- Maisey, J. G. (2005). Braincase of the Upper Devonian shark *Cladodoides wildungensis* (Chondrichthyes, Elasmobranchii), with observations on the braincase in early chondrichthyans. *Bulletin of the American Museum of Natural History* **288**, 1–103.
- Maisey, J. G. (2007). The braincase in Paleozoic symmoriiform and cladoselachian sharks. *Bulletin of the American Museum of Natural History* **307**, 1–122.
- Marcot, J. D. and Fox, D. L. (2008). StrataPhy: a new computer program for stratocladistic analysis. *Palaeontologia Electronica* **11**, 5A–16.
- Marshall, N. B. (1971). *Explorations in the life of fishes*. Harvard University Press.
- Märss, T., Afanassieva, O. B. and Blom, H. (2014). Biodiversity of the Silurian osteostracans of the East Baltic. *Earth and Environmental Science Transactions of the Royal Society of Edinburgh* **105**, 73–148.
- Marx, F. G. and Fordyce, R. E. (2015). Baleen boom and bust: a synthesis of mysticete phylogeny, diversity and disparity. *Open Science* **2**, 140434.
- Matzke, N. J. (2015). BEASTmaster: R tools for automated conversion of NEXUS data to BEAST2 XML format, for fossil tip-dating and other uses. Instructions at PhyloWiki, <http://phylo.wikidot.com/beastmaster>.

- Matzke, N. J. and Wright, A. (2016). Inferring node dates from tip dates in fossil Canidae: the importance of tree priors. *Biology Letters* **12**, 20160328.
- Meinke, D. K. (1984). A review of cosmine: its structure, development, and relationship to other forms of the dermal skeleton in osteichthyans. *Journal of Vertebrate Paleontology* **4**, 457–470.
- Miles, R. S. (1962). III.—*Gemuendenaspis* n. gen., an arthrodiran fish from the Lower Devonian Hunsrückschiefer of Germany. *Transactions of the Royal Society of Edinburgh* **65**, 59–77.
- Miles, R. S. (1965). Ventral thoracic neuromast lines of placoderm fishes. *Nature* **206**, 524–525.
- Miles, R. S. (1966). XV.—The placoderm fish *Rhachiosteus pterygiatus* Gross and its relationships. *Transactions of the Royal Society of Edinburgh* **66**, 377–392.
- Miles, R. S. (1971). The Holonematidae (placoderm fishes), a review based on new specimens of *Holonema* from the Upper Devonian of Western Australia. *Philosophical Transactions of the Royal Society of London B* **263**, 101–234.
- Miles, R. S. (1973a). Articulated acanthodian fishes from the old red sandstone of England: with a review of the structure and evolution of the acanthodian shoulder-girdle. *Bulletin of the British Museum (Natural History) Geology* **24**, 113–213.
- Miles, R. S. (1973b). Relationships of acanthodians. In *Interrelationships of fishes* (ed. P. H. Greenwood, R. S. Miles and C. Patterson), pp. 63–103. Zoological Journal of the Linnean Society, London.

- Miles, R. S. (1977). Dipnoan (lungfish) skulls and the relationships of the group: a study based on new species from the Devonian of Australia. *Zoological Journal of the Linnean Society* **61**, 1–328.
- Miles, R. S. and Dennis, K. (1979). A primitive eubrachythoracid arthrodire from Gogo, Western Australia. *Zoological Journal of the Linnean Society* **66**, 31–62.
- Miles, R. S. and Westoll, T. S. (1962). IX.—Two New Genera of coccosteid Arthrodira from the Middle Old Red Sandstone of Scotland, and their stratigraphical distribution. *Transactions of the Royal Society of Edinburgh* **65**, 179–210.
- Miles, R. S. and Westoll, T. S. (1968). IX.—The Placoderm Fish *Coccosteus cuspidatus* Miller ex Agassiz from the Middle Old Red Sandstone of Scotland. Part I. Descriptive Morphology. *Transactions of the Royal Society of Edinburgh* **67**, 373–476.
- Miles, R. S. and Young, G. C. (1977). Placoderm interrelationships reconsidered in the light of new ptyctodontids from Gogo, Western Australia. *Linnean Society Symposium Series* **4**, 123–198.
- Miller, M. A., Pfeiffer, W. and Schwartz, T. (2010). Creating the CIPRES Science Gateway for inference of large phylogenetic trees. In *Gateway Computing Environments Workshop (GCE), 2010*, pp. 1–8. IEEE.
- Miller, R. F., Cloutier, R. and Turner, S. (2003). The oldest articulated chondrichthyan from the Early Devonian period. *Nature* **425**, 501–504.
- Millot, J. and Anthony, J. (1965). *Anatomie de Latimeria chalumnae, Tome 2: Système nerveux et organes des sens*. CNRS, Paris.

- Miyashita, T. (2015). Fishing for jaws in early vertebrate evolution: a new hypothesis of mandibular confinement. *Biological Reviews* **91**, 611–657.
- Modrell, M. S., Bemis, W. E., Northcutt, R. G., Davis, M. C. and Baker, C. V. H. (2011). Electrosensory ampullary organs are derived from lateral line placodes in bony fishes. *Nature Communications* **2**, 496.
- Montgomery, J. C. (1989). Lateral line detection of planktonic prey. In *The mechanosensory lateral line* (ed. S. Coombs, P. Görner and H. Münz), pp. 561–574. Springer, New York.
- Montgomery, J. C. and Saunders, A. J. (1985). Functional morphology of the piper *Hyporhamphus ihi* with reference to the role of the lateral line in feeding. *Proceedings of the Royal Society of London B: Biological Sciences* **224**, 197–208.
- Moore, D. M. and McCarthy, I. D. (2014). Distribution of ampullary pores on three catshark species (*Apristurus* spp.) suggest a vertical-ambush predatory behaviour. *Aquatic Biology* **21**, 261–265.
- Morris, S. C. and Caron, J.-B. (2014). A primitive fish from the Cambrian of North America. *Nature* **512**, 419–422.
- Münz, H., Claas, B. and Fritsch, B. (1982). Electrophysiological evidence of electroreception in the axolotl *Siredon mexicanum*. *Neuroscience Letters* **28**, 107–111.
- Murray, R. W. (1960). Electrical sensitivity of the ampullae of Lorenzini. *Nature* **187**, 957.
- Murray, R. W. (1962). The response of the ampullae of Lorenzini of elasmobranchs to electrical stimulation. *Journal of Experimental Biology* **39**, 119–128.

- Nelson, G. J. (1969). Origin and diversification of teleostean fishes. *Annals of the New York Academy of Sciences* **167**, 18–30.
- Nelson, G. J. (1972). Cephalic sensory canals, pitlines, and the classification of esocoid fishes, with notes on galaxiid and other teleosts. *American Museum Novitates* **2492**, 1–37.
- New, J. G. (1997). The evolution of vertebrate electrosensory systems. *Brain, behavior and evolution* **50**, 244–252.
- Nicoll, R. S. (1977). Conodont apparatuses in Upper Devonian palaeoniscoid fish from the Canning Basin, Western Australia. *Bureau of Mineral Resources Journal of Australian Geology and Geophysics* **2**, 217–228.
- Norris, H. W. (1929). The distribution and innervation of the ampullae of Lorenzini of the dogfish, *Squalus acanthias*. Some comparisons with conditions in other plagiostomes and corrections of prevalent errors. *Journal of Comparative Neurology* **47**, 449–465.
- Northcutt, R. G. (1985). The brain and sense organs of the earliest vertebrates: reconstruction of a morphotype. In *Evolutionary Biology of Primitive Fishes* (ed. R. E. Foreman, A. Gorbman, J. M. Dodd and R. Olsson), pp. 81–112. Plenum, New York.
- Northcutt, R. G. (1986a). Electroreception in nonteleost bony fishes. In *Electroreception* (ed. Bullock T H and H. Wahnschaffe), pp. 257–285. John Wiley & Sons, New York.
- Northcutt, R. G. (1986b). Lungfish neural characters and their bearing on sarcopterygian phylogeny. *Journal of Morphology* **190**, 277–297.

- Northcutt, R. G. (1989). The phylogenetic distribution and innervation of craniate mechanoreceptive lateral lines. In *The mechanosensory lateral line* (ed. S. Coombs, P. Görner and H. Münz), pp. 17–78. Springer, New York.
- Northcutt, R. G. (2008). Historical hypotheses regarding segmentation of the vertebrate head. *Integrative and Comparative Biology* **48**, 611–619.
- Northcutt, R. G. and Bemis, W. E. (1993). Cranial nerves of the coelacanth, *Latimeria chalumnae* [Osteichthyes: Sarcopterygii: Actinistia], and comparisons with other craniata. *Brain, behavior and evolution* **42**, 1–76.
- Northcutt, R. G., Brändle, K. and Fritsch, B. (1995). Electroreceptors and mechanosensory lateral line organs arise from single placodes in axolotls. *Developmental Biology* **168**, 358–373.
- Northcutt, R. G. and Gans, C. (1983). The genesis of neural crest and epidermal placodes: a reinterpretation of vertebrate origins. *Quarterly Review of Biology* **58**, 1–28.
- O'Connor, A. and Wills, M. A. (2016). Measuring Stratigraphic Congruence Across Trees, Higher Taxa, and Time. *Systematic Biology* **65**, 792–811.
- O'Reilly, J. E., Puttick, M. N., Parry, L., Tanner, A. R., Tarver, J. E., Fleming, J., Pisani, D. and Donoghue, P. C. (2016). Bayesian methods outperform parsimony but at the expense of precision in the estimation of phylogeny from discrete morphological data. *Biology Letters* **12**, 20160081.
- Obara, S. (1976). Mechanism of electroreception in ampullae of Lorenzini of the marine catfish *Plotosus*. In *Electrobiology of Nerve, Synapse and Muscle* (ed. J. P. Reuben, D. P. Purpura, M. L. V. Bennett and E. R. Kandel), pp. 128–147. Raven Press, New York.

- Olive, S., Goujet, D., Lelièvre, H. and Janjou, D. (2011). A new Placoderm fish (Acanthothoraci) from the Early Devonian Jauf Formation (Saudi Arabia). *Geodiversitas* **33**, 393–409.
- Orme, D., Freckleton, R., Thomas, G., Petzoldt, T., Fritz, S., Isaac, N. and Pearse, W. (2013). caper : comparative analysis of phylogenetics and evolution in R. In *R package version 0.5.2*. <https://CRAN.R-project.org/package=caper>.
- Øravig, T. (1960). New finds of acanthodians, arthrodires, crossopterygians, ganoids and dipnoans in the upper Middle Devonian calcareous flags (oberer Plattenkalk) of the Bergisch Gladbach-Paffrath Trough. *Paläontologische Zeitschrift* **34**, 295–335.
- Øravig, T. (1961). New finds of acanthodians, arthrodires, crossopterygians, ganoids and dipnoans in the upper Middle Devonian calcareous flags (Oberer Plattenkalk) of the Bergisch Gladbach-Paffrath trough. *Paläontologische Zeitschrift* **35**, 10–27.
- Øravig, T. (1962). Y at-il une relation directe entre les arthrodires ptyctodontides et les holocephales. *Colloques Internationaux du Centre National de la Recherche Scientifique* **104**, 49–61.
- Øravig, T. (1969). Cosmine and cosmine growth. *Lethaia* **2**, 241–260.
- Øravig, T. (1971). Comments on the lateral line system of some brachythoracid and ptyctodontid arthrodires. *Zoologica Scripta* **1**, 5–35.
- Øravig, T. (1973). Fossila fisktänder i svepelektronmikroskopet: gamlafrågeställningar i ny belysning. *Fauna Flora* **68**, 166–173.
- Øravig, T. (1975). Description, with special reference to the dermal skeleton, of a new radotiniid arthrodire from the Gedinnian of Arctic Canada. *Colloques*

- Internationaux du Centre National de la Recherche Scientifique* **218**, 43–71.
- Ørvig, T. (1989). Histologic studies of ostracoderms, placoderms and fossil elasmobranchs. 6. Hard tissues of Ordovician vertebrates. *Zoologica Scripta* **18**, 427–446.
- Ota, K. G., Fujimoto, S., Oisi, Y. and Kuratani, S. (2011). Identification of vertebra-like elements and their possible differentiation from sclerotomes in the hagfish. *Nature Communications* **2**, 373.
- Ota, K. G., Fujimoto, S., Oisi, Y. and Kuratani, S. (2013). Late development of hagfish vertebral elements. *Journal of Experimental Zoology Part B: Molecular and Developmental Evolution* **320**, 129–139.
- Pan, J. (1986). Notes on Silurian vertebrates of China. *Bulletin of the Chinese Academy of Geological Sciences* **15**, 227–249.
- Pan, Z., Zhu, M., Zhu, Y. A. and Jia, L. (2015). A new petalichthyid placoderm from the Early Devonian of Yunnan, China. *Comptes Rendus Palevol* **14**, 125–137.
- Paradis, E., Claude, J. and Strimmer, K. (2004). APE: analyses of phylogenetics and evolution in R language. *Bioinformatics* **20**, 289–290.
- Patterson, C. (1975). The braincase of pholidophorid and leptolepid fishes, with a review of the actinopterygian braincase. *Philosophical Transactions of the Royal Society of London B: Biological Sciences* **269**, 275–579.
- Patterson, C. (1981). Significance of fossils in determining evolutionary relationships. *Annual Review of Ecology and Systematics* **12**, 195–223.
- Perea, D., Soto, M., Sterli, J., Mesa, V., Toriño, P., Roland, G. and Da Silva, J. (2014). *Tacuarembemys kusteræ*, gen. et sp. nov., a new late Jurassic—? earliest

- Cretaceous continental turtle from western Gondwana. *Journal of Vertebrate Paleontology* **34**, 1329–1341.
- Platnick, N. I. (1979). Philosophy and the transformation of cladistics. *Systematic Zoology* **28**, 537–546.
- Poplin, C. M. (1974). *Etude de quelques paleoniscides pennsylvaniens du Kansas*. CNRS, Paris.
- Poropat, S. F., Mannion, P. D., Upchurch, P., Hocknull, S. A., Kear, B. P., Kundrát, M., Tischler, T. R., Sloan, T., Sinapius, G. H. and Elliott, J. A. (2016). New Australian sauropods shed light on Cretaceous dinosaur palaeobiogeography. *Scientific reports* **6**.
- Pradel, A., Maisey, J. G., Tafforeau, P. and Janvier, P. (2009). An enigmatic gnathostome vertebrate skull from the Middle Devonian of Bolivia. *Acta Zoologica* **90**, 123–133.
- Pradel, A., Tafforeau, P., Maisey, J. G. and Janvier, P. (2011). A new Paleozoic Symmoriiformes (chondrichthyes) from the Late Carboniferous of Kansas (USA) and cladistic analysis of early chondrichthyans. *PloS one* **6**, e24938.
- Prichonnet, G., Di Vergilio, M. and Chidiac, Y. (1996). Stratigraphical, sedimentological and paleontological context of the Escuminac Formation: paleoenvironmental hypotheses. In *Devonian fishes and plants of Miguasha, Quebec, Canada* (ed. H.-P. Schultze and R. Cloutier), pp. 23–36. Verlag Dr. Friedrich Pfeil, München.
- Proske, U., Gregory, J. E. and Iggo, A. (1998). Sensory receptors in monotremes. *Philosophical Transactions of the Royal Society of London B* **353**, 1187–1198.

- Puttick, M. N., O'Reilly, J. E., Tanner, A. R., Fleming, J. F., Clark, J., Holloway, L., Lozano-Fernandez, J., Parry, L. A., Tarver, J. E. and Pisani, D. (2017). Uncertain-tree: discriminating among competing approaches to the phylogenetic analysis of phenotype data. *Proceedings of the Royal Society B* **284**, 20162290.
- Pyron, R. A. (2011). Divergence time estimation using fossils as terminal taxa and the origins of Lissamphibia. . *Systematic Biology* **60**, 466–481.
- Qiao, T., King, B., Long, J. A., Ahlberg, P. E. and Zhu, M. (2016). Early gnathostome phylogeny revisited: multiple method consensus. *PloS one* **11**, e0163157.
- Qu, Q., Blom, H., Sanchez, S. and Ahlberg, P. (2015a). Three - dimensional virtual histology of silurian osteostracan scales revealed by synchrotron radiation microtomography. *Journal of Morphology* **276**, 873-888.
- Qu, Q., Haitina, T., Zhu, M. and Ahlberg, P. E. (2015b). New genomic and fossil data illuminate the origin of enamel. *Nature* **526**, 108–111.
- Qu, Q., Sanchez, S., Zhu, M., Blom, H. and Ahlberg, P. E. (2017). The origin of novel features by changes in developmental mechanisms: ontogeny and three - dimensional microanatomy of polyodontode scales of two early osteichthyans. *Biological Reviews* **92**, 1189-1212.
- Qu, Q. M., Zhu, M. and Zhao, W. J. (2010). Silurian atmospheric O₂ changes and the early radiation of gnathostomes. *Palaeoworld* **19**, 146–159.
- Rambaut, A., Suchard, M. A., Xie, D. and Drummond, A. J. (2014). Tracer v1.6, Available from <http://beast.bio.ed.ac.uk/Tracer>.
- Ramírez, M. J. (2007). Homology as a parsimony problem: a dynamic homology approach for morphological data. *Cladistics* **23**, 588–612.

- Raschi, W. (1978). Notes on the gross functional morphology of the ampullary system in two similar species of skates, *Raja erinacea* and *R. ocellata*. *Copeia* **1978**, 48–53.
- Raschi, W. (1986). A morphological analysis of the ampullae of Lorenzini in selected skates (Pisces, Rajoidei). *Journal of Morphology* **189**, 225–247.
- Raschi, W., Keithan, E. D. and Rhee, W. C. H. (1997). Anatomy of the ampullary electroreceptor in the freshwater stingray, *Himantura signifer*. *Copeia* **1997**, 101–107.
- Reeder, T. W., Townsend, T. M., Mulcahy, D. G., Noonan, B. P., Wood Jr, P. L., Sites Jr, J. W. and Wiens, J. J. (2015). Integrated analyses resolve conflicts over squamate reptile phylogeny and reveal unexpected placements for fossil taxa. *PloS one* **10**, e0118199.
- Revell, L. J. (2012). phytools: an R package for phylogenetic comparative biology (and other things). *Methods in Ecology and Evolution* **3**, 217–223.
- Richter, M. and Smith, M. (1995). A microstructural study of the ganoine tissue of selected lower vertebrates. *Zoological Journal of the Linnean Society* **114**, 173–212.
- Ritchie, A. (1973). *Wuttagoonaspis* gen. nov., an unusual arthrodire from the Devonian of Western New South Wales, Australia. *Palaeontographica Abteilung A Palaeozoologie-Stratigraphie* **143**, 58–72.
- Robineau, D. (1975). The jugular vein system and its homologies in *Latimeria chalmunae* (Pisces, Crossopterygii, Coelacanthidae). *Comptes rendus hebdomadaires des seances de l'Academie des sciences. Serie D: Sciences naturelles* **281**, 45–48.

- Robinson, D. F. and Foulds, L. R. (1981). Comparison of phylogenetic trees. *Mathematical Biosciences* **53**, 131–147.
- Ronan, M. (1988). Anatomical and physiological evidence for electroreception in larval lampreys. *Brain Research* **448**, 173–177.
- Ronan, M. C. and Bodznick, D. (1986). End buds: non-ampullary electroreceptors in adult lampreys. *Journal of Comparative Physiology A* **158**, 9–15.
- Ronquist, F., Klopfstein, S., Vilhelmsen, L., Schulmeister, S., Murray, D. L. and Rasnitsyn, A. P. (2012a). A total-evidence approach to dating with fossils, applied to the early radiation of the Hymenoptera. *Systematic Biology* **61**, 973–999.
- Ronquist, F., Teslenko, M., van der Mark, P., Ayres, D. L., Darling, A., Höhna, S., Larget, B., Liu, L., Suchard, M. A. and Huelsenbeck, J. P. (2012b). MrBayes 3.2: efficient Bayesian phylogenetic inference and model choice across a large model space. *Systematic Biology* **61**, 539–542.
- Rosen, D. E., Forey, P. L., Gardiner, B. G. and Patterson, C. (1981). Lungfishes, tetrapods, paleontology, and plesiomorphy. *Bulletin of the American Museum of Natural History* **167**, 159–267.
- Roth, A. (1973). Electroreceptors in Brachiopterygii and Dipnoi. *Naturwissenschaften* **60**, 106–106.
- Roth, A. and Tschardtke, H. (1976). Ultrastructure of the ampullary electroreceptors in lungfish and Brachiopterygii. *Cell and tissue research* **173**, 95–108.
- Rücklin, M., Donoghue, P. C., Johanson, Z., Trinajstić, K., Marone, F. and Stampanoni, M. (2012). Development of teeth and jaws in the earliest jawed vertebrates. *Nature* **491**, 748–751.

- Ruta, M., Coates, M. I. and Quicke, D. L. J. (2003). Early tetrapod relationships revisited. *Biological Reviews* **78**, 251–345.
- Sakellariou, A., Sawkins, T., Senden, T. and Limaye, A. (2004). X-ray tomography for mesoscale physics applications. *Physica A: Statistical Mechanics and its Applications* **339**, 152–158.
- Sand, A. (1938). The function of the ampullae of Lorenzini, with some observations on the effect of temperature on sensory rhythms. *Proceedings of the Royal Society of London B* **125**, 524–553.
- Sanderson, M. J. and Kim, J. (2000). Parametric phylogenetics? *Systematic Biology* **49**, 817–829.
- Sansom, I. J., Davies, N. S., Coates, M. I., Nicoll, R. S. and Ritchie, A. (2012). Chondrichthyan - like scales from the Middle Ordovician of Australia. *Palaeontology* **55**, 243–247.
- Sansom, I. J., Smith, M. M. and Smith, M. P. (2001). The Ordovician radiation of vertebrates. In *Major Events in Early Vertebrate Evolution* (ed. P. E. Ahlberg), pp. 156–171. Taylor & Francis, London.
- Sansom, R. S. (2009). Phylogeny, classification and character polarity of the Osteostraci (Vertebrata). *Journal of Systematic Palaeontology* **7**, 95–115.
- Sansom, R. S., Freedman, K., Gabbott, S. E., Aldridge, R. J. and Purnell, M. A. (2010). Taphonomy and affinity of an enigmatic Silurian vertebrate, *Jamoytius kerwoodi* White. *Palaeontology* **53**, 1393–1409.
- Schaeffer, B. (1971). *The braincase of the holostean fish Macrepistius, with comments on neurocranial ossification in the Actinopterygii*. American Museum of Natural History.

- Schaeffer, B. (1975). Comments on the origin and basic radiation of the gnathostome fishes with particular reference to the feeding mechanism. *Colloques Internationaux du Centre National de la Recherche Scientifique* **218**, 101–109.
- Schaeffer, B. (1981). The xenacanth shark neurocranium, with comments on elasmobranch monophyly. *Bulletin of the American Museum of Natural History* **169**, 3–66.
- Schaeffer, B., Hecht, M. K. and Eldredge, N. (1972). Phylogeny and paleontology. In *Evolutionary biology* (ed. T. Donzhansky, M. K. Hecht and W. C. Steere), pp. 31–46. Appleton-Century-Crofts, New York.
- Schliep, K. P. (2010). phangorn: phylogenetic analysis in R. *Bioinformatics*, btq706.
- Schultze, H.-P. (1968). Palaeoniscoidea-Schuppen aus dem Unterdevon Australiens und Kanadas und aus dem Mitteldevon Spitzbergens. *Bulletin of the British Museum (Natural History) Geology* **16**, 341–368.
- Schultze, H.-P. (1992). Early Devonian actinopterygians (Osteichthyes, Pisces) from Siberia. In *Fossil Fishes as Living Animals* (ed. E. Mark-Kurik), pp. 233–242. Academy of Sciences of Estonia, Tallinn.
- Schultze, H.-P. (1996). The vertebrates of the Escuminac Formation. In *Devonian fishes and plants of Miguasha, Quebec, Canada* (ed. H.-P. Schultze and R. Cloutier), pp. 120–122. Verlag Dr. Friedrich Pfeil, München.
- Schultze, H.-P. (2016). Scales, enamel, cosmine, ganoine, and early osteichthyans. *Comptes Rendus Palevol* **15**, 83–102.

- Schultze, H.-P. and Cumbaa, S. L. (2001). *Dialipina* and the characters of basal actinopterygians. In *Major Events in Early Vertebrate Evolution* (ed. P. Ahlberg), pp. 315–332. Taylor and Francis, London and New York.
- Schultze, H.-P. and Cumbaa, S. L. (2017). A new Early Devonian (Emsian) arthrodire from the Northwest Territories, Canada, and its significance for paleogeographic reconstruction. *Canadian Journal of Earth Sciences* **54**, 461–476.
- Schwalbe, M. A., Bassett, D. K. and Webb, J. F. (2012). Feeding in the dark: lateral-line-mediated prey detection in the peacock cichlid *Aulonocara stuartgranti*. *Journal of Experimental Biology* **215**, 2060–2071.
- Shu, D.-G., Morris, S. C., Han, J., Zhang, Z.-F., Yasui, K., Janvier, P., Chen, L., Zhang, X.-L., Liu, J.-N. and Li, Y. (2003). Head and backbone of the Early Cambrian vertebrate *Haikouichthys*. *Nature* **421**, 526–529.
- Siddall, M. E. (1998). Forum. stratigraphic fit to phylogenies: a proposed solution. *Cladistics* **14**, 201–208.
- Sienknecht, U. J. (2013). Origin and development of hair cell orientation in the inner ear. In *Insights from comparative hearing research* (ed. C. Köppl, G. A. Manley, A. N. Popper and R. R. Fay), pp. 69–109. Springer, New York.
- Sire, J. Y., Donoghue, P. C. J. and Vickaryous, M. K. (2009). Origin and evolution of the integumentary skeleton in non - tetrapod vertebrates. *Journal of Anatomy* **214**, 409–440.
- Smith, A. (1998). Is the fossil record adequate. *Nature online debates* (ed. AB Smith).
- Smith, M. M. and Johanson, Z. (2003). Separate evolutionary origins of teeth from evidence in fossil jawed vertebrates. *Science* **299**, 1235–1236.

- Smith, M. M. and Sansom, I. J. (1997). Exoskeletal micro-remains of an Ordovician fish from the Harding Sandstone of Colorado. *Palaeontology* **40**, 645–658.
- Stadler, T. (2010). Sampling-through-time in birth–death trees. *Journal of Theoretical Biology* **267**, 396–404.
- Stensiö, E. A. (1927). The Downtonian and Devonian vertebrates of Spitsbergen. I, Family Cephalaspidae. *Skifter om Svalbard og Ishavet* **12**, 1–391.
- Stensiö, E. A. (1944). Contributions to the knowledge of the vertebrate fauna of the Silurian and Devonian of western Podolia. 2, Notes on Two Arthrodiras from the Downtonian of Podolia. *Arkiv för Zoologi* **35**, 1–83.
- Stensiö, E. A. (1963a). *Anatomical studies on the arthrodiran head*. Almqvist & Wiksell, Stockholm.
- Stensiö, E. A. (1963b). *The Brain and the Cranial Nerves in Fossil, Lower Craniate Vertebrates*. Universitetsforlaget, Oslo.
- Stensiö, E. A. (1969). Elasmobranchiomorphi Placodermata Arthrodiras. In *Traité de paléontologie*, vol. 4 (ed. J. Piveteau), pp. 71–692. Masson, Paris.
- Swartz, B. A. (2009). Devonian actinopterygian phylogeny and evolution based on a redescription of *Stegotrachelus finlayi*. *Zoological Journal of the Linnean Society* **156**, 750–784.
- Swofford, D. (2002). PAUP 4.0 b10: Phylogenetic analysis using parsimony. Sinauer Associates, Sunderland, MA, USA.
- Szabo, T., Kalmijn, A. J., Enger, P. S. and Bullock, T. H. (1972). Microampullary organs and a submandibular sense organ in the fresh water ray, *Potamotrygon*. *Journal of Comparative Physiology A* **79**, 15–27.

- Teeter, J. H., Szamier, R. B. and Bennett, M. V. L. (1980). Ampullary electroreceptors in the sturgeon *Scaphirhynchus platyrhynchus* (Rafinesque). *Journal of Comparative Physiology* **138**, 213–223.
- Theiss, S. M., Collin, S. P. and Hart, N. S. (2011). Morphology and distribution of the ampullary electroreceptors in wobbegong sharks: implications for feeding behaviour. *Marine Biology* **158**, 723–735.
- Thomson, K. S. (1965). The endocranium and associated structures in the Middle Devonian rhipidistian fish *Osteolepis*. *Proceedings of the Linnean Society of London* **176**, 181–195.
- Thomson, K. S. (1975). On the biology of cosmine. *Bulletin of the Peabody Museum of Natural History* **40**, 1–59.
- Thomson, K. S. (1977). On the individual history of cosmine and a possible electroreceptive function of the pore-canal system in fossil fishes. In *Problems in vertebrate evolution. Linnean Society Symposium Series* (ed. S. M. Andrews, R. S. Miles and A. D. Walker), pp. 247–271. Academic Press, London.
- Thomson, K. S. and Campbell, K. S. W. (1971). The structure and relationships of the primitive Devonian lungfish—*Dipnorhynchus sussmilchi* (Etheridge). *Bulletin of the Peabody Museum of Natural History* **38**, 1–109.
- Thorsteinsson, R. (1973). Dermal elements of a new lower vertebrate from Middle Silurian (Upper Wenlockian) Rocks of the Canadian Arctic Archipelago. *Palaeontographica Abteilung A*, 51–57.
- Tông-Dzuy, T., Phuong, T. H., Boucot, A. J., Goujet, D. and Janvier, P. (1997). Vertébrés siluriens du Viêt-nam central. *Comptes rendus de l'Académie des sciences. Série 2. Sciences de la terre et des planètes* **324**, 1023–1030.

- Trewin, N. H. (1985). Mass mortalities of Devonian fish—the Achanarras Fish Bed, Caithness. *Geology Today* **1**, 45–49.
- Tricas, T. C. (2001). The neuroecology of the elasmobranch electrosensory world: why peripheral morphology shapes behavior. *Environmental Biology of Fishes* **60**, 77–92.
- Tricas, T. C. and Sisneros, J. A. (2004). Ecological functions and adaptations of the elasmobranch electrosense. In *The Senses of Fish: Adaptations for the Reception of Natural Stimuli* (ed. G. Von der Emde, J. Mogdans and B. G. Kapoor), pp. 308–329. Kluwer Academic Publishers, Boston.
- Trinajstic, K. (1999). Scale morphology of the Late Devonian palaeoniscoid *Moythomasia durgaringa* Gardiner and Bartram, 1977. *Alcheringa* **23**, 9–19.
- Trinajstic, K., Boisvert, C., Long, J., Maksimenko, A. and Johanson, Z. (2015). Pelvic and reproductive structures in placoderms (stem gnathostomes). *Biological Reviews of the Cambridge Philosophical Society* **90**, 467–501.
- Trinajstic, K. and Long, J. A. (2009). A new genus and species of Ptyctodont (Placodermi) from the Late Devonian Gneudna Formation, Western Australia, and an analysis of Ptyctodont phylogeny. *Geological Magazine* **146**, 743–760.
- Trinajstic, K., Long, J. A., Johanson, Z., Young, G. and Senden, T. (2012). New morphological information on the ptyctodontid fishes (Placodermi, Ptyctodontida) from Western Australia. *Journal of Vertebrate Paleontology* **32**, 757–780.

- Trinajstic, K., Marshall, C., Long, J. and Bifield, K. (2007). Exceptional preservation of nerve and muscle tissues in Late Devonian placoderm fish and their evolutionary implications. *Biology Letters* **3**, 197–200.
- Trinajstic, K., Sanchez, S., Dupret, V., Tafforeau, P., Long, J., Young, G., Senden, T., Boisvert, C., Power, N. and Ahlberg, P. E. (2013). Fossil musculature of the most primitive jawed vertebrates. *Science* **341**, 160–164.
- Tuffley, C. and Steel, M. (1997). Links between maximum likelihood and maximum parsimony under a simple model of site substitution. *Bulletin of Mathematical Biology* **59**, 581–607.
- Turner, A. H., Pritchard, A. C. and Matzke, N. J. (2017). Empirical and Bayesian approaches to fossil-only divergence times: A study across three reptile clades. *PloS one* **12**, e0169885.
- van Netten, S. M. and Kroese, A. B. A. (1988). Dynamic behaviour and micromechanical properties of the cupula. In *The Mechanosensory Lateral Line, Neurobiology and Evolution* (ed. S. Coombs, P. Görner and H. Münz), pp. 247–263. Springer, New York.
- Vaškaninová, V. and Ahlberg, P. E. (2017). Unique diversity of acanthothoracid placoderms (basal jawed vertebrates) in the Early Devonian of the Prague Basin, Czech Republic: A new look at *Radotina* and *Holopetalichthys*. *PloS one* **12**, e0174794.
- Wagner, P. J. (1995). Stratigraphic tests of cladistic hypotheses. *Paleobiology* **21**, 153–178.
- Wang, M., Zheng, X., O'Connor, J. K., Lloyd, G. T., Wang, X., Wang, Y., Zhang, X. and Zhou, Z. (2015). The oldest record of Ornithuromorpha from the early cretaceous of China. *Nature Communications* **6**, 6987.

- Wang, N. and Dong, Z. (1989). Discovery of Late Silurian microfossils of Agnatha and fishes from Yunnan, China. *Acta Palaeontologica Sinica* **28**, 192–206.
- Wang, N.-Z., Donoghue, P. C., Smith, M. M. and Sansom, I. J. (2005). Histology of the galeaspid dermoskeleton and endoskeleton, and the origin and early evolution of the vertebrate cranial endoskeleton. *Journal of Vertebrate Paleontology* **25**, 745–756.
- Wängsjö, G. (1952). The Downtonian and Devonian vertebrates of Spitsbergen. IX, Morphologic and systematic studies of the Spitsbergen cephalaspids. *Norsk Polarinstitutt Skrifter* **97**, 1–611.
- Watson, D. M. S. (1937). The acanthodian fishes. *Philosophical Transactions of the Royal Society of London. Series B, Biological Sciences*, 49–146.
- Watson, D. M. S. (1954). A consideration of ostracoderms. *Philosophical Transactions of the Royal Society B* **238**, 1–25.
- Watt, M., Evans, C. S. and Joss, J. M. P. (1999). Use of electroreception during foraging by the Australian lungfish. *Animal Behaviour* **58**, 1039–1045.
- Webb, J. F. (1989). Gross morphology and evolution of the mechanoreceptive lateral-line system in teleost fishes. *Brain Behavior and Evolution* **33**, 34–43.
- Webb, J. F. (2013). Morphological diversity, development, and evolution of the mechanosensory lateral line system. In *The Lateral Line System* (ed. S. Coombs, H. Bleckmann, R. R. Fay and A. N. Popper), pp. 17–72. Springer, New York.
- Weisel, G. F. (1978). The integument and caudal filament of the shovelnose sturgeon, *Scaphirhynchus platyrhynchus*. *American Midland Naturalist*, 179–189.

- Westoll, T. S. (1936). On the structures of the dermal ethmoid shield of *Osteolepis*. *Geological Magazine* **73**, 157–171.
- Westoll, T. S. (1967). *Radotina* and other tesserate fishes. *Zoological Journal of the Linnean Society* **47**, 83–98.
- White, E. I. (1978). The larger arthrodiran fishes from the area of the Burrinjuck Dam, NSW. *The Transactions of the Zoological Society of London* **34**, 149–262.
- White, E. I. and Toombs, H. A. (1972). The buchanosteid arthrodiras of Australia. *Bulletin of the British Museum (Natural History) Geology* **22**, 379–419.
- Whitear, M. and Lane, E. B. (1983). Multivillous cells: epidermal sensory cells of unknown function in lamprey skin. *Journal of Zoology* **201**, 259–272.
- Whitehead, D. L., Tibbetts, I. R. and Daddow, L. Y. M. (1999). Distribution and morphology of the ampullary organs of the salmontail catfish, *Arius graeffei*. *Journal of Morphology* **239**, 97–105.
- Whitehead, D. L., Tibbetts, I. R. and Daddow, L. Y. M. (2000). Ampullary organ morphology of freshwater salmontail catfish, *Arius graeffei*. *Journal of Morphology* **246**, 142–149.
- Whitehead, D. L., Tibbetts, I. R. and Daddow, L. Y. M. (2003). Microampullary organs of a freshwater eel - tailed catfish, *Plotosus (tandanus) tandanus*. *Journal of Morphology* **255**, 253–260.
- Wilkens, L. A., Russell, D. F., Pei, X. and Gurgens, C. (1997). The paddlefish rostrum functions as an electrosensory antenna in plankton feeding. *Proceedings of the Royal Society of London B: Biological Sciences* **264**, 1723–1729.

- Williams, M. E. (1998). A new specimen of *Tamiodontis vetustus* (Chondrichthyes, Ctenacanthoidea) from the late Devonian Cleveland Shale of Ohio. *Journal of Vertebrate Paleontology* **18**, 251–260.
- Wills, M. A. (1999). Congruence between phylogeny and stratigraphy: randomization tests and the gap excess ratio. *Systematic Biology* **48**, 559–580.
- Winther-Janson, M., Wueringer, B. E. and Seymour, J. E. (2012). Electroreceptive and mechanoreceptive anatomical specialisations in the epaulette shark (*Hemiscyllium ocellatum*). *PloS one* **7**, e49857.
- Witmer, L. M. (1995). The extant phylogenetic bracket and the importance of reconstructing soft tissues in fossils. In *Functional morphology in vertebrate paleontology* (ed. J. J. Thomason), pp. 19–33. Cambridge University Press, New York.
- Wright, A. M. and Hillis, D. M. (2014). Bayesian analysis using a simple likelihood model outperforms parsimony for estimation of phylogeny from discrete morphological data. *PloS one* **9**, e109210.
- Wueringer, B. E. and Tibbetts, I. R. (2008). Comparison of the lateral line and ampullary systems of two species of shovelnose ray. *Reviews in Fish Biology and Fisheries* **18**, 47–64.
- Yang, Z. (1996). Among-site rate variation and its impact on phylogenetic analyses. *Trends in Ecology & Evolution* **11**, 367–372.
- Young, G. C. (1979). New information on the structure and relationships of *Buchanosteus* (Placodermi: Euarthrodira) from the Early Devonian of New South Wales. *Zoological Journal of the Linnean Society* **66**, 309–352.

- Young, G. C. (1980). A new Early Devonian placoderm from New South Wales, Australia, with a discussion of placoderm phylogeny. *Palaeontographica Abteilung A Palaeozoologie-Stratigraphie* **167**, 10–76.
- Young, G. C. (1984). Reconstruction of the jaws and braincase in the Devonian placoderm fish *Bothriolepis*. *Palaeontology* **27**, 635–661.
- Young, G. C. (1985). Further petalichthyid remains (placoderm fishes, Early Devonian) from the Taemas-Wee Jasper region, New South Wales. *Bureau of Mineral Resources Journal of Australian Geology and Geophysics* **9**, 121–131.
- Young, G. C. (1986). The relationships of placoderm fishes. *Zoological Journal of the Linnean Society* **88**, 1–57.
- Young, G. C. (1991). The first armoured agnathan vertebrates from the Devonian of Australia. In *Early Vertebrates and Related Problems Of Evolutionary Biology* (ed. M.-M. Chang, Y.-H. Liu and G.-R. Zhang), pp. 41–65. Science Press, Beijing.
- Young, G. C. (1997). Ordovician microvertebrate remains from the Amadeus Basin, central Australia. *Journal of Vertebrate Paleontology* **17**, 1–25.
- Young, G. C. (2003). A new species of *Atlantidosteus* Lelièvre, 1984 (Placodermi, Arthrodira, Brachythoraci) from the Middle Devonian of the Broken River area (Queensland, Australia). *Geodiversitas* **25**, 681–694.
- Young, G. C. (2008). The relationships of antiarchs (Devonian placoderm fishes)—evidence supporting placoderm monophyly. *Journal of Vertebrate Paleontology* **28**, 626–636.

- Young, G. C. (2010). Placoderms (armored fish): dominant vertebrates of the Devonian period. *Annual Review of Earth and Planetary Sciences* **38**, 523–550.
- Young, G. C. (2011). Wee Jasper-Lake Burrinjuck fossil fish sites: scientific background to national heritage nomination. *Proceedings of the Linnean Society of New South Wales* **132**, 83–107.
- Young, G. C. and Goujet, D. (2003). Devonian fish remains from the Dulcie Sandstone and Cravens Peak Beds, Georgina Basin, central Australia. *Records of the Western Australian Museum Supplement* **65**, 1–80.
- Young, G. C., Lelièvre, H. and Goujet, D. (2001). Primitive jaw structure in an articulated brachythoracid arthrodire (placoderm fish; Early Devonian) from Southeastern Australia. *Journal of Vertebrate Paleontology* **21**, 670–678.
- Young, G. C., Long, J. A. and Ritchie, A. (1992). Crossopterygian fishes from the Devonian of Antarctica. *Records of the Australian Museum Supplement* **14**, 1–77.
- Young, G. C. and Zhang, G. (1996). New information on the morphology of yunnanolepid antiarchs (placoderm fishes) from the Early Devonian of South China. *Journal of Vertebrate Paleontology* **16**, 623–641.
- Yu, X. (1998). A new porolepiform-like fish, *Psarolepis romeri*, gen. et sp. nov. (Sarcopterygii, Osteichthyes) from the Lower Devonian of Yunnan, China. *Journal of Vertebrate Paleontology* **18**, 261–274.
- Zhang, G.-R., Wang, S.-T., Wang, J.-Q., Wang, N.-Z. and Zhu, M. (2010). A basal antiarch (placoderm fish) from the Silurian of Qujing, Yunnan, China. *Palaeoworld* **19**, 129–135.

- Zhang, M. (1980). Preliminary note on a Lower Devonian antiarch from Yunnan, China. *Vertebrata Palasiatica* **18**, 179–&.
- Zhang, M.-M. and Yu, X.-B. (1981). A new crossopterygian, *Youngolepis praecursor*, gen. et sp. nov., from lower Devonian of East Yunnan, China. *Scientia Sinica* **24**, 89–99.
- Zhao, W. J., Zhu, M., Liu, S., Pan, Z. H. and Jia, L. T. (2016). A new look at the Silurian fish-bearing strata around the Shanmen reservoir in Lixian, Hunan province. *Journal of Stratigraphy* **40**, 341–350.
- Zhu, M. (1996). The phylogeny of the Antiarcha (Placodermi, Pisces), with the description of early Devonian antiarchs from Qujing, Yunnan, China. *Bulletin du Muséum national d'histoire naturelle. Section C, Sciences de la terre, paléontologie, géologie, minéralogie* **18**, 233–347.
- Zhu, M., Ahlberg, P. E., Pan, Z., Zhu, Y., Qiao, T., Zhao, W., Jia, L. and Lu, J. (2016). A Silurian maxillate placoderm illuminates jaw evolution. *Science* **354**, 334–336.
- Zhu, M. and Gai, Z. (2007). Phylogenetic relationships of galeaspids (Agnatha). *Frontiers of Biology in China* **2**, 151–169.
- Zhu, M. and Janvier, P. (1998). The histological structure of the endoskeleton in galeaspids (Galeaspida, Vertebrata). *Journal of Vertebrate Paleontology* **18**, 650–654.
- Zhu, M. and Schultze, H. P. (1997). The oldest sarcopterygian fish. *Lethaia* **30**, 293–304.
- Zhu, M., Wang, W. and Yu, X. (2010). *Meemannia eos*, a basal sarcopterygian fish from the Lower Devonian of China—expanded description and significance. In *Morphology, Phylogeny and Paleobiogeography of Fossil*

- Fishes* (ed. D. Elliot, J. Maisey, X. Yu and D. Miao), pp. 199–214. Verlag Dr. Friedrich Pfeil, München.
- Zhu, M. and Yu, X. (2002). A primitive fish close to the common ancestor of tetrapods and lungfish. *Nature* **418**, 767–770.
- Zhu, M., Yu, X. and Ahlberg, P. E. (2001). A primitive sarcopterygian fish with an eyestalk. *Nature* **410**, 81–84.
- Zhu, M., Yu, X., Ahlberg, P. E., Choo, B., Lu, J., Qiao, T., Qu, Q., Zhao, W., Jia, L., Blom, H. and Zhu, Y.-A. (2013). A Silurian placoderm with osteichthyan-like marginal jaw bones. *Nature* **502**, 188–193.
- Zhu, M., Yu, X., Choo, B., Qu, Q., Jia, L., Zhao, W., Qiao, T. and Lu, J. (2012a). Fossil fishes from China provide first evidence of dermal pelvic girdles in osteichthyans. *PloS one* **7**, e35103.
- Zhu, M., Yu, X., Choo, B., Wang, J. and Jia, L. (2012b). An antiarch placoderm shows that pelvic girdles arose at the root of jawed vertebrates. *Biology Letters* **8**, 453–456.
- Zhu, M., Yu, X. and Janvier, P. (1999). A primitive fossil fish sheds light on the origin of bony fishes. *Nature* **397**, 607–610.
- Zhu, M., Yu, X., Lu, J., Qiao, T., Zhao, W. and Jia, L. (2012c). Earliest known coelacanth skull extends the range of anatomically modern coelacanths to the Early Devonian. *Nature Communications* **3**, 772.
- Zhu, M., Yu, X., Wang, W., Zhao, W. and Jia, L. (2006). A primitive fish provides key characters bearing on deep osteichthyan phylogeny. *Nature* **441**, 77–80.
- Zhu, M., Zhao, W., Jia, L., Lu, J., Qiao, T. and Qu, Q. (2009). The oldest articulated osteichthyan reveals mosaic gnathostome characters. *Nature* **458**, 469–474.

Zhu, Y. A. and Zhu, M. (2013). A redescription of *Kiangyousteus yohii* (Arthrodira: Eubrachythoraci) from the Middle Devonian of China, with remarks on the systematics of the Eubrachythoraci. *Zoological Journal of the Linnean Society* **169**, 798–819.

Zhu, Y. A., Zhu, M. and Wang, J. Q. (2015). Redescription of *Yinostius major* (Arthrodira: Heterostiidae) from the Lower Devonian of China, and the interrelationships of Brachythoraci. *Zoological Journal of the Linnean Society* **176**, 806–834.